Conformational and reactivity studies of lactam esters for their suitability for transannular Dieckmann-type cyclisation towards the azabicyclooctane-scaffold

A report submitted in part fulfilment of the examination requirements for the award of PhD Pharmacy and Pharmaceutical Science, awarded by the University of Lincoln

Submitted by: Christian Weck

November 2019

1st Supervisor: Dr Tobias Gruber
Senior Lecturer, School of Pharmacy
University of Lincoln

2nd Supervisor: Dr Ishwar Singh
Associate Professor, School of Pharmacy
University of Lincoln

Declaration of Novelty

This is to certify that I am responsible for the work submitted in this thesis, that the original work is my own, except as specified in references and that neither the thesis nor the original work contained therein has been previously submitted to any institution for a degree.

Signature:

Christian Weck

Abstract

The following thesis describes a novel Dieckmann-type cyclisation of strategically modified, simple caprolactams to the medicinally interesting 7,8-dioxo-6-azabicyclo[3.2.1]octane scaffold. This scaffold is structurally related to the 1,6-diazabicyclo[3.2.1]octane, the core motif of the β-lactamase inhibitor Avibactam. The presented thesis will outline the considerations and evaluation of crucial concepts of caprolactams, their general chemistry and mechanistic studies of importance to this novel approach towards the bicyclic scaffold. The initial discovery and first attempts at optimisation are presented, which led to a study into the physicochemical behaviour of lactams. During the investigations, it was found that the scarce fundamental research on this long-known group of compounds could not provide enough insight to deliver a comprehensive understanding of the involved mechanism. For that reason, we were additionally interested in the solid-state behaviour of lactams, which led to the first ever published single-crystal structure of free δ-valerolactam without secondary components. This allowed for previously conducted theoretical experiments on the amide bond situation of δ-valerolactam to be disproven and also allowed for the abnormally fast hydrolysis of δ-valerolactam to be explained through empirical evidence. The conclusions drawn from the comparative studies on the homologous series of lactam led to a broader study on the conformational behaviour, leading hydrogen-bonding motifs, general packing in the solid-state and the effects of substitution on the amide bond of selected lactams of various ring sizes. The results from this first ever comprehensive investigation on selected caprolactam esters led to the development of a convenient, one-pot synthesis of the 7,8-dioxo-6-azabicyclo[3.2.1]octane core structure from a simple caprolactam in good yields, with the potential for the preparation of a wide variety of derivatives. This Dieckmann-type cyclisation reaction is discussed in terms of its mechanism and its possibilities for further modifications. Further synthetic effort towards the introduction of specific functional groups for the establishment of water solubility and bioactivity are presented. Parts of the here presented thesis have already been successfully published in influential peer-reviewed journals and it is expected that further such publications will follow.

Table of content

Part I - Descriptive Section

Introduction

The effective and targeted treatment of bacterial infections is one of the most important biochemical developments in the history of medicine. Before, even simple injuries, like cuts, could lead to lethal sepsis and ultimately death. This revolution was triggered by Dr Alexander Fleming's groundbreaking studies on penicillin[1]. Many medicine and chemistry related textbooks that are concerned with infections, treatments etc. denote his work as the beginning of the so-called *antibiotic-age*. Since then, a wide variety of penicillins and closely related antibiotic agents have been developed, the *β-lactam antibiotics*[2]. Even today, β-lactams are amongst the most prescribed antibiotic agents used in the treatment of infectious diseases[2]. However, the massive overprescription of penicillin and its derivatives also led to the development and spread of protective mechanisms in bacteria and many bacterial strains exhibit complete resistance against many β-lactams. Different mechanisms of resistance have been identified today, but the most concerning cause of resistance is the expression of enzymes that effectively hydrolyse β-lactam antibiotics, often referred to as *β-lactamases*. The emergence of these resistances has been reported only years after penicillin was first introduced and studies into these enzymes have shown that the expression of β-lactamases is a bacterial survival strategy, much older than the clinical treatment of infections with antibiotics[3]. Today, medicine and society might be facing a turning point, marked by the discovery of a bacterial gene called MCR-1[4]. This gene has been found to be responsible for bacterial resistance against *colistin*, a non-β-lactam, that had been thought to be the perhaps last secure line of treatment against multiresistant strains.

The need for new approaches and new agents seems overdue. Recent research has been interested not only in the development of new antibiotic agents, but also in the development of bioactive agents with potential to suppress existing resistances. One particular system that has drawn the interest of organic and medicinal chemists is the 6-azabicyclo[3.2.1]octane. The reason, it has sparked interest recently is a urea derivative with this bicyclic scaffold as its core structure, called *Avibactam* (Fig. 1.1).

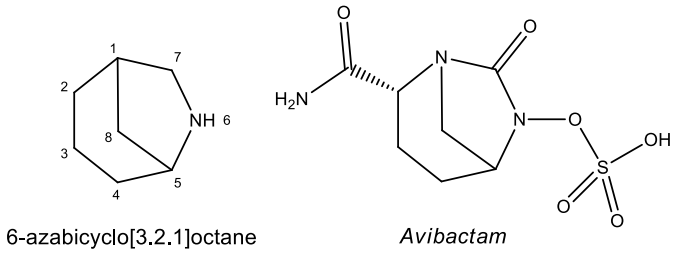

Fig. 1.1 The azabicyclo[3.2.1]octane system has drawn attention from organic and medicinal chemists through the surprising efficacy of Avibactam in the treatment of many penicillin-resistant bacterial strains.

Avibactam effectively inhibits a large number of β-lactamases through covalent binding to the active centre within these enzymes, which made the use of β-lactams antibiotics an effective treatment for

many formerly resistant bacterial strains again. Its surprising efficacy has also triggered research into a large number of structurally related compounds, but only one other of these bicyclic ureas, also known as *Diazabicycloctanes* (*DBO*) has found its way into clinical utility. The perhaps biggest disadvantage in the development of DBO related drugs is the enormous synthetic effort required for their synthesis. With more than ten consecutive steps, the preparation of potential analogues is a considerable economic detriment to their potential as a perhaps crucial contribution in the fight against antibiotic resistances. In the pursuit of a new, possible candidate with similar inhibitory properties, we were interested in the possibility to find a convenient synthetic approach to a structurally very similar scaffold, with an amide functionality instead of a urea group (Fig. 1.2).

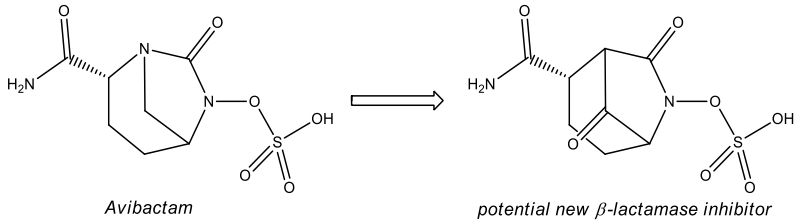

Fig. 1.2 The exchange of Avibactams urea functionality with an amide group could lead to an unprecedented new system and could contribute in the combat of growing threats of antibiotic resistances.

Avibactams mode of action relies on nucleophilic ring opening through the active centre of β-lactamases and the stability of the so formed acyl-enzyme complex, which could be lost with the transition of a urea to a lactam. However, computational studies conducted at the University of Oxford have indicated, that the introduction of a carbonyl group into the bicyclic scaffold could lead to stabilisation within those enzymes through non-covalent interactions[5]. The implementation of both of these concepts led to the evaluation of the *7,8-dioxo-6-azabicyclo[3.2.1]octane* scaffold as an alternative. The synthesis of this system has been described in literature twice before, but through long, multistep syntheses with little room for manipulation of the scaffold. We were therefore interested in developing a convenient and versatile synthetic approach to the 7,8-dioxo-6-azabicyclo[3.2.1]octane to pave the way towards this interesting system as a potential candidate to combat antibacterial resistances. The establishment, optimisation and characterisation of a total synthetic pathway towards this structure was the main objective of the here presented thesis. In the following chapters, theoretical deliberations and implementations into a novel and facile synthesis of this scaffold shall be outlined.

---

[1] A. Fleming, *Br. J. Exp. Pathol.* **1929**, *10*, 226-236.
[2] D. Steinhilber, M. Schubert-Zsilavecz, H.J. Roth, *Medizinische Chemie* 2nd edition, Deutscher Apotheker Verlage, Stuttgart, **2010**.
[3] D.Y. Wang, M.I. Abboud, M.S. Markoulides, J. Brem, C.J. Schofield, *Future Med. Chem*. **2016**, *8*, 1063-1084.
[4] Y.Y. Liu, Y. Wang, T.R. Walsh, L.X. Yi, R. Zhang, J. Spencer, Y. Doi, G. Tian, B. Dong, X. Huang, L.F. Yu, D. Gu, H. Ren, X. Chen, L. Lu, D. He, H. Zhou, Z. Liang, J.H. Liu, J. Shen, *The Lancet* **2016**, *16*, 161-168.
[5] T. Gruber *unpublished results*

Avibactam – Structure/Function relation

Bacterial resistance against β-lactam antibiotics was found to have several underlying causes. Active drug efflux, mutations on the target enzyme and reduced drug permeability have been observed mechanisms that lower the effective drug concentrations of β-lactam antibiotics in bacterial cells. However, the most clinically threatening mechanism is the hydrolytic inactivation through β-lactamases[6]. Additionally, the number of reported β-lactamases is increasing every year with more than 1400 different enzymes being reported[7]. Because of their differences in their respective modes of action, origin and intrinsic structure, β-lactamases are divided into classes, related to their biochemistry. The possibly most common classification of β-lactamases is the *Ambler classification,* which divides them into classes, A to D. Class A, C and D are often referred to as serine hydrolases, class B on the other hand are often described as metallo-β-lactamases.[8] Since the first discovery of penicillin hydrolysing enzymes in 1940, these enzymes have disseminated globally, class A and C in particular. As the need for new treatment options for bacterial infections arose and a number of new generation β-lactam antibiotics were developed, effective agents against the resistance-causing enzymes were researched. Clavulanic acid, sulbactam and tazobactam are three β-lactams with considerable clinical utility but have also been found to only be effective against certain β-lactamases (Fig. 1.3).

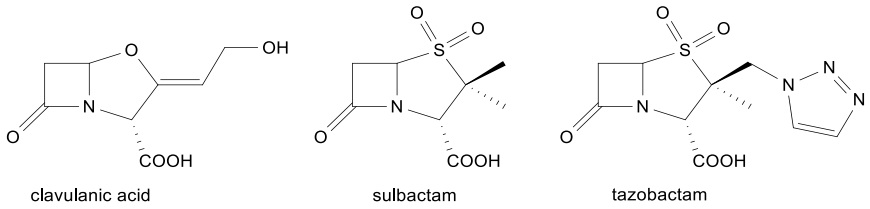

Fig. 1.3 Clavulanic acid, sulbactam and tazobactam are three β-lactamase inhibitors that are currently in clinical use, that are also β-lactams themselves. However, they are only useful against a limited number of β-lactamases.

A new class of β-lactamase inhibitors was introduced with *Avibactam,* formerly referred to as NXL-104. Avibactam was the first diazabicyclooctane (DBO) reaching clinical trails and FDA approval as an efficient new inhibitor and has now found clinical relevance. It does not show antibacterial activity itself and has to be administered alongside an effective antibacterial agent but allows for the use of previously ineffective penicillins. Its efficacy for a much wider spectrum of β-lactamases has sparked in-depth research into its biochemical behaviour, but also inspired chemists to synthesis more effective analogues. The development of DBOs has proved to be challenging, since many of its analogues require long multistep syntheses of 12 steps and more[9]. Despite these synthetic challenges, several DBOs have been synthesised and tested for biological activity, antimicrobial properties and cytotoxicity. Unfortunately, only one other DBO has been found to be clinically useful, the piperidine derivative Relebactam (Fig 1.4).

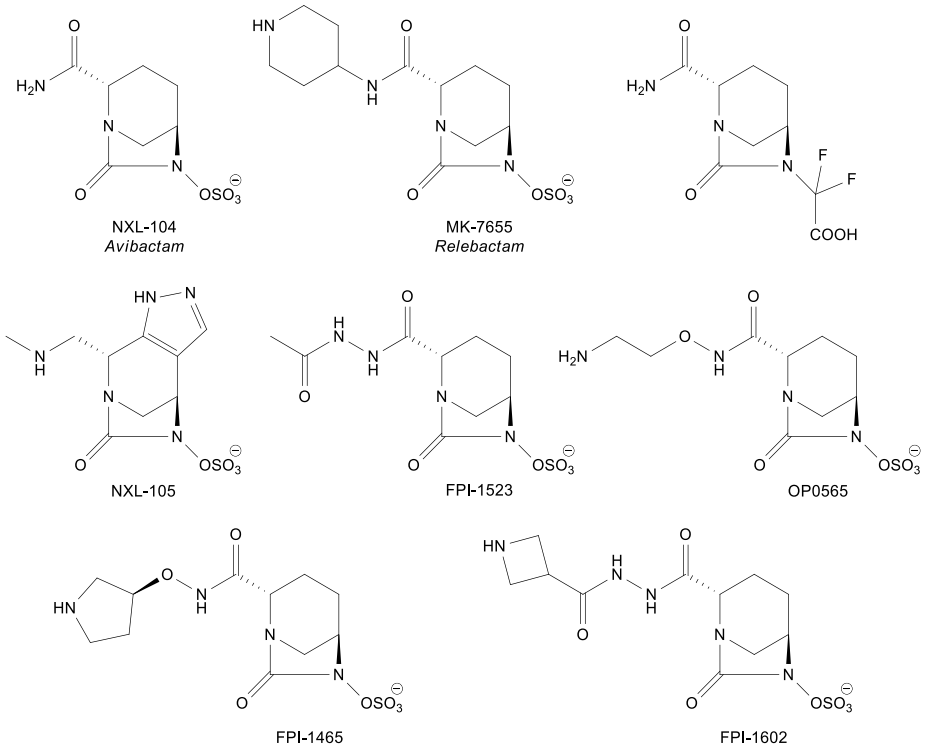

Fig. 1.4 Several diazabicyclo[3.2.1]octanes (DBO) have been synthesised and evaluated for their potential as clinically valuable drugs. So far, only Avibactam and Relebactam have found their way into clinical relevance.

Chemically speaking, Avibactam is a bicyclic urea derivative. One of the urea nitrogen atoms forms one of the bridgeheads, the other carrying a sulfactam (N-OSO_3) group. Additionally, the carbon backbone carries a carbamoyl group in α-position to the bridgehead nitrogen. The development of derivatives of Avibactam has been aimed at improving bioactivity/bioavailability whilst retaining the core scaffold. Many of these analogues show similar inhibitory action but distinctly different pharmacological properties. For example, NXL-105, a tricyclic analogue has been found to exhibit inhibitory activity against certain class A β-lactamases but is a poor inhibitor of class C enzymes. NXL-105 has also shown antibacterial activity itself with considerable effectiveness against *E. coli* and *P. aeruginosa*[9] but is not under evaluation as potential new treatment against infectious diseases caused by either.

Extensive studies into the kinetics of inhibition and crystallography of β-lactamases have revealed detailed insight into the mode of action of avibactam. It has now been generally accepted that avibactam can form an acyl-enzyme complex with a hydrolytically active serine residue in serine hydrolases. Such an acylation most likely happens with β-lactam substrates as well, but in contrast to such substrates, the avibactam-enzyme complex is significantly more stable.

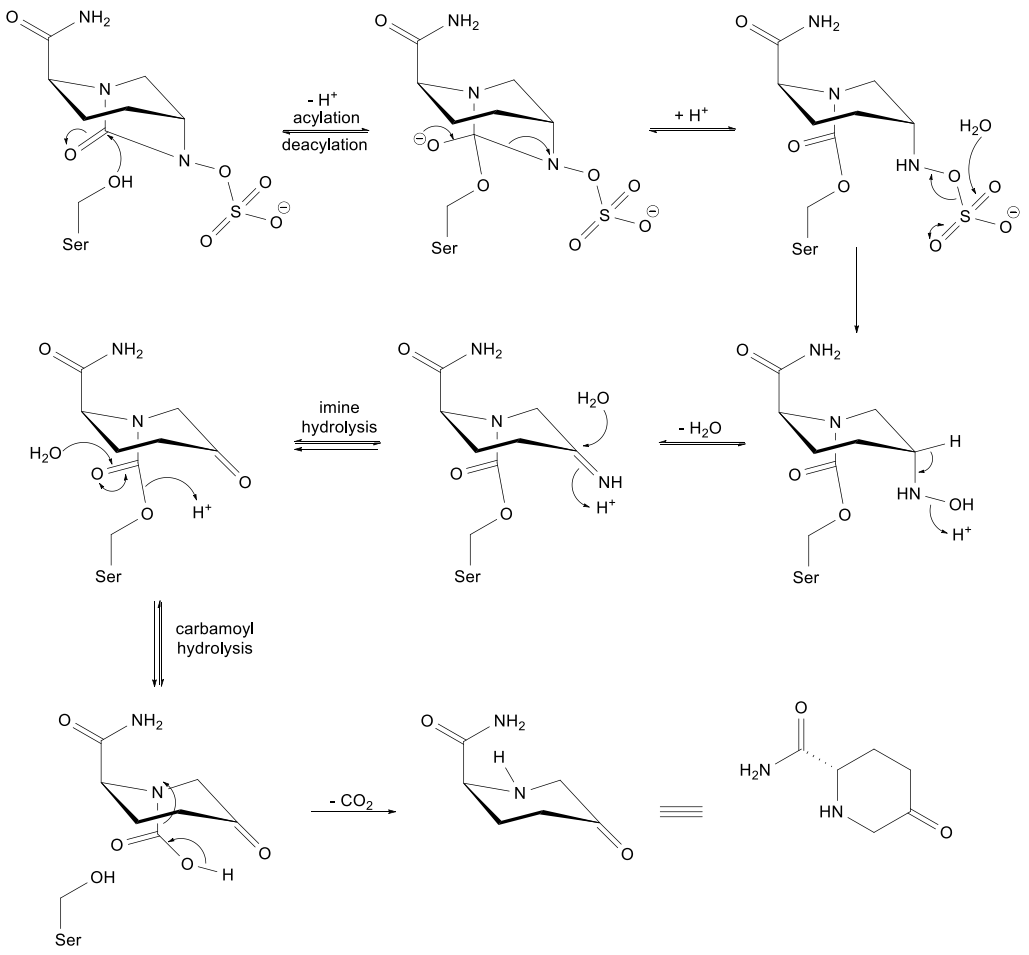

Fig. 1.5 Avibactam undergoes hydrolytic ring opening through a nucleophilic attack of an active serine residue within serine hydrolases. The subsequent reactivation of the enzyme through further hydrolytic degradation happens comparatively slowly, thus Avibactams efficacy.

It is believed that the longevity of the acyl-enzyme complex comes from the relative stability of the carbamate group formed between the enzyme and avibactam. In fact, for enzymes that are not efficiently inhibited by avibactam, hydrolytic elimination of the substrate is not thought to be a result of immediate hydrolysis of the carbamate group (Fig. 1.5). Studies have suggested that the enzymatic reactivation involves the hydrolytic transformation of the sulfonate group first. Evidence was found that the sulfate group is cleft to give a hydroxyl amine, which then undergoes imine formation through a proton mediated condensation. The imine group is further hydrolysed to give a ketone and the so formed ketone undergoes carbamate hydrolysis to give reactivated enzyme. Even though, such hydrolytic reactivation of PBPs can be found, avibactam is still considered to be much more efficient than most other β-lactamase-inhibitors. Only 1-5 avibactam molecules per β-lactamase enzyme are required for effective inhibition, compared to 10s-100s of molecules for β-lactam-based inhibitors. Avibactam appears to be superior in this respect, because the inhibition of PBPs through β-lactam-based inhibitors competes with their non-enzymatic hydrolysis whereas Avibactam is comparatively stable against such.

Evidence suggests that β-lactamases are highly optimised towards the hydrolysis of β-lactam antibacterials. Single crystal analysis of both free enzymes and enzyme-substrate complexes show that the highly functionalised β-lactams form several non-covalent connections within the active centre of PBPs. This leads to the question on how such highly optimised enzymes also recognise non-β-lactams and how inhibition of β-lactamases is realised.

Fig. 1.6 shows the acyl-enzyme complex of KPC-2, a class A serine β-lactamase from *Klebsiella pneumoniae* with avibactam. The bicyclic structure of avibactam cannot be found; instead, the active serine residue (Ser69) is found to be covalently bound as a carbamate. This carbamate also forms a network of hydrogen bonds with a threonine (Thr236) and the hydrolytically active water molecule in the active site.

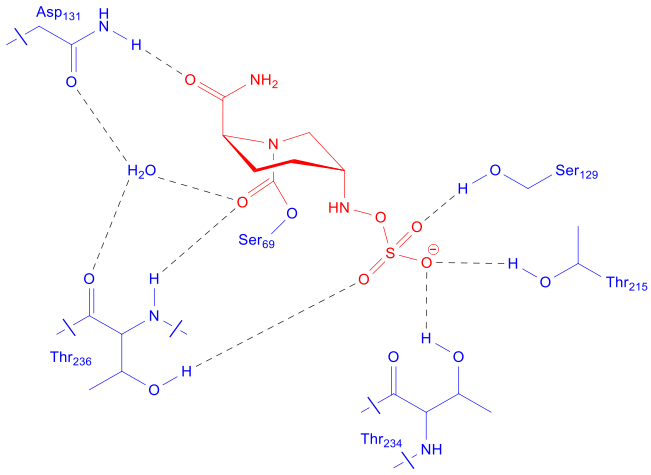

Fig. 1.6 The crystal structure of a deactivated acyl-enzyme complex of Avibactam with KPC-2, a β-lactamase from Klebsiella pneumonia shows that the active serine is involved in a carbamate bond with the ring opened Avibactam.

The *N*-sulfate group somewhat mimics the effect of carboxylic acids groups on β-lactam antibiotics. Since the carboxylic acid (or sulfate group in the case of aztreonam) functionality is a vital requirement for β-lactam antibiotics, similar enzyme-substrate interactions are most likely required for effective recognition. In the case of KPC-2, avibactams sulfate group is involved in hydrogen bonds with Ser129, Thr215, Thr 234 and Thr236. The fact that this sulfate group is hydrolysed before enzyme reactivation can occur might be another factor to be considered in terms of effective inhibition. Additionally, avibactams free carbamoyl group forms hydrogen bonding with Asp131, which further contributes to the effective recognition process. It seems fair to assume that the design and development of new active agents would require highly similar size, functional groups and functionalisation patterns.

1.1) Retrosynthetic analysis of 7,8-dioxo-6-azabicyclo[3.2.1]octane

The development of a synthetic approach to an analogue of Avibactam began with the retrosynthetic analysis of the corresponding carbon system. Retrosynthesis is a powerful tool for the organic chemist in the development of synthetic strategies. Generally speaking, retrosynthesis starts from the envisaged final product and aims at leading the organic chemist towards a feasible starting material. In contrast to applied synthesis, retrosynthesis may result in intermediary compounds that do not necessarily exist but can guide the user through a series of hypothetical synthetic steps which can then be converted into plausible transformations.

Avibactam itself is a bicyclic urea derivative in which two nitrogen atoms are embedded in a seven membered ring. It furthermore carries a sulfamate group, attached to one of the embedded nitrogen atoms, and a primary amide group attached to the carbon backbone. Stripping both additional functionalities gives avibactams bicyclic scaffold, the 7-oxo-1,6-diazabicyclo[3.2.1]octane system. The transformation of this urea to a lactam would allow two alternative systems but only retention of the nitrogen atom in position 6 will allow (retro)synthetic reattachment of a sulfate group. The resulting carbon analogue system, the 7-oxo-6-azabicyclo[3.2.1]octane has been described in literature numerous times before with convenient preparation methods. Crystallographic studies on enzyme-substrate complexes of avibactam with its target have shown that a hydrolytic ring opening of the bicyclic scaffold appears to be crucial. Such ring opening reactions can be facilitated through an increase of ring strain of the system. The retrosynthetic transformation of said carbon analogue to an oxo analogue should deliver such an increase through the change of a sp^3 to a sp^2 hybridised, bridging carbon (Fig. 1.7).

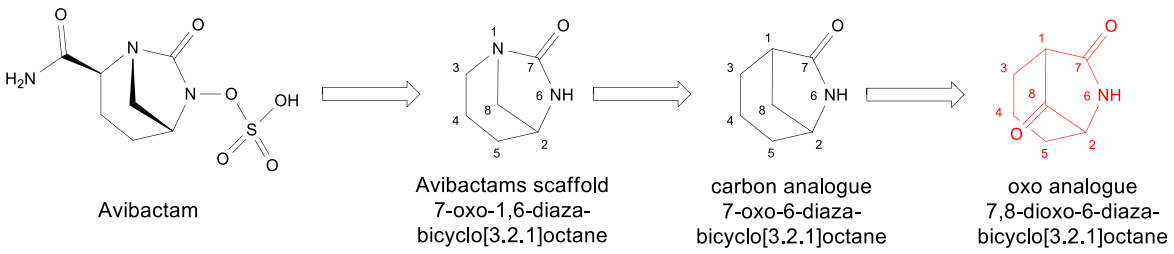

1.7 The retrosynthetic elimination of the functionalities leaves the 7-oxo-1,6-diazabicyclo[3.2.1]octane. The rational redesign and hypothetical optimisation led to the 7,8-dioxo-6-azabicyclo[3.2.1]octane as the leading motif of this project.

The introduction of an oxo group further holds two possible advantages over an unsubstituted carbon bridge:

- The resulting keto functionality should allow further modifications more easily. Considering the potential application in biologically relevant systems, this promises optimisation on crucial properties like water solubility, membrane permeability, interactions with other targets etc.
- The addition of further hydrogen bond accepting groups could be found as an advantage in the recognition by biological targets and/or superior binding properties within the active centre of target enzymes.

This ultimately led to the 7,8-dioxo-6-azabicyclo[3.2.1]octane scaffold as the main target structure for this project. The retrosynthetic analysis of polycyclic molecules usually requires a strategically chosen bond to be broken to reduce the complexity of the system in question. In the case of the 7,8-dioxo-6-azabicyclo[3.2.1]octane, three different pathways were thought to be of considerable interest, they can easily be distinguished by the size of the resulting ring (Fig. 1.8):

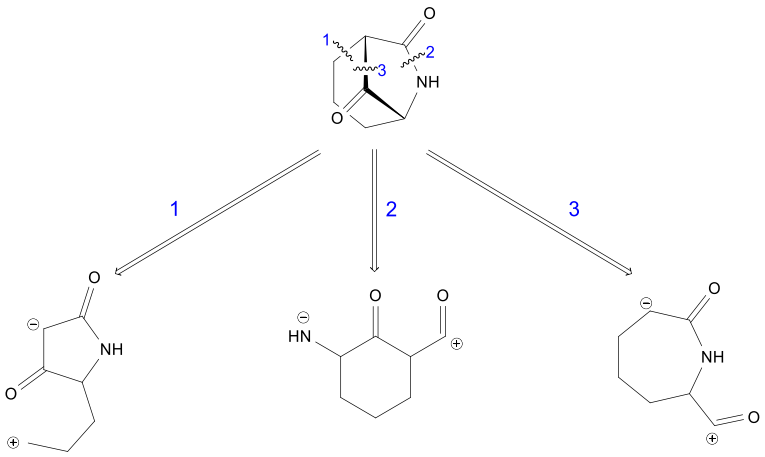

Fig. 1.8 Retrosynthetic bond breakage of the bicyclic target scaffold could lead to a large number of different structure. The three pathways that were thought to be of considerable interest would give a five-, six- or seven-membered ring as starting point.

Pathway 1 starts with a C-C bond being broken, leading to a butyrolactam. The two carbonyl functionalities would make formation of a carbanion in the displayed position presumably easy, and therefore determined the proposed charge distribution. The suggested synthetic equivalent is an oxo-butyrolactam with an alkyl bromide chain (Fig. 1.9). Such butyrolactams have been described before but are not readily commercially available and would require significant synthetic effort.

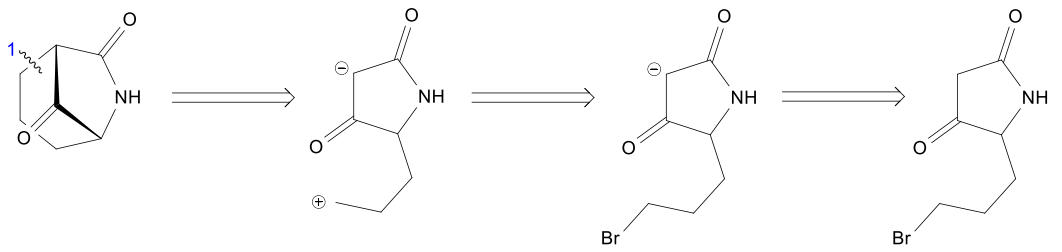

Fig. 1.9 Pathway 1 would lead to the displayed oxo-butyrolactam with an alkyl bromide side chain. Such structures have been described but would most likely require extensive synthetic preparations.

Pathway 2 starts with breaking the amide bond to give a disubstituted cyclohexanone (Fig. 1.10). Distributing the charges seems straightforward as it can be matched with the natural distribution of electron density. The resulting synthetic equivalent could be an aminocyclohexanone acyl halide, which is not commercially available as is but a potential synthesis could start from cyclohexanone or a phenol.

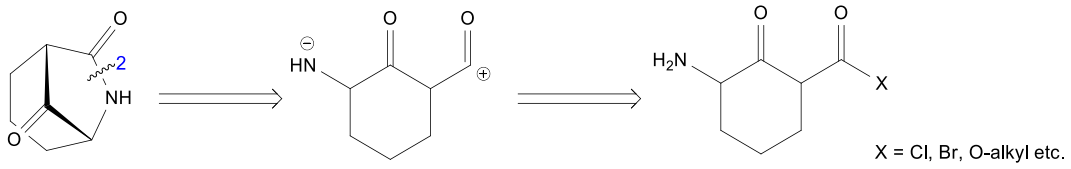

Fig. 1.10 Retrosynthetic analysis of pathway 2 shows that a comparatively simple cyclohexanone could form the starting material.

The reversal of pathway 2 from a mere retrosynthetic analysis to realistic synthetic steps quickly revealed a number of problems. The starting material would inevitably contain two stereocentres which leads to four different stereoisomers. Of these four, only the two *syn*-positioned diastereomers would allow intramolecular amide bond formation. Symmetric synthesis of this precursor would then require isolation of the *syn*-diastereomers from their respective enantiomers, or asymmetric synthesis would be required. Furthermore, a hypothetical acyl halide of the proposed aminocyclohexanone would be prone to oligo/polymerisation, less reactive ester equivalents might undergo imine condensation reactions (Fig. 1.11).

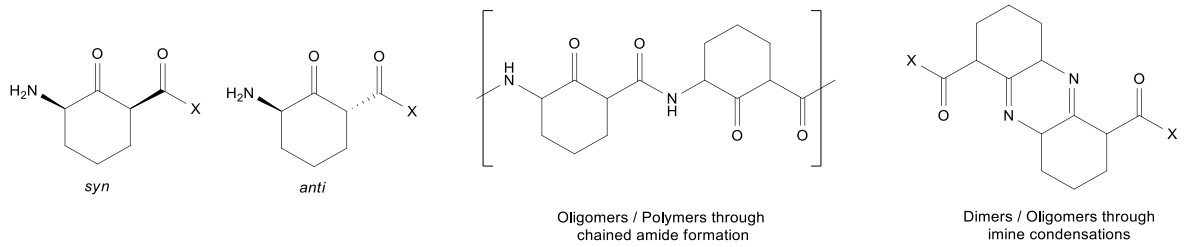

Fig. 1.11 Considerations on how pathway 2 could be implemented into synthesis shows that pathway 2 could lead to a number of synthetic challenges. The possibility of diastereomers and formation of dimers, oligomers and/or polymers would also have to be overcome.

Pathway 3 leads to a monosubstituted caprolactam with an acylium group (Fig. 1.12). A simple synthetic equivalent of this could be an acyl halide or an ester. Such a monosubstituted caprolactam is not commercially available but can be broken down further. The next logical retrosynthetic step is to break the amide bond within the caprolactam to give an acyclic synthon. The same reasoning for the charge distribution as in pathway 2 applies here, which ultimately leads to a derivative of pimelic acid. The corresponding amino acid, 2-aminopimelic acid, is in fact commercially available. The transformation of the free amino acid to acyl halides or esters could be carried out using similar procedures to other amino acids, for which a wide range of techniques are known.

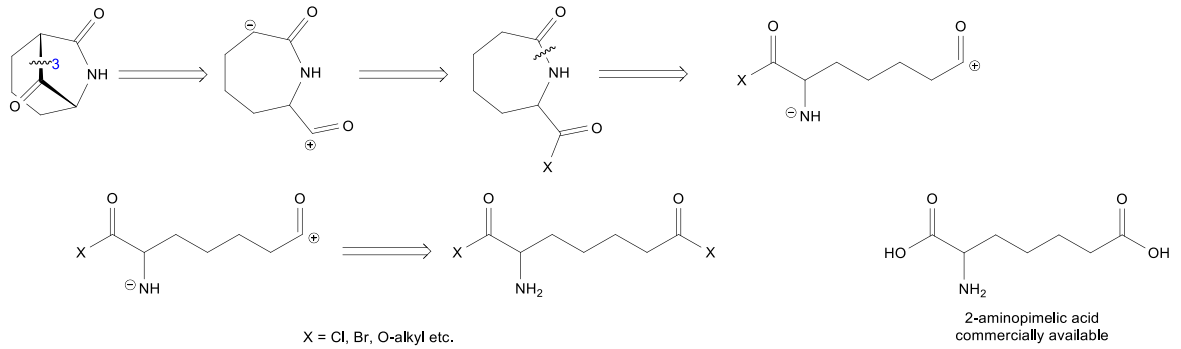

Fig. 1.12 The retrosynthetic analysis of pathway 3 lead to the commercially available 2-aminopimelic acid. Required transformations, proposed by the retrosynthesis appear to be possible as such transformations are commonly known.

The retrosynthetic analysis therefore provided 2-aminopimelic acid as a possibly viable starting material for the envisaged multistep synthesis towards the 7,8-dioxo-6-azabicyclo[3.2.1]octanes.

1.2) Previously published syntheses of the 7,8-dioxo-6-azabicyclo[3.2.1]octane scaffold

The 6-azabicyclo[3.2.1]octane has been described in literature multiple times and an array of synthetic procedures are available for the preparation of the scaffold and for strategic manipulation of it. However, synthesis of the 7,8-dioxo-6-azabicyclo[3.2.1]octane system has only been described twice before, once in the late 1980s by a Dutch group as part of their total synthesis of the alkaloid *peduncularine*, and once by a British group studying rearrangement reactions of annulated, bicyclic β-lactams.

In their total synthesis of peduncularine[10], Speckamp and coworkers started with (*S*)-malic acid and converted it into a five-membered imide, followed by the reduction to an N_{α}-ethoxy butyrolactam (Fig. 1.13). After deprotonation with lithium diisopropylamide (LDA), a silylated alkyne group was introduced to prepare the subsequent ring closure. The ring closure was accomplished through refluxing the substrate in neat formic acid for three hours and subsequent addition of a methanolic ammonia solution.

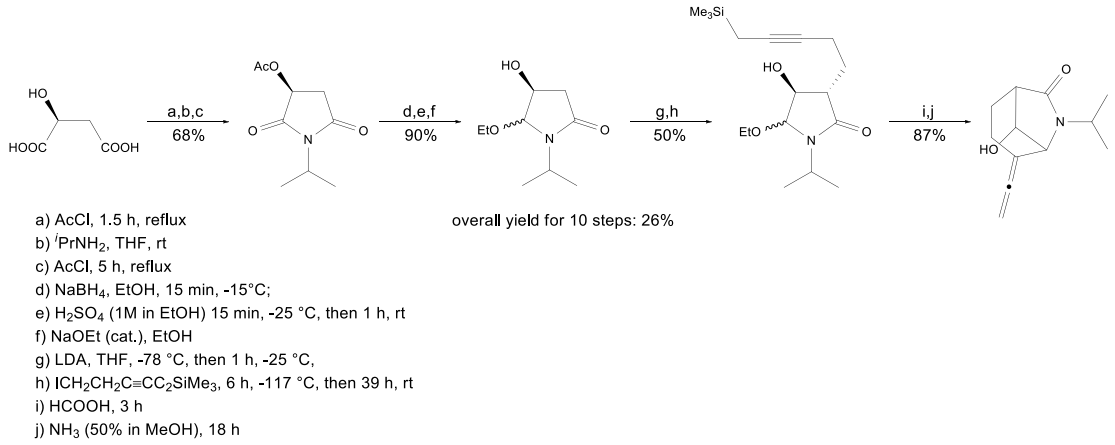

Fig. 1.13 Speckamp and co-workers have described a 10-step procedure, starting from (S)-malic acid, to give the 6-azabicyclo[3.2.1]octane scaffold in an overall yield of 26%. However, the subsequent oxidation to the 7,8-dioxo-6-azabicyclo[3.2.1]octane required another three synthetic steps.

The authors reported the 10-step procedure with a good overall yield of 26% for the preparation of the bicyclic scaffold. However, the so obtained bicyclic lactam does not have a ketone bridge at this stage, which required another three steps with 89% yield. The overall yield of this total synthesis is comparatively good, considering that 13 steps were required. This approach appears to be of tremendous synthetic effort but was also not designed for the sole preparation of the bicyclic lactam system.

A very different approach was described by Grainger and co-workers[11] (Fig. 1.14). They described a seven-step synthesis, starting with 3-bromocyclohexene, which is converted into a thiocarbamic thioanhydride through the use of a *para*-methoxyphenyl (PMP) protected amine, triphosgene and a thiocarbamic acid salt. This monocyclic urea derivative is then photocyclised, followed by elimination of a thiocarbamate group to give an annulated, bicyclic β-lactam. After stereoselective bis-hydroxylation, a semipinacol rearrangement converts the β-lactam into the PMP protected 7,8-dioxo-6-azabicyclo[3.2.1]octane scaffold in an excellent overall yield of 56% for seven steps.

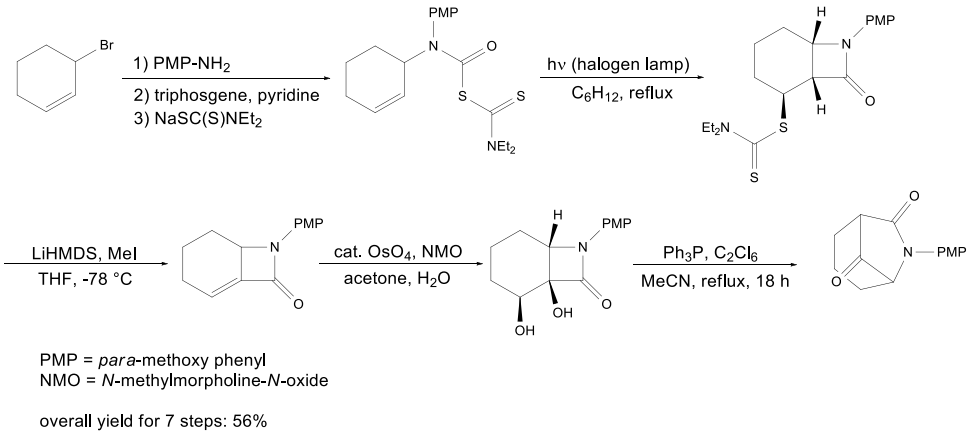

Fig. 1.14 Grainger and co-workers have described a seven-step procedure, starting with a brominated cyclohexene, to give the 7,8-dioxo-6-azabicyclo[3.2.1]octane scaffold with PMP protection with an excellent overall yield of 56%.

One debatable disadvantage of this reported approach is the use of number of expensive, hazardous and highly reactive chemicals. The commercial aspect and potential dangers from the involved chemicals is not necessarily an insurmountable challenge to experienced synthesis chemists for laboratory-scale preparations. However, the authors describe possible accessibility of derivative and potential for derivatisation, but require several further synthetic steps and focused on the versatility of this general approach to larger, bicyclic systems, rather than functionalisation.

1.4) Earlier work within the group

The groundworks on which this project is based on were carried out by Dr Tobias Gruber in his capacity as a postdoctoral researcher, University of Oxford (2010), Ms Franziska Obst as part of a Bachelor of Science Degree, University of Freiberg, Germany (2014) and Mr Christian Weck as part of a Master of Science Degree, University of Freiberg, Germany (2016). The following section shall describe the findings of importance for this project; the following information is collected from unpublished work with the explicit consent of all contributors, who should be acknowledged as this project could not have been carried out without their respective contributions. Please note: all descriptions are summarised and required substantial amounts of work.

Just as the retrosynthetic approach outlined, 2-aminopimelic acid was used as the starting material (Fig. 1.15). In a first attempt at preparing a 2-carboxy caprolactam, 2-aminopimelic acid was dissolved in toluene, fused silica (SiO_2) was added and the mixture was refluxed for 6 h. The free acid was obtained with a yield of 18%. Because the direct condensation gave such poor yields, the ring closure was to be facilitated by transforming the carboxylic acid groups into more reactive analogues. The starting material was therefore transformed into a symmetric diester through the addition of thionylchloride ($SOCl_2$) to cooled methanol/ethanol before the starting material was added. This protocol gives the respective diester of 2-aminopimelic acid as a hydrochloride in excellent yields of 90%+. After neutralisation and extraction, the so obtained esters were then refluxed in the high boiling solvent *p*-cymene. The product yield of 57% for the respective methyl ester was considerably higher than for the cyclisation of the free diacid and was considered sufficient for further synthesis whereas an ethyl ester only gave 25% yield.

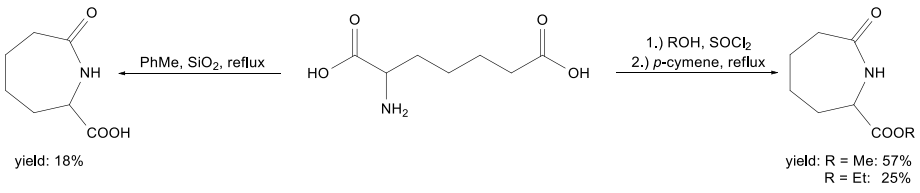

Fig. 1.15 The direct condensation of 2-aminopimelic acid to a 2-carboxy caprolactam only gave poor yields. The esterification of the ester groups and subsequent ring closure gave almost tripled product yields for the respective methyl ester, which was considered sufficient.

Experiments on the methylation of 2-aminopimelic acid using the MeOH/$SOCl_2$ protocol gave a product yield of 93% when carried out individually, the subsequent cyclisation without optimisation in *p*-cymene gave 62% (Fig. 1.16). The individual methylation step did not need further optimisation, but because the formation of this caprolactam then required an intramolecular reaction as well, it seemed plausible that intermolecular side reactions competed. It was further observed, that refluxing a solution of dimethyl 2-aminopimelate in *p*-cymene appeared to form side products with the solvent. In an attempt at optimising the cyclisation yield, experiments with various concentrations of the dimethyl ester in *p*-cymene were carried out. It was found that a concentration of about 0.08 $mol \cdot l^{-1}$ gave the best yield with 69%, with higher concentrations giving lower yields and lower concentrations not showing any further improvement. Experiments regarding the reaction time showed that the starting material was consumed within about 20 h of reflux. Longer reaction times did not improve the yield any further either.

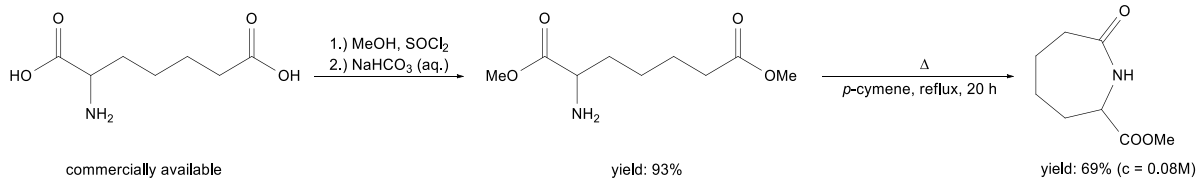

Fig. 1.16 The separation of both steps from 2-aminopimelic acid to the cyclised caprolactam ester showed that the methylation occured in almost quantitative yields. The cyclisation was optimised to a good yield of 69% through dilution.

A different approach to the caprolactam methyl ester was the Beckmann rearrangement of methyl 2-carboxycyclohexanone. However, the desired ring expansion was not observed. Instead, an isoxazol was found to be the main product (Fig. 1.17).

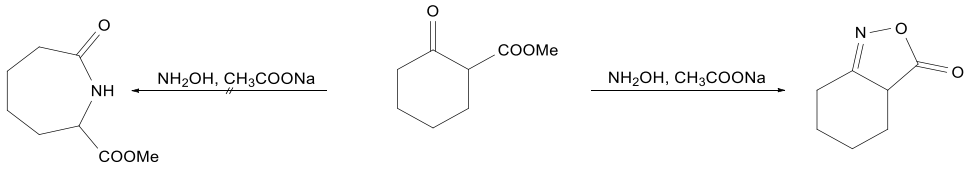

Fig. 1.17 Beckmann rearrangement of methyl-2-oxo-cyclohexanonecarboxylate did not give a caprolactam. Instead an isoxazol was found as the main product.

The cyclisation of the dimethyl 2-aminopimelate however gave an overall yield of 64% (Fig. 1.18). The so obtained methyl ester caprolactam could be saponified using a mixture of LiOH/H_2O_2 in a solvent mixture of THF/H_2O[12]. The free acid was obtained with a good yield of 70%, which adds to an overall yield of 45% starting from 2-aminopimelic acid. This saponification procedure is of particular interest for related systems, because the ester group was found to be hydrolysed without notable hydrolysis of the amide bond.

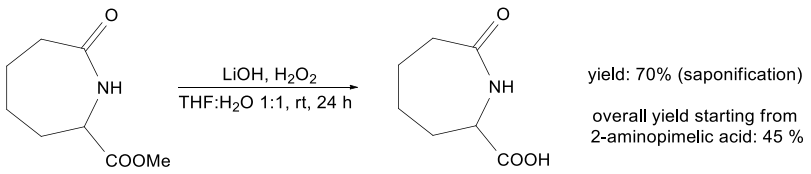

Fig. 1.18 Saponification of the ester using LiOH/H_2O_2 in THF/H_2O give the free acid conveniently without hydrolysis of the lactam bond. The good yield of 70% could allow for re-esterification to different esters.

Following the saponification, the free acid was re-esterified to give the corresponding *tert*-butyl ester. The esterification procedure used a mixture of *tert*-butyl acetate and aqueous perchloric acid, which gave a product yield of 18%, the overall yield being only 8%.

The three different caprolactam esters where then Boc protected, using two different methods (Fig. 1.19). The first used di-*tert*-butyl dicarbonate (Boc_2O) and triethylamine (NEt_3) in refluxing CH_2Cl_2 with a catalytic amount of 4-(*N*,*N*-dimethylamino)pyridine (DMAP). This procedure gave 68%, 29% and 15% for the methyl, ethyl and *tert*-butyl ester respectively. For the second method, the base was exchanged for diisopropylethylamine (DIPEA, *Hünig's base*) and CH_2Cl_2 was exchanged for toluene. This second approach gave significantly higher product yields of 86%, 72% and 95% for the three mentioned esters respectively.

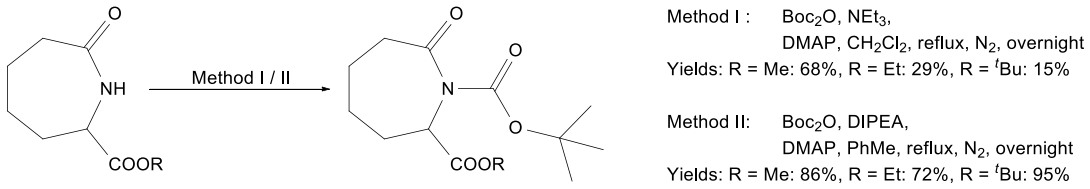

Fig. 1.19 Two methods for the Boc protection for three different caprolactam ester were tried. Method II, using Boc_2O, DIPEA, DMAP in refluxing PhMe gave superior yields for all three esters.

Alternatively, to the introduction of the Boc protection group, the introduction of a benzyloxycarbonyl or Cbz (or Z) group was tried. Three different methods were experimented with to introduce a Cbz group, but the desired Cbz protected caprolactam could not be obtained (Fig. 1.20).

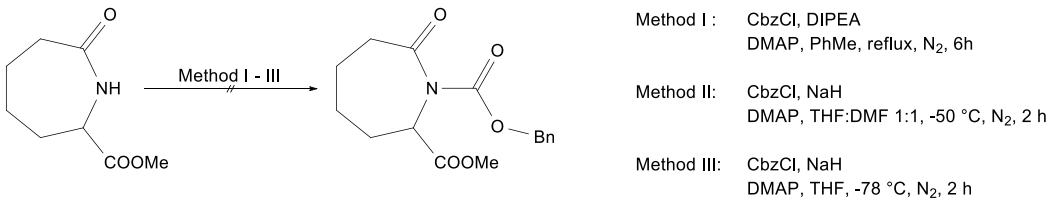

Fig. 1.20 Three different methods to prepare a Cbz protected caprolactam methyl ester were tried but none of the employed conditions gave the desired product.

Similarly to the previously described syntheses of fully saturated lactams, a desaturated caprolactam was prepared using ring closure metathesis. The required α,ω-diene is not commercially available and was synthesised. First, 2-aminopent-4-enoate was methylated using the same protocol using MeOH/$SOCl_2$ as previously described. The methylated product was obtained in quantitative yield (Fig. 1.21).

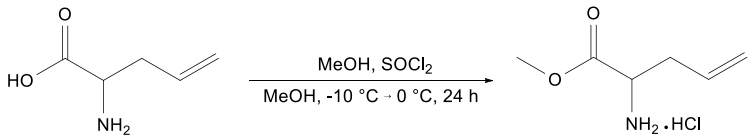

Fig. 1.21 The methylation of 2-amino-pent-4-enoic acid using the MeOH/$SOCl_2$ procedure gave the corresponding methyl ester in quantitative yield as a hydrochloride.

Next was an amide coupling of the prepared methylated amino acid with 3-butenoic acid (Fig. 1.22). Many different amide coupling procedures are known from peptide chemistry, this approach used a mixture of 1-Ethyl-3-(3-dimethylaminopropyl)carbodiimide hydrochloride (EDC·HCl) and *N*-hydroxybenzotriazole monohydrate (HOBt·H_2O). This protocol generates an activated *O*-acylurea between the acid component and the carbodiimide. Such *O*-acylureas have been found to undergo rearrangement to *N*-acylureas, which do not undergo amide coupling. This is typically avoided by vigorous cooling of the reaction mixture and can be further supported using the secondary coupling agent HOBt. The coupled peptide was obtained in a good yield of 66%.

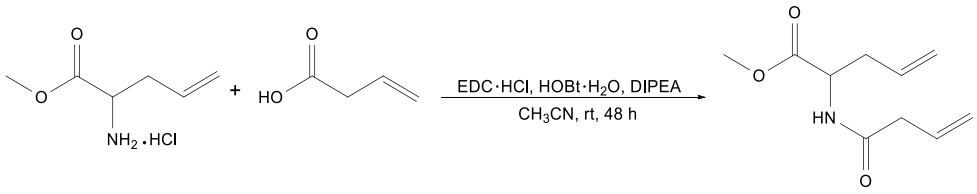

Fig. 1.22 Amide coupling of the amine and acid component using EDC·HCl and HOBt·H_2O gave the for ring closure metathesis required α,ω-dialkene in a good yield of 66%.

The obtained, coupled amide was then cyclised using the 2nd generation Grubb's catalyst for a ring closure metathesis (Fig. 1.23). Such ring closure reactions may suffer from the possibility to form dimeric species, which can be supressed under highly diluted conditions. The desaturated caprolactam was obtained in a yield of 32%.

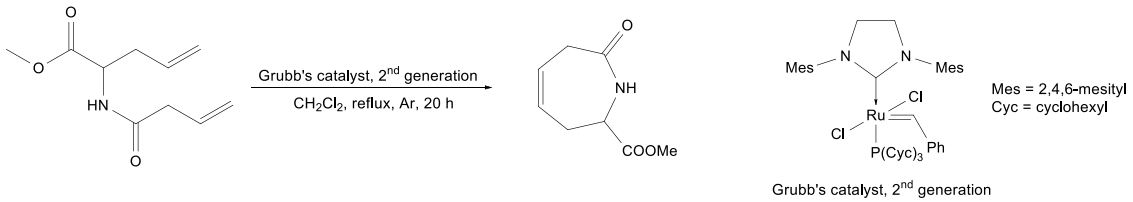

Fig. 1.23 The Grubbs catalysed ring closure metathesis only gave a product yield of 32% for the desired desaturated caprolactam methyl ester.

The obtained caprolactam would required adequate amide protection for further planned synthetic purposes. Because of the poor product yield for direct cyclisation, the desaturated peptide was Boc protected first (Fig. 1.24). The Boc protection was carried out using the same reaction conditions as for the Boc protection of the saturated caprolactam ester as previously described. The protected peptide was obtained in a good yield of 79%.

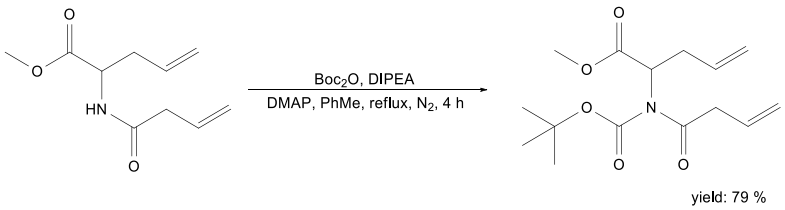

Fig. 1.24 Boc protection of this desaturated amide gave a good product yield of 79%. The additional Boc group was thought to potentially increase the product yield for the subsequent ring closure metathesis.

The so obtained Boc protected peptide was then cyclised using the same procedure as for the free peptide (Fig. 1.25). The obtained product yield remained comparatively low with 17%. Optimisation of the procedure led to an increased product yield of 35% for a protocol involving toluene as solvent and a reaction time of 6 days.

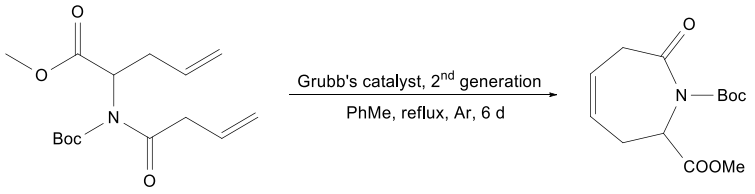

Fig. 1.25 Despite efforts to increase the product yield of the Boc protected desaturated caprolactam, the product could only be obtained with a yield of 35%.

The low yields for a number of reactions towards the envisaged 7,8-dioxo-6-azabicyclo[3.2.1]octane were considered a major obstacle towards application-relevant systems. The understanding of the underlying principles and the optimisation of these reactions therefore appeared paramount to the success of this project.

1.5) Dieckmann cyclisierung

The presented previous work had shown, that the formation of the 7,8-dioxo-6-azabicyclo[3.2.1]octane system could be achieved through the treatment of a suitable caprolactam ester with the strong base LiHMDS. This approach resembled modified procedures for Dieckmann condensations in the sense of an intramolecular ring closure between an enolate and an ester. General considerations of the Dieckmann cyclisation were therefore thought to give valuable insight into this crucial synthesis step.

Conceptually, the Dieckmann condensation is a special type of the wider family of Claisen condensation reactions. Whereas the Claisen condensation is generally the base-catalysed reaction of two esters to a β-keto ester, the Dieckmann condensation can be regarded as an intramolecular subtype, which gives cyclic β-ketonic esters[13]. A strict application of this technically excludes other ester derivatives such as amides or nitriles, but because such compounds may react through very similar mechanisms, their condensations are sometimes simply referred to as Dieckmann-type condensations.

To enable a Dieckmann condensation, a diester is deprotonated through the presence of a base (Fig. 1.26). Many classic applications of this condensation apply alkali metal alkoxides, directly added or formed *in situ* through the addition of elemental alkali metal and small amounts of the respective alcohol. However, such condensations are not exclusively limited to alkali metal alkoxides and many other bases have been shown to work similarly well or even outperform them. Often disregarded, studies have suggested, that if metal alkoxides are applied, it is the ion pair of M^+B^- that effectively reacts rather than the free base B^-[14].

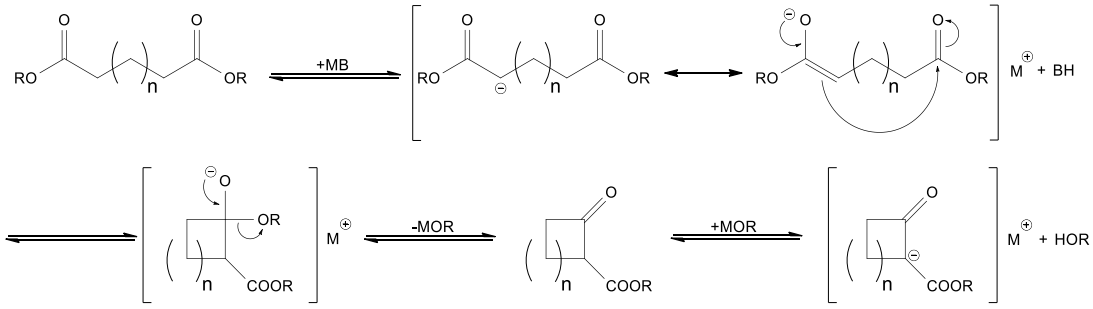

Fig. 1.26 The general mechanism of the Dieckmann condensation involves the deprotonation of a diester, the ring closure through nucleophilic, intramolecular substitution and the final elimination of an alkoxide to give β-keto esters.

Stabilised through a carbanion-enolate resonance, once deprotonation has occurred, the ring closure can proceed. Carrick and Fry have shown through ^{14}C isotope labelled experiments that the ring closure is the rate determining step[15]. The tetrahedral transition state formed will then eliminate an alkoxide residue to give a cyclic β-keto ester, which is the desired product and can often be obtained through simple aqueous work-up. Because of the increased acidity of the product and because the eliminated metal alkoxide is still present (if not somehow excluded from the equilibrium), the reaction's

equilibrium also contains the deprotonated carbanion-enolate of the cyclised β-keto ester. Each respective step of this equilibrium is reversible and can be shifted towards either the left or the right side of the equation through appropriately chosen reaction parameters. This has been demonstrated using *reverse Dieckmann condensations*[16], that if the respective eliminated alcohol is used as a solvent, drive the equilibrium can be driven towards alicyclic diesters instead of cyclic β-keto esters (Fig. 1.27).

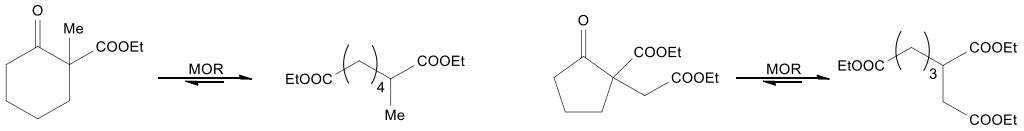

Fig. 1.27 The reverse Dieckmann condensation of cyclohexanones and cyclopentanones can be used to generate diesters with specific substitution patterns that may be prepared more easily through alternative means less conveniently.

Such reversed condensations are particularly useful if the cyclic starting material cannot undergo enolisation between its keto and ester group because enolates of β-keto esters are often comparatively stable under Dieckmann conditions. Drawn to its conclusion, this provides the concept that the enolisation of the completely reversible Dieckmann condensation is the driving force towards β-keto ester products.

Studies comparing the efficacy of ring closure experiments have shown that the Dieckmann condensation is best suited for the synthesis of five- and six-membered systems. Preparation of four-membered rings have also been shown, as well as seven- and eight-membered rings with moderate yields. When approaching larger systems, the formation of dimeric products becomes more likely, which is why larger rings such as nine-, ten- or eleven-membered rings may not be easily accessible, but even larger diketones can be prepared through Dieckmann conditions[17]. It is furthermore possible to apply the Dieckmann condensation to obtain bicyclic scaffolds, both bridged[18] and annulated[19] (Fig. 1.28).

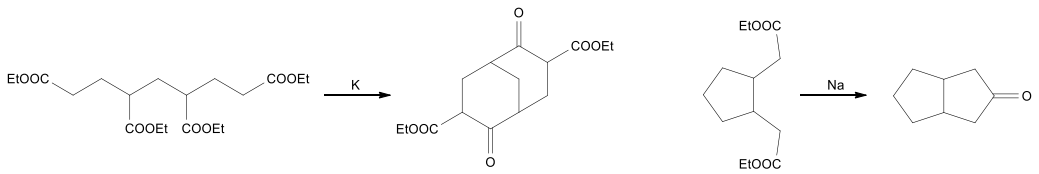

Fig. 1.28 The Dieckmann condensation is not exclusively limited to the preparation of monocyclic structures. In fact, many polycyclic systems can be prepared using Dieckmann conditions, if the starting material allows for such.

Dieckmann condensations are relatively straightforward reactions if symmetrical starting materials are being used. However, in asymmetric cases, a number of conditions have been identified to allow a certain level of control over the reaction outcome. Generally, starting materials that contain more than two ester groups will preferably give the product with the most stable cyclised enolate, as this appears to be the driving force towards possible products. However, in cases in which the enolates are

comparatively similar, other parameters may help to suppress side product formation. One such parameter is temperature, which is adequately demonstrated by Woodward and Eastman[20]. They describe that methyl 3-[(2-methoxy-2-oxoethyl)thio]propionate can either lead to 2- or 4-carbomethoxy-3-thiophanone, depending on whether the reaction is performed in refluxing diethyl ether or toluene (Fig. 1.29).

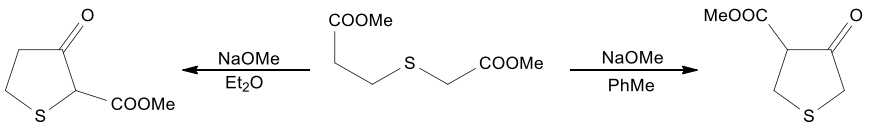

Fig. 1.29 Dieckmann condensations can be controlled to preferrably give one product, if several are possible. In the case of 3-[(2-methoxy-2-oxoethyl)thio]propionate, temperature can be used as the determining parameter for the formation of one main product.

However, it should also be noted that a change in solvent affects the solvation of all involved species as well. The importance of solvation effects may be linked to another parameter which should be considered, which is the nature and influence of the counter ion, especially in cases in which alkali metal alkoxides are involved. The cyclisation of ethyl 3-carbethoxypiperidino-1-acetate is only successful if potassium ethoxide is used, the equivalent sodium salt does not give the bicyclic product[21] (Fig. 1.30).

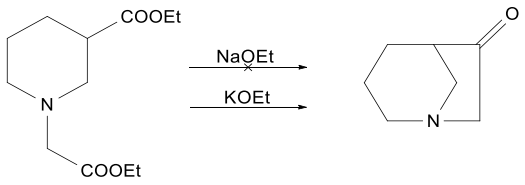

Fig. 1.30 Ethyl 3-carbethoxypiperidino-1-acetate is only cyclised successfully, if a potassium alkoxide is applied, the respective sodium salt does not lead to the bicyclic product.

Studies regarding the influence of the respective ester residue used have shown a correlation to some extent between the size of the ester and the product yield obtained. When symmetrical adipic acid esters are used, the comparison of the obtained product yields with 81% for methyl, 61% for *iso*-butyl and 57% for benzyl groups would suggest such a correlation[22]. However, the respective phenyl ester does not undergo Dieckmann condensations, suggesting that the quality of the leaving group as such is less influential as one may think.

One last factor to be considered, which might be more difficult to control is the conformational situation in the resulting tetrahedral transition states. Dutta and Biswas[23] have suggested such considerations following observations on cyclisation experiments of 2-methyl-1,2,5-tricarbethoxypentane. Theoretically, these experiments should have given a mixture of cyclopentanones and cyclohexanones. However, several studies[24] have reported, that only cyclopentanones were found (Fig. 1.31).

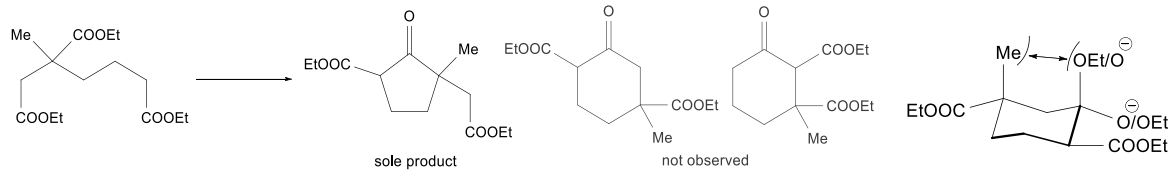

Fig. 1.31 The Dieckmann condensation of 2-methyl-1,2,5-tricarbethoxypentane only leads to the displayed cyclopentanone, not to cyclohexanones. The suggested reason can be found in the tetrahedral transition state.

It was suggested, that the 1,3-diaxial steric repulsion of a methyl group and an $-O^-$ / -OEt group in the transition state of the theoretical six membered cyclic products disfavours their formation. Considering that the Dieckmann condensation is thought to be completely reversible and seems to be driven by a thermodynamical preference, the conformational behaviour of such transition states of densely substituted starting material seems of significant importance.

1.6) Conformational behaviour of seven-membered cyclic systems

Previous work, the fact that conformational considerations for Dieckmann condensations are of importance and the envisaged use of a Dieckmann-type cyclisation for this project lead to the study of conformation behaviour of seven-membered cyclic systems. The second ring closure to a bicyclic system appeared to be the major synthetic challenge during the works of this project. Because this synthetic approach had not been undertaken before, it was considered of particular importance to understand the physicochemical behaviour of caprolactams in general. As the mechanistic considerations of the Dieckmann condensation have shown, the ring closure reaction of such condensations and related reactions is thought to be the rate determining step. Because the ring closure in the herein described caprolactam system appeared to be linked to the position of a functional group, an understanding of the general conformative behaviour of caprolactams became of interest.

Unfortunately, the physicochemical behaviour of caprolactams has generally been less intensely studied than the early discovery of ε-caprolactam and its large-scale industrial use would suggest. The much more widely studied cycloheptenes shall therefore act as a model system.

Amide bonds are often displayed as single bonds, but show certain properties usually associated with double bonds. This partial double bond character does not allow free rotation along the C-N bond and greatly restricts the angles, substituents on both sides of the amide group can adopt. In terms of lactams, this directly impacts the possible conformations, the overall ring can be found in. Comparison of caprolactams with their carbon counterparts cycloheptanes is therefore not sensible. However, it is possible to draw similarities with the monounsaturated cycloalkene cycloheptene. A perhaps more abstract concept is to regard the entire amide bond as one (arguably very large) atom within the ring. When the size of this hypothetical atom is disregarded, the conformational behaviour of such a ring

could also be approximated with cyclohexanes. Since cyclohexanes have been studied more extensively than cycloheptenes, their behaviour was considered as well.

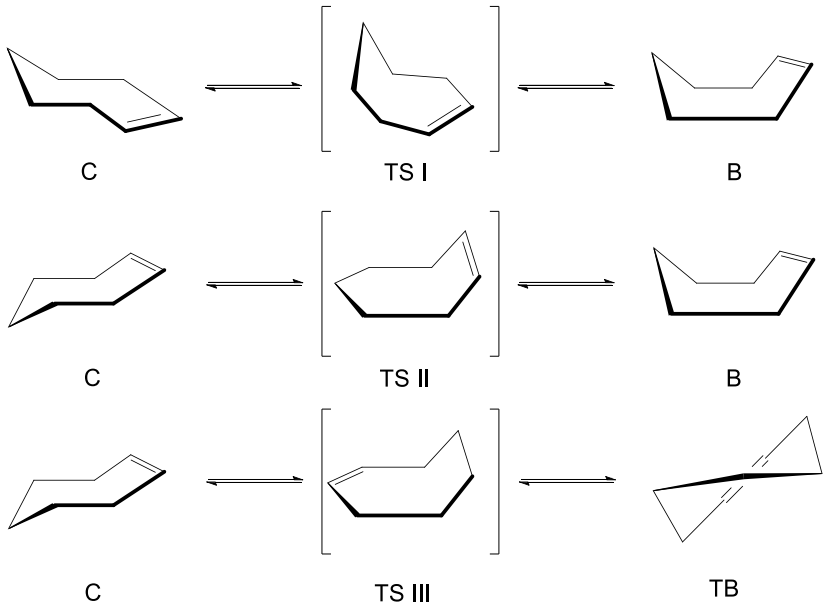

Fig. 1.31 The different conformations of cycloheptene. The chair conformation can undergo three different transitions states towards two different boat or a twisted boat conformation.

Cycloheptenes are known to adopt several different conformations, among them the (pseudo)chair, boat and a transitionary form, the twisted boat (Fig. 1.32). Under normal conditions, such as room temperature and atmospheric pressure, all of these conformations can be found in an equilibrium in which they interchange rapidly. One distinct difference between these conformations is their overall energy. Some of these conformations force their carbon atoms in unfavourable angles causing additional ring strain and are therefore disfavoured, others avoid this increase and are energetically slightly lower.

The general conformative arrangements of cyclic systems is also influenced by the position of any attached substituents. Like in cyclohexanes, substituents can adopt either axial or equatorial positions to the caprolactam ring. Just like any other system, the entire caprolactam ring will try and adopt the thermodynamically most stable and therefore energetically lowest form. Depending on how large the energetic difference between two conformations is, the more the overall equilibrium tends to shift towards one conformation in particular. The nature of a substituent, especially its size, will largely determine which conformative arrangement the ring will prefer and therefore which position is preferably found.

1.7) Conformation of the base caprolactam

As for most caprolactams, N_α-substituted caprolactams have been shown to prefer chair conformations in solution. A computational study conducted by *Gruber et. al.* has shown, that for a caprolactam with a -COOMe group in C6-position, the energy barrier between the two possible chair conformations, the $^{4}C_{1,N}$ with the respective ester group in axial position, and the $^{1,N}C_{4}$ conformation with an equatorially positioned ester, is 8 kcal · mol^{-1} as shown in Fig. 1.32[25]. Such a C6-substituted caprolactam can easily overcome this energy barrier at room temperature and both conformations can be found in solution with a ratio of roughly 1:1.

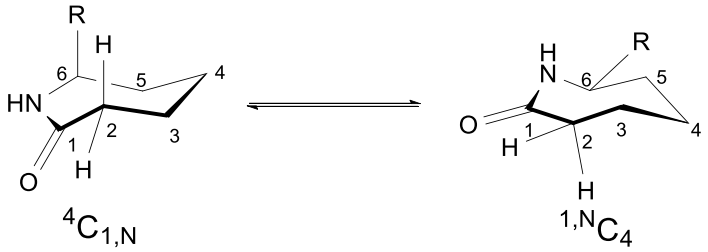

Fig. 1.32 The two chair conformation of caprolactam. The $^{4}C_{1,N}$ carries an N_α-substituent in an axial position, the $^{1,N}C_{4}$ conformation will show an equatorial position for the same substituent.

However, this study has also shown, that the introduction of a second substituent at the lactam nitrogen can change the conformational situation significantly. The authors reported the introduction of a Boc protection group at the nitrogen and discussed the results of NOE-NMR-experiments to draw conclusion about the conformational differences between the mono- and disubstituted caprolactam (Fig. 1.33). The authors argued that the sterical clash of the Boc protection group and the methyl ester in C6 position leads to a shift in the conformational equilibrium towards a more favoured axially positioned ester group. In fact, the authors reported a ratio of 70:30 in favour of the axial conformer at room temperature, but that both conformers still exchanged dynamically.

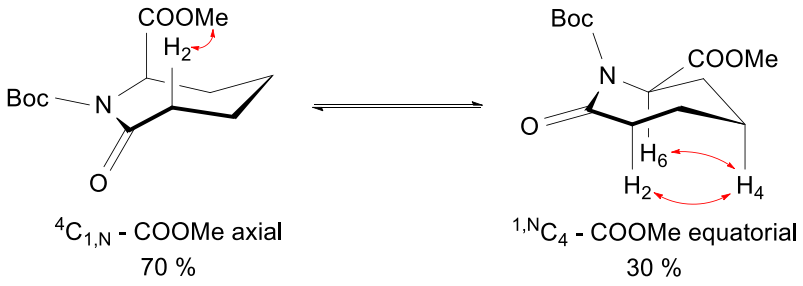

Fig. 1.33 The detection of specific transannular NOE effects revealed that in the case of a Boc protected caprolactam methyl ester, the ester group will prefer the axial position with a distribution of 70:30 to the equatorial.

1.8) Impact of solvent on reaction - The aggregation/dissociation behaviour of LiHMDS

During the first stages of this project, it became apparent that the understanding of the base-induced Dieckmann-type ring closure could be vital to the development of a convenient synthetic protocol. As the mechanistic considerations of Dieckmann condensations have shown, the influence of the applied base can change the reaction outcome entirely. Therefore, implementing concepts of organometallic chemistry such as solvation, aggregation/dissociation or coordination/chelation could offer invaluable mechanistic insight. The following descriptions are therefore dedicated to such phenomena, particularly tailored to the perhaps most prominent reagent *lithium hexamethyldisilazide* (LiHMDS) in this project. It should be mentioned that LiHMDS is per definition not an organometallic compound, but many aspects of organometallic chemistry apply to it and this clear-cut distinction shall be omitted for the sake of clarity.

One of the arguably most important concepts that has found general acceptance in the scientific community is that reactions of organometallic reagents will occur through monomeric[26], rarely also through dimeric[27] species. However, many organometallic compounds show extensive aggregation behaviour in solution. LiHMDS for example has been found to form tetrameric, dimeric and monomeric species, depending on a number of factors. A simplified explanation as to why monomers are thought to be the reactive species in most reactions can be found in crystals structures of LiHMDS species. Within the monomer, the nitrogen is comparatively open, whereas the nitrogen centres appear fully crowded in a LiHMDS dimer (Fig. 1.34).

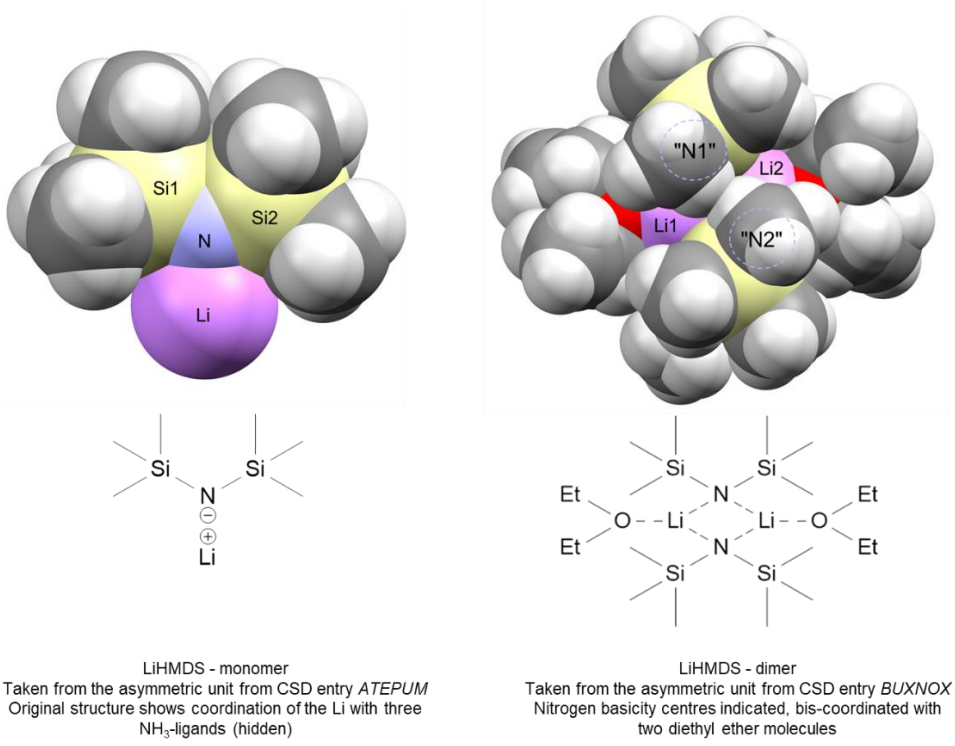

LiHMDS - monomer
Taken from the asymmetric unit from CSD entry *ATEPUM*
Original structure shows coordination of the Li with three NH_3-ligands (hidden)

LiHMDS - dimer
Taken from the asymmetric unit from CSD entry *BUXNOX*
Nitrogen basicity centres indicated, bis-coordinated with two diethyl ether molecules

Fig. 1.34 The comparison of crystal structures of LiHMDS species shows that the nitrogen is somewhat free in a monomer, but almost entirely crowded in a dimeric species.

The aggregation tendencies for LiHMDS often align with the tendencies of organolithium compounds. Generally, hydrocarbon solvents lead to higher aggregate numbers, strong ligands cause deaggregation. The two often used examples for organolithium compounds for these tendencies are pentane/hexane and THF/Et_2O solutions. Kimura and Brown have shown that this is true for LiHMDS which prefers mixtures of tetramers and dimers in hydrocarbon solvents and forms dimers and monomers in THF and most other ethers. Somewhat special are toluene and benzene, in which LiHMDS forms predominantly dimers (Fig. 1.35).

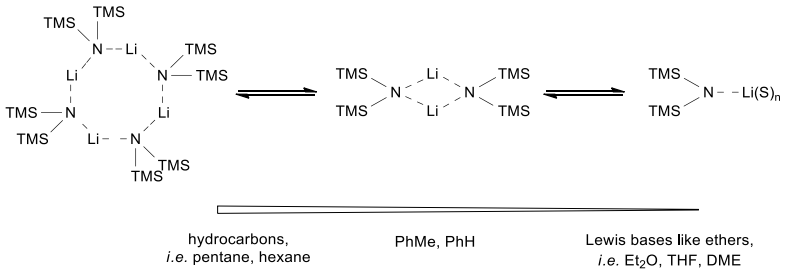

Fig. 1.35 The general trend for aggregation of LiHMDS is highly dependent on the solvent provided. As a rule of thumb, the less polar the solvent, the higher the overall aggregation.

The underlying reason for such aggregation is generally accepted to stem from the need of cations to adopt higher, rather than lower coordination. For effective coordination and therefore for a molecule to act as a ligand, there needs to be interaction between the cation and free electron pairs. Because fully saturated hydrocarbons cannot donate any free electron pairs, LiHMDS aggregates, which in turns covers lithium's coordination sphere as much as steric interference allows. For aromatic solvents, like toluene and benzene, the aromatic π electron system allows coordination to some extent, which stabilises dimers sufficiently[28]. Etheral solvents on the other hand contain oxygen atoms with free electron pairs, which are capable of coordination to cations quite well. The result is the formation of solvated monomers, which usually become the dominating species in strongly coordinating solvents like (tetrahydrofuran) THF or solvents with multiple coordination sites like dimethoxyethane (DME). An extreme example of how aggregation can affect the reactivity of reagents is the comparison of methyllithium with phenyllithium. Whereas methyllithium should be a far stronger base than phenyllithium, its tendency to form far more extensive aggregation makes methyllithium an inferior base for most applications.

As mentioned, it is generally accepted that monomers are the reactive species in most cases. Forcing dissociation into lower aggregates and even monomers can therefore impact the reactivity of organometallic reagents profoundly. A common method to force monomer formation is the addition of stochiometric amounts of chelating agents. The arguably most prominent chelators are polydentate ligands like polyamines or polyethers.

However, studies have shown that the use of such chelators offers far more structural diversity than simple formation of monomers species. For example, 2:1, 1:1 and 1:2 LiHMDS-DME complexes have been observed in solution, which most likely offer finely tuned differences in reactivity (Fig. 1.36).

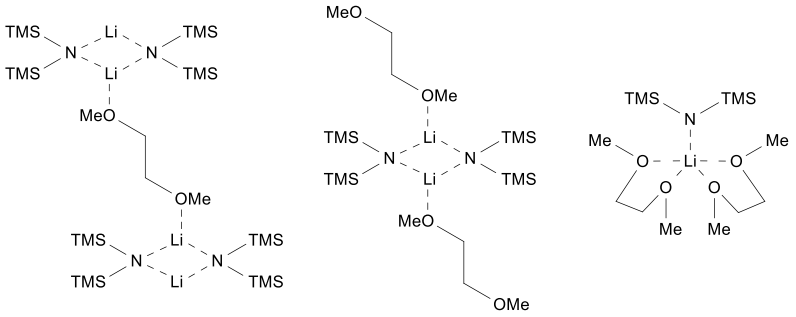

Fig. 1.36 The addition of DME to LiHMDS in hydrocarbon solutions has been found to lead to structurally diverse species, such as differently stabilised dimers or highly coordinated monomers.

For LiHMDS, the use of chelators to force monomer formation is not necessary if THF can be used as a solvent because monomeric species are the almost exclusive species in THF solutions. Nevertheless, the use of chelators does not only offer fine tuning on LiHMDS reactivity, but research into the chelation behaviour has given some insight into how lithium is chelated. Klump[29] and Reich[30] individually reported that chelated lithium species show preferences in their respective ring size. They found that five-membered rings are strongly preferred over six-membered rings; chelation does not afford four or seven-membered rings. These findings are not solely of academic interest because the metal counter ion is often chelated by intermediate states in organic reactions. However, the spectrum of LiHMDS-aggregation and coordination behaviour becomes even more complex in applied reaction systems. In a recent study, Collum and co-workers have described the deprotonation of a cyclic carbamate with LiHMDS (Fig. 1.37)[32,33].

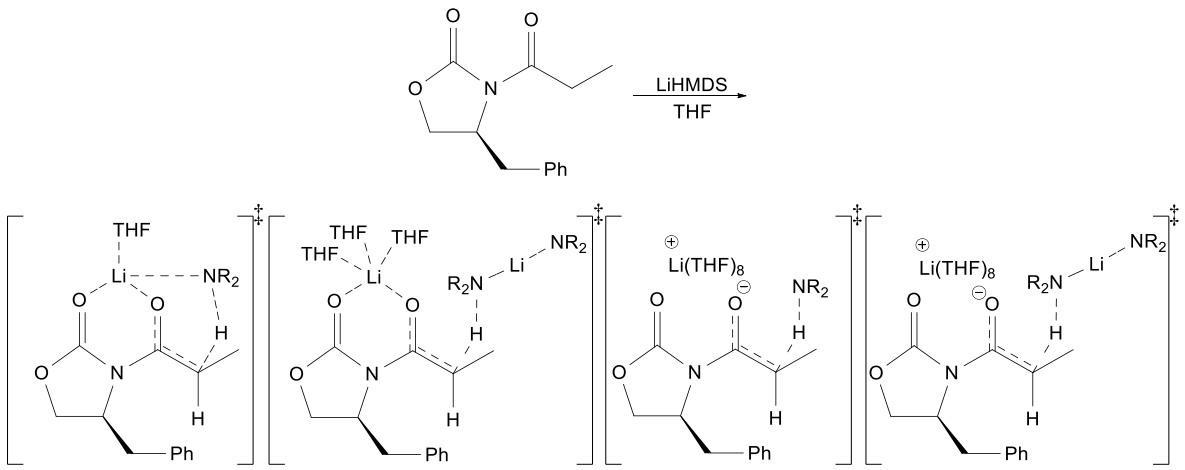

Fig. 1.37 The deprotonation of the displayed cyclic carbamate with LiHMDS will allow several complex species to be formed. As shown, lithium can be stabilised through enolates, through solvent spheres or through combinations of both.

This exemplifies that correct predictions of coordination behaviour in applied systems remains elusive. However, the synthetic utility of a single reagent like LiHMDS can also be tailored to each respective case and may lead to very different outcomes. For example, Beak and co-workers have shown that the solvent of a reaction can lead to not only different yields, but also to different enantiomeric excesses in asymmetric processes[31] (Fig. 1.38).

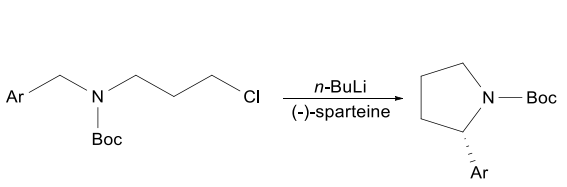

solvent	yield	ee
THF	58%	3%
^{t}BuOMe	64%	58%
Et_2O	59%	64%
Et_2O:*n*-pentane (1:1)	40%	70%
n-pentane	54%	80%
toluene	72%	96%

Fig. 1.38 The use of different solvents for this intramolecular cyclisation through n-BuLi can give very different product yields. It also shows that the solvents on either side of the aggregation spectrum may not necessarily be optimal.

It also shows, that addition of co-solvents that lower aggregation does not necessarily lead to increased synthetic efficacy. However, this in fact means that each respective synthetic process might have to go through solvent-dependent optimisation.

Other factors that should be considered are the reaction temperature[32], the addition of co-solvents and the respective ratio[33]. One more parameter that has not been discussed herein is the difference, the counter ion can make to a base. The chemistry of alkali metals in organometallic compounds and related reactions can be found to be radically different. However, changing from lithium based reagents to sodium and/or potassium can also allow delicate fine-tuning of reactions. During the synthesis of the following hydantoin derivative, chemists at Hoffmann-La Roche have found that the use of NaHMDS or KHMDS can shift stereospecific product outcome (Fig. 1.39).

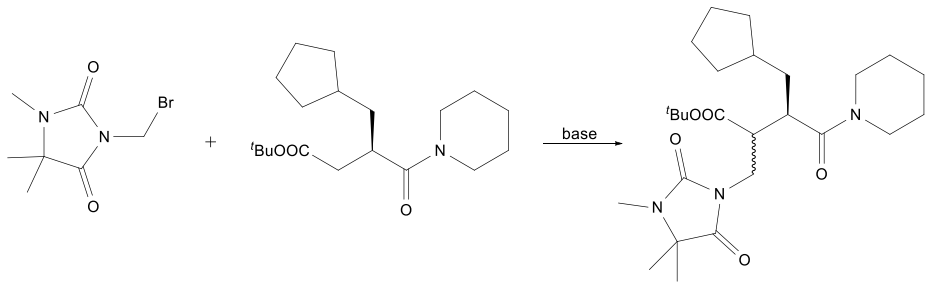

base	temp	anti/syn
LDA	-78 °C	15 : 85
NaHMDS	-78 °C	50 : 50
KHMDS	-78 °C	80 : 20
KHMDS	-60 °C	92 : 8
KHMDS	-40 °C	99 : 1

Fig. 1.39 The difference, the counterion can make, allowed for Hoffmann-La Roche chemists to achieve a 99:1 ratio of anti to syn product for a regiospecific deprotonation.

As much as these results seem unpredictable, it becomes apparent that a selection of different solvents during optimisation cycles can be a powerful tool to drive a reaction towards a preferred outcome.

1.9) Protection group chemistry

During the synthetic work of this project towards the 7,8-dioxo-6-azabicyclo[3.2.1]system through a Dieckmann-type condensation, an adequate protection group had to be introduced on the lactam nitrogen. However, as already pointed out, the Boc protection group not only protected the nitrogen, but also influenced the conformational situation fundamentally. Especially within the later synthetic stages, it also became apparent, that this group's chemistry in this azabicyclooctane system was less trivial than anticipated. Therefore, the following descriptions are dedicated to the chemistry of protection groups, the Boc group in particular.

Nitrogen is one of the most common heteroelements found in organic chemistry alongside oxygen. Organic chemists have examined its behaviour when embedded into a large number of different functionalities and developed a diverse array of strategies to manipulate nitrogen to their advantage. The necessity for these diverse strategies becomes apparent when organic chemistry is applied to biological systems. An enormous spectrum of biologically interesting compounds contain nitrogen, from amino acids to peptides, alkaloids, nucleosides and many others. Because of the plethora of different nitrogen containing functionalities and their interference with each other and other reactive functionalities makes the synthetic distinction between them invaluable. One possibility to distinguish competition between functional groups is the introduction of protection groups. With more than 350 reported protection groups[34] and strategies, a wide range of different procedures are available. Only a selected few *N*-protection groups shall be discussed under the aspects of their formation, susceptibility towards certain conditions and their cleavage.

The protection of nitrogen through the formation of respective carbamates is a comparatively common step in many multistep synthesis approaches. A number of different individual groups have been developed to satisfy a variety of requirements on their ability to withstand different conditions. Some of the more prominent groups, that found utilisation in this project, are the *tert*-butyloxycarbonyl (Boc), the benzyloxycarbonyl (Cbz) and the benzyl (Bn) group.

<u>*tert*-Butyloxycarbonyl - Boc</u>

The introduction of Boc-protection groups is most commonly performed using di-*tert*-butyl dicarbonate (also known as Boc_2O, or Boc-anhydride)[35] or 2-(*tert*-butyloxycarbonyloxyimino)-2-phenylacetonitrile (Boc-ON)[36]. Both reagents are easy to handle as they are crystalline solids at room temperature. Boc_2O has the additional advantage, that its melting point of 22-24 °C is so close to room temperature, that it can easily be molten and transferred as a liquid.

The protection of a nitrogen atom with Boc_2O often relies on a nucleophilic substitution reaction. The nucleophilic nitrogen is made to attack the susceptible carbonate carbonyl to give a carbamate, CO_2 and ^tBuOH as by-products (Fig. 1.40).

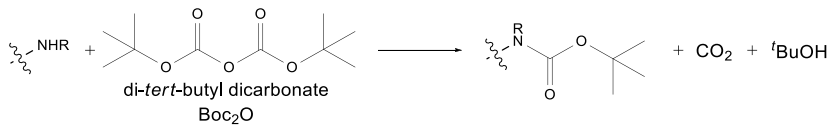

Fig. 1.40 The general Boc protection of nitrogen atoms involves a nucleophilic substitution. In case of Boc_2O, the main products are the Boc protected carbamate, CO_2 and ^tBuOH.

However, the susceptibility of Boc_2O to nucleophilic attack essentially means, that any other nucleophile could enter a competing reaction. Many procedures using Boc_2O will therefore tend to avoid humidity and the introduction of other nucleophiles. Amines often exhibit enough nucleophilicity to react on their own, for some it is necessary to introduce an additional non-nucleophilic base like Et_3N or *Hünig's base* (*N*,*N*-diisopropylethylamine or DIPEA). Amides on the other hand generally exhibit much less nucleophilicity and are not as readily Boc protected as amines[37,38,39]. One possibility to overcome the decreased nucleophilic character of amide nitrogen, is the addition of *Steglich's reagent* (4-(dimethylamino) pyridine or DMAP) to a reaction mixture. DMAP can act as a catalyst in these procedures by forming an activated pyridinium carbamate which is much more prone to nucleophilic attack by amides. Typical solvents for these protection reactions are often aprotic and include toluene, dichloromethane, or acetonitrile.

Once the Boc protection has been performed successfully, carbamates of this type are generally considered stable against even extremely basic and nucleophilic conditions. They are so stable, that even superbases, such as butyllithium reagents, can be applied. Boc protected pyrrolidine for example can be lithiated directly with *s*-BuLi in good yields (Fig. 1.41).

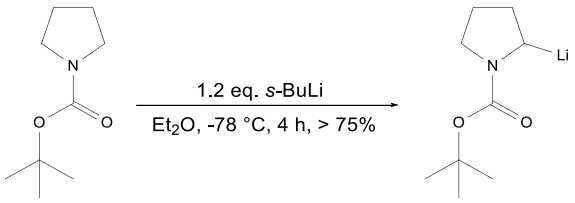

Fig. 1.41 Boc protected pyrrolidine can be conveniently lithiated using s-BuLi in Et_2O.

However, it is worth mentioning, that Boc protecting groups have also been reported to take part in intramolecular side reactions. Agami and Couty published a comprehensive review on a large number of different scenarios in which Boc carbamate groups are found to be the reactive functionality[40]. In the same sense, this carbamate is also generally thought to be stable against catalytic hydrogenolysis, but exceptions from this have been reported as well.

As much as the Boc protection group is used for reactions involving basic/nucleophilic conditions, it is very sensitive to acidic conditions. However, this can be conveniently used as a deprotection strategy for such carbamates. Many different approaches have been described, for example using trifluoroacetic acid (neat[41] or in solution[42]), HCl (as aqueous solution or in organic solvents like ethyl acetate[43]) or formic acid[44].

Acidic deprotection is believed to involve the protonation of the carbamate carbonyl, followed by the formation of a *tert*-butyl carbocation and a carbamic acid. The carbamic acid should then simply decarboxylate to give the free amine/amide.

A different approach is the use trialkylsilyl triflates for deprotection. For example, Sakaitani and Ohfune have described a procedure in which the combination of trimethylsilyl triflate (TMSOTf) and 2,6-lutidine in dichloromethane at room temperature led to quantitative product yields[45] (Fig. 1.42).

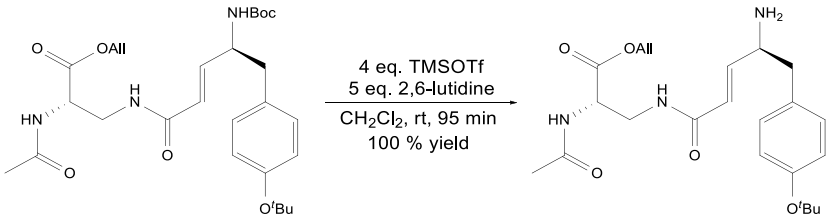

Fig. 1.42 The use of the oxophilic Lewis acid trimethylsilyl triflate (TMSOTf) in the presence of 2,6-lutidine allowed for quantitative deprotection of a Boc protection group, leaving other similar functionalities unscathed.

However, it has also been reported that the use of TMSOTf can lead to unwanted side reactions with a number of other protection groups[46,47,48]. A more selective approach involves the use of *tert*-butyldimethylsilyl triflate (TBDMSOTf) under very similar conditions[45].

Reactivity of Boc protection groups

The Boc protection group is considered one of the most useful nitrogen protection groups and is further considered to be highly stable against nucleophilic/basic conditions. However, a large number of experiments have shown, that this reluctance to engage in nucleophilic substitutions is not always given for intramolecular, nucleophilic centres. An early example under arguably harsh conditions was described by Stanetty *et. al.*[49]. They found that *N*-Boc protected aniline can undergo nucleophilic substitution in the presence of *n*-butyllithium under for this reagent rather uncommon conditions of 2.5 °C over a period of 45.5 h (Fig. 1.43).

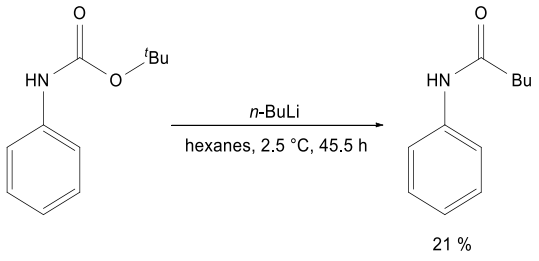

Fig. 1.43 Harsh conditions such as n-BuLi in hexanes at 2.5 °C can lead to the nucleophilic substitution of a Boc carbamate with a butyl carbanion.

Such a nucleophilic substitution might appear to be a result of the comparatively high temperature and long reaction time for a strong base and nucleophile such as *n*-BuLi. That this is not an isolated incident can be exemplified by an intramolecular ring formation, described by Beak and Lee[50]. They describe the formation of an oxazolidinone side product, associated to a diastereoselective substitution (Fig. 1.45)

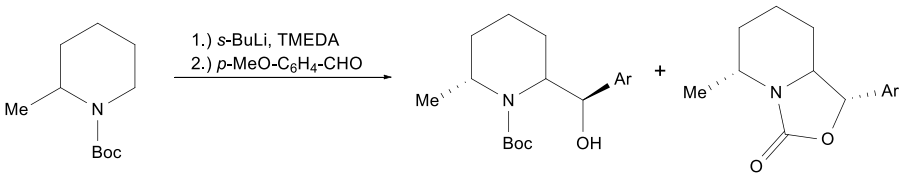

Fig. 1.44 The lithiation and subsequent introduction of a benzaldehyde can result in an intramolecular ring closure of the newly formed benzyloxide group with the Boc carbamate. However, this was only observed for the syn isomers.

They found that instead of a mixture of *syn* and *anti* isomers, the *syn* isomers undergo intramolecular cyclisation between an *in situ* formed hydroxyl group and the Boc carbonyl, resulting in a bicyclic carbamate. Such intramolecular cyclisations are also not exclusive to the use of organolithium compounds. During the synthesis of a marine alkaloid, Overman *et. al.* utilised a targeted intramolecular ring closure reaction between a free hydroxyl group and an *N*-Boc protection[51] (Fig. 1.45).

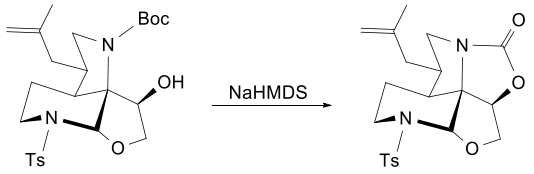

Fig. 1.45 In the total synthesis of a polycyclic natural product, the intramolecular attack of a deprotonated hydroxyl group on a Boc carbamate was used to form a desired cyclic carbamate group.

The already mentioned examples share the use of considerably strong bases. However, even less powerful bases such as K_2CO_3 in DMF can lead to such cyclisations, as shown by Rodes *et. al.*[52] and Burrows *et. al.*[53]. In these respective studies, it was found that *N*-Boc-*N'*-Bn protected *o*-phenylenediamines can undergo ring closure, to give ureas (Fig. 1.46). A different explanation on the occurrence of ureas through base-catalysed ring closure was given by Lamothe and coworkers[54]. They suggested the intermediary formation of isocyanates as a result of a rearrangement of Boc protected primary amines.

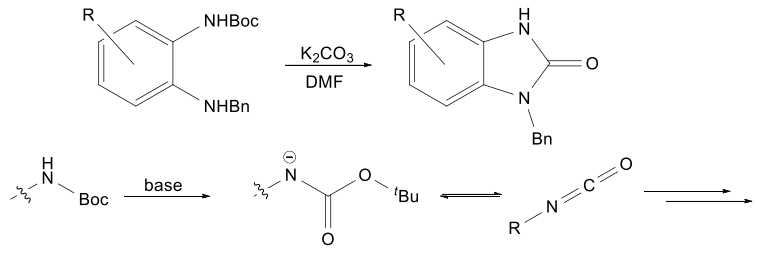

Fig. 1.46 The engagement of Boc carbamates in an intramolecular urea formation was observed when an asymmetrically diprotected o-phenylenediamine was treated with K_2CO_3. It was later suggested that the in-situ formation of an isocyanate is responsible, rather than nucleophilic substitution.

Gosh and Miller have demonstrated that such urea formations can also be used as a main synthetic approach towards hydantoins[55]. Their original experiments aimed at the introduction of a second Boc protection group on an amide, containing an *N*-Boc protected amine group. Optimisation of this procedure lead to a protocol only using Boc_2O and a catalytic amount of DMAP to conveniently form a hydantoin without the need for a base (Fig. 1.47).

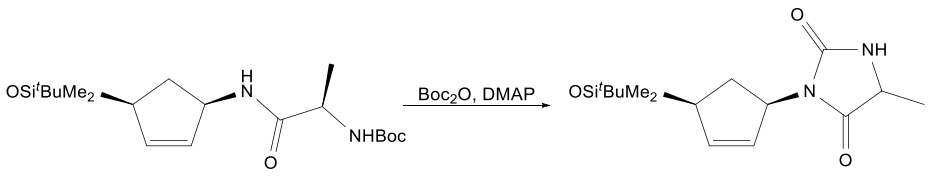

Fig. 1.47 The formation of carbamate/urea groups can be triggered through the addition of Boc_2O and DMAP without a base being present.

The previously presented reports have in common, that the Boc group engaged in intramolecular reactions with subsequent elimination of O^{t}Bu groups. Davies *et. al.* on the other hand have reported the migration of the Boc group, from a nitrogen atom to an *in situ* generated free hydroxylate (Fig. 1.49). However, it seems safe to assume, that such migrations are comparatively uncommon and most likely substrate specific.

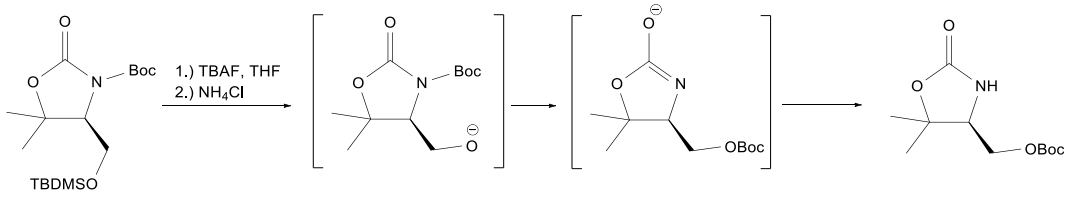

Fig. 1.48 The rearrangement of an N-Boc to and O-Boc group, described by Davies et. al. was triggered by the deprotection of an O-TBDMS group.

Benzyloxycarbonyl (Cbz)

The Cbz group resembles the Boc group in that it will form carbamates through nucleophilic attack of a nitrogen that is to be protected. This protection group is usually introduced using benzyl chloroformate (CbzCl). Alternative reagents, such as the corresponding dibenzyl dicarbonate are commercially available, but much more expensive and may only find use if CbzCl is not an option.

What sets the Cbz group apart from the Boc group, is its susceptibility to hydrogenolytic conditions. Cbz groups can be cleft under comparatively mild conditions using palladium on charcoal and hydrogen gas (Fig. 1.49).

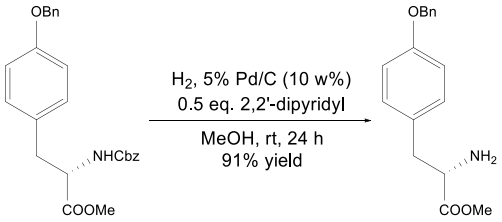

Fig. 1.49 The hydrogenolytic cleavage of a Cbz group can often be performed in the presence of other functional groups. In the here presented case, both a phenolic benzyloxy and a methyl ester group remain intact.

It is possible, to deprotect Cbz groups using acidic conditions, as well. However, the right choice of acidic reagents allows the orthogonal deprotection of Boc groups, whilst Cbz remains unscathed and *vice versa*. For example, 4M HCl in 1,4-dioxane conveniently deprotects Boc group, Cbz remains intact[56].

Benzyl (Bn)

In contrast to the Boc and Cbz protection group, benzyl protection introduces an alkyl group, rather than a carbamate. *N*-benzyl protected amines or amides can often be prepared under comparatively mild conditions using benzyl bromide and a base (Fig. 1.50). It is also possible to introduce the benzyl group indirectly to a nitrogen, by forming imines from free amines and subsequent reduction to accomplish the protection. Because of the efficacy of the former and the limitation of the latter to amines (amides cannot be introduced as easily), this group promises only little satisfaction for lactam chemistry.

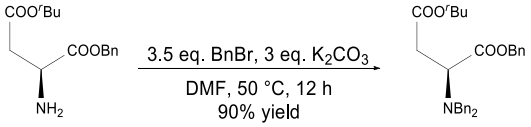

Fig. 1.50 The introduction of two benzyl groups on the same nitrogen can be performed using benzyl bromide in the presence of K_2CO_3 in DMF at relatively mild conditions.

However, the Benzyl group does offer distinct properties, that both the Boc and Cbz group may not fulfill. As an alkyl group, the electron donating effect stands in contrast to the previously mentioned carbamate groups. The methylene group, to which the nitrogen is bound also allows rotational freedom which the carbonyl group containing protection groups do not (Fig. 1.51).

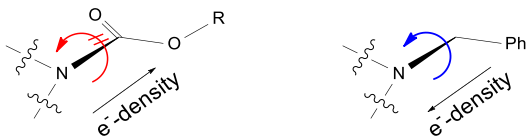

Fig. 1.51 The carbamate protection will withdraw electron density from the protected nitrogen, benzyl groups will donate. Additionally, the carbamate groups do not allow free rotation along their C-N bond, whereas benzyl groups can do so.

The deprotection of benzyl groups is generally possible through catalytic hydrogenation, just as the Cbz group. However, the conditions required are thought to be substrate specific and optimisation may be required to achieve synthetically useful yields. Another factor to consider is that examples have shown, that the catalytic hydrogenolysis of Bn groups can be performed whilst retaining stereocentres. A stereoselective synthesis, described by Davies and Ichihara, reports the catalytic deprotection of a double alkylated amine[57]. The treatment with 5% $Pd(OH)_2/C$ only deprotected the benzyl group, not the closely related phenylethyl group. The second deprotection required heavier catalytic loading with 20% $Pd(OH)_2/C$ and 3 atm of hydrogen (Fig. 1.52).

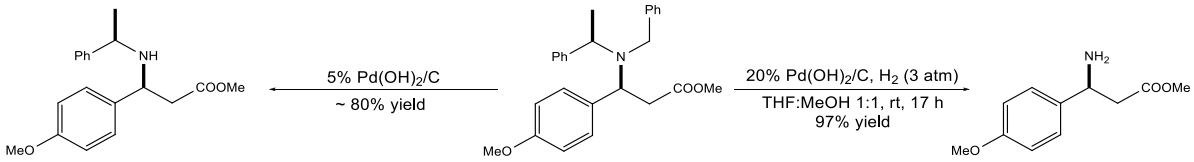

Fig. 1.52 The hydrogenolytic deprotection of benzyl and the closely related phenylethyl group can be performed whilst retaining stereocenters.

It was argued, that the difference in reaction speed is caused by the substrate's ability to align the π-system of adjacent aromatic rings to the catalyst. The phenyl group, being less hindered, would therefore react much easier. An alternative to hydrogenolysis is the use of elemental sodium in cooled liquified ammonia. This method has been reported several times to even tolerate β-lactam rings[58] (Fig. 1.53).

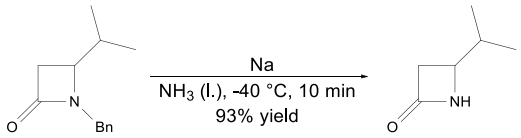

Fig. 1.53 The deprotection of a benzyl protected β-lactam ring can be done using elemental sodium in liquified ammonia. Considering the comparatively harsh conditions, the excellent yield of 93% speaks for the synthetic utility of such procedures, if the substrate can tolerate it.

1.10) Schmidt reaction

The Schmidt reaction, sometimes also referred to as the Schmidt rearrangement, is a reaction between a group of carbonyl compounds, such as carboxylic acids, aldehydes and ketones, with hydrazoic acid (HN_3) in the presence of strong acids[59] (Fig. 1.54).

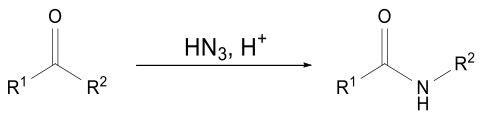

Fig. 1.54 The Schmidt reaction of a ketone with hydrazoic acid under acidic conditions will generally lead to amides. In case of cyclic ketones, lactams are obtained.

During the reaction, a nitrogen atom is inserted into a C-C bond which results in amines (for carboxylic acids), or amides (for aldehydes and ketones)[60]. A large number of different possible substrates, reagents and conditions led the Schmidt reaction to become a generalised family of related reactions. Despite this reaction being first described in 1923 by Schmidt himself, the mechanism for Schmidt reactions involving ketones is still not fully settled for the scientific community. Two possible mechanistic pathways have been proposed: a concerted mechanism[61] and a stepwise mechanism[62] (Fig. 1.55).

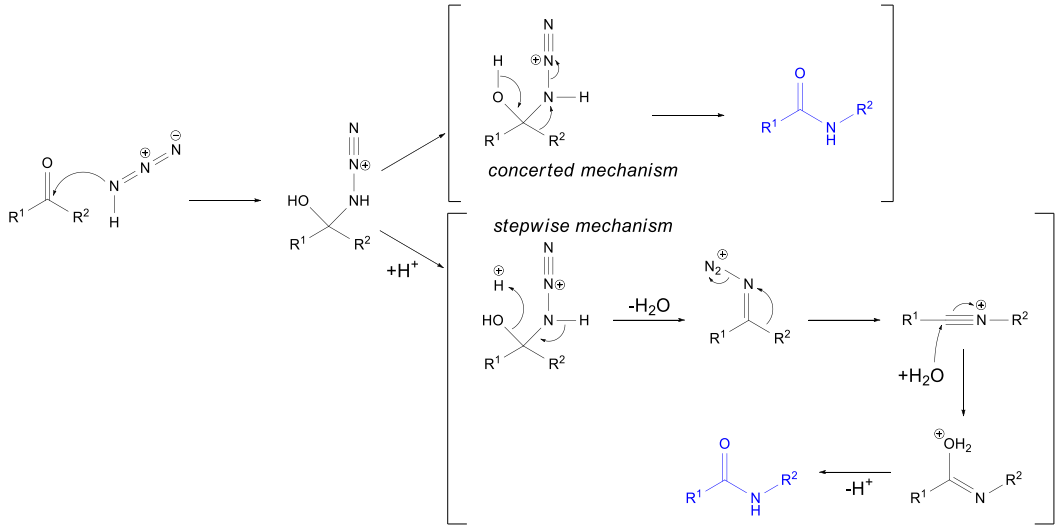

Fig. 1.55 The insertion of a nitrogen atom into a C-C bond during the Schmidt reaction has been discussed through two different mechanism, here exemplified for a ketone.

What both mechanisms have in common is the initial reaction of hydrazoic acid with a carbonyl carbon. The result, a triaz-1-yn-2-ium ion, structurally similar to cyanohydrines, will then undergo one of two ways: concerted rearrangement of a carbon bond under concomitant loss of nitrogen, or dehydration, followed by bond migration under expulsion of nitrogen. The latter would then be followed by the nucleophilic attack of eliminated water, with subsequent proton loss and tautomerization to the final amide. The Schmidt reactions are often done using Brønstedt acidic conditions, but it has also been shown that Lewis acids can trigger the rearrangement as well[63]. This allows for Brønstedt acid sensitive substrates to be open for Schmidt reactions as well.

Empirical studies have found, that the Schmidt reaction is stereospecific and substrates, in which a stereogenic carbon migrates, retain their configuration[64]. This is particularly interesting for the development of synthetic approaches for biologically active compounds, which often require asymmetric synthesis or the expensive and strenuous separation of enantiomers. Furthermore, it has been shown that the product yields vary depending on the electronic effect, substituents on the migrating carbon have[65]. Electron withdrawing groups will impede the bond migration and significantly reduce product yields, whereas electron donating groups will show the opposite effect.

[6] T. Stachyra, M.-C. Péchereau, J.-M. Bruneau, M. Claudon, J.-M. Frère, C. Miossec, K. Coleman, M.T. Black, *Antimicrob. Agents Chemother.*, **2010**, *54*, 5132-5138.
[7] H. Xiong, B. Chen, T.F. Durand-Réville, C. Jourban, Y.W. Alelyunas, D. Wu, H. Huynh, *Med. Chem. Lett.* **2014**, *5*, 1143-1147.
[8] B.G. Hall, M. Burlow, *J. Antimicrob. Chemother.* **2005**, *55*, 1050-1051.
[9] K. Coleman, *Curr. Opin. Microbiol.* **2011**, *14*, 550-555.
[10] W.J. Klaver, H. Hiemstra, W.N. Speckamp, *J. Am. Chem. Soc.* **1989**, *111*, 2588-2595.
[11] M. Betou, L. Male, J.W. Steed, R.S. Grainger, *Chem. Eur. J.* **2014**, *20*, 6505-6517.
[12] For the original procedure please see: S. Schäfer, L. Saunders, E. Eliseeva, A. Velena, M. Jung, A. Schienhorst, A. Strasser, A. Dickmanns, R. Ficner, S. Schlimme, W. Sippl, E. Verdin, M. Jung, *Bioorg. Med. Chem.* **2008**, *16*, 2011.
[13] J.P. Schaefer, J.J. Bloomfield, *Organic Reactions* **2011**, *15*, 1-46.
[14] A. Brändström, *Arkiv Kemi* **1957**, *11*, 527-590.
[15] L.W. Carrick, A. Fry, *J. Am. Chem. Soc.* **1955**, *77*, 4381-4387.
[16] W. Dieckmann, A. Groeneveld, *Ann.* **1901**, *317*, 27-109.
[17] N.J. Leonard, C.W. Schimelpfenig Jr., *J. Org. Chem.* **1958**, *23*, 1708-1710.
[18] A) H. Stetter, O.E. Bander, W. Neumann, *Chem. Ber.* **1956**, *89*, 1922-1926.; B) H. Stetter, B. Schafer, H. Spangenberger, *Chem. Ber.* **1956**, *89*, 1620-1624.
[19] R.P. Linstead, E.M. Meade, *J. Chem. Soc.* **1934**, 935-946.
[20] R.B. Woodward, R.H. Eastman, *J. Am. Chem. Soc.* **1946**, *68*, 2229-2235.
[21] C.R. Clemo, J. Ormston, G.R. Ramage, *J. Chem. Soc.* **1931**, 3185-3190.
[22] H. Walther, W. Treibs, K. Michealis, *Chem. Ber.* **1956**, *89*, 60-69.
[23] J. Dutta, R.N. Biswas, *J. Indian Chem. Soc.* **1961**, *38*, 385-390.
[24] A) M.W. Goldberg, F. Hunzike, J.R. Billeter, H.R. Rosenberg, *Helv. Chim. Acta* **1947**, *30*, 200-205.; B) D.K. Banerjee, *J. Indian Chem. Soc.* **1940**, *17*, 453-462.; C) N.K. Chakraverty, D.K. Banerjee, *J. Indian Chem. Soc.* **1946**, *23*, 377-379.
[25] T. Gruber, A.L. Thompson, B. Odell, P. Bombicz, C.J. Schofield, *New J. Chem.* **2014**, *38*, 5905-5917.
[26] M. Schlosser, *Struktur und Reaktivität polarer Organometalle*, Springer, Berlin, **1973**.
[27] A) G.E. Hartwell, T.L. Brown, *J. Am. Chem. Soc.* **1966**, *88*, 4625-4629.; B) M.Y. Darensbourg, B.Y. Kimura, G.E. Hartwell, T.L. Brown, *J. Am. Chem. Soc.* **1970**, *92*, 1236-1242.; C) J.F. McGarrity, C.A. Ogle, Z. Brich, H.R. Loosli, *J. Am. Chem. Soc.* **1985**, *107*, 1810-1815.
[28] B.Y. Kimura, T.L. Brown, *J. Organomet. Chem.* **1971**, *26*, 57-67.
[29] G.W. Klumpp, *Recl. Trav. Chim. Pays-Bas* **1986**, *105*, 1-21.
[30] H.J. Reich, K.J. Kulicke. *J. Am. Chem. Soc.* **1996**, *118*, 273-274.
[31] S. Wu, S. Lee, P. Beak, *J. Am. Chem. Soc.* **1996**, *118*, 715-721.
[32] B.L. Lucht, D.B. Collum, *J. Am. Chem. Soc.* **1995**, *117*, 9863-9874.
[33] A.J. McNeil, D.B. Collum, *J. Am. Chem. Soc.* **2005**, *127*, 5655-5661.
[34] P.J. Kocieński, *Protecting Groups* 3rd edition, Georg Thieme Verlag, Stuttgart, **2005**.
[35] B.M. Pope, Y. Yamamoto, D.S. Tarbell, *Org. Synth. Coll. Vol. VI* **1988**, 418.
[36] M. Itoh, D. Hagiwara, T. Kamiya, *Bull. Chem. Soc. Jpn.* **1977**, *50*, 718-721.
[37] Y. Ohfune, M. Tomita, *J. Am. Chem. Soc.* **1982**, *104*, 3511-3513.
[38] D.L. Flynn, R.E. Zelle, P.A. Grieco, *J. Org. Chem.* **1983**, *48*, 2424-2426.
[39] L. Grehn, K. Gunnarsson, V. Ragnarsson, *Acta. Chem. Scand.* **1986**, *B40*, 745-750.
[40] C. Agami, F. Couty, *Tetrahedron* **2002**, *58*, 2071-2724.
[41] E. Wünsch, E. Jaeger, L. Kisfaludy, M Löw, *Angew. Chem. Int. Ed. Engl.* **1977**, *16*, 317-318.
[42] R.M. Williams, J. Cao, H. Tsujishima, *Angew. Chem. Int. Ed.* **2000**, *39*, 2540-2544.
[43] F.S. Gibson, S.C. Bergmeier, H.J. Rapoport, *J. Org. Chem.* **1994**, *59*, 3216-3218.
[44] R.B. Hamed, J. Mecinovic, C. Ducho, T.D.W. Claridge, C.J. Schofield, *Chem. Comm.* **2010**, *46*, 1413-1415.
[45] M. Sakaitani, Y. Ohfune, *J. Org. Chem.* **1990**, *51*, 870-876.
[46] U. Schmidt, R. Utz, A. Lieberknecht, H. Griesser, B. Potzolli, J. Bahr, K. Wagner, P. Fischer, *Synthesis* **1987**, 236-241.
[47] H. Vorbrüggen, K. Krolikiewicz, *Angew. Chem. Int. Ed. Engl.* **1975**, *14*, 818.
[48] Y. Hamada, T. Shioiri, *J. Org. Chem.* **1986**, *51*, 5489-5490.
[49] P. Stanetty, H. Koller, M. Mihivilovic, *J. Org. Chem.* **1992**, *57*, 6833-6838.
[50] P. Beak, W.K. Lee, *J. Org. Chem*. **1993**, *58*, 1109-1117.
[51] R. Downhawm, F.W. Ng, L.E. Overman, *J. Org. Chem.* **1998**, *63*, 8096-8097.
[52] A. Orjales, R. Mosquera, L. Labeaga, R. Rodes, *J. Med. Chem*. **1997**, *40*, 586-593.
[53] K.J. Fordon, C.G. Crane, C.J. Burrows, *Tetrahedron Lett.* **1994**, *35*, 6215-6216.

[54] M. Lamothe, M. Perez, V. Colovray-Gotteland, S. Halazy, *Synlett* **1996**, 507-508.
[55] A. Gosh, M.J. Miller, *Tetrahedron Lett.* **1995**, *36*, 6399-6402.
[56] R.M. Valerio, P.F. Alewood, R.B. Johns, *Synthesis* **1988**, 768-789.
[57] S.G. Davies, O. Ichihara, *Tetrahedron Lett.* **2000**, *41*, 6025-6028.
[58] A) G.D. Annis, E.M. Hebblethwaite, S.T. Hodgson, D.M. Hollinshead, S.V. Ley, *J. Chem. Soc., Perkin Trans. 1* **1983**, 2851-2856.; B) M. Shibasaki, Y. Ishida, G. Iwasaki, T. Iimori, *J. Org. Chem.* **1987**, *52*, 3488-3489.; C) T. Yamada, H. Suzuki, T. Mukaiyama, *Chem. Lett.* **1987**, 293-296.; D) R.M. Williams, B.H. Lee, M.M. Miller, O.P. Anderson, *J. Am. Chem. Soc.* **1989**, *111*, 1073-1081.
[59] A) K.F. Schmidt, *Angew. Chem.* **1923**, *36*, 511.; B) K.F. Schmidt, *Ber. Dtsch. Chem. Ges.* **1924**, *57*, 704-723.; C) H. Wolff, *Org. React.* **1946**, *3*, 307.
[60] S. Grecian, J. Aube *Organic Azides* John Wiley & Sons Ltd., Chichester, **2010**, 191-237.
[61] A) R.D. Bach, G.J. Wolber, *J. Org. Chem.* **1982**, *47*, 239-245.; B) L.E. Fike, H. Shechter, *J. Org. Chem.* **1979**, *44*, 741-744.
[62] R.A. Abramovich, E.P. Kyba, *The Chemistry of the Azido Group*, Wiley, London, **1971**.
[63] J. Aubé, G.L. Milligan, *J. Am. Chem. Soc.* **1991**, *61*, 8965-8966.
[64] A) J.H. Boyer, J. Hamer, *J. Am. Chem. Soc.* **1955**, *77*, 951-954.; B) J.H. Boyer, F.C. Canter, J. Hamer, R.K. Putney, *J. Am. Chem. Soc.* **1956**, *78*, 325-327.; C) H.-L. Lee, J. Aubé, *Tetrahedron* **2007**, *63*, 9007-9015.
[65] G.L. Milligan, C.J. Mossman, J. Aubé, *J. Am. Chem. Soc.* **1992**, *57*, 1635-1637.

Chapter 2) Synthesis of a bicyclic oxo-γ-lactam from a simple caprolactam derivative

2.1) Abstract

A new synthetic approach towards the bicyclic 6-azabicyclo[3.2.1]octane system *via* Dieckmann-type condensation is presented. This bicyclic system can be broken down into a butyrolactam, a cyclohexanone or a caprolactam retrosynthetically, depending on which ring bridging bond is broken. For the aim of this project, the caprolactam system was chosen as a starting point. For the Dieckmann-type ring closure to proceed, a strategically modified caprolactam derivate with an ester group in C2 position was synthesised as starting material. Addition of the strong, non-nucleophilic and sterically demanding base LiHMDS yielded the desired bicyclic lactam. The considerations of the conformative behaviour and reaction conditions are discussed; the subsequent optimisation of the synthetic protocol is reported. Furthermore, structural elucidation of the final product and the successfully acquired single crystal X-Ray diffraction data of several intermediate products and the final lactam is presented.

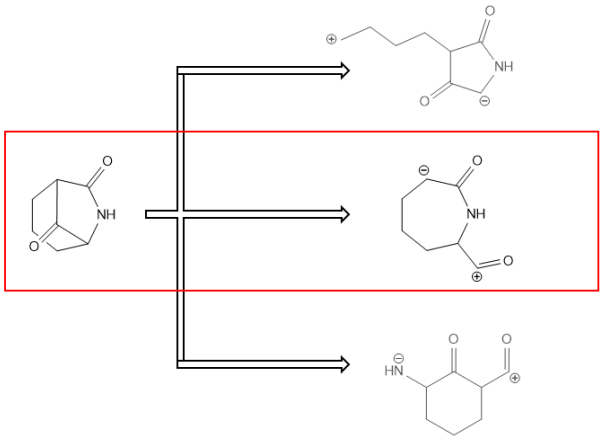

Fig. 2.1 Retrosynthesis of the7,8-dioxo-6-azabicyclo[3.2.1]octane shows that three possible approaches can be found: a five membered lactam, a cyclohexanone or a caprolactam as starting points.

2.2) Introduction

The 6-azabicyclo[3.2.1]octane system has been identified as the leading structural motif in a number of biologically active molecules. Several compounds from natural and non-natural sources have been found to contain this bicyclic scaffold. Some of these contain further functional groups, others have more extensive bridged and/or annulated ring systems, perhaps of more interest to application-based research, others have shown potential for new pharmaceuticals. Unfortunately, only little research has been undertaken to investigate these promising compounds, which may help combat a lot of modern challenges of medicine. *Azaprophen* for example has been shown to have strong antimuscarinic receptor ligand properties, similar to atropine (Fig. 2.2).

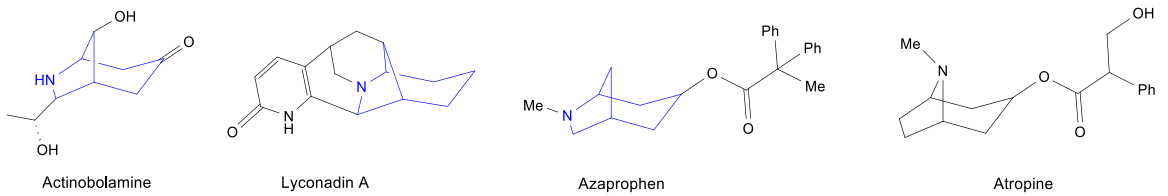

Fig. 2.2 The azabicyclo[3.2.1]octane scaffold was found in several biologically active compounds. Azaprophen, a strong antimuscarinic receptor ligand shows striking similarities to atropine.

The potential of this system comes to light even more when compared to its closely related isomer the 8-azabicyclo[3.2.1]octane scaffold. It is arguably best known as one of the leading motifs in cocaine. The major difference between these two systems, is the precise position of the nitrogen atom, embedded in the carbon chains. Within cocaine, the nitrogen atom forms the monoatomic bridge, spanning over a cycloheptane ring. In the 6-azabicyclo[3.2.1]octane scaffold, the nitrogen atom is found within that seven membered ring and is part of the diatomic bridge (Fig. 2.3).

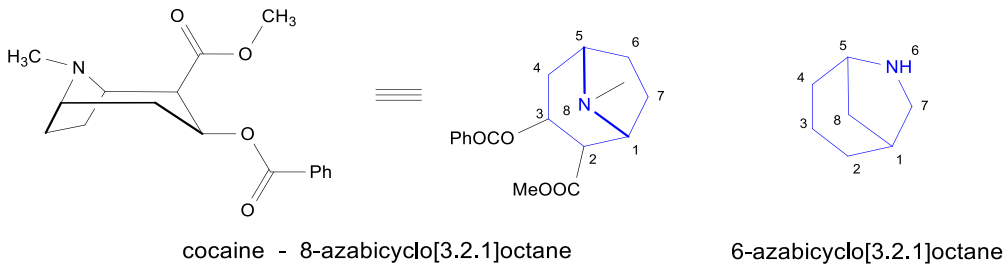

Fig. 2.3 Direct comparison of the bicyclic amine scaffold of cocain shows the close relation to the 6-azabicyclo[3.2.1]octane system.

Considering the potential of this system, the development of a simple, target oriented synthesis of the 6-azabicyclo[3.2.1]octane scaffold could be of great interest to medicinal chemists. A fast, convenient and multifunctional synthetic route could give rise to broad, fundamental research on its structure-function relations, possible derivates or even for the development of novel polycyclic structures.

Many of the already described compounds are, simply put, polycyclic amines with varying degrees of substitution. However, one of these compounds which is not an amine, is *Avibactam*. Chemically, Avibactam is a urea derivative with both of the urea nitrogen atoms being part of a seven-membered ring (Fig. 2.4). One of them is further incorporated into the carbon bridge as one of its bridge heads, the other nitrogen atom carrying a sulfate group. It has sparked the attention of medicinal chemists in the recent past, as it has been proven to be an effective inhibitor for certain enzymes involved in the development of bacterial resistances against penicillin derivatives. These enzymes, known as *β-lactamases* or *Penicillin binding proteins* (PBPs) have caused tremendous struggles in the treatment of infectious diseases. Many penicillin derivates that were approved and used as first line of treatment for bacterial infections, are no longer effective due to the expression of these β-lactamases in bacteria.

However, combination treatment of some previously penicillin-resistant bacteria strains with Avibactam and a penicillin derivate is successful again.

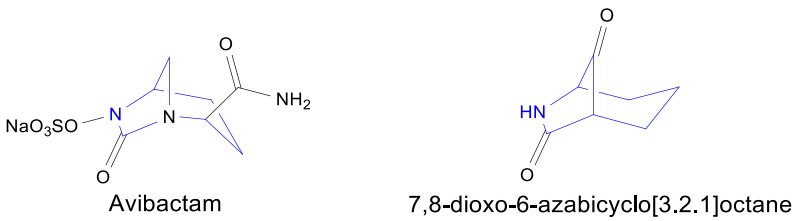

Fig. 2.4 Avibactam is a bicyclic urea derivative of the 7-oxo-1,6-diazabicyclo[3.2.1]octane scaffold. The hypothetical excision of one nitrogen atom leads to the in this work presented system.

Avibactam itself does not show any antibacterial effect, it does not inhibit bacterial cell growth, but pseudo-irreversibly binds to the active centre of many β-lactamases. Intense research has shown that the mode of action origins from a nucleophilic attack from a serine residue within the active centre of PBPs and subsequent ring opening of one of the urea bonds. The perhaps most interesting aspect is that urea derivatives are generally considered to be amongst the least reactive carbonyl compounds. However, this is arguably one of Avibactams advantages. An unreactive carbonyl should also less likely suffer from unwanted side reactions, such as the hydrolysis of carbonyl-nitrogen bonds. On the other hand, an unreactive species might not be as effective, as a more activated counterpart.

Structurally related to ureas are amides. Whereas electron density is distributed over two nitrogen atoms and the carbonyl group in a urea, there is only one nitrogen present in an amide. The loss of some degree of electron distribution from a urea to an amide, or to a lactam, comes with an increase in carbonyl reactivity. This increased reactivity might also increase its efficiency towards enzyme inhibition, potentially making the 7,8-dioxo-6-azabicyclo[3.2.1]octane a novel candidate in the fight against multi-resistant bacterial strains.

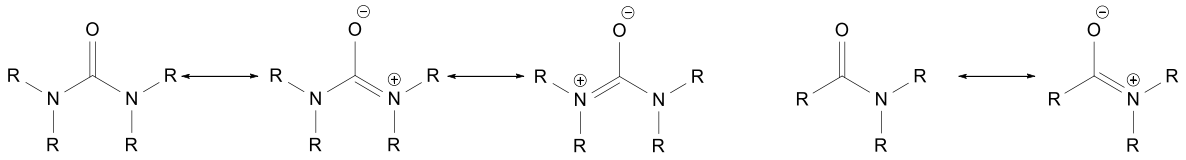

Fig. 2.5 Whereas ureas exhibit electron density distribution over two nitrogen atoms, amides only contain one nitrogen resulting in less resonance stabilisation.

The retrosynthetic breakdown delivered a straightforward, relatively simple approach from the envisaged bicyclic oxo-lactam to the commercially available 2-aminopimelic acid. Reversing the retrosynthesis steps gave a first approach, consisting of the following steps:

- Esterification of 2-aminopimelic acid as this would become necessary for later steps
- First cyclisation to give the caprolactam base ring
- Introduction of a protection group on the lactam nitrogen
- Second cyclisation through regioselective deprotonation and intramolecular ring closure

Previous work in the Gruber work group had established workable procedures for these individual steps and had investigated different aspects of the precursor syntheses. However, because the Dieckmann-type second ring closure had only been possible in poor yields, any potential application and further development required optimisation. This chapter will outline the synthetic efforts to optimise the product yield of the desired bicyclic product through different parameters like solvent, temperature and base.

2.3) Theoretical considerations

The possibly most important step in this synthetic approach to create a convenient and fast route to the 7,8-dioxo-6-azabicyclo[3.2.1]octane scaffold was thought to be the second cyclisation. As this particular synthesis has not been described in literature before, a number of different facets of the reaction were considered. The designated starting material for this transformation was a caprolactam ester. Previous work had proven that this reaction could be carried out successfully by the addition of the strong, non-nucleophilic base lithium hexamethyldisilazide (LiHMDS). Following the general mechanism for the Dieckmann cyclisation, a deprotonation of the α-lactam position and subsequent intramolecular attack of the newly formed enolate on the ester group should be the occurring process. For this general approach to be optimised further, the following factors were considered.

1) The initial system exhibits two CH-acidic positions with relatively similar overall acidity. The distinction between the α-lactam and the α-ester position would require a regioselective approach of both positions. Regioselectivity is a common challenge and similar cases of regioselective deprotonation of one out of two possible CH-acidic centres can be successful if the right base is applied.
2) The base itself could not be a strong nucleophile to avoid nucleophilic transformations of the substrate. Esters of simple alcohols are usually not considered to be overly reactive and often require moderate to strong nucleophiles or comparatively harsh reaction conditions. Nonetheless, they are known to undergo nucleophilic substitution with nucleophiles such as dialkyl amines as side reactions in significant amounts. However, the base had to be strong enough to deprotonate a lactam without the need of further activation.

3) For the successful ring closure reaction to occur, the lactam nitrogen required adequate protection. Any protection group that could be considered would have to be stable under strongly basic conditions. Furthermore, since a connection between the C6-substitution, steric clash of additional *N*-substitution and the conformational behaviour had been found, the size of the protection group was another point to be considered.
4) It seemed reasonable to work on the assumption that the ring closure would only occur if the ester group adopted an axial position. Chapter 1 has given details about the concepts and the previously published investigations on the conformational behaviour of this system. Because conformational equilibria are dependent on other factors such as temperature, this would have to be considered for any possible reaction condition.

The impact of each of the mentioned factors cannot be isolated from the others and had to be examined in conjunction for every optimisation experiment. As an example, as Chapter 1 has outlined, considerations of LiHMDS's aggregation behaviour is dependent on several factors, including temperature, solvent etc. The following section shall be divided into experiments and results that were obtained separate from the bicyclisation experiments first and then lead to the results of the optimisation efforts.

2.4) Results and Discussion

During the synthesis of Boc protected lactam **3**, single crystalline material for SC-XRD analysis could be harvested. The structure has been described in literature before, found in a triclinic space group. This newly crystallised material was found to crystallise in a polymorphic cell to the previously described structure (CSD entry *BOLHOB*[66]).

Single crystal structure of polymorph II of lactam **3**

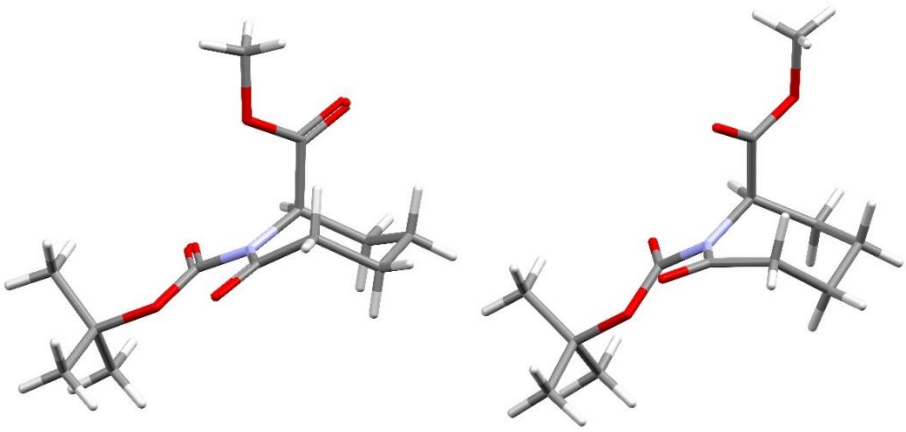

Polymorph I Polymorph II

*Fig. 2.6 The two polymorphs of lactam **3** were found in a similar conformation. The main differences were found in the crystal packing.*

Polymorph II of lactam **3** was found in the orthorhombic space group *Pbca* with one molecule in the asymmetric unit. The caprolactam ring adopts a chair conformation similar to its polymorph I, the ester group is found in an axial position to the lactam ring. Comparison of bond lengths and angles showed no unusual values and are similar to the already published polymorph. One outstanding bond length is the C-N bond length of the lactam bond. Most amide bonds exhibit a bond length of around 1.346 Å for tertiary amides[67] but lactam **3** shows a C-N length of 1.423 Å. This indicates a relatively weak bond and perhaps a lower degree of partial double bond character compared to many other amides and lactams in general. This is further supported by the torsion angle between C3-N1-C8-C7 with an absolute value of 32.44 °, which is significantly higher than the expected co-planar bonds of most amides. The combination of a significantly elongated bond and a torsion angle with significant difference to co-planarity suggests that this caprolactam tends towards an amide with considerably less double bond character along the amide bond.

The crystal structure shows only very few and weak hydrogen bonds, which exclusively involve the lactam carbonyl and the methyl ester protons. The contact C1-H1C···O3 was found with a distance of d(D-H···A)=3.622 Å and an angle of <(DHA)=169.41 °; the contact C1-H1B···O3 with a distance of d(D-H···A)=3.440 Å and an angle of <(DHA)=139.09 °. MeO groups are considered relatively weak acceptors, which is reflected in the comparatively weak hydrogen bonds. Apart from these, a number of hydrophobic interactions can be found. A look into the crystal packing shows that the hydrogen bonds connect the molecules along the crystallographic *b* axis in chain like structures (Fig. 2.7). In each respective chain, the MeO groups interact with the lactam carbonyl of the next molecule, which also interacts with the MeO group of neighbouring molecule, expanding further in the sense of $(MeO_X)\cdots(C{=}O_{Y+1})\cdots(MeO_{X+2})\cdots(C{=}O_{Y+3})$. The chains are connected between each other through bridging interactions of the respective other partner in the sense of $(C{=}O_Y)\cdots(MeO_{X+1})\cdots(C{=}O_{Y+2})\cdots(MeO_{X+3})$. These interconnected chains form a sheet-like pattern along the crystallographic *a,b* plane.

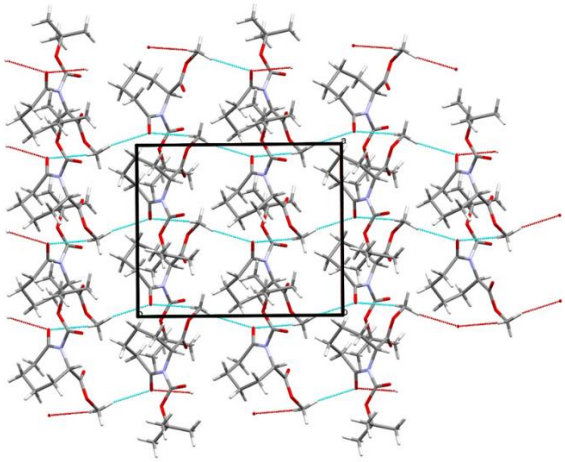

Fig. 2.7 The connections between the lactam carbonyls and the methoxy groups lead to chains and further connect to sheets along the crystallographic a,b plane.

Within each respective sheet, the *tert*-butyl groups of the Boc protection groups point outwards of the sheets, forming a hydrophobic outer layer (Fig. 2.8). These hydrophobic layers than interact with the next sheet to complete the crystal structure along the *c* axis.

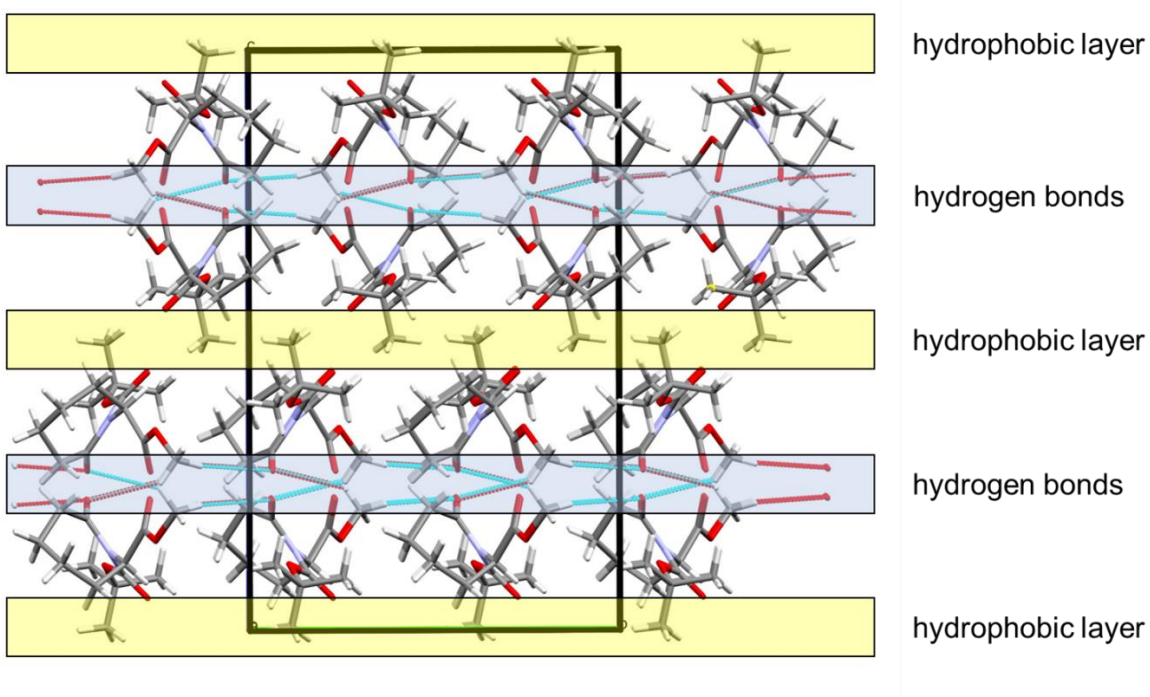

*Fig. 2.8 Lactam **3** forms molecular bilayers through hydrogen bonds, these bilayers are connected through hydrophobic interactions between them.*

Comparison of both polymorphs

The comparison of both polymorphs shows a high degree of similarity (Fig. 2.9). The caprolactam ring adopts roughly the same conformation for both polymorphs, the ester groups are found in an axial position in both cases. The bond lengths and angles show roughly the same numerical values but one torsion angle, which is distinctly different and arguably quite surprising. As already mentioned, amides are generally known to exhibit partial double bond character which usually leads to planarity along the amide bond. This can also be found in polymorph I with a torsion angle of -0.49 Å. Polymorph II exhibits a much wider torsion angle between C3-N1-C8-C7 with a value of -32.44 °. This would suggest, that the high deviation from co-planarity in polymorph II is a result of its different packing. This would than also suggest that the earlier hypothesis of lactam **3** exhibiting less partial double bond character would not necessarily be true in solution. As this could influence the behaviour and reactivity of lactam **3**, further studies towards the amide bond situation in Boc protected lactams are in order (this shall be discussed further in Chapter 4). However, it is not possible to draw a definite conclusion from this.

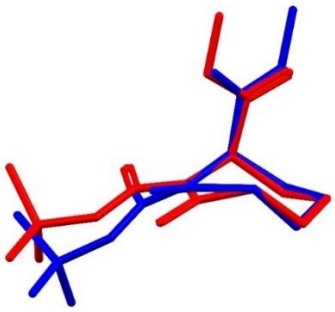

Fig. 2.9 Comparison of polymorph I (red) and II (blue) shows that the caprolactam rings adopt roughly the same conformation, but that the different torsion angles along the amide bond are different.

Optimisation of the Dieckmann-type cyclisation

Table 1.1 summarises the chosen reaction conditions for the initial cyclisation protocol, all attempts at optimisation and the reaction entries using different substrates. A typical reaction was performed as follows: the starting material (lactams **3 - 7**) was dissolved in water-free solvent (THF, *n*-hexane, toluene), the temperature was adjusted (rt to -100 °C), the base was added (Li/Na/KHMDS) (Fig. 2.10). The reaction mixture was stirred for 30 min, aqueous, saturated NH_4Cl was added to quench residual base and the crude mixture was further worked-up. The bicyclic lactam **1a** was successfully synthesised with a yield of 8% for the initial set of parameters. Please note, the synthesis of lactams **4** and **5** is outlined in the appendix, the synthesis of **6** and **7** is described in Chapter 1 under *earlier work within the group*.

Tab. 1.1 The respective reaction entries, their substrates, reaction conditions and isolated product yields (if obtained). The reaction time of 30 min between first addition of the base and quenching was kept unless other specified

Entry	Substrate	Base	Solvent	Base Eq.	Temp. [°C]	Yield [%]
1	**3**	LiHMDS	THF	1.1	-78 (30 min)	8
2	**3**	LiHMDS	THF	1.1	-78 (1 h)	8
3	**3**	LiHMDS	THF	1.1	-78 (3 h)	8
4	**3**	LiHMDS	THF	1.1	-78 (6 h)	8
5	**3**	LiHMDS	THF	1.1	-85	8
6	**3**	LiHMDS	*n*-hexane	1.3	-85	8
7	**3**	LiHMDS	toluene	1.3	-85	11
8	**3**	LiHMDS	THF	1.1	rt	0
9	**3**	LiHMDS	THF	1.1	0	0
10	**3**	LiHMDS	THF	1.3	-85	8
11	**3**	LiHMDS	THF	1.3	-100	7
12	**3**	LiHMDS	THF	2.1	-85	12
13	**3**	KHMDS	THF	1.3	-85	8
14	**3**	KHMDS	THF	2.1	-85	13
15	**3**	NaHMDS	THF	1.3	-85	7
16	**3**	NaHMDS	THF	2.1	-85	11
17	**4**	LiHMDS	THF	1.3	-85	0
18	**4**	KHMDS	THF	1.3	-85	0
19	**4**	KHMDS	THF	2.1	-85	0
20	**5**	LiHMDS	THF	1.3	-85	0
21	**6**	LiHMDS	THF	1.1	-85	0
22	**7**	LiHMDS	THF	1.1	-85	15

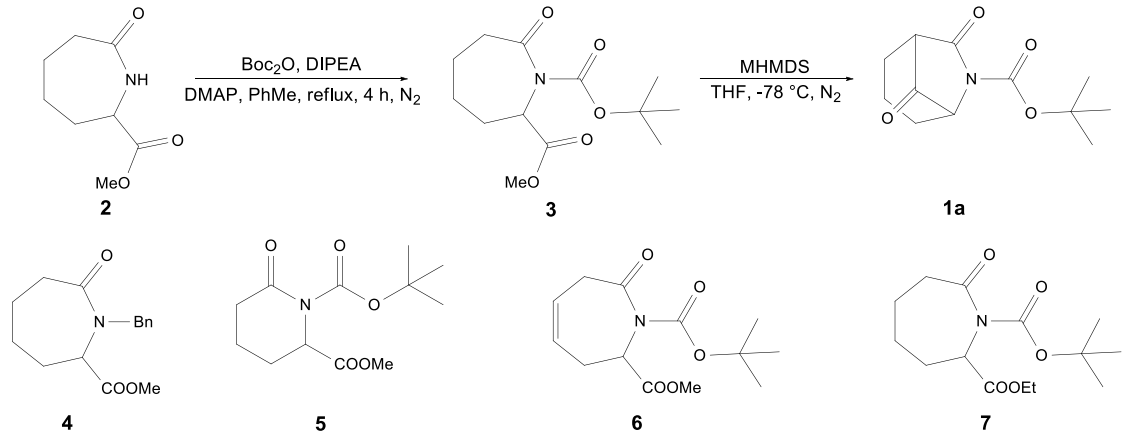

*Fig. 2.10 The initial protocol started with lactam **3** using LiHMDS in THF at -78 °C for 30 min. Besides the reaction conditions, different substrates were used to help elucidate the reaction mechanism.*

Coolant and reaction time

The initial procedure was outlined to let the reaction mixture stir for 30 min, but longer reaction times were investigated as well. Faster addition of the base increased the temperature to up to -50 °C uncontrollably and the product yield decreased significantly. Instead, reaction times of 1 h, 3 h and 6 h were investigated but the product yield was found to be around 8 % consistently. This led to the conclusion that as long as the reaction mixture is kept cooled, the bicyclisation occurs within the first few minutes of adding the base.

First reactions were performed using a dry ice/acetone mixture as coolant. However, it was observed that maintaining the reaction temperature below -73 °C whilst also keeping the reaction time below 30 min failed. To keep the reaction time short, the use of frozen ethyl acetate as a coolant was introduced. This gave a reaction temperature of around -85 °C, allowed to keep the temperature below -80 °C during the addition of the base, and the reaction time of 30 min. All further entries apart from the temperature-dependent were therefore performed using this coolant.

Solvent

THF was initially chosen as a solvent for its use in similar reactions and its inertness against many highly reactive reagents/reactants. Since the strong base LiHMDS was going to be used for the deprotonation of the caprolactam, any solvent that would possibly undergo deprotonation itself was not considered. This essentially excluded most strongly polar solvents, such as DMSO, alcohols and acidic carbonyls. The solvent also had to have a freezing point below at least -70°C since this was believed to be the upper limit of tolerance for the reaction.

Consideration of the mechanism of the Dieckmann condensation suggested that the choice of solvent could also influence the outcome from a very different perspective. Deprotonation of a carbonyl usually results in the formation of a carbanion. Many mechanisms in organic chemistry can be explained using such a carbanion to a satisfying degree. A more accurate description of such a carbanion would be the fully outlined resonance structure with its enolate. However, both of these structures do not necessarily display the true nature of these species because they usually do not take into account that a counter ion is always required. Organometallic chemistry demonstrates that the solvent can have major influence on the reaction outcome of metal ion-containing species and was therefore chosen as first parameter to be changed. *n*-Hexane and toluene were tried instead of THF. *n*-Hexane as solvent did not seem change the reaction outcome, cyclisations in toluene showed a slight increase in the product yield to 11 %. Against the theoretical considerations, the different solvents did not seem to influence the reaction outcome as significantly as expected. It seems that phenomena like aggregation/dissociation or solvent stabilisation either have no effect on this cyclisation, or that the observed yields were roughly equal by coincidence. However, the base LiHMDS was purchased as a THF/*n*-heptane/ethyl benzene solution. The exact amount of THF within the supplied solvent mixture is not known. This gives a concentration of around 0.4 mol·l^{-1} max., assuming the reagent's solvent was pure THF. As already discussed in Chapter 1, the use of co-solvents can have a substantial effect on product yields and even small amounts of THF (Fig. 2.11) may be enough to influence the aggregation/solvation dramatically.

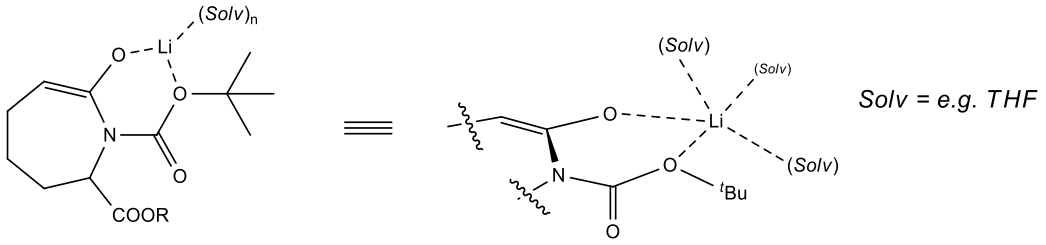

*Fig. 2.11 The deprotonation of lactam **3** could lead to a chelated lithium enolate. The lithium counterion is most likely further solvated by a full solvent sphere in case of THF.*

Unfortunately, the aqueous work-up with toluene as a solvent was found to be much more demanding than in THF or *n*-hexane. The organic and aqueous layers formed finely dispersed emulsions, which only fully separated after about 45 mins. It was decided that the slight increase in yield did not justify the time-consuming work-up and THF was used for all following reactions.

Temperature

As already mentioned, it was observed that the addition of the base increased the temperature of the reaction system quite drastically, which required the addition speed and reaction time to be adjusted accordingly. These experiments were not meant to change the temperature as a parameter but did so indirectly. The temperature as a condition by itself was studied as well. Since one of the main objectives

was to create a protocol with as much synthetic convenience as possible, room temperature and ice as readily available coolant were tried. However, none of the conducted experiments yielded any product. This suggests that the fast addition of the base does not necessarily inhibit product formation, but that the rise in temperature seems to be the main reason for this. As outlined before, it was thought that regioselectivity and the suppression of side reactions were particularly important to the selective deprotonation and successful ring closure. It seems plausible that the regioselectivity is lost at these comparatively high temperatures. Furthermore, it was not possible to recover any starting material after the temperature-dependent experiments above -78 °C. This strongly indicates that side reactions occur at these temperatures but unfortunately, none of the resulting side products could be identified.

A further decrease in temperature did not improve the yield either. THF as the solvent has a melting point of -108 °C. It was observed, that if THF is cooled below about -100 °C, its viscosity seems to drastically increase. It was thought that a significantly increased viscosity could influence the reaction itself beyond the temperature as a parameter because viscosity directly influences the molecular movement within any given system. To avoid any such additional factors, -100 °C was the lowest temperature that was to be tried. However, ~ -100 °C did not seem to influence the yield. A plausible explanation is that -78 °C allows enough kinetic control of the reaction to promote the bicyclisation, but further cooling might only influence the reaction speed rather than its actual occurrence.

Concentration

Another factor that was studied was the concentration of the reaction system (Fig. 2.12). Both the amount of solvent and the amount of added base were varied to investigate dilution of all compounds involved vs. increasing the concentration of only the base.

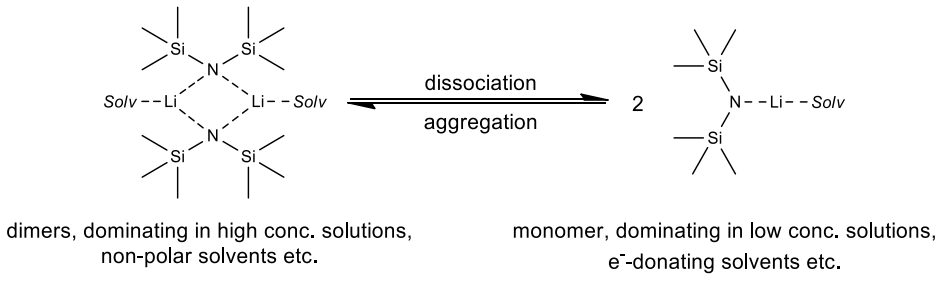

Fig. 2.12 The aggregation and dissociation of solvated LiHMDS largely depends on the solvent. More polar solvents will generally lead to dissociated, e.g. monomeric species, less polar solvents will promote aggregation.

Concentration related entries showed that further dilution of the entire reaction mixture did not improve the product yield, but the addition of more equivalents of base showed a slight increase. The increase of LiHMDS from 1.1 eq to 2.1 eq led to an increase of product yield from 8% to 12%. This non-linear increase in product yield could have several plausible reasons. On one hand, the addition of more base

could simply shift the reaction's equilibrium towards the products and therefore increase the yield. On the other hand, it is also possible that the solvation of LiHMDS and its availability for effective deprotonation impacts the outcome. This could mean that 1.1 eq of the base should technically provide sufficient molecules, but because not all of them are available for the deprotonation, a larger number of base molecules could be required to provide at least 1.0 eq of monomers. It is also possible, that the base plays a much more complex role in the reaction mechanism. Considering that the aggregation/dissociation of such reagents can be highly diverse, such diversity could lead to different reactivities for all species involved. This could mean that more base is needed because of either some unexpected side reaction, or that the generally accepted mechanism for the Dieckmann condensation simply does not apply to the here presented system.

Counterion

As already discussed, the counterion of metal ion-based reagents can change the direction and outcome of a reaction. To study the influence of the counterion on the reaction, NaHMDS and KHMDS were applied as well. The addition of just 1.3 eq of both the sodium and potassium base gave a product yield of 8 %, adding 2.1 eq increased the yield slightly to 13 % for NaHMDS and 12 % for KHMDS. Analysis of all reaction products gave no indication of any newly formed compounds or a change in the reaction outcome other than the slight increase in yield. As discussed for LiHMDS, its not possible to pinpoint one explanation as the underlying reason. The different counterions did not seem to change the reaction system either.

Different substrates

To test, whether this reaction protocol could be used to cyclise different starting materials, lactams **4** to **7** were synthesised. This was thought to give more insight into the occurring reaction mechanism, because the majority of discussed concepts do not necessarily limit the success of this protocol to only saturated caprolactams. A change in protection group, the influence of the ring size, the possibility to cyclise desaturated caprolactams and the effect a different ester pendant would have, were studied.

Protection Group

Previous work had shown, that the Cbz protected caprolactam could not be obtained easily through similar synthesis but benzyl protection was performed successfully (Fig. 2.13). The two main differences between Boc and Bn that were expected are the aromatic nature of the Bn group and the lack of a carbonyl group within the Bn group. Entries number 17 to 19 show that none of the conducted cyclisation experiments gave a benzyl protected bicyclic lactam.

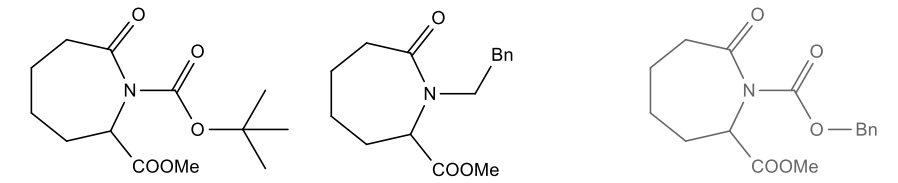

Fig. 2.13 To test whether the Dieckmann-type cyclisation could also be used for other caprolactam derivatives, differently protected caprolactams were investigated. It was further thought, that different outcomes could help to elucidate the underlying reaction mechanism.

The initial protocol with 1.3 eq. LiHMDS was expanded to 1.3 and 2.1 eq of KHMDS to study if the counterion shows different outcomes for this new substrate. However, no product could be found. This suggested that the Bn group does not lead to cyclisation products for this protocol. It is commonly known that CH-acidity increases with an increase of electron withdrawing effects on a potential deprotonation site. The electron releasing effect of the Bn group could disfavour the deprotonation as the first step. This would tie in with the observed cyclisation of the Boc protected caprolactam since the Boc group shows electron withdrawing effects. Another plausible explanation could be the flexibility of the Bn group in comparison to the Boc group. The Boc protected caprolactam shows extensive planarity across the carbamate functionality, which is supported by the single crystal structures of lactam **3**. The planarity along the Boc group restricts the movement of the protection group and only allows rotation of the *tert*-butyl group itself. The relatively fixed Boc group forces the ester group into an axial position as already mentioned. However, the Bn group is presumably more flexible along the CH_2-C_{arom} bond and could therefore adopt a more favourable position towards an equatorially positioned ester group. Another explanation could be the lack of another carbonyl group for a hypothetical chelation. Literature has shown extensive research towards the effect of chelation of counter ions in CH-deprotonation procedures. This suggested that a similar chelation between the lactam and the Boc carbonyl group could be crucial to the bicyclisation. A Bn protected lactam does not have this additional carbonyl group and might therefore not form a complex with the base's counterion, making the successful deprotonation impossible.

Other substrates

Experiments to cyclise a smaller lactam ring were conducted on an equivalent valerolactam. No evidence of any bicyclic product was found during these experiments (Fig. 2.14). The theoretical bicyclic product, an azabicyclo[2.2.1]heptane has been described in literature before and is known to be stable. However, the here presented cyclisation protocol does not seem to be able to produce this system from a valerolactam ester in the same way, as for the caprolactam. The arguably most likely explanation is the ring strain of the product. It is possible, that the energy barrier to form the keto bridge is too high under the reaction conditions and that the equilibrium within the entire system is not driven towards the

bicyclic product. It is also possible that the conformation of the six-membered ring does not allow the cyclisation to occur. As mentioned before, the position of the ester group is believed to play a major role in a successful cyclisation. It was already shown that the ester group adopts an axial position in the respective caprolactam ester. But the differences in conformational behaviour of six-membered lactams might not allow the ester group to be positioned in close enough proximity for an enolate to attack nucleophilicly.

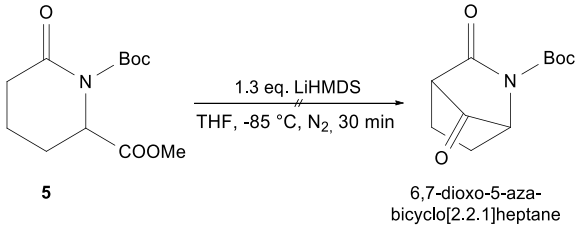

Fig. 2.14 The preparation of a 6,7-dioxo-5-azabicyclo[2.2.1]heptane through the same Dieckmann-type reaction from a valerolactam was not successful. Similar systems have been described in literature, but this Dieckmann-type condensation does not seem to be effective here.

Following this, we also found no evidence of the unsatured caprolactam **6** to undergo cyclisation under the presented protocol (Fig. 2.15). If the explanations of disfavorable ring strain and conformational behaviour can be true for the six-membered lactam, they can also be applied to other related systems. Double bonds within cyclic molecules are known to change both ring strain and conformational behaviour drastically. Its conformational behaviour tends to be more closely related to the behaviour of cyclopentane, assuming that the double bond and its restricted movement can be regarded as one atom in this respect. In addition to the already restricted amide bond, a second double bond within the lactam ring would make comparison with a cycloheptadiene more accurate. But whether either the ring strain of the theoretical product or the conformations of the starting material actually prohibit the formation of bicyclic products and what part they take in this, is unclear.

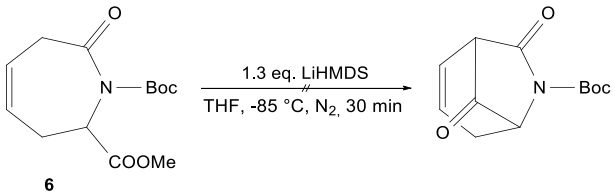

*Fig. 2.15 The desaturated caprolactam **6** was subjected to the same cyclisation protocol but no product formation was observed. Just as for the valerolactam **5**, the increased ring strain could be a possible explanation.*

Ester

Another parameter that was to be investigated was the difference the ester pendant could have. The original synthesis, starting from 2-aminopimelic acid eventually gave the methyl ester **3** but could be changed to give the respective ethyl ester. The original investigations into Dieckmann condensations

had shown that different esters would give less product yield with an increase in the alcohol's size. However, what seemed to be of importance here was the steric demand the parent alcohol would pose. For the purpose of investigating this influence, the methyl ester lactam was saponified and subsequently re-esterified to give the ethyl ester, followed by Boc protection and the cyclisation protocol. The change from a methyl to ethyl ester increased the product yield from 8% to 15%.

The arguably simplest explanation is that the ethyl ester has a higher steric demand than the methyl ester, which therefore improves the kinetic regioselectivity of the LiHMDS base and promotes deprotonation of the α-lactam position. This then also strongly indicates that deprotonation of the α-ester position is a major factor to be considered and is not overcome by the sterically demanding base and the lowered temperature during the reaction. Up to 80% (determined by NMR) of the starting material could be recovered from the reaction mixture for the initial protocol. These findings could suggest that the α-ester position is deprotonated in the process, forms a stable intermediate which does not react further to the bicyclic product and that the monocyclic lactam is regenerated during work-up (Fig. 2.16). However, it is possible that the recovery of starting material is unrelated to the deprotonation process, that only a small percentage of the starting material is in fact deprotonated in α-ester position and that this intermediate does react to give side products that could not be analysed.

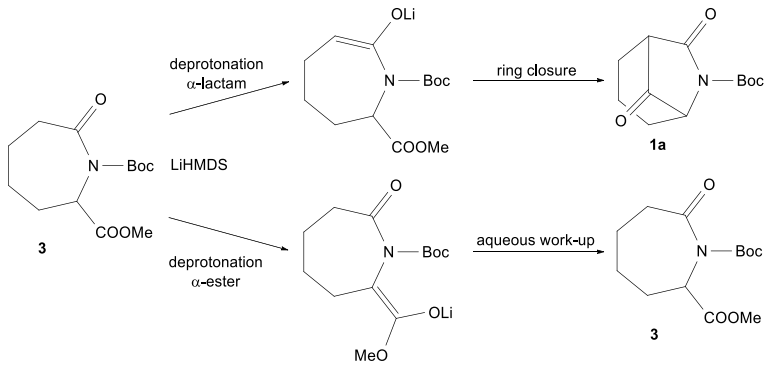

*Fig. 2.16 The deprotonation of lactam **3** can give two different enolates of which only one would give the bicyclic product. The ester enolate might be stable enough to give the starting material back through aqueous work-up.*

Structural identification of the bicyclic product

Confirmation of a 7,8-dioxo-6-azabicyclo[3.2.1]octane being produced required a series of different analytical methods and experiments. One particular challenge was to prove that the acquired product was the desired bicyclic compound and not a, for example, dimerised, bridged side product. This appeared to be much more complex than initially expected. *Gas chromatography* with *mass spectrometric* detection (GC-MS) of the presumed product gave conflicting results. The Boc protected bicyclic product has a calculated molecular mass of 238.12 $g \cdot mol^{-1}$. The acquired gas chromatographs showed two distinct peaks, both presented with significant integrals.

This indicated that either the product was not pure and was heavily contaminated with an unknown compound, or that decomposition occurred during the analysis. NMR-spectroscopy did not indicate a mixture of two main components and the thermal decomposition of Boc protected molecules has been described before[68]. The mass spectra did not show peaks with m/z=238 but did show peaks at m/z=139, which indeed matches the molecular mass of the free bicyclic lactam. However, this could only be considered an indication, but did not necessarily prove it. Liquid chromatography with subsequent mass spectrometric analysis using ESI (*electron spray ionisation*) showed more conflicting results. Only one peak in the chromatograms was found, suggesting that the injected samples were not a mixture of compounds (assuming that all of the injected components eluted). This in turn supported the theory that the heat used for GC-analysis might decompose the product and that the sample used for the analysis only contained one component. The mass spectra did show peaks around m/z=238.12, which would indicate the product. Peaks found at m/z=478.24 and 510.26 on the other hand would also match hypothetical dimeric species (Fig. 2.17).

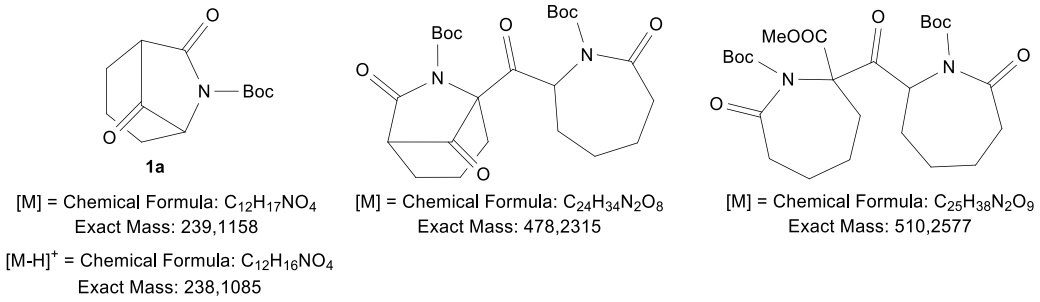

*Fig. 2.17 The mass spectra, recorded of the presumed product showed peaks that could match both the bicyclic ketone **1a** or dimeric species, such as displayed.*

The results could therefore be interpreted in two ways:

1) The desired bicyclic product was formed
   - ➔ GC-MS-analysis suffered from the thermal decomposition
   - ➔ LC-MS-analysis suggested a pure sample and the ESI-technique produced dimeric adducts which could be found as well as the monomeric product
2) The desired product did not form
   - ➔ GC/LC-MS analysis showed compounds of a very similar structure, such as a covalently bound dimeric species, but not the actual product

Considering that mass spectrometric analysis techniques could not prove the presumed structure of the acquired product, NMR-spectroscopic experiments would have to unequivocally prove an accurate structure, the MS results could only support a conclusive theory. Acquired NMR spectra did indicate the generally presumed structure of a lactam, containing a keto group and a Boc group. However, simple assignment of all signals and comparison of proton signal integrals was not fully convincing that the monomeric lactam was formed.

Close examination of the proton spectra showed that most signals within the upfield ranges of chemical shift (3 ppm – 0 ppm) display relatively complex signal splitting. Assuming that a lactam, hence cyclic structure is present, these complex patterns would come from various couplings of the backbone protons and their non-equivalence of the axial and equatorial proton on each respective CH_2 group. However, the two signals at 4.39 ppm and 2.99 ppm respectively exhibited a much less complex splitting. Comparison of their respective integrals indicated that these signals could come from the bridgehead protons H2 and H6. Proton signal coupling usually stems from ^3J-couplings between two protons. Long-range couplings (over more than three bonds) are usually only observed under certain structural conditions like multiple bond conjugation. H2 and H6 should exhibit *doublets of doublets* from their coupling with their neighbouring CH_2 groups. The initially acquired data confirmed this, but did show signal broadening, which hinted towards an underlaying signal, that the original resolution could not properly display.

To artificially improve resolution, data manipulation with "*zero filling*" and "*apodization*" was carried out. After data manipulation of the measured FIDs, the received spectra showed better resolved splitting, especially for the signals at 4.39 ppm and 2.99 pm. Both signals now revealed a distinct *doublet of doublets of doublets* pattern, with one coupling constant being shared between them (Fig. 2.18). Two of the doublet splittings can easily be explained by the protons' respective CH_2 neighbours. Both signals in question showed roughly the same constant, which is a further indicator that the two signals couple with each other. This, assuming the assigned bicyclic structure is in fact correct, would require H2 and H6 to couple over four bonds, along the presumed keto bridge. Coupling patters over four bonds are known, they are predominantly displayed along aromatic or conjugated multiple bond systems. However, there are cases in which protons in structurally fixed *W*-conformations can show ^4J-coupling with constants of about 2 Hz and lower.

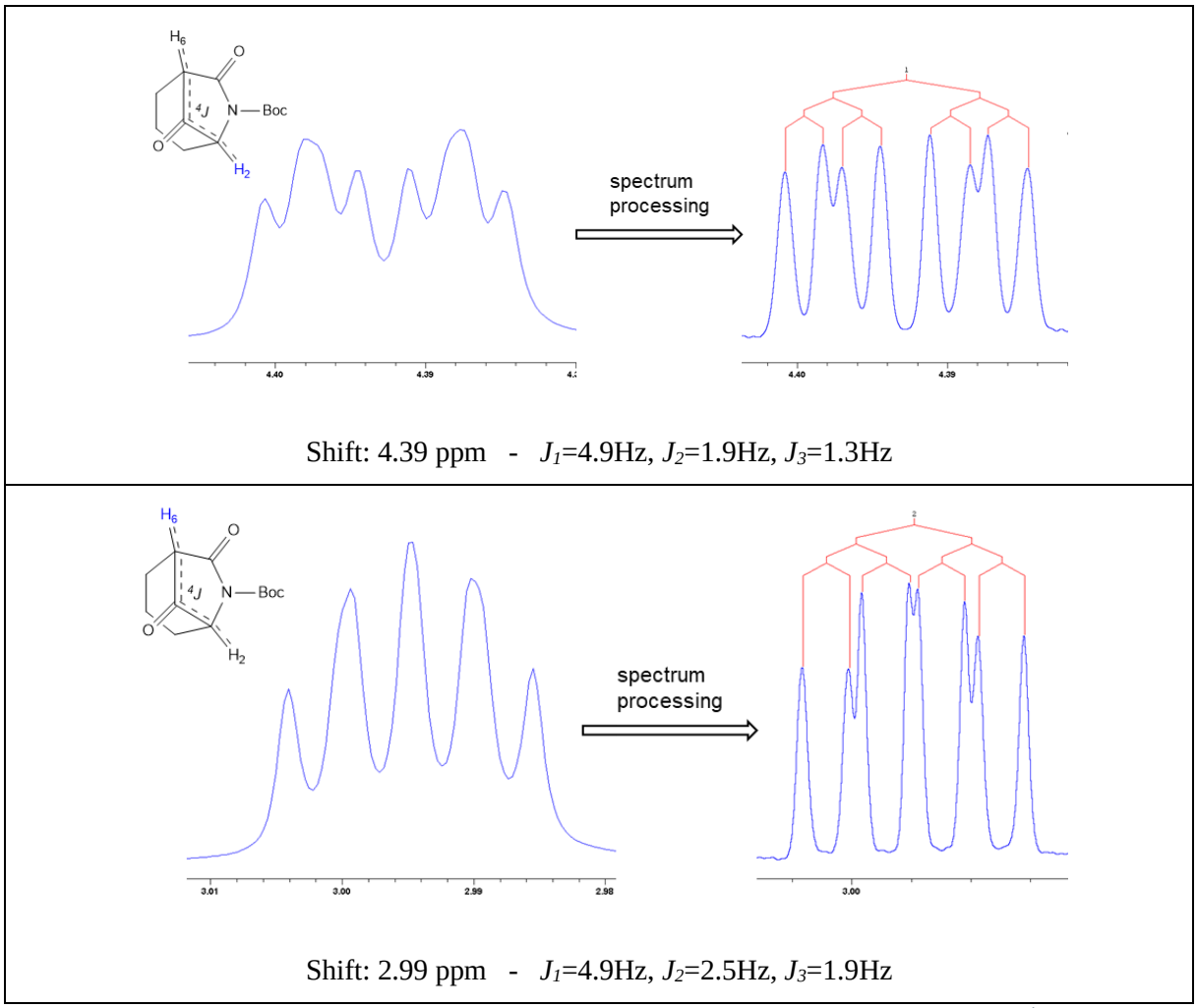

*Fig. 2.18 Processing the spectra of the presumed bicyclic ketone **1a** revealed that the H2 and H6 exhibit a ^4J coupling over the keto bridge. Fixed 'W'-conformations of cyclic systems are known to show these uncommon patterns.*

This particular motif of a structurally fixed W-formation of two protons over four bonds can be found in the monomeric bicyclic lactam. Dimeric species would likely be too flexible to exhibit such couplings. It was therefore concluded that the assigned structure was correct and the azabicyclo[3.2.1]octane scaffold was formed.

Lactam **1a** readily forms a white, crystalline solid but all initial attempts at crystallisation for *single crystal X-RAY diffraction* (SC-XRD) analysis failed. Most crystallisation experiments resulted in polycrystalline material, amorphous solid and/or heavily twinned crystals. Most of these experiments used the *slow-evaporation crystallisation* approach, which had shown success on similar structures before. Instead of slow-evaporation crystallisation, *vapour-diffusion crystallisation* methods were also applied and gave single crystalline material eventually. It is worth mentioning, that the crystal used for the final structural determination was in fact a twinned crystal, but the acquired data was of satisfactory quality to solve the twinning. The single crystal analysis did not show the expected ketone **1a**. Instead we found the bicyclic lactam featuring a *geminal* diol function instead of the keto bridge (Fig. 2.19). The solvents used (ethyl acetate and cyclohexane) were not anhydrous grade but were not expected to contain excessive amounts of water either.

It was concluded that the growth of single crystalline material from the ketone **1a** suffered from interactions with water diffused into the solvents from air and that the closed vapour-diffusion set limited the diffusion of water into the solvents and therefore allowed slow growth of single crystals of **1a**. The formation the a very similar hydrate had already been described in literature before, observed in a crystal structure as in the here presented case[69].

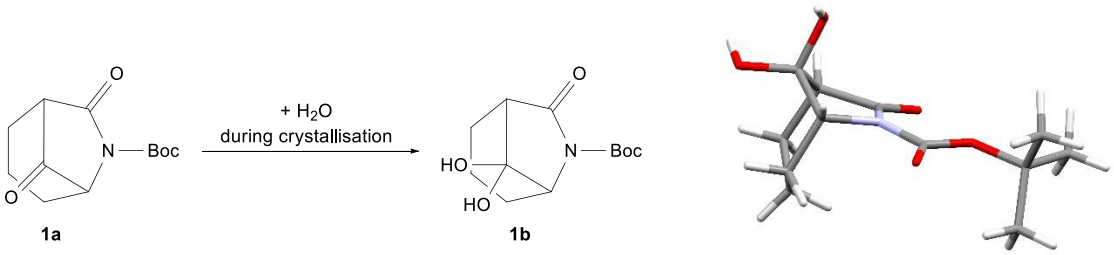

*Fig. 2.19 Slow-solvent evaporation crystallisation of **1a** remained largely unsuccessful. However, vapor-diffusion crystallisation eventually gave single crystalline material, but instead of ketone **1a**, the gem. diol **1b** was found.*

Lactam **1b** crystallised in the triclinic space group $P\bar{1}$ with both enantiomers (*R*,*R*) and (*S*,*S*) being present. Diastereomers were not to be expected, since a hypothetical (*R*,*S*) form of the product would only form if the bridging group could connect C2 and C6 through the caprolactam ring, instead of above. The reaction is therefore not asymmetric, but the stereocenter of the starting material must determine the nature of the second stereocenter. Both enantiomers in the asymmetric unit show the same conformational arrangement and will therefore be described as one for the sake of clarity. Lactam **1b** shows that the caprolactam ring adopts a pseudo-boat conformation, with the diol bridge standing in an endo-position to the carbon backbone of the ring. On top of the caprolactam, the lactam group forms an additional butyrolactam ring with the diol bridge, which exhibits an envelope conformation itself. Comparison of the bond lengths and angles show that the lactam C-N bond is slightly elongated with 1.394 Å in comparison to many other amides and lactams.The slight elongation could be a direct result from the rain strain formed by the bicyclic system, which could force the carbon and nitrogen atoms apart. However, the SC-XRD data of both polymers of the monocyclic starting material suggests that the amide bond stretches when the Boc group is introduced. It seems that the electron withdrawing effect of the Boc group causes this elongation, but it is impossible to say to what extend ring strain plays into this for the bicyclic system at this point. This confirms the hypothesis that despite the stretched C-N bond, the lactam group still has partial double bond character and therefore is movement restricted.

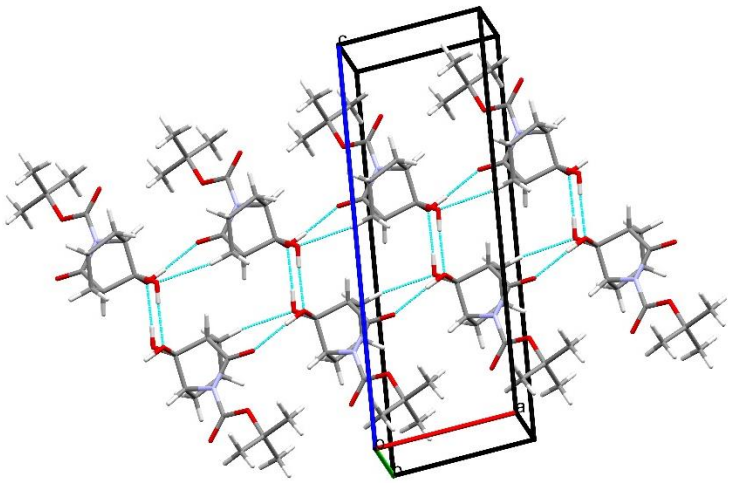

*Fig. 2.20 The most dominant interactions in the crystal packing of **1b** found were hydrogen bonds between the gem. diol groups. They are found to form chain like structures along the crystallographic a axis.*

The packing of hydrate **1b** is dominated by hydrogen bonds between the diol groups. Two molecules form dimers between the diol groups with the $R_2^2(8)$ graph set descriptor. The diol groups of both molecules of that dimer further connect to another respective dimer over hydrogen contacts with the lactam carbonyl groups of one of the monomers. This alternating connection system creates a chain like structure along the crystallographic *a* axis (Fig. 2.20). These chains are interconnected over relatively weak C-H···O contacts along the *b* axis between the diol groups and the carbon backbone of the lactam ring. This arrangement forms layers of dimers in the crystallographic *a,b* plane, with the *tert*-butyl groups pointing outwards. This can be described as a sheet-like overall structure. The sheets are connected *via* hydrophobic interactions between each other. It is believe that the hydrophobic interactions of the sheets between each other are relatively weak and cause stacking errors, which further explains the challenging crystallisation and the extensive twinning of the crystals that were eventually used.

2.5) Summary and Conclusion

After thorough consideration of many aspects of reaction conditions, a successful synthesis of the azabicyclo[3.2.1]octane was found in a Dieckmann-type cyclisation reaction. The initial reaction protocol only gave a yield of 8%, several attempts at optimisation have been performed. The following parameters were investigated on their respective influence:

- Addition speed of the base: as long as the decreased reaction temperature is maintained, the addition speed did not seem to influence the outcome, 30 min is sufficient for the reaction to take place
- Solvent: *n*-hexane, toluene and THF were tried but THF was found to be the best option in terms of yield and practicality

- Temperature: it seemed that as long as the temperature is not allowed to rise too quickly during the addition and kept below a certain threshold (-70 °C seemed appropriate), the temperature did not seem to affect the yield
- Amounts of added base: doubling the base eq. showed a slight rise in yield, but it was not possible to prove a link between the yield and the amount of base directly
- Counterion of the base: Li-, Na- and KHMDS were tried but the counterion did not seem to influence the reaction outcome
- Protection groups: The Boc protected caprolactam was found to successfully undergo cyclisation, the Cbz group could not be introduced, the Bn protected caprolactam was not found to undergo cyclisation
- Six-membered lactam: the equivalent valerolactam was not found to undergo this Dieckmann-type cyclisation under the applied conditions
- Desaturated caprolactam: A desaturated caprolactam was tried but was not found to undergo this Dieckmann-type cyclisation under the tried conditions
- Size of ester: The change from the initially studies methyl to and ethyl ester has shown an increase in yield by almost 100%

Once acquired, the bicyclic product lactam **1a** was characterised using several analysis techniques and the structure was confirmed. Furthermore, single crystalline material suitable for SC-XRD analysis was obtained. The acquired data showed that the bicyclic lactam did not crystallise as the expected ketone **1a** but as the geminal diol **1b**.

The following principles were therefore concluded: this Dieckmann-type cyclisation can successfully yield the 7,8-dioxo-6-azabicyclo[3.2.1]octane scaffold starting from a strategically modified caprolactam. Certain reaction conditions do not seem to majorly influence the reaction outcome as long as they are kept within a threshold like concentration, temperature, addition speed of the base or its counterion, or the solvent. Other factors have been found to not allow the precursor lactam **3** to be cyclised such as different protection groups, a different ring size or an additional double bond.

However, after all conducted studies, the reaction mechanism seems to be more complex than initially anticipated. The experiments around different substrates indicated that factors like the conformational behaviour or ring strain could play a major role in the cyclisation but it was not possible to directly connect these to the reaction mechanism.

Nonetheless, only a small selection of conditions and substrates, that were arbitrarily chosen were tested. It is possible that other factors, that were not tested in this study, could lead to a drastically improved yield. For example, the addition of chelating agents, different bases such as *lithium diisopropylamide* (LDA) or *lithium tetramethylpiperidide* (LTMP), larger esters or different protection groups could change the reaction system entirely. Further studies were aimed at the investigation of more possibilities to improve the yield and to further elucidate the reaction mechanism.

2.6) Appendix

Preparation of an equivalent valerolactam

A look into literature on valerolactams revealed that 2-carboxyl valerolactams are synthetically available through cyclisation of 2-aminoadipic acid. A procedure by Meister[70] describes the reflux of 2-aminoadipic acid in water for 3 h to give the free valerolactam acid in good yields, without the need for further purification (Fig. 2.21).

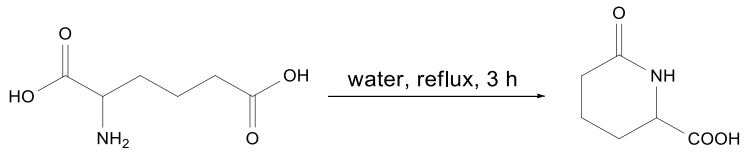

Fig. 2.21 Refluxing 2-aminoadipic acid has been described to give a valerolactam acid by A. Meister in good yields and purity.

First attempts at this comparatively simple condensation only resulted in the recovery of the starting material, no product was found to be formed. Because 2-aminoadipic acid is comparatively expensive, it was decided to follow the same synthetic approach that was employed to give the respective caprolactam ester. The first step was the equivalent esterification of 2-aminoadipic acid through the $SOCl_2$/MeOH protocol.

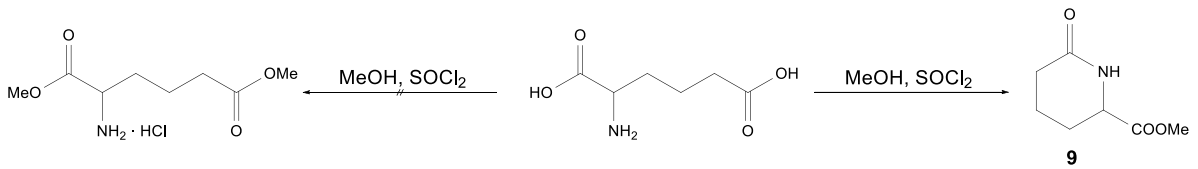

Fig. 2.22 The methylation of 2-aminoadipic acid did not result in its corresponding diester but readily gave the valerolactam methyl ester without the need for further synthetic steps.

To our surprise, the dimethyl ester was not obtained. Analysis of the product revealed that the valerolactam had readily formed in the reaction mixture (Fig. 2.22). As pointed out in the proposed mechanism of the esterification of 2-aminopimelic acid, it seems reasonable that the formation of HCl in the $SOCl_2$/MeOH mixture should protonate the amino group to give a hydrochloride. Assuming that the same proposition should be true for the aminoadipic acid, the protonated amine group would have to nucleophilicly attack the newly formed ω-ester group to form a lactam.

Considering that the empirical evidence clearly proves that the product is formed, there appears to be some thermodynamic driving force which allows the formation of the lactam. Previously published work on diethyl 2-aminoadipate hydrochloride salt described a successful cyclisation when the diethyl ester was gently refluxed in EtOH or the presence of dilute KOH-solution with pH of "only" 8[71]. This indicates, that at least the diethyl ester of the hydrochloride salt does not undergo ring closure readily. It also indicates, that the presence of another proton acceptor such as OH^- can then trigger the condensation reaction. Following this, two theories were put forward:

1.) The hydrochloride salt forms an equilibrium with free amine and the free amine is capable of reacting to give the lactam and therefore drives the equilibrium towards the product
2.) The esterification and a subsequent ring closure condensation are kinetically superior to the acid-base reaction of the free HCl with the amine and the lactam simply forms faster than the hydrochloride.

Acids and their corresponding bases are well-known to form equilibria. It is also very well documented that the irreversible reaction of one component in an equilibrium can be enough to enforce one particular mechanistic pathway. Taken to its conclusion, this would mean that free amine would undergo ring closure comparatively easy because it would compete with the protonation reaction. Considering that HCl is a strong acid with a pK_a of -7 in water[72] and that the solvent for this reaction was methanol, which should enhance the acidity of free HCl, 2-aminoadipic acid should undergo ready and complete protonation. Whether this solution still contains considerable amounts of the free amine is debatable. However, since the resulting valerolactam seems stable under these conditions, even trace amounts of free amine could be enough to undergo cyclisation. A hypothetical reaction of a hydrochloride salt to the free amine and the subsequent intramolecular condensation would liberate one equivalent of HCl and one equivalent of methanol. Simplified, this would mean that one molecule would react to give three product molecules, which should be entropically favoured to some extent. Furthermore, six-membered rings are generally considered particularly stable which could also contribute to a favoured formation of the lactam.

On the other hand, the sole argument of the ring closure reaction simply being faster than the protonation seems unlikely. The free HCl in the $SOCl_2$/MeOH mixture is most likely already present, even before the starting material is brought into this mixture. Based on the assumption, that the esterification step needs to proceed before a ring closure can occur, the acid-base reaction should compete kinetically already. However, it should be mentioned that both of these theories are largely dependent on the assumptions made from the proposed reaction mechanism. It could also be possible, that since no efforts were made to fully elucidate this mechanism, these assumptions are not fully accurate.

The resulting methyl ester readily crystallised and gave suitable single crystals for SC-XRD. Because SC-XRD data of the free acids of both the five- and seven-membered lactams were available, the equivalent free acid of valerolactam was targeted. The methyl ester was available after the successful cyclisation and saponification with the previously successful protocol using $LiOH/H_2O_2$ in THF/H_2O mixtures was performed. The saponification gave the desired free acid in a good yield of 79% with satisfying purity without the need for time consuming purification procedures (Fig. 2.23).

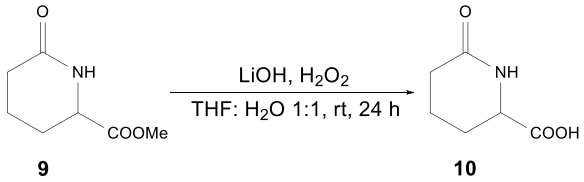

Fig. 2.23 Saponifying the valerolactam methyl ester with the $LiOH/H_2O_2$ procedure gave the free acid in good yield of 79%.

Because the main focus remained on systems that could help elucidate the behaviour of the Dieckmann-type cyclisation of caprolactam ester, it was decided to not pursue a wider variety of different valerolactam esters. Instead, a Boc protected valerolactam methyl ester was thought to give valuable insight into its larger equivalent. Similar to the previously mentioned Boc protection reaction, the same reaction conditions were used to synthesise the Boc protected methyl ester of valerolactam. A good yield of 81% of the product was achieved (Fig. 2.24). Unfortunately, this product was obtained as a viscous oil and multiple attempts at crystallisation through different methods remained unsuccessful.

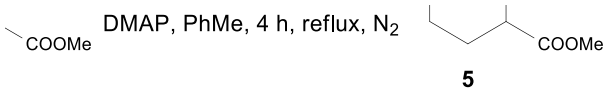

Fig. 2.24 Just as with the respective caprolactam ester, the Boc protection using Boc_2O, DIPEA and DMAP gave a good yield of 81% for the Boc protected product.

Earlier work had shown that the introduction of a Boc protection group changes the conformational behaviour of the investigated caprolactam ester. It was suspected, that the size of the sterically demanding Boc group played the key determinant in its influence on the position of a N_α-positioned ester group. The NMR studies clearly indicated that large protection groups could force such an ester group in the normally unfavoured axial position. Because of the electron withdrawing nature of this particular protection group, the investigation of the influence of a protection group, which would not withdraw electron density became of interest. Even alkyl groups such as methyl could function well as *N*-protection. However, because it was planned to eliminate the protection group after successful cyclisation, most normal alkyl groups were not considered. A classic electron donating protection group in peptide synthesis is the benzyl group. This group was thought to serve several aspects:

1.) Benzyl groups are electron donating and could therefore influence the deprotonation kinetics of the Dieckmann-type cyclisation
2.) Even though the protected nitrogen atom carries a freely rotating CH_2 group, instead of a fixed carbamate group, Bn was thought to be comparable in its steric demand
3.) Bn protection is classically deprotected through hydrogenolysis and usually withstands strongly basic conditions which were required for the Dieckmann-type cyclisation

The synthesis of a Bn protected caprolactam ester was derived from peptide chemistry and involved the reaction of the caprolactam with NaH in DMF at 0°C with subsequent addition of benzyl bromide.

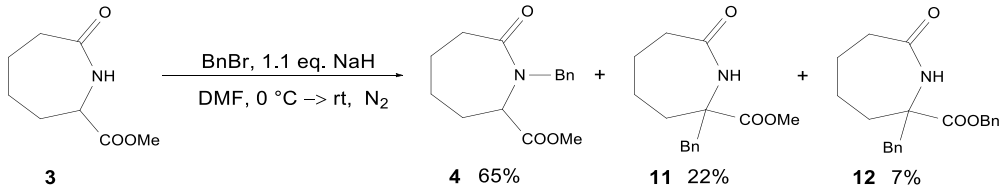

Fig. 2.25 The benzyl protection of this caprolactam ester gave the desired main product and two further side products.

The main product was obtained in a moderately good yield of 65%. However, two side products were found as well. Two free caprolactams with second N_α-substitution, with one retaining the methyl ester, the other being re-esterified with another benzyl group with 22% and 7%, respectively (Fig. 2.25). Because the starting material has three acidic positions (NH, α-ester, α-lactam), only 1.1 eq of the base were added in an effort to avoid side reactions. The NH was believed to be the most acidic position, which is reflected in the ratio of products. Assuming that the nitrogen undergoes deprotonation preferably before the acidic carbon atoms, the formation of the main product seems straightforward.

Mechanistically, *N*-benzylated caprolactam should not react back to the free lactam under the applied conditions. It was therefore believed that the substitution in N_α-position would have to proceed before *N*-benzylation occurs. This pointed towards a kinetic phenomenon, rather than a thermodynamic. The applied base NaH was not provided as a pure compound, but as a suspension in mineral oil. This is common practice, because NaH as a pure compound is highly reactive, whereas the suspension is relatively safe to handle. NaH is also known not to dissolve in most organic solvents. Reactions are thought to only occur on the surface of the NaH-particles because of its insolubility. This could mean, that the α-ester could be deprotonated kinetically to give a carbanion and the corresponding enolate of the ester in an equilibrium.

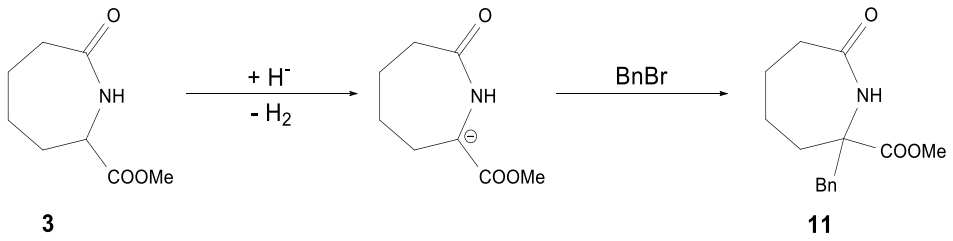

*Fig. 2.26. Deprotonation of the N_α-position could give the disubstituted caprolactam **11**. This side product was obtained with a yield of 22%.*

The carbanion should be able to react with benzyl bromide in the sense of a nucleophilic attack rather easily, which would explain the first side product (Fig. 2.26). However, this theory cannot explain the transesterification. A very different explanation could come from previously mentioned work by Masschelein *et. al.*[73]. In their work on very similar butyrolactam esters, they describe a base induced rearrangement of Boc protection groups onto the N_α-carbon atom (Fig. 2.27).

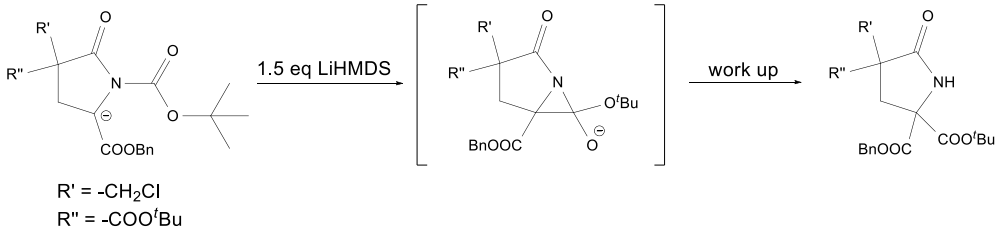

Fig. 2.27 A published article by Masschelein et. al. describes the formation of N_α,N_α -diesters through rearrangement of a Boc protection group. The authors hypothesise a three membered transition state to explain the rearrangement.

Applied to the benzyl protected caprolactam, the N_α-benzylated product could form after such a rearrangement. This would not only explain the formation of the mono benzylated side product, but could also explain why no *N*-benzylated dibenzylation product was found.

The formation of the transesterification product can still not be satisfyingly explained. The authors of the rearrangement only describe the observation of N_α-diesters, without transesterification. We would like to offer a highly speculative explanation following a hypothetical species, which could be formed by both mechanisms. However, no empirical evidence was found for this hypothesis and it should be regarded as such. As mentioned, a kinetic deprotonation of the α-ester position would lead to a carbanion and through the equilibrium, also to an enolate. Such an enolate could attack benzyl bromide nucleophilicly to form a benzylated keten acetal. The formation of such species from esters through deprotonation and treatment with trimethylsilyl chloride (TMSCl) is known. The relative stability of such silylethers and ease of their formation is thought to stem from the oxophilic nature of silicon. This also explains the tendency to only silylate enolates, not carbanions. Benzyl bromide is far less likely to undergo a similar reaction but such a species could also be generated through the mentioned rearrangement. Once the *N*-benzylation has proceeded and a second deprotonation has occurred, the resulting enolate might form an oxazoline system as an intermediate.

4-Oxazolines have been described in literature as very reactive, they undergo ring opening quite easily[74]. Once the transesterification has occurred, the second benzylation might take place, explaining the introduction of the second benzyl group. The introduction of the second benzyl group would have to take place after the rearrangement because enolisation of the ester group becomes impossible. With the introduction of water through the aqueous work-up, water could attack the stabilised enol to give a tetrahedral transition state from which a methoxide ion could be expelled and the dibenzylated product forms (Fig. 2.28).

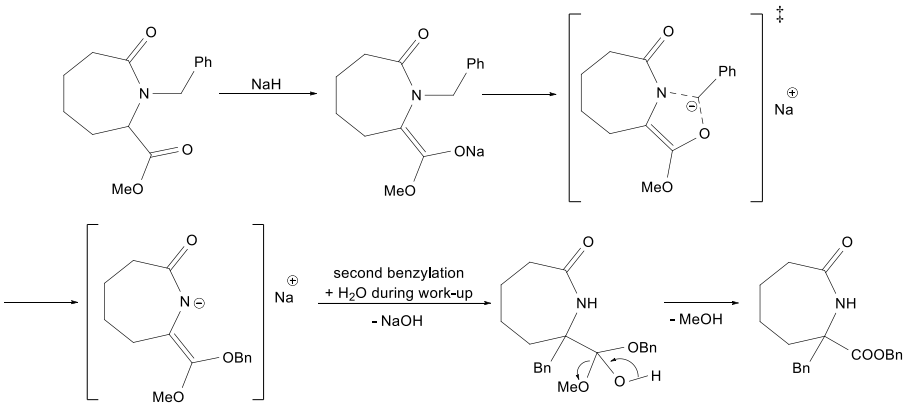

*Fig. 2.28 A suggested mechanism on the transesterification of methyl ester **3** to the dibenzylated caprolactam **12** would involve the formation of a five-membered ring as a transition state. However, no empirical proof was found for this highly speculative mechanism.*

This, again, seems unlikely, benzyl alcohol is considered a comparatively good leaving group and the proposed stepwise mechanism cannot sufficiently explain why methanol is liberated instead. A hypothetical, concerted mechanism involving the attack of a hydroxide ion, the elimination of methanol and the ring opening might explain this.

---

[66] T. Gruber, A.L. Thompson, B. Odell, P. Bombicz, C.J. Schofield, *New. J. Chem.* **2014**, *38*, 5905-5917.
[67] F.H. Allen, O. Kennard, D.G. Watson, L. Brammer, A.G. Orpen, *J. Chem. Soc. Perkin Trans. II* **1987**, 1-19.
[68] K.E. Krakowiak, J.S. Bradshaw, *Synth. Commun.* **1996**, *26*, 3999-4004.
[69] M. Betou, L. Male, J.W. Steed, R.S. Grainger, *Chem., Eur. J.* **2014**, *20*, 6505-6517.
[70] A. Meister, *J. Biol. Chem.* **1954**, *210*, 17-35.
[71] A) A. Sadiq, N. Sewald, *Org. Lett.* **2013**, *15*, 2720-2722.; B) S.-B. Huang, J.S. Nelson, D.D. Weller, *Syn. Comm.* **1989**, *19*, 3485-3496.
[72] Autorenkollektiv *Organikum* 24th edition, Wiley-VCH Verlag GmbH Co. KGaA, Weinheim, **2015**.
[73] K.G.R. Masschelein, C.V. Stevens, N. Dieltiens, D.D. Claeys, *Tetrahedron* **2007**, *63*, 4712-4724.
[74] E. Vedejs, J.W. Grissom, *J. Am. Chem. Soc.* **1987**, *110*, 3238-3246.

Chapter 3) – The Missing link in the homologous Series of Lactams: The X-Ray Structure of Valerolactam

3.1) Abstract

Whereas many lactams have been characterised through single-crystal X-RAY diffraction (SC-XRD), the simple, unsubstituted δ-valerolactam had not been described in literature before as a structure solely by itself. Because of this missing piece in the homologous series, conclusions drawn from previously published structures of valerolactams had to be drawn under the assumption that free δ-valerolactam would behave equally to published solvates or coordinated complexes. The acquisition of appropriate data for a free δ-valerolactam was found to be much more challenging than initially anticipated. However, for the first time, the acquisition and description of its SC-XRD data is presented. Furthermore, the acquired data will be brought into a wider context by completing the SC-XRD data for the homologue series of lactams. Particular interest shall be paid to the intermolecular hydrogen bonding patterns and the lactam bond properties.

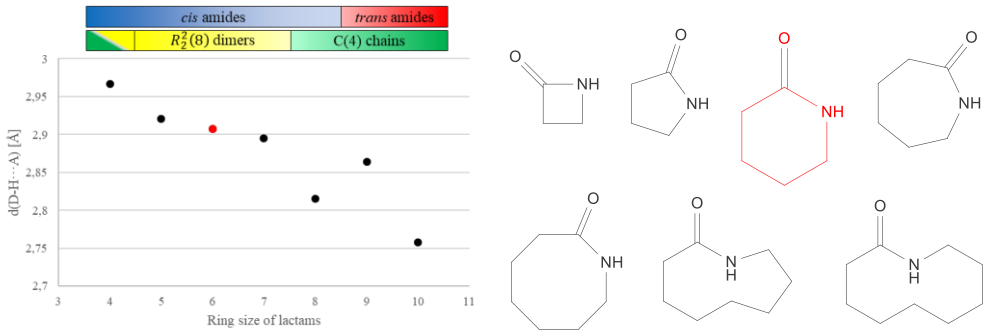

Fig. 3.1 The acquisition of the first full SC-XRD data set of free δ-valerolactam finally allows comprehensive studies on the homologous series of lactam.

3.2) Introduction

The lactam functionality can be found in a plethora of naturally and non-naturally occurring sources, with the arguably most prominent representative, the β-lactam antibiotics, a ground-breaking milestone in modern medicine. This class of antibiotics is characterised by its β-lactam ring, which not only impacts many chemical aspects, but also functions as their pharmacophore. Another, well-known example, especially for the industrial relevance of lactams, is ε-caprolactam. First described in the 18th century, ε-caprolactam rose to become of widespread importance for its use as the starting material of the polyamide *Perlon*®. Its discovery and commercial success also paved the groundworks for a wide variety of other polyamides and polyaramides such as *Kevlar*. Other simple lactams could therefore be found to be of groundbreaking importance as well.

Technically, every cyclic peptide classes as a lactam per definition but despite this seeming importance, lactams as a compound class have not been particularly well researched in the past. Studies on their reactivity or physicochemical behaviour are comparatively rare. An example of this lack of fundamental research into lactams is the uncertainty of why their non-linear hydrolytic stability to the ring size occurs.

Both the four-membered and the six-membered lactam (β-propiolactam and δ-valerolactam respectively) show significantly increased hydrolysis rates (Fig. 3.2). This can easily be explained by an increase in ring strain for β-propiolactam, but this is unlikely for δ-valerolactam. It was hypothesized that the two most likely explanations are either a weakened amide bond or special conformational behaviour to facilitate nucleophilic attack from water molecules. However, neither of these explanations have been fully elucidated unequivocally yet[75].

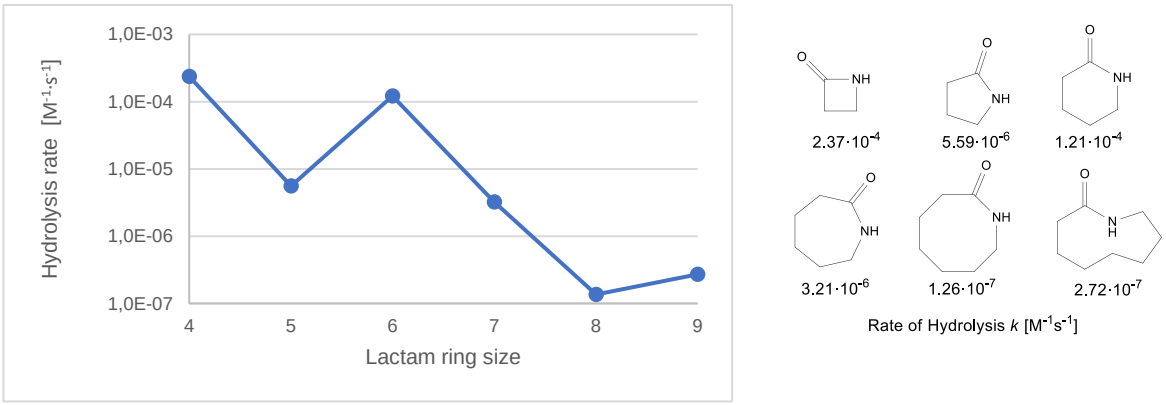

Fig. 3.2 The rate of hydrolysis for the homologous series of lactams shows the unusual trend of δ-valerolactam being hydrolysed much faster than both γ-butyro and ε-caprolactam.

Fundamental research into the understanding of compounds largely depends on analytical experiments being conducted and the acquired data being processed and evaluated. One of the potentially most important modern analysis methods within the toolbox of chemists is the acquisition of single crystal structural data (SC-XRD). SC-XRD can give a variety of different information about any compound that can be measured with this technique. It can elucidate the existing structure of highly complex molecules like enzymes; it can allow the analysis of lengths and angles of covalent and non-covalent interactions within just one or many molecules. Furthermore, unexpected macroscopic phenomena of crystalline material can be understood through analysis of certain microscopic patterns. For this reason, many chemists use SC-XRD and its potential to explain empirical observations, that cannot be explained by spectroscopy or spectrometry. One of the arguably biggest disadvantages of this analysis method is the need for single crystalline material. Many compounds do form solids at room temperature. However, even if the melting point of any given compound lies within a convenient range, the formation of single crystallites does not always occur readily.

Considering that lactams can be found as part of many more complex structures, we were surprised that the commercially available and rather inexpensive δ-valerolactam had not been described as a single crystal structure by itself. Several publications have described this simple lactam as crystalline solvates, as ligands coordinated to Lewis acids[76] or as part of larger molecular structures[77]. However, interactions with a solvent or coordination to a metal ion can influence the molecular arrangements of the overall electronic distribution of a molecule.

As it is always difficult to quantify the effects caused by such circumstances on the crystallised compound, structures that do contain secondary molecules do not necessarily exhibit the same behaviour as the corresponding free compound itself. For that reason, acquisition of single crystal structure data, free of such secondary compounds, is desirable if the respective structure is to be compared to chemically related structures that have been described free of secondary components.

3.3) Results and Discussion

Harvesting a suitable crystal and subsequent preparations

Growing and harvesting single crystals which are suitable for SC-XRD can be challenging. Liquids and gases have to be cooled below their respective melting points and need to be crystallised in a controlled way; air and/or humidity-sensitive compounds usually require special techniques; other compounds tend to form amorphous solids, which cannot be determined by SC-XRD. Furthermore, single crystallites very often need special preparation before they can be used for SC-XRD. The crystallites usually need to be immersed in special oils and are too big for direct use, which in turns usually requires a crystallographer to cut the crystals into appropriate shards. They further often require parts of the crystallite to be cut off, or adhered, smaller crystals need to be removed.

Most of the smaller members of the homologous series of lactams have been characterised by SC-XRD. They readily form crystalline solids at room temperature which made crystallographic characterisation possible without the necessity of modern, sophisticate methods for growing and harvesting crystals. The majority of work was done by Winkler and coworkers[78] in the 1970s, compiling most simple lactams, with δ-valerolactam being the exception.

According to the supplier *Merck KGaA*©, δ-valerolactam has a melting range of 38-40 °C, which suggested that SC-XRD data acquisition should be fairly straightforward, once single crystalline material was harvested. First examination of a commercially obtained sample of δ-valerolactam showed a crystalline solid with no obvious reason why the acquisition of single crystal structural data would be problematic. However, during the preparations to harvest a potentially suitable crystal, an unexpected phenomenon was observed. The solid material could be taken out of the sample bottle, but once a sample was put on a microscopy slide, the solid sample seemingly liquified within a matter of minutes. Crystallites with the size range of hundreds of millimetres liquified within a matter of seconds, larger samples took longer to liquify.

This made initial attempts at harvesting a suitable sample and subsequent preparation impossible. These preparations took too long for δ-valerolactam and all crystallites liquified too quickly. Literature research could not readily deliver an explanation on why this occurred, and it was suggested that the light from the microscope used for the examination/preparation could have been enough of a source of heat to reach the melting point. The samples where therefore cooled and stored in a dry ice container.

The cooled, harvested crystals remained solid for long enough for all preparations to take place and only the edges of most crystallites were liquified. Unfortunately, the so harvested crystals did not give useful data.

Since cooling the crystals seemed to slow down what appeared to be a melting process, we suspected that the crystallites had partially molten around the edges, which could have recrystallised uncontrollably when brought into the cold nitrogen gas stream of the SC-XRD machine. It should be mentioned at this point, that these initial attempts at acquiring data did result in a data set of δ-valerolactam. However, the acquired data was of no satisfying quality and the refinement process revealed evidence for heavy disorder.

According to the supplier, δ-valerolactam is suggested to be stored at 8 °C. However, when the sample bottle was left to stand at room temperature, the content was still solid after more than 72 h. The liquification only takes places, once a sample is taken from the bottle and brought into contact with fresh air. This suggested that δ-valerolactam did not in fact melt, but liquified through the contact with air.

A look into properties of the related lactams showed that ε-caprolactam is known for its hygroscopy. When left to stand in air, ε-caprolactam tends to form oil-like, highly viscous layers in which a residual amount of solid remains. Hygroscopy, the tendency to absorb water from the surrounding air is a well-known property of many solid compounds. However, there are substances known to absorb so much water from the air, that they readily dissolve in the absorbed water due to their high solubility. This as *deliquescence*[79] known phenomenon can be observed for salts like sodium hydroxide or calcium chloride. We concluded that δ-valerolactam might exhibit similar deliquescence. Whereas similar sized samples of ε-caprolactam took hours to liquify, δ-valerolactam seemed to simply liquify faster. Another possible explanation which would show the same outcome could be the formation of a eutectic system of δ-valerolactam and water.

A eutectic system is defined as homogenous mixtures of different compounds that exhibit a melting point below the melting points of the respective pure components. If δ-valerolactam absorbed water from the air and the superficially absorbed water would form a eutectic system, the resulting liquified layer could allow more water to reach deeper layers of the liquifying crystals. Both of these plausible reasons would be slowed down considerably by decreased temperature. Lower temperatures could lead to a decreased solubility of δ-valerolactam in water or the temperature could be too low even for a eutectic system to melt. The main difference would be that the formation of such a eutectic system might be controlled to give sharply defined hydrates, but because the main objective was the acquisition of appropriate data, no further research was undertaken in this direction. Furthermore, any such eutectic would represent a binary system in which δ-valerolactam would be influenced by water.

As already mentioned, certain compounds require single crystal preparation under inert conditions. The preparation of suitable single crystals for SC-XRD characterisation of many pyrophoric, organometallic compounds is done under strict exclusion of air. Special equipment for work under inert conditions are commercially available, but the investment in such equipment is only sensible if large numbers of potential samples justify such an investment. The University of Lincoln does not possess such equipment. However, the general principle is fairly simple. A vessel is usually filled with liquid nitrogen which simply evaporates to give a cool stream of nitrogen gas. The stream is than directed to the work surface that crystals would be prepared on, often in the form of a table-like surface which can be placed under a microscope. It was thought that such a sophisticated piece of equipment would not be necessary in the case of δ-valerolactam, we anticipated that a general avoidance of humidity could allow single crystals to be prepared fast enough for a measurement to be successful. We therefore built a simple set-up that allowed a focused stream of nitrogen gas to be directed onto a work surface on which the crystals were then successfully prepared.

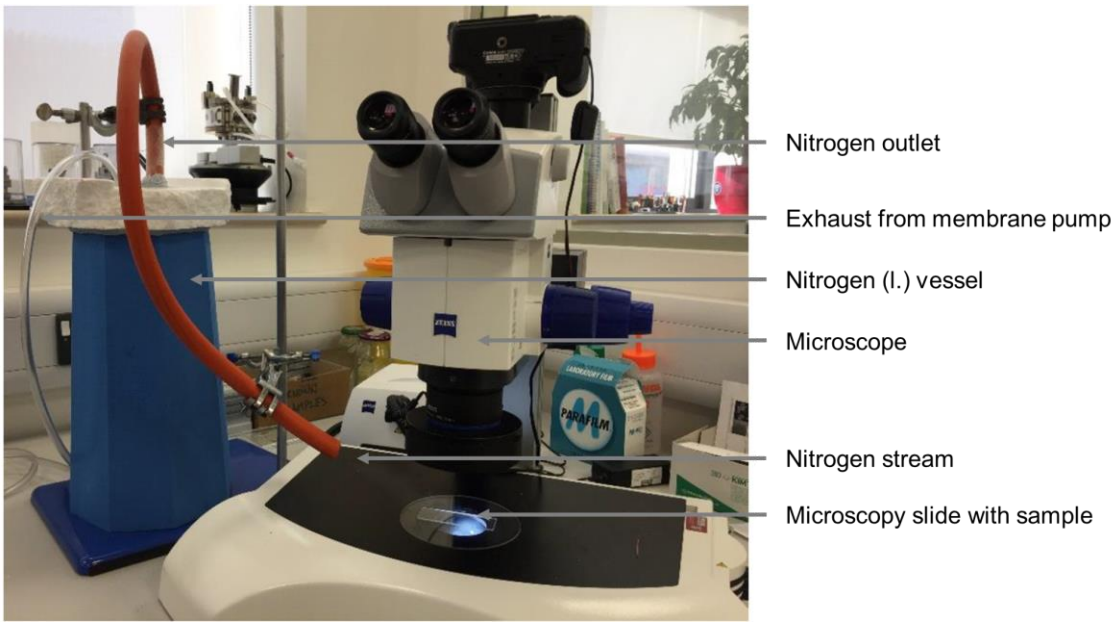

Fig. 3.3 A self-made cooling device allowed for the successful acquisition of single crystal structural data of δ-valerolactam.

Figure 3.3 shows the set-up used for the preparation of the δ-valerolactam crystals. An insulated vessel was filled with nitrogen. The exhaust line of a membrane pump was directed into the liquid nitrogen to force a relatively constant stream of nitrogen to be liberated from the vessel. The vessel was sealed to allow the evolving gas to be channelled through a second line of tubing which was directed at the workstation under the microscope.

Single crystal structure

The successfully measured and refined single crystal structure of δ-valerolactam presented itself in the monoclinic space group $P2_1/c$ with only one molecule in the asymmetric unit. The molecules were found in a half-chair conformation in the crystal with striking similarity to related systems like cyclohexene. Direct comparison with the other homologous lactams did not show any significantly different bond lengths or angles. There are however discrepancies with theoretical calculations done on δ-valerolactam. The length of the amide bond had been calculated to be 1.372 Å, the empirically found length was found to be shorter with 1.3344 Å. The found amide bond length fits better with the corresponding amide bond lengths within the homologous series of lactams. Additionally, calculations predicted the torsion angle along the amide bond to be -25.0 ° (MNDO-calculations[80]) or -17.8 ° (*ab initio*-calculations[81]). The empirical data showed a torsion angle of -2.8(2) °, which is much closer to planarity than what the predictions suggested.

This also fits better with previously described single crystal structures of lactams, which generally exhibit almost co-planarity along their amide bonds due to their partial double bond character. Other experiments in the gas phase had also suggested that conformations other than the half-chair are possible[82]. However, the presented crystal structure only displays one of presumably more possible conformations and does not exclude the possibility of others.

A more factual description of the half-chair conformation can be given through atom C2 and C3. Both exhibit a slight deviation from the amide bond plane (0.417 Å for C2, 0.325 Å for C3) which is comparable to a described structure of cyclohexene (0.366 Å and 0.373 Å respectively)[83].

A look at the crystal packing presents intermolecular dimers of the amide groups with hydrogen bonds between N-H···O=C. They are best described by the common amide dimer graph set descriptor $R_2^2(8)$, which can also be found for many small to middle sized lactams. Both the distance of 2.907 Å and the angle of 176.3 ° suggest that this amide-amide contact is moderately strong. Since unsubstituted lactams do not contain any other functionality that could form more complex structures other than interactions of the backbone, this dimerisation appears the be the major stabilisation factor within the crystal. A wider view showed long C-H···O contacts with a length of 3.4210 Å with a descriptor of $R_2^2(10)$, which connect the dimers with each other in chain-like structures along the crystallographic *b* axis. These chains then arrange in sheet-like structures along the *a* axis (Fig 3.4) in which all the amide planes are found to be parallel to each other. The sheets between themselves are arranged in a zig-zag fashion, with an angle of 65.6 ° between the planes.

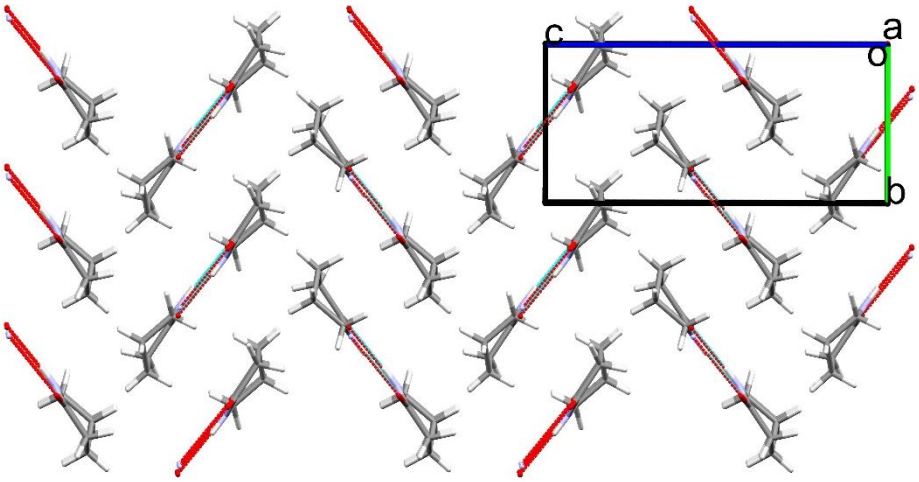

Fig. 3.4 The crystal packing of this δ-valerolactam structure shows that the chains, formed by the amide-amide dimers, form sheets themselves. The sheets display an angle of about 66 ° between each other.

Polymorph **B**

As already mentioned, initial attempts at harvesting and preparing a suitable single crystal after cooling the entire sample with dry ice gave a set of data with only unsatisfying goodness. The following descriptions of this polymorph are to be viewed under this aspect and no final conclusions should be drawn from this. For the sake of clarity, the following polymorph shall be denoted as data set/polymorph **B**.

Polymorph **B** was measured as a triclinic space group *P-1*, one molecule can be found in the asymmetric unit. Comparison of the bond lengths and angles did not show any unusual values. The C-N lactam bond is found to be 1.315 Å, which is only slightly shorter than in polymorph **A**. However, this is shorter than the previously mentioned calculated values (Δ[d(C-N)=0.057 Å]). The torsion angle along the amide bond was found to be -4.85 °. This again is a lot more similar to polymorph **A** and co-planarity than it is to the theoretically calculated values. The lactam ring itself is found in a very similar conformation like polymorph **A** with C3 and C4 deviating from the mean amide plane by 0.383 Å and 0.337 Å respectively. This leads to a half-chair conformation for **B** as well. The main difference between the polymorphs here is the direction of how C3 and C4 stand away from the amide plane, which is reversed for the respective polymorphs (Fig. 3.5).

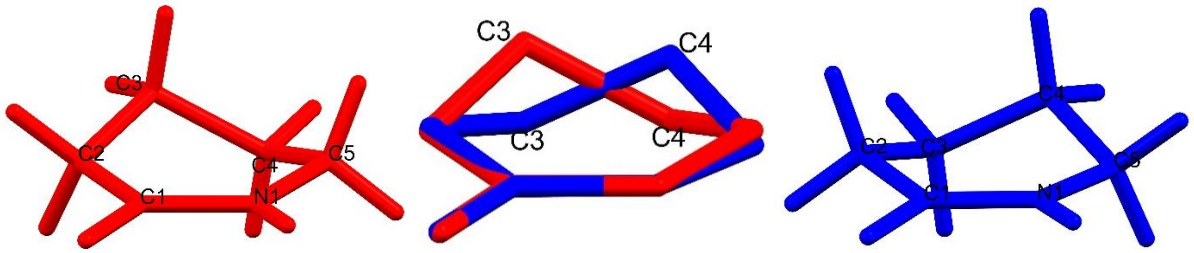

*Fig. 3.5 Comparison of the two measured polymorphs shows that the overall conformation of the lactam ring is similar, but that the deviation of C3 and C4 from the amide plane is reversed. Polymorph **A** blue; Polymorph **B** red.*

Polymorph **B** shows amide dimer formation, just as polymorph **A** does, the same graph set descriptor $R_2^2(8)$ applies to **B** as well. Both the distance and angle of the amide connection are very similar.

The packing of **B** on the other hand shows distinct differences to its polymorph. Whereas **A** displays a zig-zag-type arrangement of the amide dimers, **B** exhibits stacked planes along the crystallographic *b* axis. Within those planes, all amide groups are parallel to each other (Fig. 3.6).

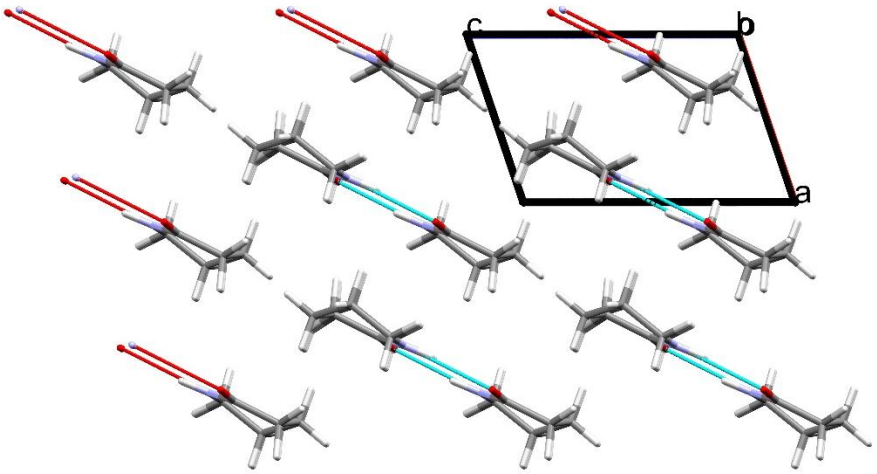

*Fig. 3.6 The packing of polymorph **B** is different from **A** in that it does not form zig-zag arranged sheets, but that the molecular sheets are formed parallel to each other.*

3.4) Summary and Conclusion

Comparison within the homologous series

Until now, the single crystal structures of samples for the four-to ten-membered lactam rings have been described. However, some of these structures were measured under different conditions than under which the here presented data were acquired. For example, the structures of ε-caprolactam, η -caprylolactam and θ-pelargolactam were measured at room temperature. Whereas the published data for ε-capro- (CSD entry: CAPLAC) and η -caprylolactam (CSD entry: CAPRYL) are well resolved and refined, the published data for the θ-pelargolactam (CSD entry: PELARG) shows heavy disorder. The three-membered ring could not be measured because the unsubstituted three-membered lactam has not been successfully isolated and characterised so far.

The amide bond lengths of these lactams can be found between 1.328 Å and 1.335 Å, which is on average only slightly shorter than for secondary amides in general (1.334 Å[84]). One exception from is the ten-membered θ-pelargolactam which exhibits a significantly longer amide bond length of 1.426 Å. It has not been fully explained why this particular bond length is elongated to this extend. It is possible that this is part of a trend for larger lactams. The next larger lactam, the eleven-membered caprinolactam[85], has been described in literature before and a single crystal structure does exist but only of the lactam's hydrochloride. However, because of the mentioned heavily disordered data, this value has to be considered very careful and might not reflect the factually accurate behaviour of θ-pelargolactam.

As it is to be expected, N-H···O=C contacts can be found for all the unsubstituted lactams. Comparing the structure of these hydrogen bonds shows that the smaller rings (4-7) tend towards dimeric contacts with the $R_2^2(8)$ motive, the larger rings (8-10) display a tendency to form C(4) chains. The only exception from this tendency is the four-membered β-propiolactam, which exhibits both $R_2^2(8)$-dimers and C(4) chains. An explanation for the trends observed can be found in the increasing steric demand of the carbon backbone of the rings. The comparatively small four-membered rings form dimers because this seems to be the most favourable interaction possible. Because the carbon backbone only consists of two carbons, the amide groups are able to stack close enough to also form the C(4)-chain interactions. The γ-butyrolactam rings are only slightly larger, but this increase in size seems to be enough to disable the additional formation of the C(4)-chain interaction. Once the rings have reached a certain size, with the cut-off being the eight-membered ζ-enantholactam, the ring seems to be too large to even form dimers and the molecules resort to the formation of C(4)-chains as their leading motif.

A look into the nature of the amide bonds shows that starting from β-propiolactam to the ζ-enantholactam the amide bond displays a *cis*-structure, the larger rings show *trans*-amide bonds. The transition from *cis* to *trans* cannot be directly linked to the leading hydrogen bond motif. Caprolactam, which presents *cis*-structure forms amide dimers, ζ-enantholactam which also presents *cis*-structure, forms C(4) chains. One explanation could come from the nature of the lactam bond. Amide bonds are considered comparatively stable. An equilibrium between an open chain *vs.* closed ring has not been observed for simple lactams dissolved in inert solvents as it has been for sugars. Considering that the amide bond is not able to rotate freely either, it seems plausible that during the formation of those lactams, a *trans*-amide bond is preferred, and a *cis*-amide bond will not convert into a *trans*-bond by itself and *vice versa*. This could mean, that *cis*-caprylolactam could exist, but the considered data simply do not reflect this. Different synthetic approaches could therefore proof this concept and lead to both forms of larger lactams.

Comparison of the donor (D)-acceptor (A) lengths (d(DH···A)) within the homologous series of lactams shows a decline from β-propiolactam to ζ-enantholactam, with 2.927 Å and 2.815 Å respectively. The influence of the transition from $R_2^2(8)$ to C(4) interactions between ε-capro- and ζ-enantholactam on the strength of the interactons is not quite clear. Both ζ-enantho- and η-caprylolactam (2.864 Å) exhibit shorter N-H···O contacts than all the other lactams. Furthermore, comparison of the donor-acceptor angles shows a significant difference between β-propiolactam and all other lactams (apart from θ-pelargolactam). The five-to nine-membered lactams show an average <(DHA) angle of 171.9 ° with a median of 170.8 ° and fall within a range of about ± 5.5 °. β-Propiolactam however has a slightly lower <(DHA) angle of 152.8 °.

This led to the following conclusions:

- The size of the carbon backbone determines the ability to form hydrogen bonding patterns and influences the packing of the crystal through this. The smaller rings are able to form the seemingly preferred amide dimers, the larger rings can only form C(4)-chains because of their steric hinderance.
- β-Propiolactam is particularly small and can form both dimers and chains. The formation of both interactions seems to be preferential over shorter contacts. This can easily be explained by the fact that two strong interactions are most likely energetically favourable over one that is only slightly stronger.
- β-Propiolactam shows slightly widened (DHA) angles because both hydrogen bonding patterns allow the energetic loss to be compensated, whereas all other lactams only show either dimers or chains and therefore form the generally preferred angles closer to 180 °.
- The smaller, *cis*-positioned lactams show a decline in hydrogen bond lengths, the *trans*-positioned η-caprylolactam shows a slight elongation of the equivalent hydrogen contact. We believe that this trend results from a combination of the position of the amide bond and the hydrogen bonding pattern. ε-Caprolactam, which is still able to form dimers follows the initial trend of a slow but steady decline. ζ-Enantholactam, which shows *cis*-amide bonds but has to adopt C(4)-chains, compensates the less favourable hydrogen bonding pattern by forming shorter hydrogen bonds. η-Caprylolactam shows longer hydrogen bonds again, because of the transition from *cis*- to *trans*-amide bonds.

Hydrolytic stability

As already mentioned, lactams have not been studied as thoroughly as other compound classes have. On the other hand, ring opening reactions, especially through hydrolysis / nucleophilic attack have been investigated in several studies. This particular interest was sparked by the discovery of the enzymatically accelerated hydrolysis of β-lactam systems. As discussed, empirical evidence shows, that β-propiolactam and δ-valerolactam exhibit somewhat anomalies within the homologous series in this respect. The accelerated hydrolysis of propiolactam rings can easily be explained by the higher ring strain in comparison to other lactams, but this does not fully explain the accelerated hydrolysis of δ-valerolactam. One possible explanation was that δ-valerolactam could have a significantly longer and therefore weaker amide bond in comparison to the other lactams. This explanation was supported by theoretical studies that predicted longer amide bonds for δ-valerolactam. However, the acquired single crystal data would dispute this. Studies by Imming *et. al*. have suggested, that valerolactams, if unrestricted, adopt conformations that could allow easier access of a nucleophile to the carbonyl carbon. This facilitated attack would sufficiently explain valerolactam's anomaly in terms of hydrolysis but was never supported by SC-XRD data of the free δ-valerolactam. The fact that the amide bond of valerolactam falls well within the range of amide bond lengths for other free lactams clearly suggests

that bond length is not the determining factor for the hydrolysis. We therefore conclude that Immings hypothesis of conformational facilitation of nucleophilic attack is more likely to be correct.

---

[75] P. Imming, B. Klar, D. Dix, *J. Med. Chem.* **2000**, *43*, 4328-4331.
[76] A) G. Bolla, A. Nangia, *Chem. Comm.* **2015**, *51*, 15578-15581.; B) F. Marchetti, G. Pampaloni, S. Zacchini, *RSC Advances* **2013**, *25*, 10007-10013.; C) J.L. Bear, R.S. Lifsey, L.K. Chau, M.Q. Ahsan, J.D. Korp, M. Chavan, K.M. Kadish, *J. Chem. Soc., Dalton Trans* **1989**, *1*, 93-100.; D) C. Munhoz, P.C. Isolani, G. Vicentini, J. Zukerman-Schpector, *J. Alloys Compd.* **1998**, *275*, 782-784.
[77] A) J. Pabba, B.P. Rempel, S.G. Withers, A. Vasella, *Helv. Chim. Acta* **2006**, *89*, 635-666.; B) S.R. Ramakumar, K. Venkatesan, H.P. Weber, *Helv. Chim. Acta* **1977**, *60*, 1691-1696.; C) M. Wu, D. Ma, *Angew. Chem., Int. Ed.* **2013**, *52*, 9759-9762.
[78] A) F.K. Winkler, J.D. Dunitz, *Acta Cryst. B* **1975**, *31*, 268-269.; B) F.K. Winkler, P. Seiler, *Acta Cryst. B* **1979**, *35*, 1920-1922.; C) F.K. Winkler, J.D. Dunitz, *Acta Cryst. B* **1975**, *31*, 276-278.; D) F.K. Winkler, J.D. Dunitz, *Acta Cryst. B* **1975**, *31*, 281-283.
[79] A.D. McNaught, A. Wilkinson *IUPAC. Compendium of Chemical Terminology*, 2nd edition, Blackwell Scientific Publications, Oxford, **1997**.
[80] A) L. Treschanke, P. Rademacher, *J. Mol. Struct. (Theochem)* **1985**, *122*, 35-45.; B) L. Treschanke, P. Rademacher, *J. Mol. Struct. (Theochem)* **1985**, *122*, 47-57.
[81] N. Kuze, H. Funahashi, M. Ogawa, H. Tajiri, Y. Ohta, T. Usami, T. Sakaizumi, O. Ohashi, *J. Mol. Spectrosc.* **1999**, *198*, 381-386.
[82] R.G. Bird, V. Vaquero-Vara, D.P. Zaleski, B.H. Pate, D.W. Pratt, *J. Mol. Spectrosc.* **2012**, *280*, 42-46.
[83] R.M. Ibberon, M.T. Telling, S. Parson, *Cryst. Growth Des.* **2008**, *8*, 512-518.
[84] F.H. Allen, O. Kennard, D.G. Watson, L. Brammer, A.G. Orpen, *J. Chem. Soc. Perkin Trans. II* **1987**, 1-19.
[85] F.K. Winkler, J.D. Dunitz, *Acta Cryst. B* **1975**, *31*, 283-286

Chapter 4 - Does the exception prove the Rule? – A comparative study of supramolecular synthons in a series of lactam esters

4.1) Abstract

Chapter 3 had investigated the first published SC-XRD data set for free δ-valerolactam and had concluded that the conformational situation of this six-membered lactam is most likely to be responsible for its abnormal rate of hydrolysis within the homologous series of lactams. This chapter will focus on the studies of the conformational behaviour of N_α-ester/acid substituted lactams in general. Particular focus was paid to the complex relations between ring size, strategically selected substitution, the dominating amide bonding pattern and their effect on selected bond lengths and angles along the amide bond. For these studies, a number of new lactams were synthesised, and eight new SC-XRD structures were acquired. It was found that smaller esters will prefer an equatorial position, larger esters will adopt the axial site. Introduction of *N*-substitution will likely lead to axially positioned esters, with enantholactams being excluded from this general trend, which seem to accommodate equatorial esters and *N*-substitution through their ring size. With increasing ring size and steric demand of ester pendants, the amide bonding pattern transitions from the preferred $R_2^2(8)$ amide dimers, to C(4)-chains. One enantholactam displays a somewhat unique bonding pattern amongst the studied structures with the formation of $R_2^2(8)$ N-H···O/C-H···O=C heterodimers. The studied free acids are also to be excluded from the general trends as their strong hydrogen bonds seem to dominate the packing of their respective compounds and lead to different binding motifs. The introduction of the electron withdrawing Boc group leads to a significant elongation of the amide bond. For one studied example, it was found that this leads to hydrolytic susceptibility which should be considered for synthetic application of complex lactam systems.

4.2) Introduction

Lactams, *i.e.* cyclic amides, are a classic subgroup of carbonyl compounds and can also be considered heterocycles. The general group of lactams is comparatively widely spread, cyclic amides can be found in many biological systems or artificial environments. For many aspects of chemical research, it is of utmost importance to understand the chemical and physicochemical behaviour of parent compounds to draw conclusions on more complex systems. Studies concerning reactivity, such as stability against all kinds of reagents, kinetics and conformational behaviour build the fundamental background knowledge that is very often required to fully understand unprecedented problems. Lactams have been somewhat neglected in this respect as there has been only little fundamental research into their fundamental properties

One particularly important property of amides is their characteristic tendency to form partial double bonds along the C-N bond. One of the resulting consequences is the formation of both *cis*- and *trans*-positioned amides, depending on their respective substitution.

And despite the fact, that the bonding situation within the homologous series of lactams is generally considered quite consistent, experiments on the hydrolytic stability of lactams have shown anomalies that could not be explained simply by comparing typical parameters of the amide bonds. Both the four-membered and the six-membered lactams hydrolyse significantly faster than their neighbours within the homologous series. Thorough, unbiased comparison of the amide bond situation within the lactams has not been possible so far, because SC-XRD data of the free, unsubstituted δ-valerolactam was not available. For example, one single crystal structure of a neodymium perchlorate, coordinated with eight δ-valerolactam molecules, shows that the amide bond lengths can differ significantly (1.300 Å – 1.339 Å) for the same compound[86]. Following the successful acquisition of the first SC-XRD data set for δ-valerolactam, Chapter 3 concluded with the confirmation of a suggested explanation on the seeming discrepancy in hydrolysis rates among simple lactams. It was confirmed that the particular nature of the lactam bond, *i.e.* the length, does not seem to be the determining factor in these cases. It seems that the original suggestion made by Imming *et. al.*, that δ-valerolactam exhibits special conformational behaviour which enables facilitated nucleophilic attack is likely to be correct.

The already presented experimental approach to utilise a Dieckmann-type cyclisation on strategically substituted caprolactams had raised the question about our fundamental understanding of the conformational situation in those lactams and the influence on this experimental approach. We found that such studies had not been done on the conformational behaviour of lactams and especially N_{α}-substituted lactam esters. A look into the literature showed, that only very few free lactams with this specific substitution pattern had been described in terms of their physicochemical behaviour.

To investigate and understand these systems in a wider context than just the eminent caprolactams, a series of new lactams had to be synthesised for a more comprehensive comparison. The newly synthesised lactams were characterised by SC-XRD and a comparative investigation was started together with previously acquired data sets and already published structures.

The following descriptions focus on the studies on the relation between the structure of the investigated lactams and the respective position of N_{α}-substituted ester and acid groups, observed hydrogen bonding motifs and the packing in the crystalline state. All the herein discussed results come from obtained single crystal structural data, which means that they cannot be universally applied to the same compounds in solution. However, this does allowed the analysis of the bonding situation of the amide bonds and should advance our general understanding of the amide bond in substituted lactams.

4.3) Synthesis of a number of novel lactams

As mentioned before, initial research into published SC-XRD data on N_{α}-substituted lactam esters and acids showed that only very few structures under these criteria had been published. Even though many of the compounds had been described in literature in general, only few of them had been crystallised

and analysed. For that reason, it was decided that a more comprehensive study would require a number of lactam esters to be synthesised and characterised. Since the main objective of this study was to support our understanding of the conformational behaviour of caprolactam esters, it was decided that esters, their free acids and corresponding Boc protected lactams should function as related model systems (Fig. 4.1).

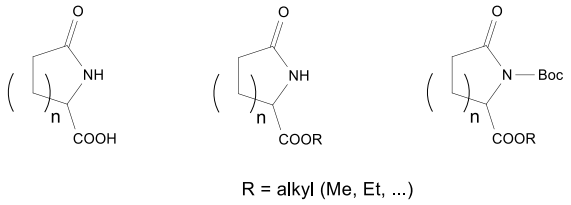

Fig. 4.1 Comprehensive studies on the conformational situation, the bonding and the packing patterns of lactam esters required more compounds to be synthesised. N_{α}-substituted lactam acids, esters and their respective Boc protected lactams were targeted.

γ-Butyrolactams

The already studied caprolactam esters had been synthesised either through the cyclisation of 2-aminopimelic acid or *via* Grubb's catalysed ring closure metatheses. Equally demanding synthesis was not thought to be necessary as the free acid, sold under pyroglutamic acid, is readily commercially available and was to be esterified. Pyroglutamic acid itself had already been characterised with SC-XRD. The esterification of pyroglutamic acid to its corresponding methyl and ethyl ester seemed straightforward. An analogue procedure to the esterification of 2-aminopimelic acid was chosen because of the low synthetic effort and the excellent yield in previous uses.

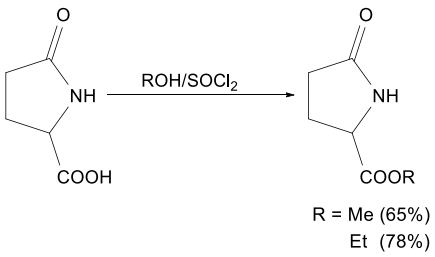

Fig. 4.2 The esterification of pyroglutamic acid using the ROH/$SOCl_2$ method gave good yields of 65% and 78% for the methyl and ethyl ester respectively.

Just like the esterification of 2-aminopimelic acid, thionyl chloride was added to cooled alkyl alcohol and subsequent addition of pyroglutamic acid gave the corresponding esters with good yields of 65% for the methyl and 78% for the ethyl ester (Fig. 4.2). These yields were determined by NMR, because the raw product mixtures contained side products, contrary to earlier experience with this procedure. TLC analysis gave no evidence of separation of the main products from its side products and because the crude product mixture was of a viscous, oily nature, recrystallisation did not succeed. Furthermore, because of the amounts of starting materials used, the product mixture only consisted of about a few millilitres, adding challenge to an option of distillation as purification.

It was therefore decided, that since a different esterification method would have to be used for secondary and/or tertiary alcohol ester such as *iso*-propyl or *tert*-butyl esters, the methyl and ethyl ester should be synthesized through a different approach again. An attempt at using a *Fischer esterification* for the methyl and ethyl esters was made. Pyroglutamic acid was dissolved in chloroform, the respective primary alcohol and sulfuric acid were added, and the mixture was refluxed using an inverted *Dean-Stark* trap. TLC analysis of the reaction mixture gave no indication of the desired ester being formed after 24 h and the attempt was declared unsuccessful.

Following these initial attempts, it was decided to use the *Steglich esterification* next. The Steglich esterification is a synthetically more demanding protocol, which uses a carbodiimide as an activating agent for carboxylic acids and *Steglich's base* (*N*,*N*-dimethylpyridine-4-amine, *DMAP*) as a catalyst. This procedure has the distinct advantage that sensitive, and also sterically demanding substrates like *tert*-butanol can be esterified. To synthesise the desired esters, pyroglutamic acid was dissolved in dry dichloromethane together with a small amount of DMAP and the respective alkyl alcohol before the mixture was cooled to 0 °C. The cooling of the mixture is recommended to supress side reactions of intermediates that form during the reaction. Following a standard protocol, dicyclohexyl carbodiimide (*DCC*) was utilised as carbodiimide component, which was added once the reaction mixture had been cooled. The generally accepted mechanism is displayed in Fig. 4.3 for a methyl ester and starts with an acid-base reaction between the carboxylic acid and the carbodiimide. The resulting carboxylate is thought to attack the diimide carbon to form an *O*-acyluronium. The so formed uronium intermediates are known to undergo rearrangement side reactions, which can be avoided by a decrease in reaction temperature, hence the cooling to 0 °C. If this possible side reaction is avoided, the mechanism then suggests a nucleophilic attack of the DMAP catalyst on the acid components' carbonyl carbon, to give an activated DMAP ester species. The activated ester is then thought to be re-esterified by the provided nucleophile, *i.e.* the alkyl alcohol to ultimately give the desired ester.

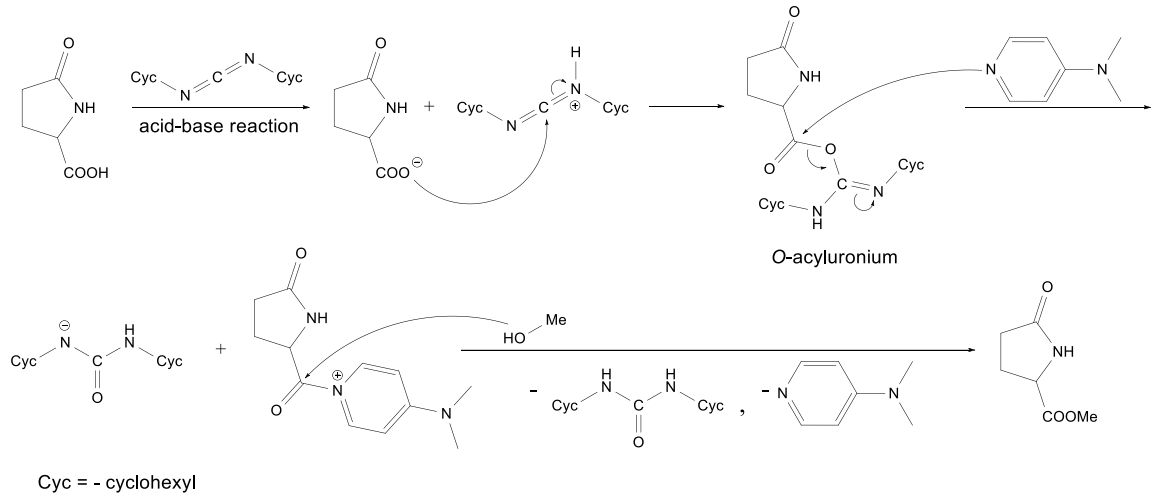

Fig. 4.3 The mechanism for the Steglich esterification, here shown for pyroglutamic acid and methanol. The first step is the formation of an O-acyluronium species, which forms an activated ester with DMAP, which then reacts with the alcohol component to give the desired product.

Apart from the already mentioned methyl, ethyl, *iso*-propyl and *tert*-butyl ester of pyroglutamic acid, the (-)menthyl ester was prepared as well (Fig. 4.4). The menthyl ester was prepared as a model system to investigate three different aspects:

1.) What synthetic effort would be required to form these esters and could this potentially be used as an alternative to form more esters of the studied caprolactam system
2.) Could a menthyl ester be used to separate the resulting diastereomers of a lactam ester
3.) How would each of the sterically demanding menthyl enantiomers arrange around the lactam ring and could that be used to influence potential Dieckmann cyclisations as lain out in Chapter 2

Both (+) and (-)menthol are available as enantiomerically pure materials. Only the (-)menthyl ester was prepared initially, the equivalent enantiomer was planned to be prepared once the (-)menthyl ester was successfully prepared and investigated. Table 4.1 shows the obtained product yields for all five initially tried esters.

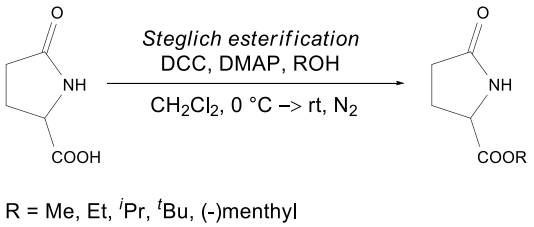

Fig. 4.56 The Steglich esterification procedure was used to prepare five pyroglutamate esters of varying size.

Table 4.1 All five pyroglutamate esters could be prepared successfully, but the methyl and ethyl ester could not be solidified and the (-)menthyl ester did not yield single crystalline material, suitable for SC-XRD.

Pyroglutamic acid	-	Crystalline solid	SC-XRD data available
Methyl ester	15 %	Viscous oil	No SC-XRD data
Ethyl ester	23 %	Viscous oil	No SC-XRD data
*iso-P*ropyl ester	67 %	Ready solidification	SC-XRD data acquired
*tert-B*utyl ester	8 %	Ready solidification	SC-XRD data acquired
(-)Menthyl ester	71 %	Ready solidification	No SC-XRD data

All five ester were successfully prepared using the Steglich esterification, with different product yields. The lowest yield was observed for the *tert*-butyl ester with only about 8% product yield, which might simply be a result of the unoptimized reaction conditions and the steric hindrance. The comparatively low yields of the methyl and ethyl ester cannot be as easily explained. However, this was less relevant because the $SOCl_2$/ROH procedure had been proven to give appropriate yields for synthesis and the Steglich esterified products were only prepared for analytical purposes. Both the *iso*-propyl and (-)menthyl ester were formed in good yields of 67% and 71%, respectively.

The subsequent purification procedure appeared to be straightforward at first, TLC analysis indicated good chromatographic separation after liquid-liquid extractive work-up. However, once the crude product mixtures were subjected to column chromatographic purification, it was observed that the vast majority of obtained fractions contained small amounts of dicyclohexyl urea as an impurity. The formation of this urea derivative is of no surprise, the reaction mechanism itself suggests this. Unfortunately, the acquired, chromatographed products still contained small amounts of dicyclohexyl urea. Dicyclohexyl urea is a crystalline compound which appears to crystallise readily, even from mixtures in which it only forms a minor component. In fact, many crystallisation attempts with the slightly impure products gave single crystals of dicyclohexyl urea, rather than the lactam esters. A second column chromatographic purification step was required to fully separate the impurity from the products, which could then be crystallised successfully. Considering that the Steglich esterification of pyroglutamic acid gave good yields for the *iso*-propyl and (-)menthyl ester, but that the purification seemed time consuming (but possible), it was decided that this method could be a viable option for the synthesis of larger ester of caprolactams.

Unfortunately, both TLC and column chromatography did not show any signs of successful separation of the diastereomers of the pyroglutamic acid (-)menthol ester. It is possible, that chromatographic separation *via* analytical high-performance liquid chromatography (HPLC) and its preparative equivalent could separate the diastereomers. However, because preparative HPLC purification on gram-scaled syntheses is considerably expensive, time consuming and not readily available at the University of Lincoln, it was concluded that the menthyl ester could not be used to separate the lactam ester enantiomers for the here presented purposes. The introduction of enantiomerically pure chiral auxiliaries is a relatively common method for the separation of enantiomeric mixtures and has been shown to work multiple times. A possible explanation why this did not seem to be a workable option for this pyroglutamic acid ester is that the presumed interactions of the two different diastereomers with SiO_2 as a stationary phase are too similar to separate them efficiently enough. Considering that pyroglutamate esters are comparatively small molecules with only two functional groups other than CH_X-groups, a lack of sufficient interaction seems plausible.

The methyl and ethyl pyroglutamates were obtained as viscous oils, which unfortunately did not crystallise by themselves even after several weeks. Multiple attempts at crystallising them through slow solvent evaporation and through rapid cooling and subsequent controlled warming did not give any single crystalline material. On the other hand, the *iso*-propyl, *tert*-butyl and (-)menthyl pyroglutamates readily solidified at room temperature. Both the *iso*-propyl and *tert*-butyl esters gave single crystals suitable for SC-XRD analysis *via* slow solvent evaporation crystallisation, the (-)menthyl ester only gave twinned crystals and/or amorphous solids. Several further attempts at crystallising the menthyl ester with *solvent diffusion crystallisation* did not succeed either.

Another attempt was made at obtaining a single crystalline sample through controlled cycled cooling and re-heating. Unfortunately, the menthyl ester seemed to decompose when heated to its melting point around and above 110 °C. And despite continuous efforts to obtain SC-XRD date for the menthyl ester, no suitable material could be obtained so far (Fig. 4.5).

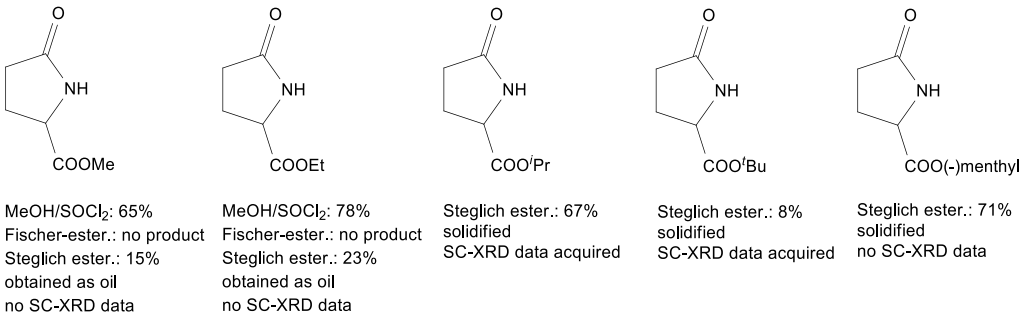

Fig. 4.5 Five pyroglutamate esters were synthesised through different procedures, the iso-propyl and tert-butyl esters were analysised through SC-XRD successfully.

This left the structural analysis with SC-XRD data for the *iso*-propyl and *tert*-butyl pyroglutamate, which shall be presented and discussed later on.

δ-Valerolactams

Our studies on the mechanism of the Dieckmann-type cyclisation of caprolactam esters had led to the synthesis of equivalent valerolactams. The details of the synthesis of a Boc protected valerolactam methyl ester are presented in Chapter 2. Some of the newly synthesised valerolactam precursors could be successfully crystallised. The respective free acid and its methyl ester crystallised readily after their synthesis and it was possible to acquire SC-XRD data for both. Unfortunately, the Boc protected methyl ester could only be obtained as an oil and all attempts at crystallisation remained unsuccessful (Fig. 4.6).

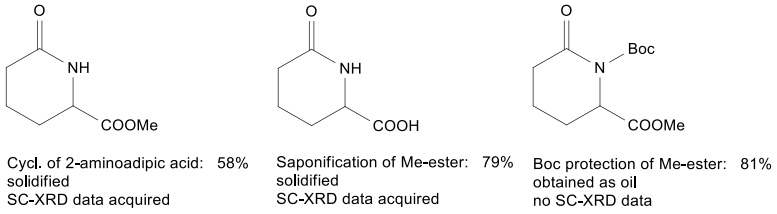

Fig. 4.6 The synthesis of two valerolactam esters and one acid yielded SC-XRD data for the free lactam methyl ester and the free acid. For details on the synthesis, please see Chapter 2.

ε-Caprolactams

As already discussed in Chapter 1, the caprolactam esters were synthesised started from 2-aminopimelic acid which was esterified and subsequently cyclised. The resulting caprolactam methyl ester has also been saponified and re-esterified to give the ethyl ester. The resulting free acid and both the methyl and ethyl ester had already been characterised by SC-XRD successfully. As further discussed in Chapter 2, it was found that the change from a methyl to an ethyl ester had shown an increase in product yield after Dieckmann-type cyclisation.

The experiments on how to esterify pyroglutamic acid were designed to establish a procedure that could also be used for the caprolactam acid (Fig. 4.7) besides the intention to acquire structural data.

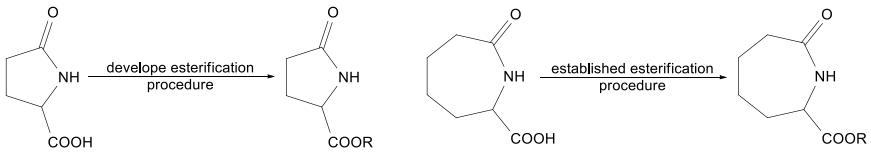

Fig. 4.7 The development of an esterification procedure for pyroglutamic acid was carried out as a model for the establishment of an equivalent procedure for caprolactam esters.

The Steglich esterification protocol gave moderately good yields for *iso*-propyl and menthyl esters and it was planned to employ this protocol to produce analogue caprolactam esters. Following the same procedure, the free caprolactam ester, prepared through saponification of the corresponding methyl ester, was tried. Unfortunately, the free acid did not show any signs of dissolution in CH_2Cl_2. However, because the free acid did dissolve in *iso*-propanol, even though only slowly and incompletely, it was attempted to proceed with the esterification. To overcome the solubility issue, a large excess of *iso*-propanol was added to the mixture to serve both as a reagent and co-solvent with CH_2Cl_2. TLC analysis of the reaction mixture did not show any indications of a potential product and the reaction was declared unsuccessful after 72 h. CH_2Cl_2 was initially chosen as solvent, because the original procedure by Neises and Steglich found CH_2Cl_2 to work well for a large number of substrates[87] (Fig. 4.8). However, the authors also mention that DMF can be used for esterifications of substrates with low solubility in CH_2Cl_2. Identical to the first attempt, the free caprolactam acid did not visibly dissolve in DMF either. Despite this, the procedure was carried out and a second attempt, using a large excess of *iso*-propanol as co-solvent was tried as well. Again, TLC analysis did not show any signs of product formation within 72 h and these esterification attempts were declared unsuccessful as well.

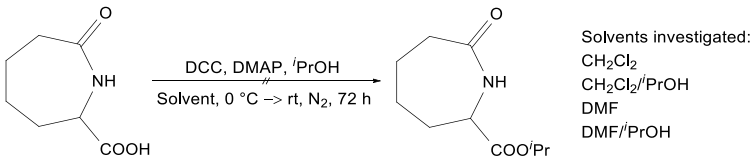

Fig. 4.8 Attempts at esterifying the free caprolactam acid using the Steglich esterification did not succeed. Four different solvent systems were investigated, but the free acid did not appear to dissolve in either.

Another attempt to find a viable synthetic procedure was made, trying to transform the free acid into an acyl chloride. Despite the fact, that pyroglutamic acid had not served well as a model system for the Steglich esterification, it was decided that the cost of 2-aminopimelic acid justified the use of pyroglutamic acid as a model again. A well-known method to produce acyl chlorides is the reaction of carboxylic acids with $SOCl_2$ which can then be treated with alcohols to give esters. However, attempts at synthesising the respective acyl chloride of pyroglutamic acid were not successful. Microscale preparations of the free caprolactam acid with $SOCl_2$ and subsequent one-pot alcoholysis did not show signs of product formation either (Fig. 4.9).

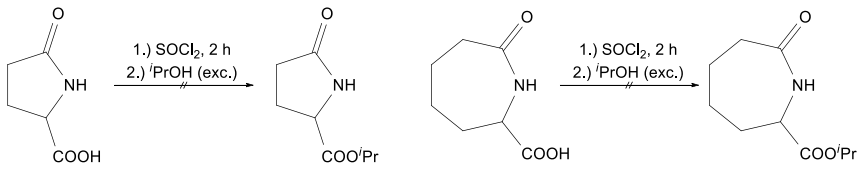

Fig. 4.9 The formation of an acyl chloride with $SOCl_2$ and subsequent alcoholysis with iso-propanol did not yield the respective esters, neither for pyroglutamic acid nor for the free caprolactam acid.

Because all attempts at generating further caprolactam esters were found to be unsuccessful, it was decided that the established synthetic approach starting from 2-aminopimelic acid was to be revised. Caprolactams are synthesised on an industrial scale using the *Beckmann rearrangement*. A very inexpensive starting material for the Beckmann rearrangement is cyclohexanone. In a first step, this ketone is transformed into a ketoxime through the condensation reaction of cyclohexanone and hydroxylamine. Once the ketoxime is formed and purified, the rearrangement is performed in which one of the substituents on the carbonyl carbon migrates to bind to the nitrogen. However, previous work has shown that Beckmann rearrangement would not lead to a caprolactam for the required starting material, a cyclohexanone ester (Fig. 4.10).

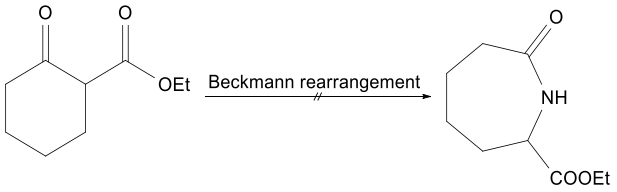

Fig. 4.10 The Beckmann rearrangement of ethyl-2-oxo-cyclohexanecarboxylate did not give the caprolactam ethyl ester as a potential precursor.

Closely related to the Beckmann rearrangement is the *Schmidt rearrangement*. Ring expansion through Beckmann reactions require the initial formation of oxime compounds first, the Schmidt reaction on the other hand can proceed to the ring expansion directly from a suitable ketone in a one-pot reaction (Fig. 4.11).

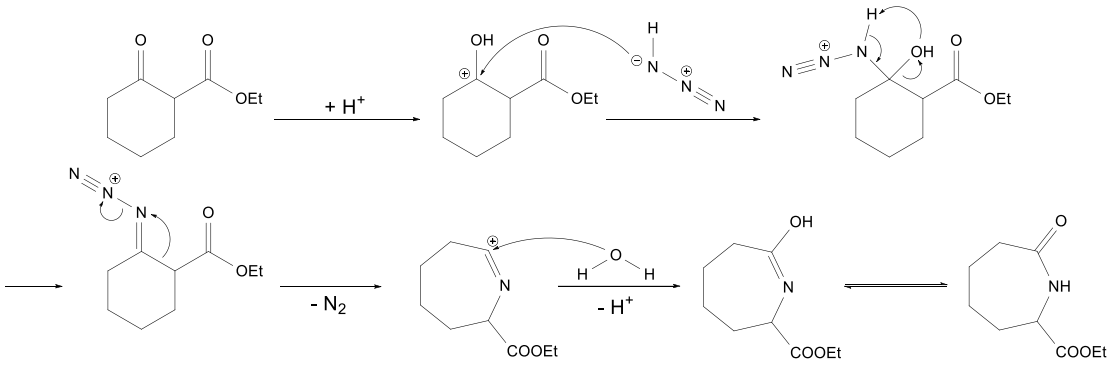

Fig. 4.11 The Schmidt rearrangement of ethyl-2-oxo-cyclohexanecarboxylate involves the acid promoted in situ generation of hydrazoic acid, which will lead to ring expansion under the loss of elemental nitrogen from an intermediary diazoimine.

The mechanistic details, regioselectivity and current research have already been discussed in detail in Chapter 1. One point to highlight that should be mentioned is the discussion for the Schmidt rearrangement over the Beckmann rearrangement. The use of hydrazoic acid should always be considered very carefully for its highly toxic and readily explosive properties. Beckmann rearrangements do not require the use of just hazardous reagents. However, since Beckmann rearrangement was not an option, the Schmidt rearrangement was investigated instead. Additionally, the manual handling of hydrazoic acid is not required itself. Most protocols operate using a strong acid, which is required for the ring expansion as well, and sodium azide, which is far less hazardous to handle. The hydrazoic acid is generated *in situ* and usually readily dissolves in the reaction solvent, often chloroform. Whereas the pure hydrazoic acid is an explosive liquid itself, solutions with less than 15% (v/v) are not considered explosive anymore[88].

Initial experiments were carried out using ethyl-2-oxocyclohexane carboxylate as starting material. This commercially available and significantly less expensive compound was subjected to Schmidt reaction conditions and gave the caprolactam ethyl ester in a moderate yield of 44%. Evaluation of both synthetic routes, methylation of 2-aminopimelic acid and subsequent cyclisation *vs*. ring expansion of the cyclohexanone derivates showed that the use of the Schmidt rearrangement gave a moderately lower yield. However, considering that the Schmidt reaction involved less practical work and that the caprolactam ethyl ester would give a significantly better yield for the envisaged Dieckmann-type ring closure, the benefits justified the hazards for the Schmidt rearrangement to be taken forward (Fig. 4.12).

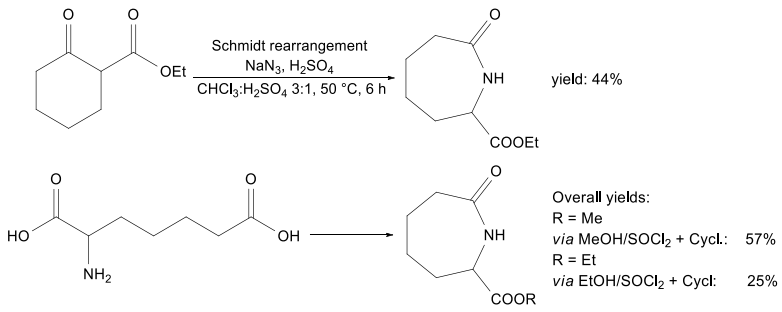

Fig. 4.12 The much more hazardous Schmidt rearrangement seemed justified over the previously applied procedure for its much better economic turnout because of the comparatively expensive 2-aminopimelic acid.

As pointed out in Chapter 2, the deprotonation of the α-ester position in the discussed caprolactam esters was thought to compete with the desired deprotonation of the α-ester position. To study the effect, the substitution of this acidic proton would have on the conformational behaviour and the subsequent Dieckmann-type ring closure, the introduction of a methyl group on that position was investigated. The introduction of a methyl group in the correct position proved to be fairly simple by adding methyl iodide to a solution of the cyclohexanone ester in acetone in the presence of K_2CO_3 as a base.

Chromatographic purification had to be carried out twice to obtain a pure product, but it was observed that the crude product mixture could be used for a Schmidt rearrangement after bifold liquid-liquid extraction without a loss of product yield. Following this, the Schmidt rearrangement was carried out equivalent to the non-methylated analogue. The so formed caprolactam product was received in a good yield of 74%, and therefore in a higher yield than its non-methylated analogue, which had already been anticipated (Fig. 4.13). Literature on Schmidt rearrangements with different substrates had shown that electron withdrawing groups on the migrating carbon seem to decrease the product yield, electron donating groups increase the yield and promote higher regioselectivity. The additional electron donating effect of the methyl group supported this. The obtained free, methylated lactam also solidified readily, but slow evaporation crystallisation did not yield single crystalline samples suitable for SC-XRD. However, the controlled growth of single crystals from a molten sample provided suitable samples for SC-XRD. The subsequent Boc protection gave good yields of 64%, but the purified product did not solidify and all attempts at crystallisation remained unsuccessful.

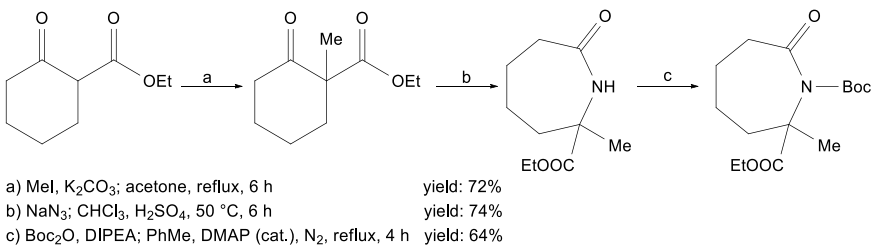

Fig. 4.13 The introduction of a methyl group in N_α-position of the caprolactam was possible through methylation of the precursor with a comparatively simple nucleophilic substitution. An equivalent introduction on 2-aminopimelic acid might have not been as easily achieved.

Hydrolysis of the amide bond during saponification

Because the mentioned re-esterifications of the free caprolactam acid were thought to have failed because of low solubility of the starting material. The introduction of a Boc group was then thought to aid with solubility and saponification of a Boc protected caprolactam was investigated. Considering that Boc protection groups are generally stable against basic and nucleophilic conditions, the previously employed procedure for saponification of lactams was applied again. 2D-NMR-analysis of the obtained product did not show the expected free acid of a caprolactam. Instead, *N*-Boc-2-aminopimelic acid was found to be the main product with only little impurities (Fig. 4.14). Saponification of different lactams had not shown any indication of ring opening before. An explanation for this hydrolysis was derived from the obtained SC-XRD data later on and shall be discussed in conjunction with the presentation of that data.

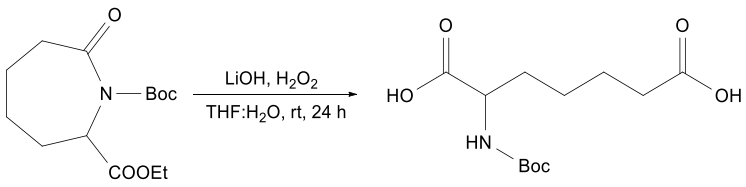

Fig. 4.14 The saponification of this Boc protected caprolactam ester did not result in a caprolactam, but the hydrolysis of the amide bond was observed.

Alongside the synthesis of valerolactams, the studies on the Dieckmann-type cyclisation had also led to three different benzylated caprolactam esters. Both monobenzylated caprolactams were found to solidify after several days and multiple attempts at obtaining single crystals were made. Unfortunately, all of these attempts remained unsuccessful.

ζ-Enantholactams

2-Aminosuberic acid, the equivalent starting material for enantholactams, is not readily commercially available. However, because the Schmidt rearrangement had shown success in the establishment of a far less expensive and more versatile route to caprolactams, it was decided to prepare enantholactams through an equivalent procedure. Because esters of 2-oxocycloheptane carboxylic acid were found to be much more expensive, but synthetic procedures starting from cycloheptanone are well-documented, it was decided to synthesise the respective ester before subsequent ring expansion (Fig. 4.15).

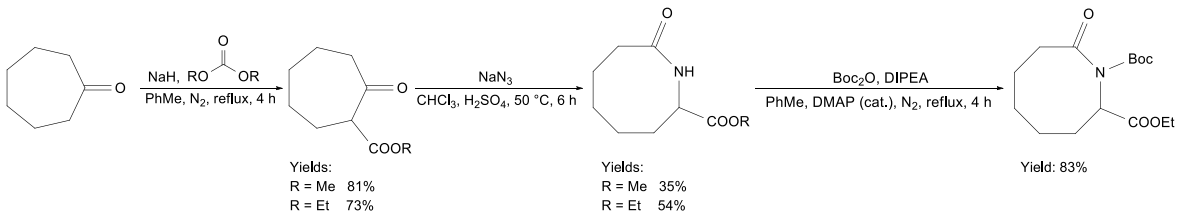

Fig. 4.15 The preparations of enantholactams through Schmidt rearrangement of cycloheptanone carboxylic acid esters gave the enantholactams in moderate yields. The respective ethyl ester was further Boc protected for subsequent cyclisation experiments.

This comparatively straightforward reaction gave good yields for both methyl and ethyl esters and did not require further adjustments. Following simple column chromatographic purification, the cycloheptanone derivatives were then subjected to the same Schmidt reaction conditions as the equivalent cyclohexanone with a moderate yields of 35% and 54% for the methyl and ethyl ester, respectively. The free enantholactams solidified readily and single crystalline samples could be harvested after simple recrystallisation using slow solvent evaporation.

Because the Boc protected valerolactam ester could not be crystallised, the enantholactam ethyl ester was then Boc protected under the same conditions as before. The ethyl ester was chosen, because the resulting bocylated enantholactam was also planned to be used in bicyclisation experiments. And because the equivalent caprolactams had shown, that ethyl esters seemed to undergo bicyclisation with better yields, synthetic efforts were focused on the ethyl ester.

The desired Boc protected enantholactam was obtained with good yields of 83%. The purified product was obtained as a viscous oil, but recrystallisation gave single crystalline samples suitable for SC-XRD analysis.

4.4) Crystallography

For the here presented studies, a number of new lactams were synthesised but only eight of these new compounds could be taken under consideration. Other compounds could not be characterised because they did not solidify at room temperature or it was not possible to harvest suitable single crystals. A list of all synthesised compounds, their apparent state of matter at room temperature and whether suitable crystals could be obtained is displayed in Table 4.2. Several other lactams that were obtained in earlier work within the group shall be taken into account for all considerations but are not listed below.

Table 4.2 All newly synthesised lactams, whether they solidified at room temperature and whether single crystalline material was obtained

Compound / Identification number (if applicable)	Structure	SC-XRD data availability
Methyl pyroglutamate	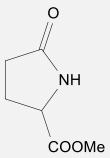	No oil
Ethyl pyroglutamate	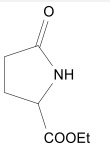	No oil
iso-Propyl pyroglutamate **1**	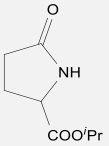	Yes
tert-Butyl pyroglutamate **2**	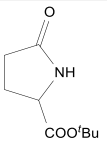	Yes
(-)Menthyl pyroglutamate	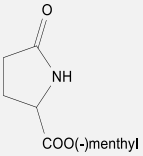	No Solid but no single crystals
Methyl 6-oxopiperidine carboxylate **3**	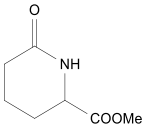	Yes
6-oxopiperidine carboxylate **4**	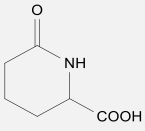	Yes

1-*tert*-Butyl 2-ethyl 6-oxopiperidine 1,2-dicarboxylate	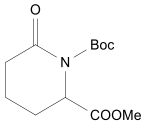	No Viscous oil
1-Benzyl 2-methyl 7-oxoazepane 2-carboxylate	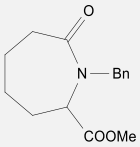	No Solid but no single crystals
Methyl 2-benzyl-7-oxoazepane 2-carboxylate	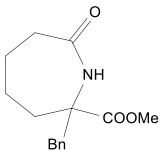	No Solid but no single crystals
Benzyl 2-benzyl 7-oxoazepane 2-carboxylate	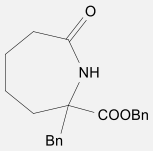	No Viscous oil
Ethyl 7-oxoazepane carboxylate	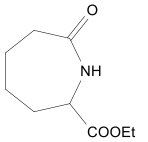	No Solid but no single crystals
1-*tert*-Butyl 2-ethyl 7-oxoazepane 1,2-dicarboxylate	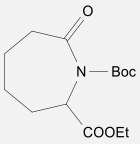	No Viscous oil
Ethyl 2-methyl-7-oxoazepane carboxylate **5**	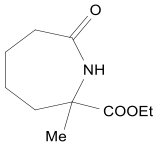	Yes
1-*tert*-Butyl 2-ethyl 2-methyl-7-oxoazepane 1,2-dicarboxylate	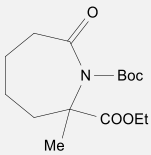	No oil
Methyl 8-oxoazocane carboxylate **6**	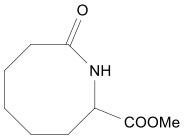	Yes
Ethyl 8-oxoazocane carboxylate **7**	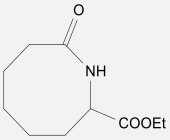	Yes

1-*tert*-Butyl 2-ethyl 8-oxoazocane 1,2-dicarboxylate **8**	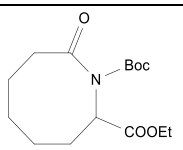	Yes
N-Boc-2-aminopimelic acid **9**	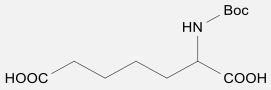	Yes

Please note: for all considerations of axially or equatorially positioned N_α-substituents, the amide plane C_α-N-C(O)-C_ω will be used as the mean plane.

Pyroglutamates 1 und 2. The *iso*-propyl ester **1** was found to crystallise in the triclinic space group *P-1*, with one molecule found in the asymmetric unit. The lactam ring was found to adopt a slight envelope conformation with C2 standing slightly above the amide plane towards the ester group. This distance however was only found to be 0.196 Å, which makes the ring appear almost planar on first sight. This envelope conformation is less prominent than in its parent lactam's, which shows a distance of 0.371 Å for the same atoms (CSD entry: NILYAI[89]).

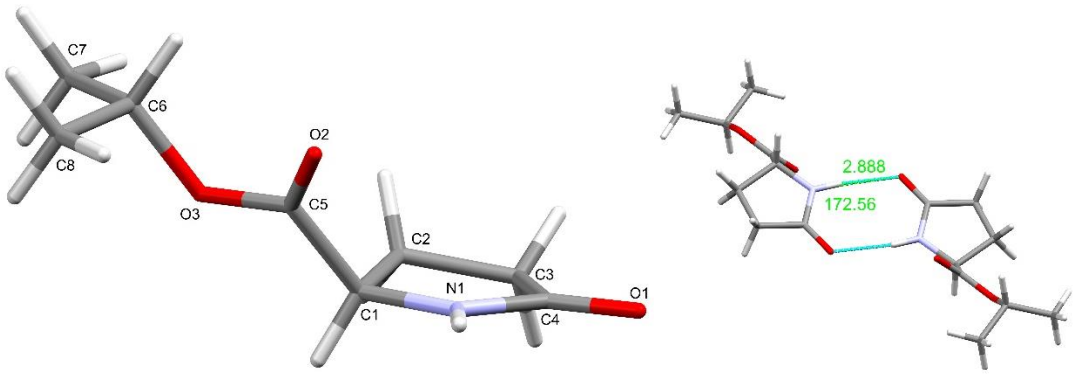

Fig. 4.16 ***Left****: The asymmetric unit of pyroglutamate* ***1*** *only contains one molecule.* ***Right****: The amide groups are found to be arranged in amide-amide dimers.*

The position of the ester group is less easily described (Fig. 4.16). The angle between C1-C5 and the amide plane was found to be 41.7 °. This is neither a clear axial position, which would usually mean higher angles, towards 90 °, nor a clear equatorial position which would tend towards 0 °. Analysis of the bond lengths and angles did not show any unexpected values. A look into the hydrogen bonds showed that the most prominent interaction seemed to be the N1-H1N···O1=C4 contact, which connects two molecules to a dimer (Fig. 4.16). The hydrogen bond length of d(D-H···A) = 2.888 Å and the angle of >(DHA) = 172.6 ° suggested a mutual contact of moderate strength and is only slightly shorter than for the parent lactam (d(D-H···A) = 2.921 Å; >(DHA) = 172.4 °). The two molecules in each dimer are symmetry connected through an inversion centre which leads to the graph descriptor $R_2^2(8)$ for this interaction, no further strong hydrogen bonds were found. The so formed dimers were found to be connected to the next set of dimers through another $R_2^2(8)$ contact between C3-H3A···O1=C4, which, once expanded in both directions, gives the appearance of a step-wise chain-type structure (Fig. 4.17).

These chains expand into the crystallographic *a* axis; the *iso*-propyl groups point outwards, away from the lactam dimers. A closer look revealed that the chains themselves are interconnected through short contacts between C6-H6···C4, which connects the chains to sheets along the crystallographic *a,c* plane.

As mentioned, the *iso*-propyl groups point outwards of the chains and H1A, H2A and H3B atoms pointing outwards as well. This could be interpreted as a hydrophobic surface, but a *spacefill* model reveals that these groups do not cover the entire surface and could leave enough space for further non-hydrophobic interactions. The here described sheets seem to stack through hydrophobic interactions.

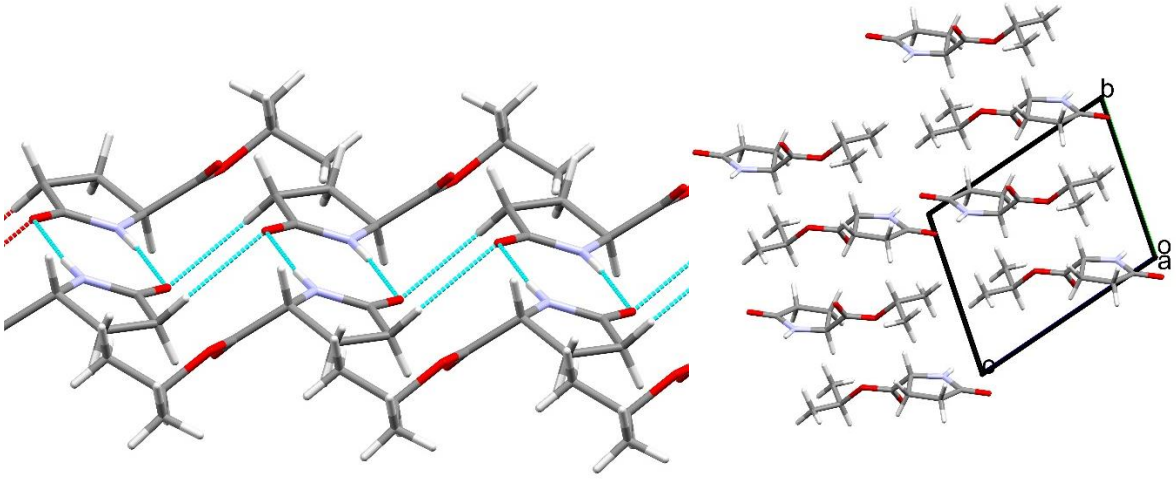

Fig. 4.17 ***Left****: The combination of amide-amide and amide-ring contacts results in this step-wise chain like structure.* ***Right****: The formation of sheet-like structures within the a,c plane can be found.*

The *tert*-butyl ester **2** was found in the monoclinic space group *C2/c*, previously published data described a polymorph with an orthorhombic space group (CSD entry: DICXET[90]). Similar to the *iso*-propyl ester, lactam **2** exhibited only one molecule in the asymmetric unit and the lactam ring itself is found to adopt an envelope conformation. Contrary to **1**, C2 stands away from the ester group and is slightly further away from the amide plane with a distance of 0.329 Å.

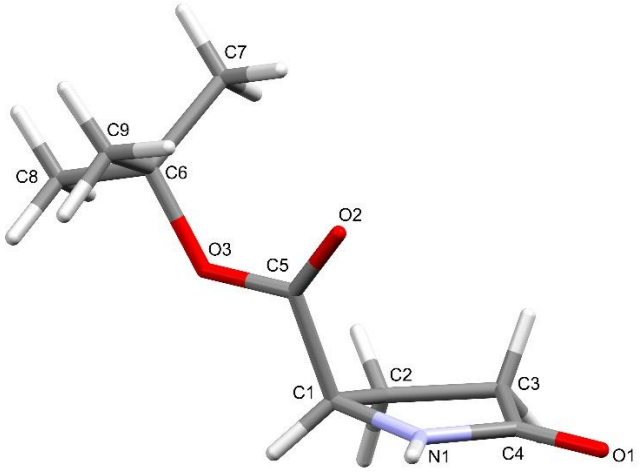

Fig. 4.18 The asymmetric unit of tert-butyl ester ***2*** *contains one molecule, similar to* ***1****. However, contrary to* ***1****, the ester group is found in a clear axial position in* ***2****.*

The ester group in **2** presents itself in a clear axial position (Fig. 4.18) to the amide plane with an angle of 64.7 °; the bond lengths and angles do not show any unexpected values for lactam **2** either. The hydrogen bonds however are somewhat more diverse. The amide groups are connected through hydrogen bonds between N1-H1N···O1=C4, similar to lactam **1**, but the amide groups are arranged in C(4)-chains (Fig. 4.19). Ring A therefore connects to ring B with a N_A-H_A···O_B contact, molecule B in turns connects to the next ring with a N_B-H_B···O_C contact. A close look into the positioning of the rings towards each other shows that ring A and B are tilted by 32.7 °, ring A and C however are found to be parallel again. Ring A and C can be found to be connected to each other as well *via* the two contacts between C1-H1···O1=C4 and also through the less usual contact of C3-H3B···O3. The combination of both of these interactions can be described with $R_2^2(8)$ again.

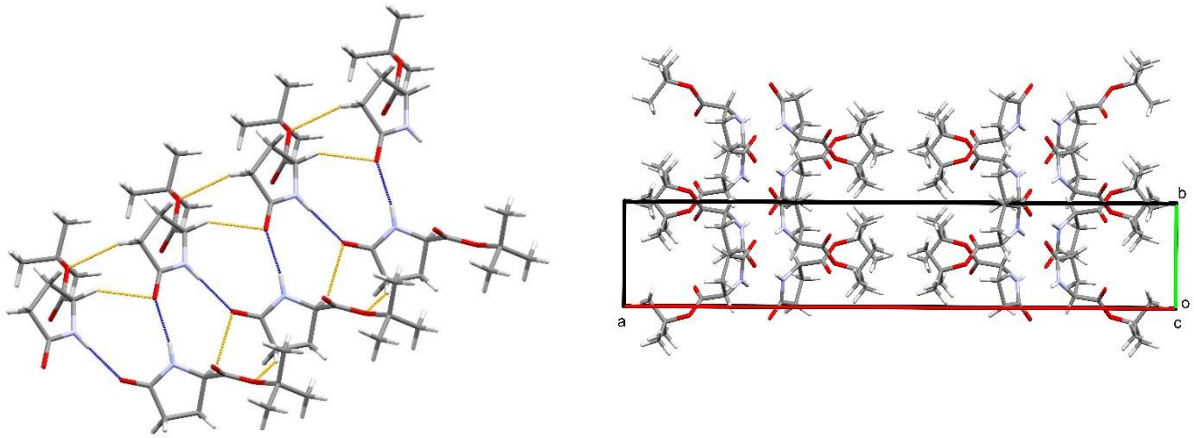

Fig. 4.19 ***Left****: The C(4)-chains between the lactam groups connects the lactam rings in the crystallographic a axis.* ***Right****: The packing of lactam* ***2*** *shows that the chains arrange in bilayered structures, of which two occupy the asymmetric unit.*

A wider look into the overall structure shows that the contacts O1-N1, O1-C1 and O3-C3 in conjunction form a molecular chain along the crystallographic *b* axis. The arrangement of the molecules can be neatly described by a screw axis, four of which can be found within the unit cell, one in each quadrant. The chains themselves are further connected to the next chain over the relatively weak C3-H3A···O1=C4 contacts, with $R_2^2(8)$. The *tert*-butyl groups do not interact through any strong contacts. However, Fig. 4.20 shows that they do arrange in a noteworthy pattern. The dimer chains are connected with each other, which in turns forms sheet-like structures along the *b,c* plane. The surface of these sheets is covered by the hydrophobic *tert*-butyl groups almost entirely. Within one unit cell, two of these sheets can be found, they seem to only be connected through hydrophobic interactions between the *tert*-butyl groups.

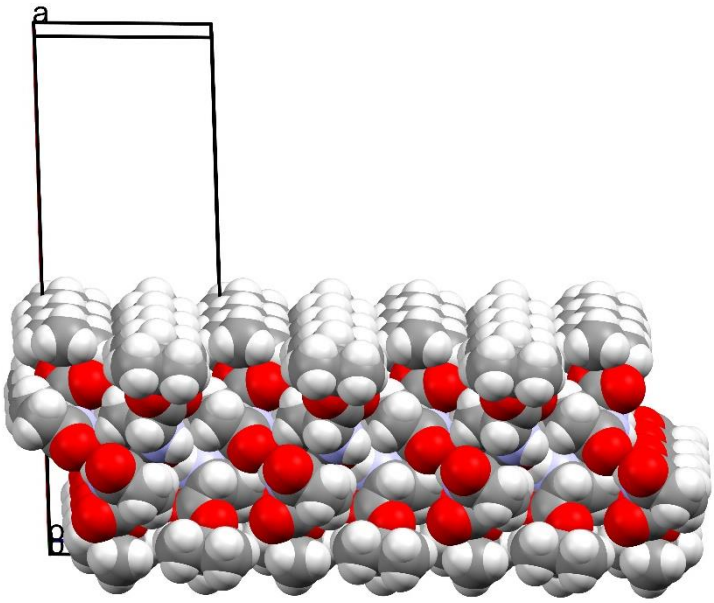

*Fig. 4.20 The tert-butyl groups in lactam **2** point outwards of bilayered sheets, which are held together through the amide interactions. The spacefill model shows significant coverage with hydrophobic groups.*

Valerolactams 3 und 4. The methyl ester of pyrohomoglutamic acid was found to crystallise in the monoclinic space group $P2_1/c$ with one molecule found in the asymmetric unit. The bond lengths and angles do not show any significant disparity with other investigated lactams. However, the torsion angle between C5-N1-C1-C2 is found with a value of 23.9 °, which is comparatively high for a partial double bond. Considering the normal bond length of d[N(1)-C(5)] = 1.344 Å suggests that the amide bond retained its partial double bond character, but further suggests that the amide group is forced to adopt such an uncharacteristic angle to accommodate other effects such as the packing. If the amide plane C5-N1-C1-C2 is used as the starting point for the determination of the position of the ester group, an angle of 37.4 ° can be found between them. This suggests a tendency towards an equatorial position. However, taking into account that the amide plane itself is only an average and that the torsion angle along the atoms, used for the plane, is relatively big, the realistic ester-amide group angle could be debated.

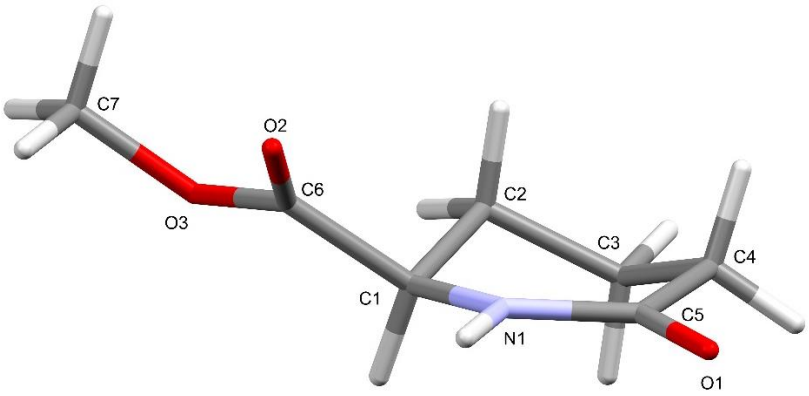

*Fig. 4.21 The numerical angle between the mean amide plane of lactam **3** and its ester group was found to be 37.2 °, but because the torsion angle along the amide bond is comparatively high itself, this angle does not necessarily reflect the equatorial position well.*

Fig. 4.21 does support the argument of a more equatorially positioned ester group. The two carbon atoms in the carbon backbone of the lactam ring both stand out of the amide plane in opposite directions: C2 shows a distance of 0.359 Å, C3 a distance of -0.395 Å. This lets the lactam ring appear in a half-chair conformation, which on the other hand is not as apparent due to the debatable planarity of the amide bond. The perhaps most prominent non-covalent interaction that can be found is the N1-H1N···O1 contact between the amide groups, the contact is not found to show an unexpected long or distorted hydrogen bonds. Methyl ester **3** is found to form amide dimers with the common descriptor $R_2^2(8)$, similar to its corresponding parent lactam (See Chapter 3; CSD entry: HIQJOJ[91]). Besides the dimeric contacts, O1 is further involved in a contact between C1-H1···O1 with another molecule outside of the dimer itself. If the initial dimer was named as A and B, this weak interaction could than be denoted as $C1_C$-$H1_C\cdots O1_A$. The lactam ring, here shown as ring C (Fig. 4.22), then forms another dimer with a ring D in the sense of $N1_C$-$H1N_C\cdots O1_D$, and ring D is than connected back to ring A through another comparatively weak $C4_A$-$H4_A\cdots O1_D$ contact. This arrangement gives the overall appearance of a network within the chains, connecting both into the *b* and *c* direction, in which the amide dimers are stacked with an angle of 64.7 ° for the amide dimer planes.

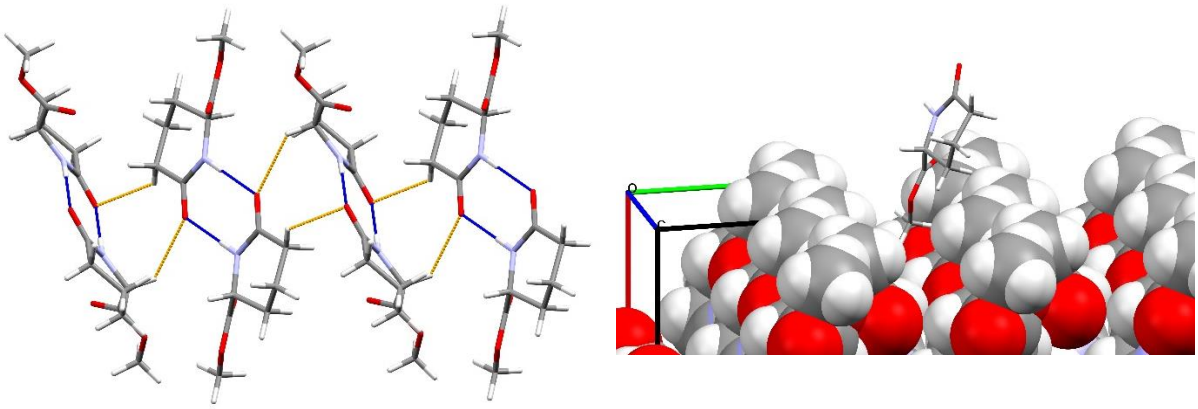

*Fig. 4.22 Methyl ester **3** forms amide dimers that are further connected through weak hydrogen bonds of the lactam carbonyls to the next set of dimers. The outwards pointing methyl groups do not cover the entire outer surface and leave enough space for connections into the hydrophilic areas.*

When extended, the network continues along the *b*,*c* plane. A spacefill model of the resulting layer shows that the outer surface is again covered by the methyl groups of the ester functionalities, *e.g.* the alkyl residue. However, in contrast to the *tert*-butyl ester **2**, the methyl groups do not cover the entire surface and allow hydrogen contacts between the layers (Fig. 4.22). The weak C7-H7B···C6 is found as the connection, with a very long distance of 3.726 Å and an angle of 144.2 °.

Free pyrohomoglutamic acid was found to crystallise in the monoclinic space groups $P2_1/n$ and just as for the methyl ester **3**, one molecule is found in the asymmetric unit. The bond lengths and angles of acid **4** do not show significant deviations from other lactams, the free acid exhibits almost co-planarity along the amide bond. In contrast to **3**, the free acid group is found to adopt a more or less clear axial position with an angle of 67.2 ° to the mean amide plane.

The lactam ring itself adopts a half-chair conformation with C2 and C3 standing out of the plane with distances of -0.463 Å and 0.277 Å respectively (Fig. 4.23).

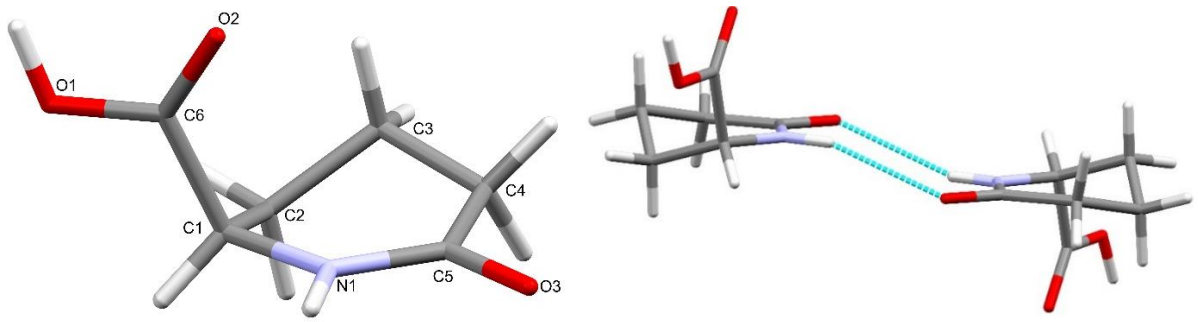

Fig. 4.23 ***Left****: The free acid from of lactam* ***4*** *adopts a clear axial position. The ring further adopts a half-chair conformation.* ***Right****: the dimeric amide-amide contacts are found to be staggered, which has not been observed for any of the other investigated lactams.*

A look into the hydrogen bonds of the free acid shows that several contacts can be found. The amide-amide interaction in lactam **4** is a dimeric amide hydrogen bond with $R_2^2(8)$ symmetry (Fig. 4.23). However, **4** does show one particular property, that was not observed in other structures investigated. The amide regions of both partners of one dimer do not align, but are staggered, with the two amide planes showing a distance of 0.872 Å from each other. The N1-H1N···O3 is also found to be significantly longer than most other studied amide contacts with a length of 3.158 Å and an angle 150.2 °. Whether this rather weak interaction is a result of the misalignment, the misalignment being a result of weak interaction or whether these are completely unrelated observations cannot be said with certainty.

Apart from the amide dimers, the free acid groups are involved in a O-H···O contact with the lactam carbonyl oxygens, forming acid-lactam C(7)-chains. With a length of 2.584 Å and an angle of 170.3 °, this interaction appears to be the determining contact in the structure which could explain the misalignment of the amide planes, if the acid-lactam contacts dominate the dimeric amide-amide interaction.

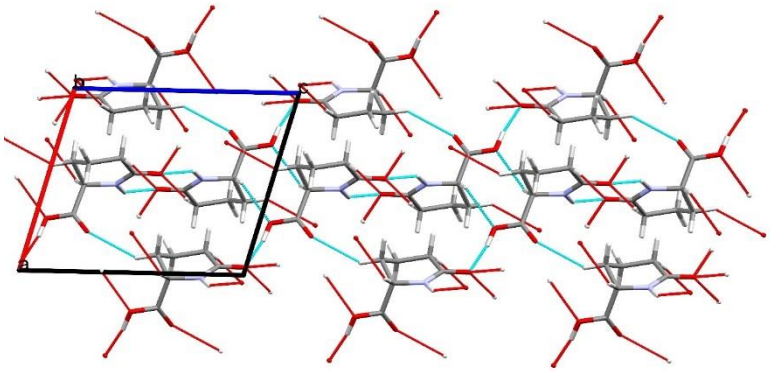

Fig. 4.24 Lactam ***4*** *shows several hydrogen contacts in all crystallographic directions, which creates a three-dimensional network. Chain- or sheet-like structures could not be found.*

Apart from the already mentioned interactions, there are further interactions of the amide functionality to be found. The lactam carbonyl oxygen atom O3 is also involved in a moderate to strong O1-H1O···O3 contact with the acid group of another molecule and a comparatively weak interaction between C4-H4B···O3. The latter connects two molecules in a somewhat dimeric fashion, well-described with $R_2^2(8)$ as well. Apart from the already mentioned contacts, further contacts that can be found are C1-H1···O1 and C2-H2B···O2. The combination of all of these interactions creates a three-dimensional network in all directions and chain- or sheet-like structures could not be found (Fig. 4.24).

Caprolactam 5. The N_α-disubstituted caprolactam **5** was found to crystallise in the monoclinic space group $P2_1/c$ with one molecule in the asymmetric unit. None of the bond lengths or angles within the molecule appear to be unusual. The lactam ring was found in a boat conformation, which is thought to be the energetically most favourable conformation for the structurally related cycloheptenes (Fig. 4.25). In contrast to the previously described lactam esters/acid, caprolactam **5** carries two substituents in N_α-position. The ester group adopts a clear axial position with an angle of 60.7 ° to the amide plane, the methyl group therefore adopts an equatorial position.

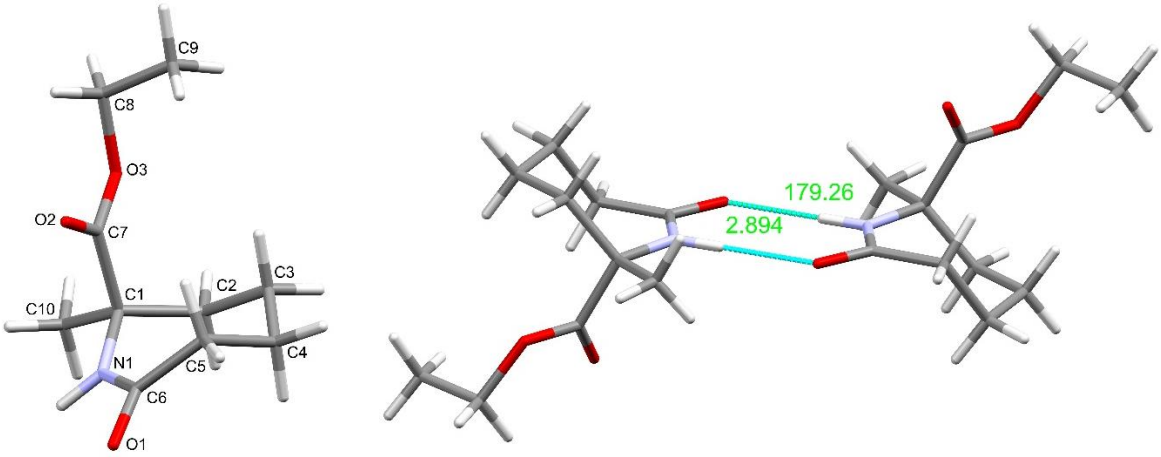

Fig. 4.25 ***Left****: Caprolactam* ***5*** *adopts a pseudo-boat confirmation, its ester group stands in a clear axial position.* ***Right****: 5 forms amide dimers, with comparatively normal lengths and angles.*

A look into the hydrogen bondings shows, that lactam **5** forms amide dimers, the N1-H1N···O1 interactions do not seem to show any abnormalities (Fig. 4.25). It seems that the addition of a methyl group did not influence the amide bonding pattern. However, methyl groups are considered relatively small and only exhibit a comparatively small steric demand. It is plausible, that bigger groups, or substituents with strong influence on the electronic distribution to adjacent substituents would have a much more drastic effect on the amide hydrogen contacts. O1 is further involved in a contact between C5-H5A···O1, which connects to another molecule. Both of these interactions can be described with the $R_2^2(8)$ descriptor, the combination of both, if extended, form a chain-like structure along the crystallographic *a* axis (Fig. 4.26). The so formed chains of amide dimers are connected to the next chain through a less usual interaction between C2-H2B···O3, a contact between a ring carbon and the methoxy oxygen of an ester group.

The connections extend along the *c* axis and can be described with the $R_2^2(10)$ descriptor. The so formed layers are then connected to the next set of molecules through the C2-H2A···O2, which therefore creates a full three-dimensional network (Fig. 4.26).

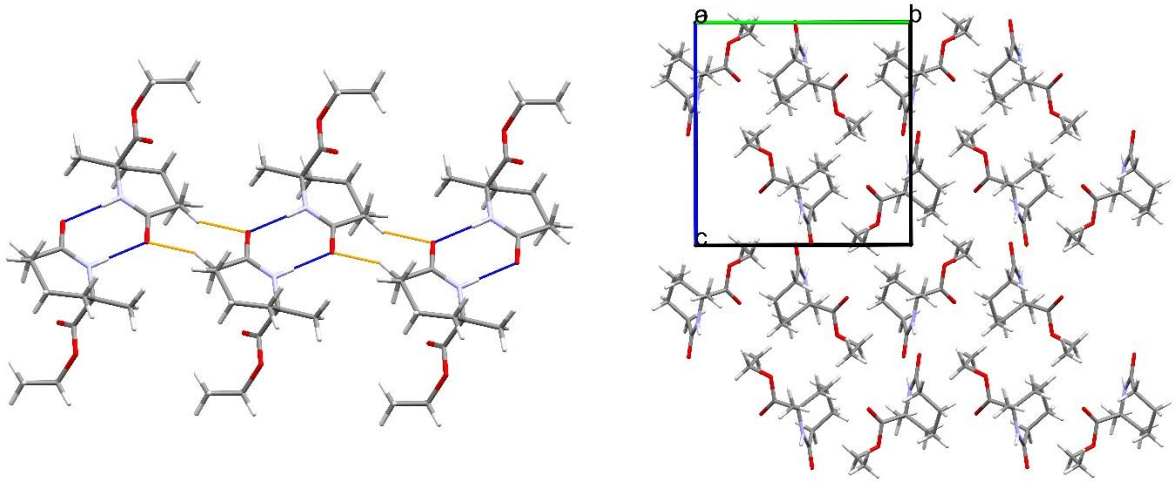

Fig. 4.26 ***Left****: Similar to valerolactam methyl ester* ***3****, caprolactam* ***5*** *forms amide dimers which are connected through interactions of the lactam carbonyls with each other.* ***Right****: The three-dimensional network does not show formation of sheet-like structures as observed for other investigates lactams.*

Enantholactams 6-8. Enantholactam **6** was found to crystallise in the orthorhombic space group $P2_12_12_1$ with one molecule in the asymmetric unit. Comparison of the bond lengths and angles did not show any unexpected values, however the torsion angle along the amide bond was found to be -7.4 °. Considering that the valerolactam methyl ester **3** exhibits a torsion angle of ~24 ° and considering that the bond length along the amide bond of **6** with d[N(1)-C(7)] = 1.350 Å, this seems to be a mere effect of the crystal packing. The overall conformation resembles its parent lactam (CSD entry: ENANOL[92]), as can be seen in an overlay of the two structures (Fig. 4.27). The ester group was found in an equatorial position, the angle between the ester group and the mean amide plane is 23.6 °.

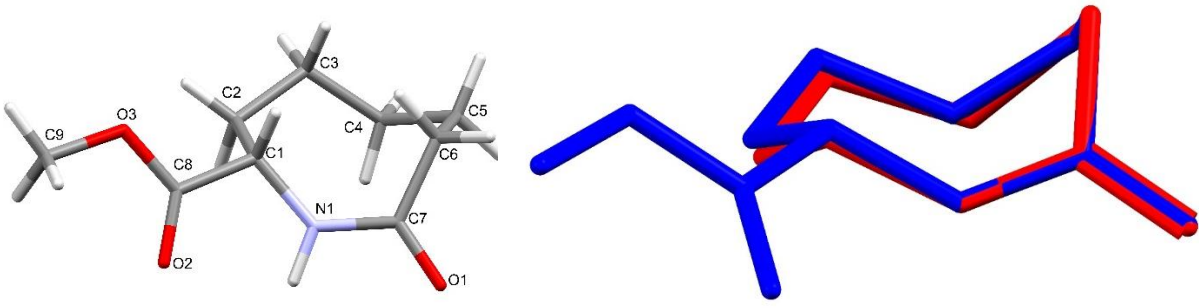

Fig. 4.27 ***Left****: The ester group of enantholactam* ***6*** *is found to adopt a clear equatorial position.* ***Right****: Comparison with the parent lactam ENANOL shows a high level of similarity, it appears as if the methyl ester group has little effect on the conformation in the solid state.*

Table 4.2 Summary of all involved hydrogen contacts with respective lengths and a short descriptions of the connectivity with other interactions

I	N1-H1···O3 O3···H1N-N1	Lactam nitrogen-Methoxy oxygen contact, d = 3.464 Å, connects two rings in conjunction with *II*, *IV* and *VI* and forms chains along *a* axis. Distance between the amide plane: 1.443 Å
II	C1-H1···O1 O1···H1-C1	Lactam carbonyl – Lactam ring contact, d = 3.247 Å, connects chains in conjunction with *I*, *IV* and *VI*
III	C2-H2A···O1 O1···H2A-C2	Lactam carbonyl – Lactam ring contact, d = 3.540 Å, connects chains formed through *I*, *II*, *IV* and *VI* with next sets of chains along *b* axis
IV	C6-H6B···O1 O1···H6B-C6	Lactam carbonyl – Lactam ring contact, d = 3.537 Å, connects transannularly close hydrogens in conjunction with *III*
V	C6-H6A···O2 O2···H6A-C6	Ester carbonyl – Lactam ring contact, d = 3.396 Å, connects chains formed through *I*, *II*, *IV* and *VI* with next sets of chains along *c* axis
VI	C9-H9B···O2 O2···H9B-C9	Ester carbonyl – Methyl ester group, d = 3.230 Å, connects rings to chains in conjunction with *I*, *II*, *IV* and *VI*

For the sake of clarity, the interactions shall be examined first and then brought into a bigger context of their individual role in the superior packing. Table 4.3 gives an overview of all hydrogen bonds with short descriptions of their respective connectivity that can be found in the crystal structure. All previously examined structures either displayed amide dimers with the descriptor $R_2^2(8)$, or C(4)-chains, which are also commonly found in literature[93]. However, methyl ester **6** shows a different bonding pattern. The amide nitrogen does not form a hydrogen bond with a lactam carbonyl, but with the methoxy oxygen of the ester group of another molecule. Alkoxy oxygens are usually considered weak hydrogen bond acceptors[94] but have also been found in other for this study examined structures before. This particular connection between the lactam nitrogen and the alkoxy group was not observed for any of the other structures. If contact *I* is expanded, it becomes visible that the lactam rings arrange in a chain-type structure in conjunction with contacts *II*, *IV* and *VI* in the direction of the crystallographic *a* axis. The combination of contacts *I* and *VI* can be described with $R_2^2(8)$, but in contrast to the other examined structures, these contacts form heterodimers in the form of N-H···O/C-H···O=C.

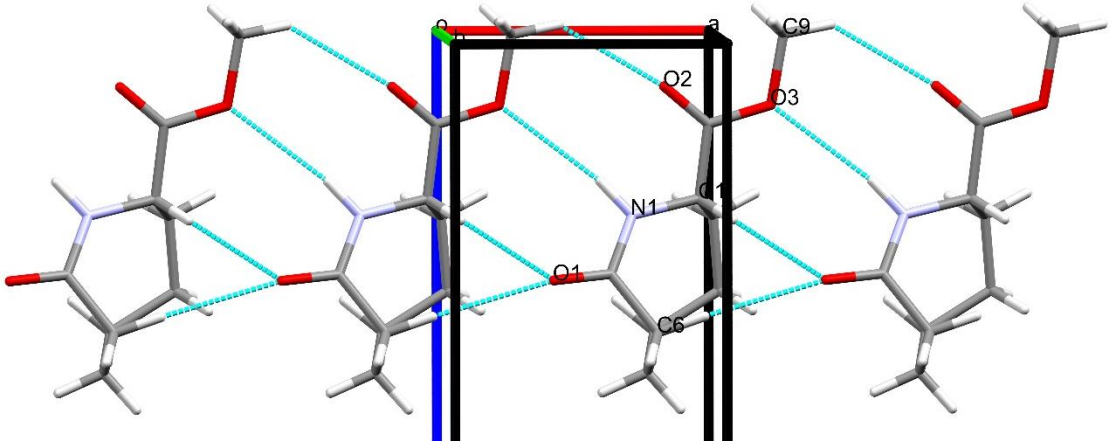

*Fig. 4.28 In contrast to other investigated lactams, enantholactam **6** does not show hydrogen contacts between the amide hydrogen and a carbonyl group. Instead, an uncommon connection to a methoxy oxygen can be found.*

As already mentioned, the formation of this chain-type structure is further supported by the contacts *II* and *IV*, which exhibit a motif that has not been seen before for any of the smaller lactam rings (Fig. 4.28). Both contacts *II* and *IV* connect the lactam carbonyl oxygens in bifurcated hydrogen bonds with C1 and C6. A *spacefill* model of the structure shows, that the hydrogens H1, H2 and H6 are considerably close to each other and even overlap (Fig. 4.29), *e.g.* their distance is shorter than the sum of their Van-der-Waals radii. One usually accepted criterium for the determination of a positive interaction is that if two atoms are closer to each other than the sum of their respective Van-der-Waals radii, which would mean that these protons interact positively.

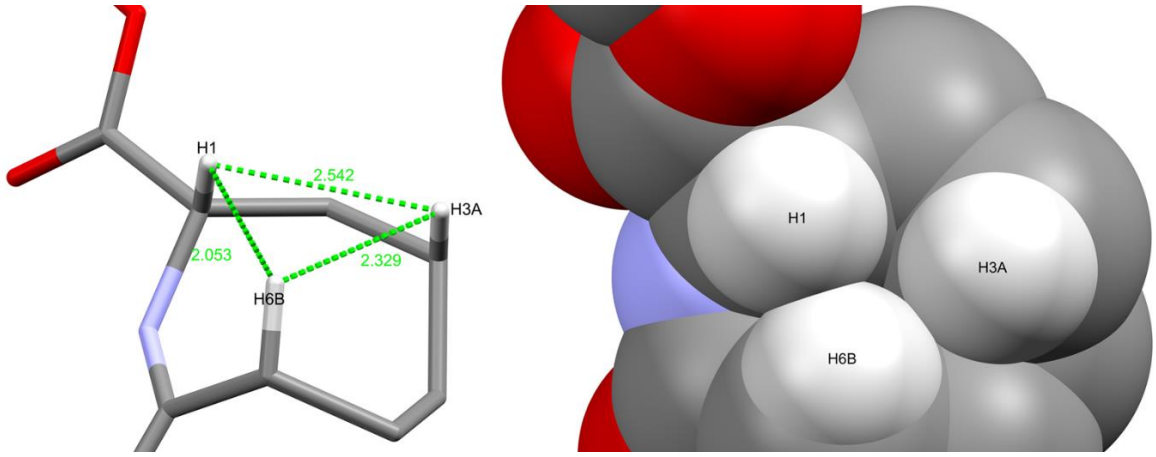

*Fig. 4.29 A spacefill model of enantholactam **6** reveals that protons H1, H3A and H6B are considerably close to each other. Whether this is a positive interaction, cannot be said.*

Overlap 1: d(H1-H6B) = 2.053 Å	<(C1-H1···H6B) = 109.1 ° <(C6-H6B···H1) = 124.1 °
Overlap 2: d(H6B-H3A) = 2.329 Å	<(C6-H6B···H3A) = 111.4 ° <(C3-H3A···H6B) = 107.9 °
"Overlap 3": d(H3A-H1) = 2.542 Å	<(C3-H3A···H1) = 92.1 ° <(C1-H1···H3A) = 91.2 °

Comparison of the lengths shows that H1 clearly overlaps with H6B, H6B overlaps with H3A with a longer distance but there is no overlap between H3A and H1. However, the angles between the protons are very low and, depending on the accepted range of angles for hydrogen bonds, would not be considered anymore. It remains debatable whether these should be considered positive interactions or just a result of the crystal packing. These presumably short contacts shall be evaluated under a different aspect as well. Amongst the different types of ring strain, the so-called *Prelog-strain* or *transannular ring strain*[95] denotes that cyclic structures can experience an increase in their overall energy, if substituents on the ring are forced too close together. It is believed that this strain comes from steric repulsion and that any cyclic structure will try to accommodate for that by adopting conformations that avoid this steric clash. Even though hydrogen atoms are among the smallest possible substituents on a carbon atom, they have been shown to cause ring strain for certain cyclic structures[96]. In the case of lactam **6**, it seems very much plausible to assume that the transannular overlap of the mentioned hydrogen atoms causes an increase in the ring strain of the enantholactam ring. However, it does seem that the overall stabilisation through the entire packing, and the bifurcated lactam carbonyl contacts compensate for this presumably unfavourable conformation.

Lactam carbonyl O1 is involved in another hydrogen contact, apart from the already mentioned. Contact *III* refers to a contact between the lactam carbonyl and H2A on the lactam ring. These contacts are formed along the *b* axis and connect the chains formed through contacts *I*, *II*, *IV* and *VI* with each other. These layers are than connected further through contact *V* which is formed in the general crystallographic *c* direction. This completes the contacts to form a three-dimensional network (Fig. 4.30).

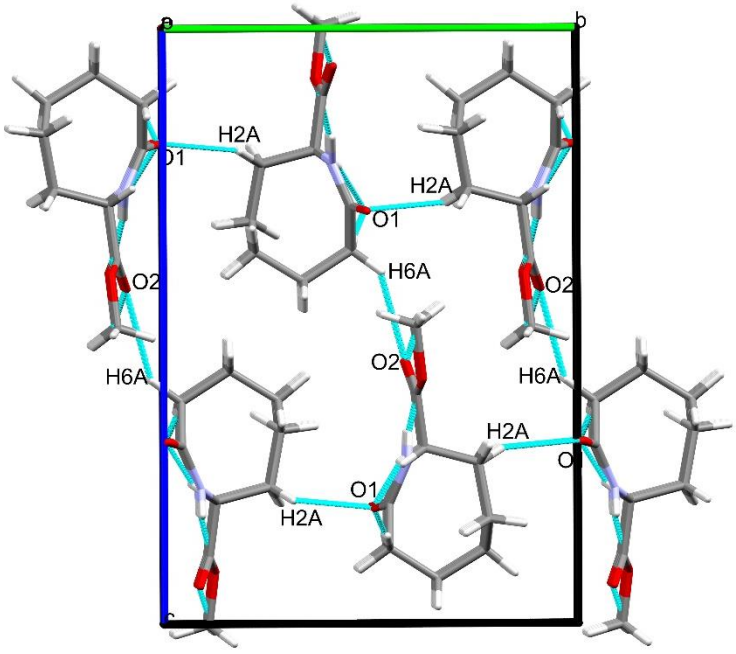

*Fig. 4.30 The combination of the hydrogen contacts I-VI forms a complex, three-dimensional network in the crystal packing of enantholactam **6**.*

Enantholactam **7** was found to crystallise in the monoclinic space group $P2_1/c$ with two molecules in the asymmetric unit. Comparison of all bond lengths and angles did not reveal any unexpected properties but structural overlay of the parent lactam, the methyl ester **6** and the ethyl ester **7** shows that **7** adopts a different conformation (Fig. 4.31). However, different conformations are to be expected from a presumably flexible system like an eight-membered lactam ring.

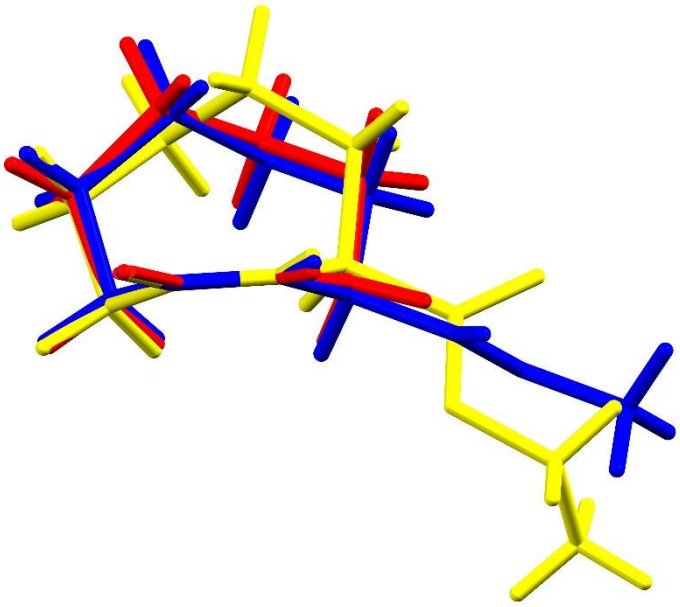

*Fig. 4.31 An overlay of the three structures of ENANOL (red), methyl ester **6** (blue) and ethyl ester **7** (yellow) shows that the ethyl ester **7** shows a different conformation to its corresponding parent lactam and its methyl ester.*

Despite of the bond angles not showing unexpected values, the amide groups are not fully planar for ethyl ester **7**. With respective torsion angles of 13.2 ° and 14.7 ° it is debatable whether they can be considered planar or not. The valerolactam methyl ester **3** had been found to exhibit a torsion angle of 23.9 ° which is almost twice as wide. Comparison of the respective bond lengths shows that the amide bonds (both for the O=C and the N-C bonds) are roughly equal (Ring A: d[N(1)-C(7)] = 1.339 Å; Ring B: d[N(2)-C(17)] = 1.340 Å) but also fall well within the normal ranges for the lactam bonds. It seems that the widened torsion angles are more likely a result of packing effects, rather than the lactams exhibiting a reduced partial double bond character. The packing could for example allow this increased strain on the double bond to be compensated by the reinforcement of hydrogen bonds or only allow certain hydrogen bonds to be formed in the first place. Unfortunately, it is not possible to determine why these torsion angles along the amide bonds occur and how much packing effects take part in this with the available data.

Several different hydrogen bonds can be found in the acquired structure of **7**. As already mentioned, the asymmetric unit contains two molecules, both of which form hydrogen bonds. They are summarised in tables 4.4 and 4.5, depending on which ring they are formed by. For the sake of clarity, all connections will be addressed by their respective ring and number.

Table 4.3 Summary of all involved hydrogen contacts with respective lengths and a short descriptions of the connectivity with other interactions

Ring A

I	N2-H2N···O1	Amide contact, d=2.817 Å, connects ring A with ring B in C(4)-chains
II	C20-H20···O1	Connects to ester group (ring B), d=3.512 Å, connects to the same molecule as *VIII*, *IX*, *X*
III	N1-H1N···O4	Amide contact, d=2.819 Å, connects to ring B, completes the C(4)-chains
IV *V*	C11-H11···O2 C16-H16···O2	d=3.296 Å / d=3.609 Å, Connect the two protons H11 and H16 which are in relative proximity to ring B, transannular connection
VI *VII*	C1-H1A···O5 C6-H6A···O5	d=3.303 Å / d=3.623 Å, Connect to the ester carbonyl oxygen of ring B, forms chains with interactions *IV*, *V*
VIII *IX* *X*	C19-H19···O3 C9-H9···O6 C10-H10···O4	d=3.393 Å / d=3.406 Å / d=3.567 Å; Connect ring A and B in conjunction with the amide contacts

Table 4.4 Summary of all involved hydrogen contacts with respective lengths and a short descriptions of the connectivity with other interactions

Ring B

I	N1-H1N···O4	Amide contact, d=2.819 Å, connects ring B with ring A in C(4)-chains
II	C10-H10···O4	d = 3.567 Å, Connects to ester group (ring A), connects to the same molecule as VIII, IX, X
III	N2-H2N···O1	Amide contact, d=2.817 Å, connects to ring A, completes the C(4)-chains
IV *V*	C11-H11···O2 H16-C16···O2	d=3.296 Å / d=3.609 Å, Two close transannular protons, connect to the lactam carbonyl oxygen O2
VI *VII*	O5···C1-H1A O5···C6-H6A	d=3.303 Å / d=3.623 Å, Connect to the ester carbonyl oxygen of ring A, forms chains with interactions *IV*, *V*
VIII *IX* *X*	C9-H9···O6 C19-H19···O3 C10-H10···O4	d=3.406 Å / d=3.393 Å / d=3.567 Å, Connect ring B and A in conjunction with the amide contacts

Comparison of the overall list of interactions shows certain similarities. Contacts I and III for both rings connect the amide groups between in the two rings. These are the strongest interactions within the structure, they are comparatively short with d(D-H···A) 2.819 Å and 2.817 Å respectively, among the studied lactams which suggest relatively strong amide connections.

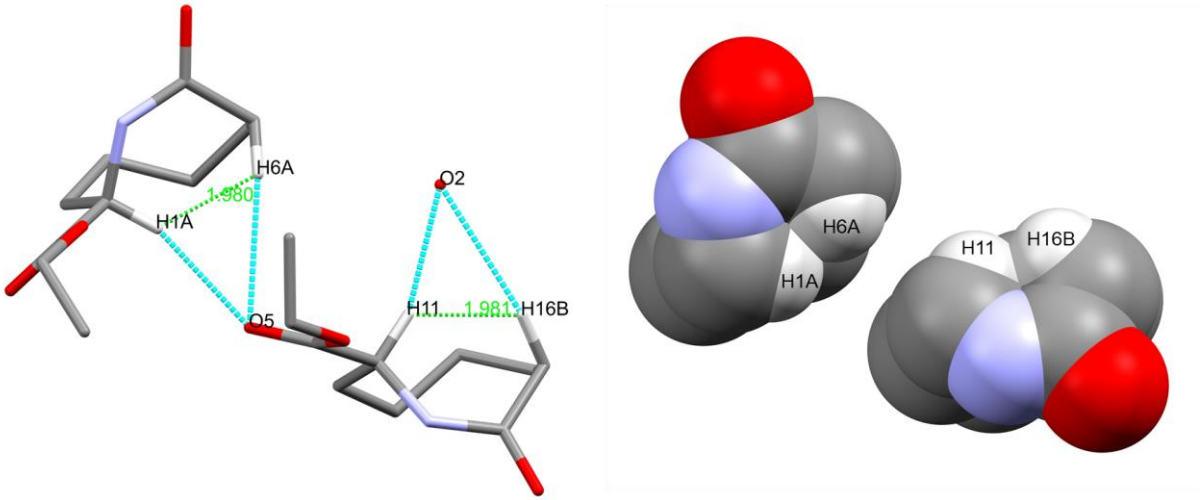

*Fig. 4.32 The short distances between H1A and H6A as well as H11 and H16B might be a direct result of their respective bifurcated hydrogen contacts. The two protons within one respective ring also show overlap in a spacefill model of lactam **7**.*

Another set of hydrogen bonds that are similar for both rings are connections *IV* and *V*, *VI* and *VII*, which involve the bifurcated contacts of the ester carbonyl oxygens with two ring protons each. As figure 4.32 shows, the two protons on each respective ring for these interactions are comparatively close to each other. A *spacefill* model also shows that the protons overlap, a similar overlap had already been observed for the respective methyl ester **6**.

Ring I: d(H6A-H1A)=1.980 Å	>(C1-H1A···H6A) = 123.5 ° >(C6-H6A···H1A) = 113.6 °
Ring II: d(H11-H16B)=1.981 Å	>(C11-H11···H16B) = 123.1 ° >(C16-H16B···H11) = 114.2 °

In the case of lactam **7**, it seems plausible to assume that the transannular overlap of the mentioned hydrogen atoms causes an increase in the ring strain of the enantholactam ring. It seems that the overall stabilisation through the entire packing, and the bifurcated ester carbonyl contacts, seem to compensate for this. The interactions *II* and *VIII*, *IX* and *X* are comparatively weak interactions between the ring carbons and the alkyl residue on the ester group and the two oxygen atoms in the ester group.

Analysis of all found interactions leads to the conclusion that the amide hydrogen bonds are the most dominant interaction and determine the general packing of enantholactam **7**. The amide contacts form C(4)-chains along the crystallographic *a* axis. These chains are supported by the bifurcated contacts between the transannular positioned hydrogen atoms and the ester carbonyls. The combination of these interactions connects chains along the *a*,*b* plane and extends in both directions. The lactam backbones point outwards along the *c* axis, the ester groups point towards the opposite direction on the *c* axis as can be seen in figure 4.33.

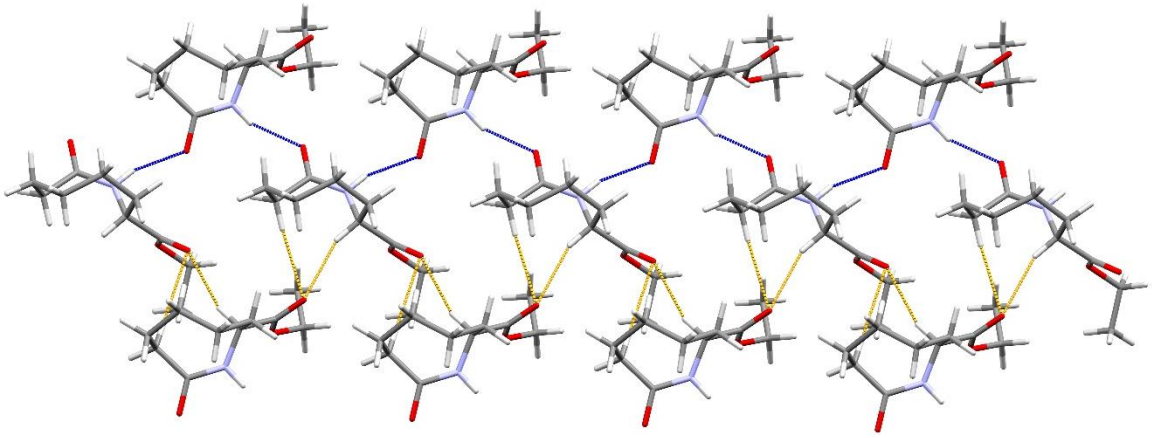

Fig. 4.33 The combination of the C(4) amide chains (blue) and the bifurcated, transannular carbonyl contacts (orange) forms chains along the a axis and extend into the a,b plane.

This set of chains is met by a second layer of chains on top of the first one. The ester groups connect the two layers through the interactions *II*, *VIII*, *IX* and *X* and therefore form a symmetry related bilayer of the chains. A spacefill model of that bilayer shows that the surface on both sides is covered by hydrophobic groups, effectively shielding the internal structures from outside interactions. This had already been observed for the *tert*-butyl ester **2** but whereas the *tert*-butyl groups were forming the hydrophobic surface (fig. 4.34), it is the lactam rings for this enantholactam that points outwards of the layers. The bilayers are connected through further hydrophobic interactions between them.

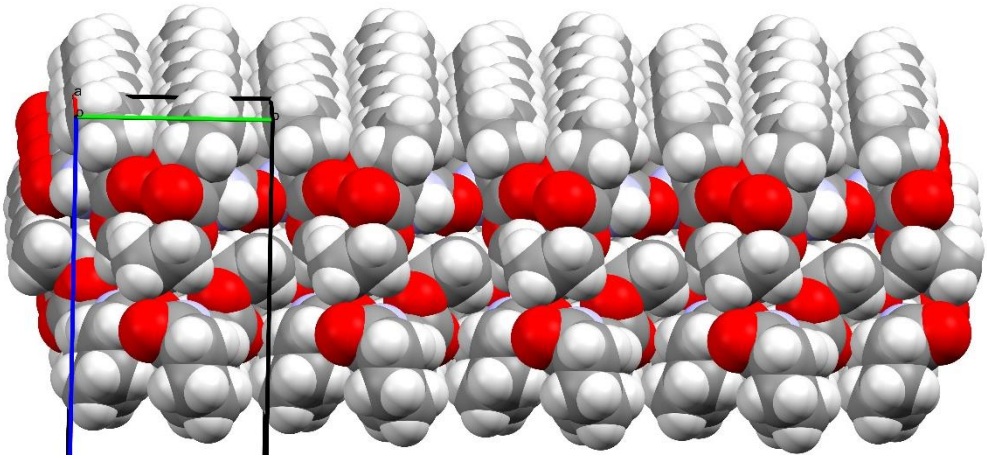

*Fig. 4.34 As already observed for pyroglutamate **2**, enantholactam **7** forms molecular bilayers, which are held together by hydrogen contacts and display hydrophobic surfaces on the outside. Contrary to **2**, the lactam ring backbones form the hydrophobic surface in **7**.*

The Boc protected enantholactam **8** was found to crystallise in the monoclinic space group $P2_1$ with one molecule in the asymmetric unit. A comparison of the bond lengths and angles revealed that the C-N bond of the lactam group is particularly long with d(N1-C7)=1.402 Å, the corresponding C=O is slightly shortened with d(O1-C7)=1.219 Å. Additionally, the torsion angle along the amide bond is particularly wide with <(C6-C7-N1-C1)=27.9 °. It was already observed that the torsion angle for the free lactam **7** was comparatively large with 13.2 °/14.7 ° but the respective bond lengths/angles were not out of the ordinary.

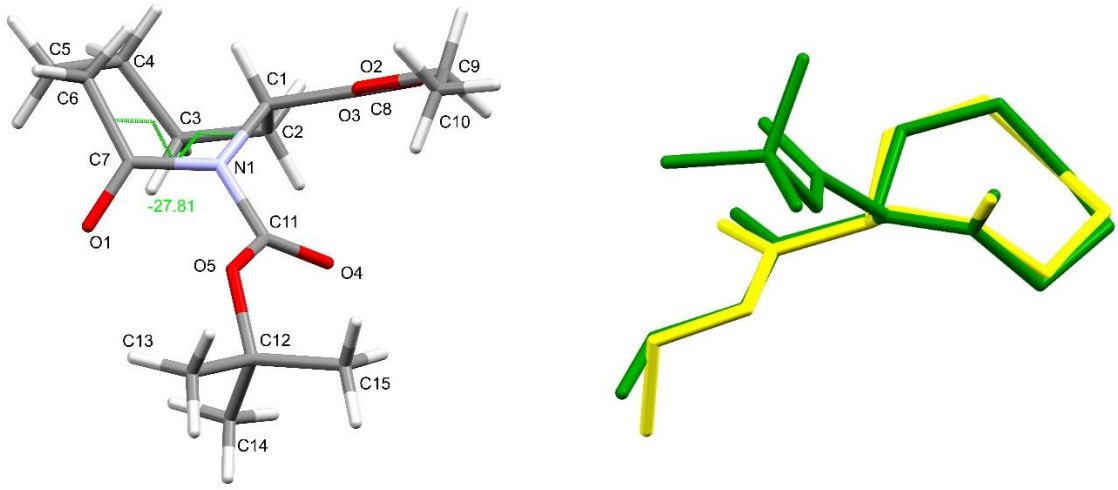

Fig. 4.35 ***Left****: The torsion angle along the amide bond in* ***8*** *is found to be the highest amongst all investigated lactams with 27.8 °.* ***Right****: Comparison of Boc protected enantholactam* ***8*** *(green) and the free lactam* ***7*** *(yellow) shows that the Boc protection does not seem to influence the conformation.*

The overall conformation of the Boc protected enantholactam **8** resembles its synthetic starting material, ethyl ester **7**. The ester group is found to adopt an equatorial position, standing away from the amide plane at an angle of 55.4 °. The study on conformative behaviour of caprolactams by *Gruber et. al.* had suggested, that on an equivalent caprolactam, the Boc protection group and the ester group experience steric repulsion. The caprolactam ring therefore adopts a conformation in which the ester group stand axially to the ring, avoiding the steric clash with the Boc group. This does not seem to be the case for the enantholactam **8**. However, the general conformational situation in enantholactams should be considered more flexible than for caprolactams due to the additional CH_2-group. The angle between a plane along the ester group (O3-C8-O2-C1), and a plane along the carbamate group (N1-C11-O4-O5) is found to be 28.6 °: It is plausible, that the conformational flexibility of the eight-membered ring allows the ester group to adopt an equatorial position without the steric clash that respective caprolactams might experience.

Just as already observed for the other two enantholactams **6** and **7**, synthesised for this study, the Boc protected lactam **8** shows transannular contacts, between H1 and H6A and between H1 and H4A (Fig. 4.36).

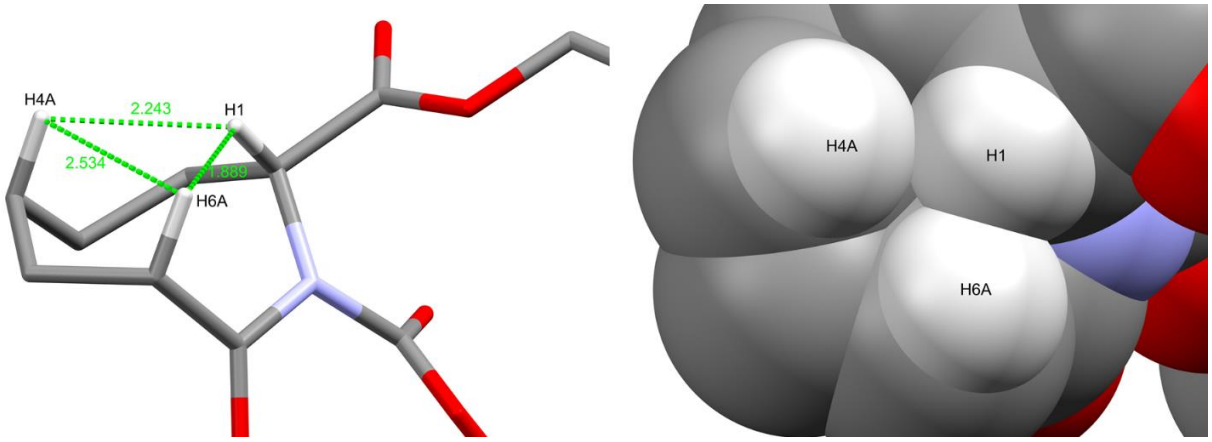

*Fig. 4.36 Just as for the other investigated enantholactams **6** and **7**, the Boc protected lactam **8** shows transannular, short hydrogen distances, which can be displayed as an overlap in a spacefill model.*

Overlap 1: d(H1-H6A)=1.889 Å	<(C1-H1⋯H6A)=125.5 ° <(C6-H6A⋯H1)=114.8 °
Overlap 2: d(H1-H4A)=2.243 Å	<(C1-H1⋯H4A)=116.8 ° <(C4-H4A⋯H1)=106.4 °

The contact between H1 and H6B is relatively short, compared to the other already described transannular contacts. Again, it is very much debatable whether this accounts for an actual positive interaction or not.

***N*-Boc-2-aminopimelic acid 9**. The diacid **9** was found to crystallise in the monoclinic space group *P21/n*, with one molecule in the asymmetric unit (Fig. 4.37). Comparison of the bond lengths and angles do not show any unexpected values for a Boc protected amino acid. Similar to other amino acids, the free proton on the carbamate nitrogen forms hydrogen bonds with the neighbouring acid group to give dimers and can be described by the graph set descriptor $R_2^2(10)$ (Fig. 4.37). The distance d(D-H⋯A) of 2.933 Å, accompanied by an angle of 174.4 ° is slightly longer than most of the studied lactams, but not overly so.

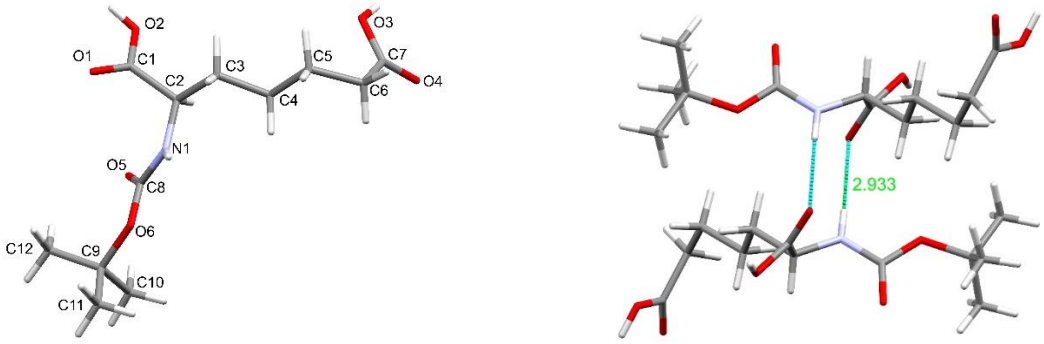

*Fig. 4.37 **Left**: The asymmetric unit of the Boc protected 2-aminopimelic acid. **Right**: The carbamate-acid interaction between N1 and O2.*

Both free acid groups are involved in OH-carbonyl contacts, alongside one acid-acid (O2-H2O···O4) and one acid-carbamate (O3-H3O···O5) contact. The acid-acid interaction shows a distance of 2.606 Å with an angle of 162.5 ° and connects the α- and ω- positioned acid groups intermolecularly to form C(10)-chains in the crystallographic *b* direction. The acid-carbamate contact is found to be slightly longer with 2.664 Å and an angle of 163.3 °, which is to be expected for the carbamate carbonyl, which can be considered a weaker H-bond acceptor in this case. The combination of both acid contacts connects three molecules through the system O3(A)-H3O(A)···O5(B)-O2(B)-H2O(B)···O4(C)-O3(C)-H3O(C)···O5(A) to heterotrimers with a less common descriptor $R_3^3(22)$. Additionally, two potential hydrogen contacts can be found between the carbamate carbonyl and two methyl groups of the *tert*-butyl group. However, both contacts (C10-H10B···O5, d=3.074 Å, 116.4 °; C12-H12C···O5, d=3.020 Å, 115.1 °) have considerably low angles and are below the generally used guideline for hydrogen bonds (<(DHA) > 120 °)[97]. If these were to be considered, they might influence the free rotation of the *tert*-butyl group which might therefore show a tendency to favour certain angles. Two more weak C-H···O contacts complete the interactions and the combination of all above mentioned contacts create a three-dimensional network with no clear formation of distinct supramolecular structures (fig. 4.38).

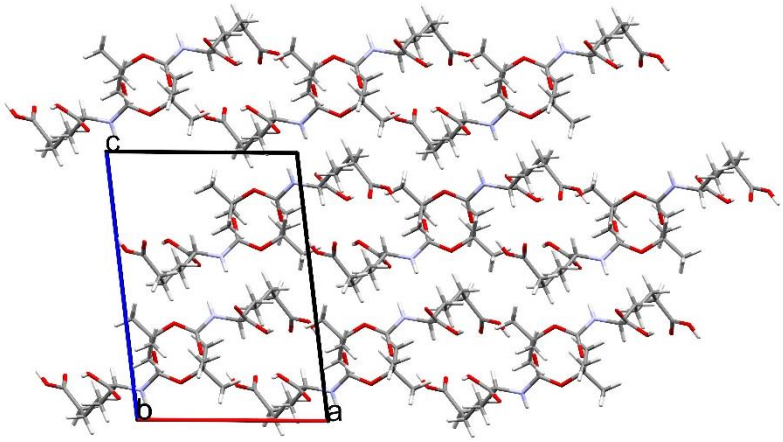

*Fig. 4.38 The combination of all interactions in enantholactam **8** gives a three-dimensional network, with no observable preferences of supramolecular structures.*

Comparison of the acquired data with already published structures

The above described structures shall now be put into a wider context by comparing them to a selected group of previously published structures. A list of the considered CSD entries is given in table 4.6 but will not be described individually. The results of the comparative studies will be split into the respective lactams first before overall conclusion will be drawn. Please note that all conclusions are drawn from a small size of available data and might not necessarily reflect overall tendencies for similar compounds that have not been studied.

Table 4.6 The following lactams were investigated alongside the newly synthesised lactams

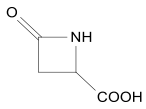 PELJUM[98]	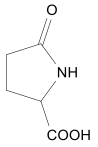 PYRGLU01[99]	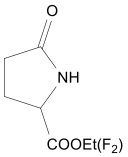 ABOQOA[100]	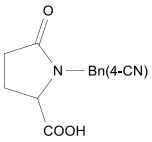 YAYMAO[101]	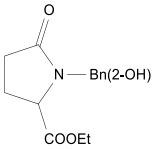 YEKQOX[102]
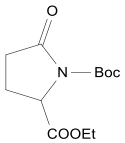 CEVBUC[103]	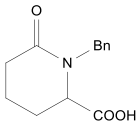 WALWOY[104]	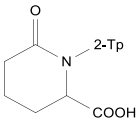 LOQCOL[105]	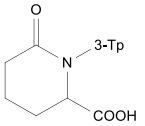 LOQCUR[105]	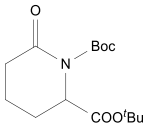 BAKYOC[106]
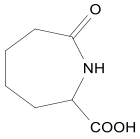 BOLHIV[107]	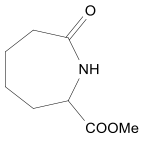 BOLHER[107]	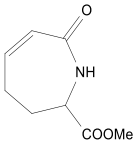 BOLJIX[107]	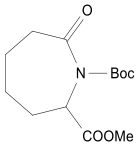 BOLHOB[107] (polymorph 1)	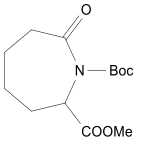 BOLHOB01[108] (polymorph 2)

Butyrolactams

Within the small sample group of butyrolactams, the envelope conformation appears to be the default. This is not unexpected considering that none of the analysed five-membered rings displayed desaturation. The angle, at which the C2 atom deviates from the mean amide plane varies between 7.4 ° and 28.4 °. The N_{α}-carboxyl substituents seem to adopt an equatorial position for less sterically demanding esters (exemplified by the diflouroethyl ester) and the free acid. With growing steric demand, this seems to change towards axial substituents. The *iso*-propyl ester appears to signify this transition, the next larger studied *tert*-butyl ester clearly adopts an axial position. Introduction of substituents on the lactam nitrogen also seems to promote adoption of axial positions, which can easily be explained by a steric clash between both substituents on the lactam ring. The size of the substituents also seems to be a determining factor for the main interaction between the lactam functionalities. Small esters seem to prefer $R_2^2(8)$ amide dimers, larger esters exhibit C(4)-chain structures. The free acid seems to be an exception from this, mainly because the comparatively strong acid interactions interfere with sole amide contacts.

Valerolactams

The considered valerolactams only contain two esters, a methyl and *tert*-butyl ester, which makes conclusive comparison difficult. The small methyl ester was the only structure found to show an equatorially positioned ester, the *tert*-butyl ester and all free acids adopt axial conformations. Free δ-valerolactam and the methyl ester were found to crystallise with $R_2^2(8)$ amide dimers as their apparent leading motif, the free acids show C(7)-chains. It should be mentioned, that the majority of the studied lactams show *N*-substitution, which excludes these from forming hydrogen bonds with the amide functionalities.

Caprolactams

Within the group of studied caprolactams, no tendency for certain conformations of the caprolactam rings were found. However, it seems plausible that the position of N_α-carboxyl substituents influences the entire ring structure. The methyl ester and the free acid were found to adopt equatorial positions, whereas all other examined structures show clear axial substituents such as secondary N_α-substitution, introduction of a double bond into the backbone and *N*-derivatisation. All of the studied caprolactams exhibit $R_2^2(8)$ amide dimers as their leading packing motif, but only comparatively small esters could be taken under consideration. It is possible, that larger esters would result in C(4) motifs.

Enantholactams

Every of the studied enantholactams show N_α-esters in equatorial position. The very small sample size has to be taken into account for this. However, considering that every other *N*-substituted lactam showed axial N_α-substituents, this could be an indication of a potential transition, depending on the ring size. Another indicator for such a transition can be found within the torsion angles starting from the lactam carbonyl carbons over the nitrogens to the ester carbonyl carbons ($C{=}O_{lactam}$-N-C_{chiral}-$C{=}O_{ester}$). Whereas all other lactams exhibit a wide range of torsion angles along this specific sequence, all studied enantholactams show angles between 149.1 ° and 154.6 °. It also seems, that the torsion angle along the amide bond tends to widen with an increase in the size of the respective ester residue. Free ζ-enantholactam and the respective ethyl ester form C(4)-chains, the methyl ester exhibits an alternative packing mode which had not been observed for any of the other studied lactams.

Analysis of spacefill models showed that short, transannular H-H contacts were found for the three studied enantholactams. This is could be a direct effect of the ring size and therefore the increased conformational flexibility of enantholactams over the smaller rings. However, this is to be expected for other enantholactams as well and seems to be related to Prelog-strain. Whereas this particular ring strain is sometimes denoted as 1,5-transannular ring strain, in the here presented structures, 1,4-positioned protons were found to show spacefill overlap.

General comparisons

The above-mentioned findings for the individual ring sizes shall now be brought into a general concept for lactams. The properties, that drew particular interest were the amide bond lengths, the adoption of axial *vs.* equatorial conformations of N_α-esters and the hydrogen bonding patterns, both for the amide groups and in conjunction with the analysed carboxylic acid functionalities.

Length of amide bonds

Amongst all the for this study examined structures, it was found that the amide bond lengths do not seem to be influenced by the ring size, the N_α-substitution, the leading packing motif or the crystal packing in general. The observed slight variation in C-N distance (1.31–1.35 Å) for this respective bond is to be expected. However, introduction of a Boc protection group on the amide nitrogen changes this considerably. Direct comparison of the amide bond lengths between the studied Boc substituted lactams with their respective parent lactams shows a significant increase. The experimental importance of this was reflected by the empirical observation made during the unexpected hydrolysis of the Boc protected caprolactam ethyl ester. Whereas the $LiOH/H_2O_2$ protocol had only resulted in saponification of the ester for all unprotected lactams, the same procedure had led to hydrolytic ring opening for this *N*-Boc derivatised lactam. As mentioned in Chapter 3, our findings on δ-valerolactam had led to the conclusion that the amide bond lengths do not necessarily determine the rate of hydrolysis for the homologous series of lactams. However, the significant elongation of amide bonds through the introduction of electron withdrawing substituents on the lactam nitrogen appears to change their hydrolytic stability again. What remains unknown is the extent to which both of these factors influence hydrolysis. Nevertheless, these findings are to be considered carefully for any synthetic approach that involves the use of potentially hydrolytic conditions and possibly for reactions involving nucleophiles as well.

Position of esters

The analysed structures led to two general trends on the adoption of axial *vs.* equatorial conformations for the studied lactams. Firstly, it seems that esters with a high steric demand such as *iso*-propyl or *tert*-butyl ester will tend to occupy the axial positions, less demanding esters will prefer equatorial conformations. Secondly, *N*-substitution, especially with large protection groups, seems to force most esters into the axial conformation even if that is disfavoured for the free lactam. However, there also seem to be certain exceptions from these trends. Free carboxylic acids follow the trend of small esters and seem to prefer the equatorial over the axial conformation, but do not appear to be influenced by *N*-substitution. An easy explanation can be given by their small size, but their ability to form strong hydrogen bonds is most likely a determining factor for this behaviour as well. Enantholactams seem to prefer for their ester groups to adopt an equatorial position. It is possible, that enantholactams with large esters and *N*-substitution might adopt axial sites. Unfortunately, this theory cannot neither be proven nor disproven at this point.

The acquired data therefore lead to the final conclusion: the equatorial position is favourable; steric demand and repulsion will force conformationally flexible substituents into an axial site. We further believe that enantho-, and possibly larger lactams, allow their substituents to avoid steric clash which therefore allows the preferred equatorial position.

Amide-amide contact patterns

Within the studied group of lactams, two general motifs were found to dominate the amide hydrogen bonding patters of free lactams: the dimerization in $R_2^2(8)$ symmetry and the formation of C(4)-chains. Smaller sized lactams (five- to seven-membered) with low steric demand seem to prefer dimerization, larger esters and larger lactams seem to prefer C(4)-chains. This trend was already observed within the homologous series of lactams and is further supported by this comparative study. The impact of this patters on physicochemical behaviour cannot be evaluated with certainty. However, the formation of small aggregates *vs.* oligomeric structures could influence aspects like dissolution kinetics, reactivity etc.

General H-bonding patterns

Alongside the findings of the amide interactions in the solid state, the structures containing free carboxylic acid groups had to be considered from a different perspective. It seems that lactams with such free acid groups will often form C(7)-chains between the acid OH and the lactam carbonyl groups. It also seems that the formation of these acid interactions supersede the formation of sole amide-amide contacts. However, the combination of amide and acid contacts, both in oligomeric forms such as chains and in cyclic structures seems common as well. A number of different cyclic motifs was found for varying lactam ring sizes; $R_3^3(13)$ trimers were found for a propiolactam (CSD entry: PELJUM), $R_2^2(10)$ for a butyrolactam (CSD entry: PYRGLU01) or a $R_2^2(8)$ acid-amide heterodimers for a caprolactam (CSD entry: BOLHIV). The acid-amide heterodimer should be considered an exception and are usually only observed for amide/carboxylic acid co-crystals.[109,110]

4.5) Summary and Conclusion

Only little research on N_α-substituted lactams has been published and only very few compounds have been structurally characterised by single crystal analysis. To increase the sample size for the here presented studies, several new lactams of varying sizes were synthesised, but not all of them could be analysed with SC-XRD. Comparative investigation of the available and eight newly acquired data sets allowed several comprehensive conclusions to be drawn. It was found, that besides the well-known amide packing motifs of $R_2^2(8)$ amide dimers and C(4)-amide chains, a new descriptor was found: $R_2^2(8)$ amide-acid heterodimers. It was also found that the presence of free carboxylic acid groups usually leads to C(7)-chains. Apart from these moderately strong contacts, the majority of structures further exhibit weak C-H···O contacts. The importance of such weak interactions might not necessarily play a determining role in the presented compounds but has been described as one stabilising factor in protein chemistry[111]. The length of the amide bond in lactams does not seem to be influenced by their conformation or the introduction of N_α-substituents. Introduction of electron withdrawing groups on the nitrogen atom however appears to change their reactivity and their susceptibility towards hydrolysis.

The conformation itself is influenced by the size of N_α-substituents. Small ester groups will often adopt equatorial positions, larger esters will tend towards axial sites. Furthermore, it seems that as soon as the lactam ring reaches a certain size itself, these substituents will remain in the equatorial position. The turning point for this transition was found to be the size difference between capro- and enantholactams. The size of such N_α-substitution also influences the overall tendency to form strong interactions. It seems that the formation of amide-amide dimers is the preferred default, which prevails until steric hinderance of large groups forces a change to chain-type structures. These findings support the in Chapter 2 mentioned hypothesised importance of the positioning of N_α-esters on the Dieckmann cyclisation of caprolactams and shall be further investigated and considered in the following Chapter.

---

[86] L.R.F. Carvalho, L.B. Zinner, G. Vincentini, G. Bombieri, F. Benetollo, *Inorg. Chim. Acta* **1992**, *191*, 49-56.
[87] B. Neises, W. Steglich, *Org. Syn.* **1985**, *63*, 183.
[88] A) M.E. Kopach, M.M. Murray, T.M. Braden, M.E. Kobierski, O.L. Williams, *Org. Process Res. Dev.* **2009**, *12*, 152-160.; B) R.B. King, *Encyclopedia of Inorganic Chemistry* 2nd Edition, Wiley-VCH, Weinheim, **2005**.
[89] R. Goddard, O. Heinemann, C. Kruger, I. Magdo, F. Mark, K. Schaffner, *Acta Cryst. C* **1998**, *54*, 501-504.
[90] J. Wagger, S.G. Grdadolnik, U. Groselj, A. Meden, B. Stanovnik, J. Svete, *Tetrahedron: Asymm.* **2007**, *18*, 464-475.
[91] C. Weck, E. Nauha, T. Gruber, *Cryst. Growth Des.* **2018**, *18*, 7248-7253.
[92] F.K. Winkler, P. Seiler, *Acta Cryst. C* **1979**, *35*, 1920-1922.
[93] C. Weck, E. Nauha, T. Gruber, *Cryst. Growth Des.* **2019**, *19*, 2899-2911.
[94] G.R. Desiraju, T. Steiner, *The Weak Hydrogen Bond in Structural Chemistry and Biology* OUP, Chichester, **1999**.
[95] A.D. McNaught, A. Wilkinson, *IUPAC, Compendium of Chemical Terminology* 2nd edition, Blackwell Scientific Publications, Oxford, **1997**.
[96] E.L. Eliel, N.L. Allinger, S.J. Angyal, G.A. Morrison, *Conformational Analysis* 3rd edition, Wiley & Sons, New York, **1967**.
[97] P.A. Wood, F.H. Allen, E. Pidcock, *CrystEngComm* **2009**, *11*, 1563-1571.
[98] A.J. Mora, M. Brunelli, A.N. Fitch, J. Wright, M.E. Baez, F. Lopez-Carrasquero, *Acta Cryst. B* **2006**, *62*, 606-611.
[99] Z. Taira, W.H. Watson, *Acta Cryst. B.* **1977**, *33*, 3823-3827.
[100] P.K. Mykhailiuk, I. Kishko, V. Kubyshkin, N. Budisa, J. Cossy, *Chem. Eur. J.* **2017**, *23*, 13279-13283.
[101] J. Chen, T. Sheng, S. Hu, S. Xiang, R. Fu, Q. Zhu, X. Wu, *J. Solid State Chem.* **2012**, *192*, 255-262.
[102] R.S. Mulla, M.T. Walden, D.S. Yufit, T. Desa, E. Lurie-Luke, J.A.G. Williams, *Tetrahedron* **2017**, *73*, 6410-6420.
[103] P. Rajalakshmi, N. Srinivasan, R.V. Krishnakumar, I.A. Razak, M.M. Rosli, *Acta Cryst. E* **2013**, *69*, 567-568.
[104] J. Sivy, V. Vrabel, S. Marchalin, P. Safar, *Asian J. Chem.* **2015**, *27*, 2635-2638.
[105] V. Vrabel, J. Sivy, P. Safar, S. Marchalin, *Acta Cryst. C* **2014**, *70*, 817-822.
[106] J. Marin, C. Didierjean, A. Aubry, B. Guichard, G. Guichard, *J. Org. Chem.* **2002**, *67*, 8440-8449.
[107] T. Gruber, A.L. Thompson, B. Odell, P. Bombicz, C.J. Schofield, *New J. Chem.* **2014**, *12*, 5905-5917.
[108] C. Weck, F. Obst, E. Nauha, C.J. Schofield, T. Gruber, *New J. Chem.* **2017**, *41*, 9984-9989.
[109] S. Saha, G.R. Desiraju, *J. Am. Chem. Soc.* **2018**, *140*, 6361-6373.
[110] A.M. Moragues-Bartolome, W. Jones, A.J. Cruz-Cabeza, *CrystEngComm* **2012**, *14*, 2552-2559.
[111] M. Mottamal, T. Lazaridis, *Biochemistry* **2005**, *44*, 1607-1613.

Chapter 5) – Optimisation of the synthesis of 7,8-dioxo-6-azabicyclo[3.2.1]octanes from caprolactams

5.1) Abstract

Previous chapters have outlined the introduction and initial efforts to optimise a Dieckmann-type cyclisation of N_α-substituted caprolactams and crystallographic studies on the behaviour of lactams in the solid state. Following these studies, further attempts at optimising the ring closure are presented. After a number of targeted experiments, a simple one-pot synthesis starting from a free, unprotected caprolactam to the desired 7,8-dioxo-6-azabicyclo[3.2.1]octane was accomplished. This pathway is able to replace previous multistep approaches with better overall yields and without the need for strong bases such as LDA. Furthermore, a detailed mechanism for the proceeding ring closure is proposed. Reaction conditions, the impact of substrate variability and synthetically important physicochemical properties are discussed. The obersavtion of stable carbonic acid esters and hemiketals is described, their formation and certain aspects of their stability is presented, and the respective compounds are being characterised.

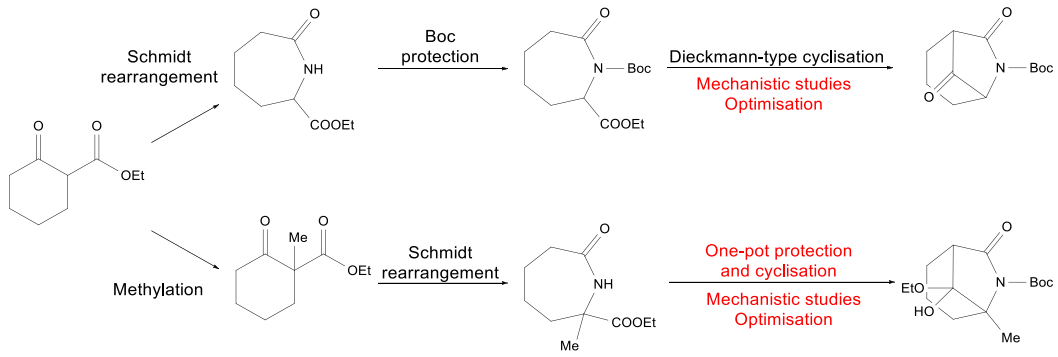

Fig. 5.1 The following Chapter will discuss a more detailed mechanistic investigation of this Dieckmann-type cyclisation, which resulted in the development of a one-pot synthesis of Boc protection and bicyclisation from a simple caprolactam.

5.2) Introduction

As outlined in Chapter 2, multiple attempts to optimise a Dieckmann-type cyclisation to obtain 7,8-dioxo-6-azabicyclo[3.2.1]octanes had remained largely unsuccessful. Despite all efforts to increase the yield beyond 15%, a viable approach for further synthetic purposes had remained elusive. However, the previously discussed experiments indicated several factors, that seemed to be of essential importance for the success of such a synthetic approach. The protection group, the conformational behaviour of the lactam ring and the application of a suitable base were suggested to play determinant roles. Other factors such as temperature or concentration were also found to influence the reaction outcome, but it was suggested, that these only indirectly influenced the outcome through the main determinants.

A Boc protection group seemed necessary for the viability of a Dieckmann-type cyclisation, a benzyl protected caprolactam could not be cyclised. It was thought that the benzyl group would pose similar steric demand to the Boc group, which was expected to play a key role in the reaction. The other main difference between these two protection groups is the effect they have on the electronic situation within the caprolactam. Whereas carbamate protection groups can be counted as electronic withdrawing, the benzyl group is attributed to electron donating groups.

This influence of the Boc group on the electronic distribution of lactams was found in crystallography studies again. It was found that Boc protected lactams exhibit considerably longer amide bonds than their parent lactams. A few selected *N*-benzyl-type substituted lactams had further supported this general concept by showing that these lactams did not exhibit elongated amide bonds.

It was initially suggested that the steric demand of the Boc group would force an N_α-positioned ester group in the axial position which appeared to be another key role. Chapter 4 had concluded, that this was not exclusively related to Boc groups, but to *N*-substitution in general. This supported the suggestion that the electronic structure was indeed the key determinant in the distinct differences between the Boc and the Bn protection of caprolactams for this cyclisation.

Another factor that was outlined to play a major role was the conformational situation in general. It is well-known that the different sized cycloalkene rings show distinct conformational behaviour. Amide and therefore lactam bonds have been shown to adopt certain characteristics of double bonds due to their partial double bond character. This makes comparisons to the very well-studied cycloalkenes easier than to the less well-studied lactams themselves. These theoretical considerations were now planned to be further supported by empirical evidence. Experiments on the cyclisation of systems, other than caprolactams, like a valerolactam or an unsaturated caprolactam had remained unsuccessful. The studies on the conformational behaviour in the solid state supported the concept that different lactam sizes or the introduction of double bonds would supress bicyclisation towards dioxoazabicyclo scaffolds.

It was also found, that the change from a methyl to an ethyl ester seemed to increase the yield by almost twofold. Following the crystallography studies, we concluded that this could be a direct result of the influence of the ester size. It was found that with increasing size of the ester functionality an axial position becomes more favourable for N_α-substituents. This further supported the concept of conformation being a main determinant for the success of any Dieckmann-type cyclisation of these lactams.

Furthermore, evidence was found that the amount of base seemed to have an effect to some extent. A twofold increase in base equivalents seemed to also increase the product almost twofold. And while the counter-ion was not found to directly impact the product yield on the scale that the previous study had worked on, it was also appreciated that the only base used was of the hexamethyldisilazide type. While certain bases do not promise success because of their nucleophilic nature or their steric demand, other potentially viable options had not been investigated, such as lithium diisopropyl amide (LDA).

The findings from chapters 2, 3 and 4 were now to be tested for their potential to help elucidate the reaction mechanism. It was thought that a thorough understanding of how the reaction proceeds could lead to the successful optimisation of this approach to enable widespread synthetic application.

Key Factors	Influencial factors
Conformational situation *N*-Protection group Ring size	Temperature Base (amount, type, counter-ion, etc.) Concentration Ester size

5.3) Results and Discussion

As mentioned, a number of factors were identified as key factors, others were found to likely influence these key factors. The following targeted experiments were designed to support the proposed theories.

Variations of lactam ring size and studies

The initial reaction studies had already led to experiments on the same Dieckmann-type cyclisation of valerolactams instead of caprolactams. Several attempts had remained unsuccessful in the preparation of an azabicyclo[2.2.1]heptane. The conclusions in Chapter 4 had suggested, that protected valerolactams would adopt conformations in which N_{α}-positioned esters would stand axially to the ring. The fact that the preparation of the respective bicyclic products had failed suggested that the ring strain was the prohibiting factor, rather than the conformation. Our studies on the conformational behaviour of lactams in the solid state had led to the synthesis of similar enantholactams. To test whether the theories on conformation *vs*. ring strain were correct, a Boc protected enantholactam ethyl ester was therefore subjected to the cyclisation protocol that had shown success on caprolactams (Fig. 5.2).

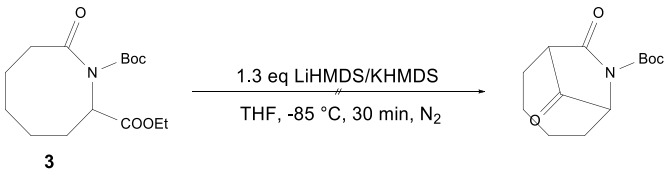

*Fig. 5.2 The Dieckmann-type cyclisation of Boc protected enantholactam ethyl ester **3** did not give any bicyclic product. Following the previously mentioned conclusions on the behaviour of such lactams, this could be a result of the reluctance for the ester group to adopt an axial position.*

Neither LiHMDS, nor KHMDS were found to successfully cyclise enantholactam **3**. Chapter 4 had indicated that N_α-substituents on enantholactams would not adopt an axial position as easily as for equivalent caprolactams. The unsuccessful cyclisation was therefore thought to be a direct result of this. Because of the increased size of the lactam ring, the ester group would not have to adopt an axial position and would therefore face away from the ring. It seems safe to assume that for a successful cyclisation to happen, a carbanion formed through α-lactam deprotonation would have to be able to nucleophilicly attack the ester group. It is possible, that disubstituted enantholactams with similar substitution patterns to the presented allow for N_α-esters to adopt an axial position in solution. However, if that was the case, it is plausible that this would still be energetically disfavoured and therefore disfavour ring closure in the mechanistic sequence of a Dieckmann-type cyclisation.

Variations on the base

Initial studies on the caprolactam methyl ester have shown, that an increase in the applied base could also increase the product yield. 1.1 eq. of MHMDS had led to 7-8 % of the product, 2.1 eq. had resulted in 11-13 %. To see if an extreme increase in the base would lead to a further increase in the product yield or whether this would lead to side products, 10 eq. of LiHMDS were used. Chapter 3 had concluded that the counter-ion did not seem to influence the reaction outcome on a less excessive scale. However, considering that 10 eq. could change the mechanism drastically, the counter-ions could have an effect on this scale. It was therefore decided, that 10 eq. of NaHMDS and KHMDS were to be tried as well (Fig. 5.3).

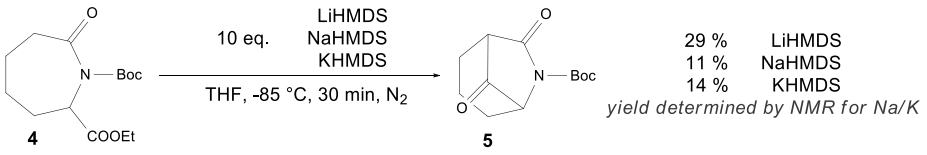

Fig. 5.3 To test, whether a large excess of base would increase the yield, 10 eq. of MHMDS bases were applied. The yield was found to increase to 29%, 11% and 14% for lithium, sodium and potassium respectively.

Indeed, an increase of LiHMDS to 10 eq. also gave an increase of product yield up to 29%. This non-linear increase suggested that the amount of base influences the reaction mechanism, but also that more base does not automatically result in more product. It appeared that the large excess either shifted an existing equilibrium, or that interference with the reaction mechanism occurred, that was not fully understood yet. Despite repeated column chromatographic purification attempts, the product for the experiments using NaHMDS and KHMDS was not obtained pure. The formation of product was confirmed, and the yield determined by NMR, but these analyses had also shown an impurity. Extensive 2D-NMR analysis then suggested, that the product impurity would be of highly similar structure than the main ketone product. ^{13}C-NMR experiments had shown a signal at 98.7 ppm, which had not been observed for any other compound with a similar structure in this project (Fig. 5.4). Carbon NMR signals around 100 ppm are comparatively unusual[112] but can be found for certain classes of compounds such as ketals or acetals. As an example, 2,2-dimethyl-1,3-dioxolane, the ethylene ketal of acetone, shows a signal around 108 ppm in carbon NMR experiments[113].

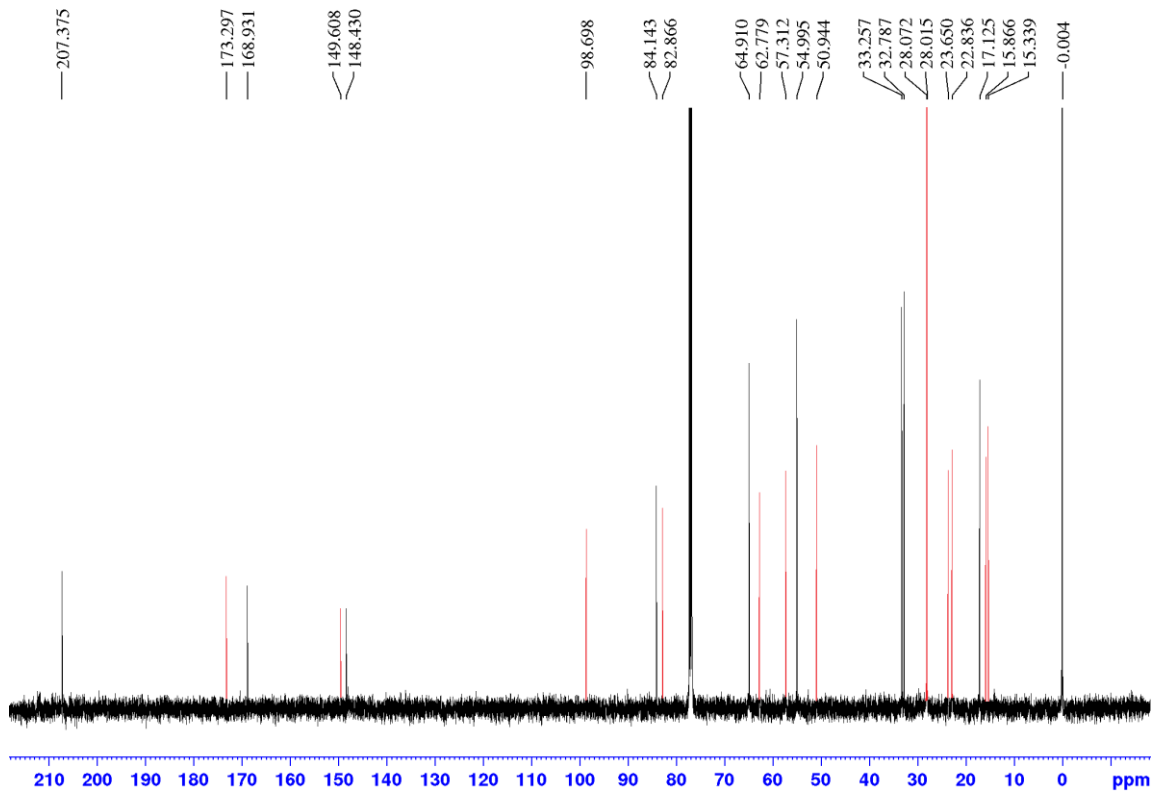

*Fig. 5.4 The ^{13}C-NMR spectrum, acquired from a sample of the presumed pure ketone **5** showed a number of signals that indicated an impurity of roughly equal amounts to the desired product. The signal at 98.7 ppm indicated the formation of a ketalic species (highlighted in red).*

According to the general mechanism for Dieckmann condensations, the nucleophilic attack of the through deprotonation formed carbanion leads to a hemiketalic species, which then reacts further to give a ketone. Hemiketals are considered to be unstable in many cases and give ketones through the elimination of one equivalent of the respective alcohol.

However, the mechanism explicitly states, that such a hemiketalic species is formed and such ketalic species show signals around the range of 100 ppm in carbon NMR experiments. Following this theory, the re-evaluation of the 2D-NMR experiments led to the conclusion, that the product mixture of the Na/KHMDS experiments consisted of the desired bicyclic ketone and an ethoxy hemiketal (Fig. 5.5).

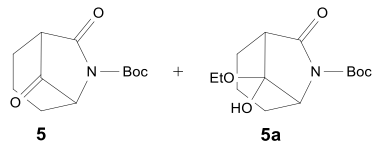

*Fig. 5.5 The analysed product from the NaHMDS and KHMDS cyclisation experiments were found to contain both the bicyclic ketone **5** and its respective ethoxy hemiketal **5a**.*

The NaHMDS experiment gave a ratio of roughly 65 to 35, KHMDS gave 55 to 45 for the ketone and hemiketal, respectively. The formation of such a hemiketalic species had not been observed for any of the LiHMDS experiments and raised the question of the influence of the counter ion again. The counter-ion is neglected in many reaction mechanisms in organic chemistry, but this clearly indicated, that the counter-ion played a role in this cyclisation that had not been fully understood.

The next logical conclusion that followed, was the re-evalutation of the importance of the Boc protection group. It is known, that the stabilisation of metal ions through chelation from functional groups can play a significant role. It had already been observed, that the Boc protection group, a carbonyl containing carbamate group, could lead to successful bicyclisation, the benzyl group that does not contain such a carbonyl group, does not (Fig. 5.6).

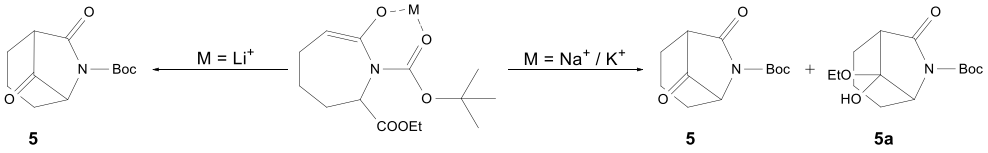

Fig. 5.6 When 10 eq. of MHMDS-base are used, a difference in the product formation was observed: LiHMDS only gave the respective ketone, NaHMDS and KHMDS gave a mixture of ketone and a stable ethoxy hemiketal.

According to the mechanism of Dieckmann condensations, the next step following a chelation would be the nucleophilic attack of the enolate on the ester group to give a tetrahedral hemiketalic species. The ethoxy group on the bridging carbon atom would be the mechanistic result (for an ethyl ester) alongside a free hydroxylate ion. The fact, that this species was only found for the Na- and KHMDS experiments led to the conclusion, that the increased ion radius of Na^+ and K^+ could play a role (Li^+ - 76 ppm, Na^+ - 102 ppm, K^+ - 138 ppm for hexacoordinated species[114]). The free hydroxylate anion would still require a counter-ion to be present in proximity, but this counter-ion could already be chelated by the lactam carbonyl and the carbamate group. In case of the smaller Li^+ ions, this chelation could be strong enough to force the hemiketal to eliminate the negative net charge by expulsion of an ethanolate ion. The result would be ketone.

This ketone would also not be able to undergo CH-deprotonation again, because the bicyclic structure would not allow the formation of an enolate again, according to *Bredt's rule*[115]. For the larger Na^+ and K^+ ions, the hydroxylate could be stabilised through the larger counter-ions, which could allow for the electrostatic attraction whilst maintaining chelation to some extent (Fig. 5.7).

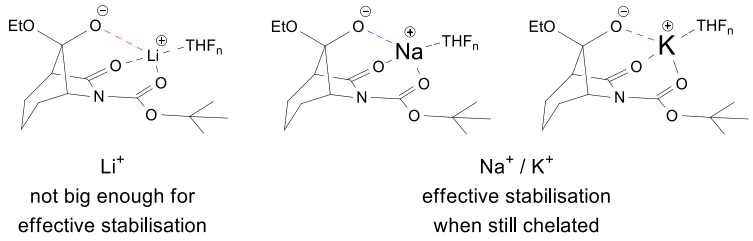

Fig. 5.7 Considering the size difference of the three counter-ions that were used and that these counter ions are likely to be chelated during the reaction, stabilisation of hemiketals through the larger ions might be the reason for the first observation of such stable hemiketals.

In all three cases, the mildly acidic, aqueous work-up with saturated NH_4Cl, which was introduced to quench any residual base, would then simply generate non-charged species. Any eliminated ethanolate would react to give ethanol, a bicyclic hydroxylate would be transferred to a free hemiketal. The stability of such hemiketals is always debatable, but the NMR-analysis had clearly indicated that this was the case for this bicyclic system. Several NMR studies were conducted following this, which shall be presented and discussed later on in this chapter.

To further expand the understanding of this system, instead of using sterically demanding bases, NaH as a strong, non-nucleophilic base with very little steric hinderance, was used. As expected, no indication of product formation was found. It was already hypothesised, that a large base would be necessary to allow regioselectivity between the two CH-acidic positions, the α-ester and the α-lactam position. This experiment supported this and also led to another conclusion about the reaction mechanism and the low product yields. It was observed, that the majority of the starting material could be recovered after work-up and chromatography for most of the experiments, including many experiments with LiHMDS as a base. LiHMDS was employed because of its steric hinderance, but no empirical prove was found that its steric demand was enough to establish sufficient regioselectivity. Considering, that the hypothesised reaction mechanism requires the ester group to stand in an axial position, the α-ester proton might not be crowded enough to avoid deprotonation, even in the case of MHMDS bases. Such a deprotonation would generate an enolate, similar to the α-lactam position. If the concept of chelation is allowed for the lactam enolate, it must also be allowed for an ester enolate. The crystal structures of the Boc protected caprolactams had supported this suggestion. An ester enolate could therefore also experience chelation. This can be further supported by the fact, that enolates are generally thought to show carbon-carbon double bond character and can therefore be considered co-planar as well.

Such an enolate would therefore not distinguish between the previous axial or equatorial position of that ester group. It seems that under the employed conditions, the so formed hypothetical enolate is stable for the duration of the experiment. Aqueous work-up would then simply regenerate the ester and the result would be the starting material with no chemical transformation (Fig. 5.8).

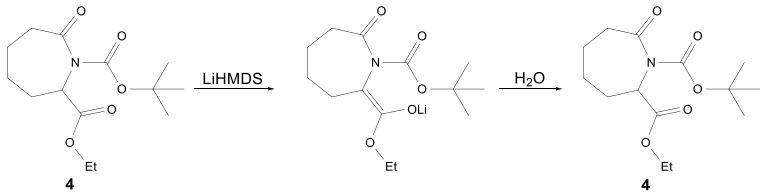

Fig. 5.8 The use of the sterically hindered base LiHMDS seems to not be regioselective enough for a selective deprotonation of the α-lactam position. Formation of an ester enolate instead seems to form a stable species, that regenerates the starting material after aqueous work-up.

The choice of MHMDS bases was largely based on their steric hinderance. The basicity was considered to only be secondary because it was anticipated, that the bicyclisation would have to be controlled through kinetic means, not necessarily through thermodynamic. Experiments using NaH gave no bicyclic product, which reinforced the concept for the need of a sterically hindered base. As explained in Chapter 2, lithium diisopropylamide (LDA) is another strong, non-nucleophilic base and was chosen for further experiments. First experiments using 1.3 eq. of LDA gave a promising yield of 30% of bicyclic ketone **5**. Because the large excess of LiHMDS had increased the yield further, 10 eq. of LDA were applied as well, but only insignificantly increased the yield further to 32%. The increased basicity led to the reconsideration of the bicyclisation reaction from a thermodynamic perspective. It seemed that if such a strong base is applied, the amount of base will not affect the reaction outcome as much as with the weaker base LiHMDS. A simple, thermodynamic explanation is that the reaction system allows about 30% of the starting material to proceed to its ketone product. This can be supported by the experiments conducted using different time frames and the temperature. If 1.3 eq. of LiHMDS are used, the reaction seems to proceed within the first 30 min, which indicates that the thermodynamic equilibrium has already been reached. A further decrease in temperature below -78 °C also did not seem to increase the product yield and was only conducted as sole means of practical convenience. Again, this supports the theory, that the thermodynamic equilibrium was reached. Following this argument, the large excess of LiHMDS however would shift such an equilibrium towards the side of the products, which was also supported by the experiments. The thermodynamically dominating base LDA could transform as much of the starting material as the system thermodynamically allows and a further increase beyond 1.3 eq. would not drastically change that outcome anymore. This would mean, that the addition of even more than 10 eq. of LiHMDS could further increase the product yield. However, because the base was applied as a premade solution and further addition of even more of this solution would also change the concentration of the mixture entirely. This theory was therefore not further investigated, as it appears to go beyond a practical scope.

However, the dissection of the thermodynamic and kinetic aspects of both bases is difficult. pK_a values for LDA are often listed as being stronger than LiHMDS by a magnitude of 10, which is generally considered a thermodynamic phenomenon. However, LDA is also a slightly smaller base which influences its kinetic behaviour as well. The reaction kinetics can therefore not be ruled out entirely as a determinant.

Variation on substrate

The experiments involving the variation of the base had concluded, that the deprotonation of the α-ester position most likely interfered with the successful bicyclisation, despite the use of sterically strongly hindered bases. To test this theory, the N_α-disubstituted caprolactam that was previously synthesised previously was used for further experiments (Fig. 5.9).

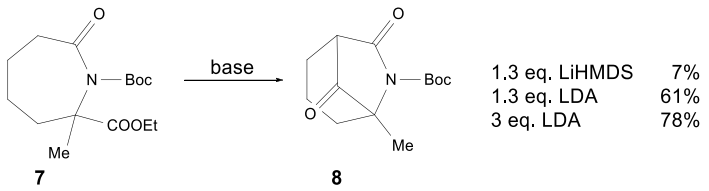

7 **8**

*Fig. 5.9 The Dieckmann-type cyclisation with N_α-disubstituted caprolactam **7** gave a poor yield of 7% for 1.3 eq. LiHMDS but good yields of 61% and 78% for 1.3 eq. and 3 eq. for LDA, respectively.*

The initial reaction protocol employing 1.3 eq. of LiHMDS gave a product yield of 7% for the N_α-methylated bicyclic ketone. 1.3 eq. LDA on the other hand gave a good product yield of 61%, 3 eq. of LDA further increased the yield to 78%.

This led two major conclusions. Firstly, the change from LiHMDS to LDA allowed the bicyclic lactam to be formed as the main product. It was already discussed, that LiHMDS and LDA mainly differ in their basicity, but also in their steric demand. However, one more factor that had not been considered so far is the reaction products formed after these two bases have undergone an acid-base reaction. LDA will give diisopropylamine, LiHMDS on the other hand will give hexamethyldisilazane (HMDS). HMDS itself can be used as a base but is also used as a silylating agent to transform alcohols into silyl ethers[116] (Fig. 5.10) in for example GC-MS derivatisation procedures. This also led to the re-evaluation of LiHMDS as a base for the deprotonation mechanism. Once LiHMDS successfully deprotonated the α-lactam position, we hypothesised the formation of a lithium enolate. The other reaction product must be HMDS, which could act as a silylating agent, and form a TMS-enolate. Furthermore, following the hypothesised reaction mechanism, one of the proposed intermediates is a hemketalic species with a free hydroxylate group. HMDS could also act as a silylating agent once the ring closure has occurred to give a TMS ketal. Even though the possible silylation of any intermediates is not been proven on this system so far but would support the observed empirical outcomes.

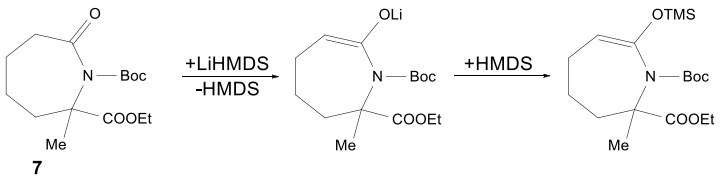

Fig. 5.10 HMDS, which can be used as a silylating agents could form a silyl ether with a lithium enolate. The resulting silyl ether might not undergo cyclisation.

Number 2: the elimination of the second CH-acidic position changed the reaction system entirely. This observation supported several of the previously formed theories on the reaction mechanism. For LiHMDS induced cyclisations of **7**, the starting material could not be recovered. It had been hypothesized, that the Dieckmann-type cyclisation could come to an end, if that position was deprotonated and that the resulting enolate was stable enough to then be recovered, once water was introduced into the system. Without this second acidic position, this enolate cannot form and the α-lactam position undergoes deprotonation, leading to cyclisation.

One more factor that is to be considered comes from the examination of the SC-XRD data of lactam **7**. The data shows that the ester group occupies the axial position. One of the overall conclusions of Chapter 4 was that a substituent in that respective position on a caprolactam most likely prefers the equatorial position because of steric repulsion. Following the concept, an additional substituent could than force the axial position of the ester. This would be especially true, if *N*-substitution with another comparatively large group is introduced. The two largest group, the *N*-Boc and the ester group in the case of lactam **7**, would avoid steric clash by the ring adopting the conformation with the least steric repulsion, *i.e.* the axial position for the ester group. It was further concluded, that the position of the ester group plays a determining factor in the possible nucleophilic attack of any formed lactam enolate. It is therefore plausible, that the changed conformational situation in caprolactam **7** also has an effect on the ring closure. However, it is not possible to fully dissect both effects and their individual extend at this point.

Optimisation to a multistep one-pot synthesis

The previous experiments had shown, that the bicyclisation of an N_{α}-disubstituted caprolactam gave good product yields and appeared to be superior to non-methylated caprolactam. Because of the significantly better yield, it was decided that refocussing the synthetic efforts to the methylated caprolactam **7** promised greater success due to the higher possible throughput. The bottleneck reaction here was the synthesis of the caprolactam itself through Schmidt rearrangement. The hazardous nature of the reaction conditions required the synthesis of this precursor to be limited to small scaled batches. About 1.0 g of the cyclohexanone starting material was typically used, which gave around 0.8 g of the caprolactam product. The entire precursor product was then Boc protected, using equal amounts and concentrations as for the same protection reaction of the non-methylated caprolactam.

To our surprise, during the resynthesis of the Boc protected lactam **7**, the bicyclic product **8** could be found in the crude product mixture and could be isolated with a yield of about 6% (Fig. 5.11). This discovery led to the investigation of the protection procedure. An outline of the reaction protocol is given below.

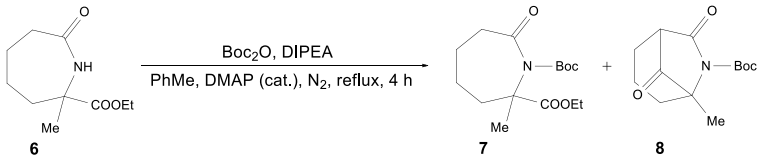

*Fig. 5.11 During the resynthesis of Boc protected precursor **7** for bicyclisation, it was found that the bicyclic product **8** had readily formed in 6% yield.*

Compound	Mass / Volume / Amount Syn. equivalents	Concentration in 100 ml toluene
Ethyl 2-methyl-7-oxoazepane-2-carboxylate **6**	0.8 g / $4.02 \cdot 10^{-3}$ mol 1 eq	$4.02 \cdot 10^{-3}$ mol·l^{-1}
Di *tert*-butyl dicarbonate; Boc_2O	2.63 g / $1.21 \cdot 10^{-2}$ mol 3 eq	$1.21 \cdot 10^{-1}$ mol·l^{-1}
Diisopropylethylamine; DIPEA	0.62 g / 0.82 ml / $4.82 \cdot 10^{-3}$ mol 1.2 eq	$4.82 \cdot 10^{-2}$ mol·l^{-1}
4-Dimethylamino pyridine; DMAP	100 mg (cat.) / $8.18 \cdot 10^{-4}$ mol	$8.18 \cdot 10^{-3}$ mol l^{-1}

Procedure:

1.) The reagents were dissolved in water-free toluene
2.) Reflux of the reaction mixture
3.) The reaction was quenched with aqueous, sat. NH_4Cl and stirred for 90 min
4.) Liquid-liquid extraction of the crude product mixture
5.) Purification with column chromatography

The discovery of already bicyclised product in the product mixture after the protection reaction led to the following questions:

1.) Could the procedure be modified to increase the yield of the bicyclic product
2.) Could the protection and the bicyclisation reaction be combined into a one-pot synthesis
3.) Could the mechanism of this unexpected bicyclisation be explained through the already gathered information on the Dieckmann cyclisation of these caprolactams

The formation of the already bicyclised product had not been observed for the non-methylated caprolactam. As pointed out before, the much more successful cyclisation of caprolactam **7** compared to **4** was attributed to two factors: the elimination of the acidic α-ester proton and the changed conformational situation due to the second substituent in N_α position. To test the synthetic availability of the bicyclised product directly through the protection reaction, a number of experiments were conducted. The understanding of the determining factor for the bicyclisation was thought to be key. To eliminate as many variables as possible, the first experiments were carried out using the Boc protected precursor **8** (Fig. 5.12).

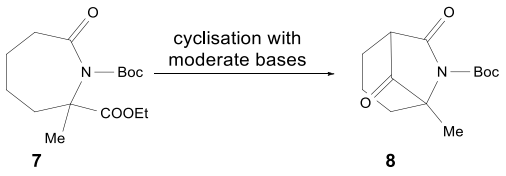

*Fig. 5.12 To investigate, whether the cyclisation of lactam **7** would also occur when less powerful bases are applied, a number of experiments were planned, using DIPEA and KO^{t}Bu.*

It seemed plausible, that a two-step process occurred during the protection reaction. The intended Boc protection would be the logical first step, after the bicyclisation proceeded, even though in a low yield. To test, whether the presumed second step could be reproduced as an isolated reaction, the already protected caprolactam **7** was subjected to the same reaction conditions as for the protection reaction. The bicyclic product was indeed found with a yield of about 6%, with toluene as a solvent (Fig. 5.13).

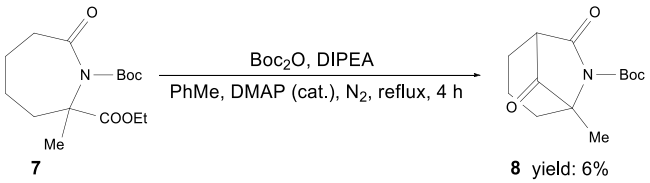

*Fig. 5.13 Subjecting monocyclic, Boc protected lactam **7** to Boc protection conditions gave the bicyclic ketone **8** in a yield of 6%. Despite the low yield, this proved that powerful bases like LiHMDS or LDA are not necessary.*

One experiment using THF as solvent gave roughly the same yield. Despite the yields being too low for synthetic applications, this indicated that a bicyclisation with only DIPEA was possible. It was therefore tested, whether an extreme increase of the base concentration could drive the reaction to the bicyclic product. Caprolactam **7** was therefore dissolved in DIPEA, which for this experiment acted as both base and solvent. However, no product was found after refluxing the mixture for 4 h.

This led to the conclusion, that either the reaction conditions or the combination of reagents was responsible for the bicyclisation. The Boc protection procedure employed DIPEA as a non-nucleophilic base, strong enough to deprotonate the amide functionality. To test, whether a different base could still lead to the formation of the bicyclic product, another two experiments were conducted using KO^{t}Bu as a base, once with and once without Boc_2O. The experiment without Boc_2O did not give any product, the one with the electrophile gave product with a yield of about 9% (Fig. 5.14). It seemed that the addition of Boc_2O was one of the key factors and that the strength of the base was not overly important. That the strength of the applied base had an effect, had already been indicated by the experiments using LiHMDS/LDA. But the much weaker base DIPEA had still resulted in product being formed.

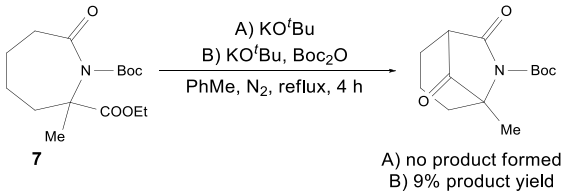

*Fig. 5.14 Subjecting lactam **7** to KO^{t}Bu alone did not give any bicyclic product, but the addition of Boc_2O resulted in a product yield of 9% for the bicyclic product **8**.*

A fresh aspect was delivered by the resynthesis of the precursors. During the routine synthesis of all precursors, the Schmidt rearrangement was the limiting factor. The hazardous nature of this reaction required the preparation of the free lactam **6** in small batches. This was usually directly subjected to Boc protection using the same procedure that had already shown good yields. However, to safe time, the product of three Schmidt reaction batches were combined for the protection reaction while remaining the same amount of solvent, effectively increasing the concentration of all reagents by threefold. TLC analysis of the raw product mixture gave no unexpected results and the reaction mixture was worked-up in the usual manner. To our surprise, the compound presumed to be the Boc protected lactam **7** was not found to be formed as the main product (Fig. 5.15). ^{1}H and ^{13}C NMR analysis indicated that this new compound would have to contain two individual Boc groups. The integration of proton spectrum signals had also indicated that the α-lactam position had undergone deprotonation and most likely a substitution of some sort. However, the possibly most surprising observation was a signal at 107.2 ppm. A signal in this unusual chemical shift range for these systems was found to be the bridging hemiketalic carbon for **5a**. Further 2D-NMR analysis then confirmed the theory, that this newly formed compound was in fact an already bicyclic caprolactam of ketalic nature. All gathered evidence suggests that the bridging sp^3 hybridised carbon carries both and ethoxy group and a carbonic acid ester of itself and *tert*-butanol.

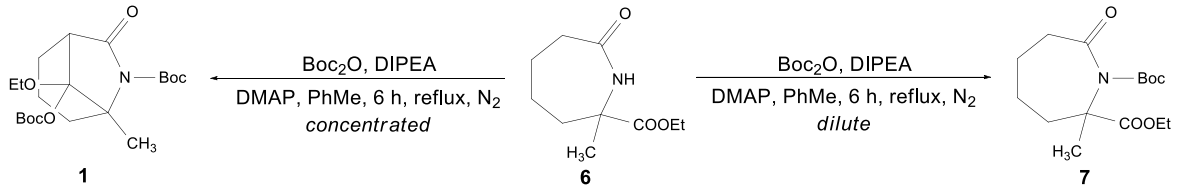

*Fig. 5.15 During the resynthesis of **7** an increase of concentration of all involved reagents did not lead to the expected monocyclic lactam **7**, but to the bicyclic ketal **1**.*

A repeat of the synthesis confirmed that this product could be reproduced if the Boc protection reaction is carried out in higher concentrations than the initial procedure suggested. The ready formation of a bicyclic species directly led to the re-evaluation of the considerations about the base. It had been thought that the deprotonation of the α-lactam position would require a strong base like LiHMDS or LDA. However, the analysis of SC-XRD data had revealed, that Boc protected lactams showed significantly elongated amide bonds. This had not been considered before and led to the following conclusion: the electron withdrawing effect of an additional carbamate group on the lactam nitrogen might increase the acidity of the α-lactam position. It is plausible, that the changed electronic distribution along the amide bond would also have impact on the lactam carbonyl group. And furthermore, a different electronic density on a carbonyl carbon through electron withdrawing groups increases the acidity of α-carbonyl protons. The effect of *N*-Boc substitution was thought to be most likely small compared to other groups, especially considering the position.

To combine all the gathered information, the most plausible explanation is that the α-lactam protons are acidic enough to be deprotonated with DIPEA. For the bicyclisation to then occur, Boc_2O as an electrophile has to be present. The presence of Boc_2O could be necessary to react with the hemiketalic hydroxylate and form a product which cannot react back to the starting materials. It seems that the concentration here is a crucial condition, but it remains unknown how this effects the reaction's mechanism in detail.

Bicyclic ketal **1** was obtained with a good yield of 65% directly from the unprotected lactam **6**. However, the obtained bicyclic product was not a free ketone, which is what the project had originally aimed for. It was therefore desirable to also find a simple method to generate the ketone from the hemiketal. As the carbonic acid ester group was thought to be the stabilising factor of the ketalic product, the elimination of this group drew the focus. Carbonic acid esters, such as dimethyl carbonate, are often prone to nucleophilic attack and hydrolysis. The crude product mixture of the Boc protection was treated with water to hydrolyse residual Boc_2O and facilitate the subsequent chromatographic purification. But the bicyclic carbonate had not been hydrolysed with just water, even after 90 mins of stirring at elevated temperatures. Looking further ahead, the synthetic plan was outlined to contain a deprotection step after successful bicyclisation. And a classic deprotection procedure for Boc protected nitrogen compounds is the treatment with aqueous acid solutions.

To test whether acidic conditions could form the desired deprotected bicyclic lactam right away, carbonate **1** was dissolved in a 0.5 M DCl solution in 1:1 mixture of MeOD-d_4:D_2O and proton spectra of the mixture were recorded. The recorded spectra show, that only one group of the typical Boc signals remain, the ketalic carbon is still observable. This suggests, that acidic, aqueous work-up with dilute HCl solutions instead of pH neutral can give the bicyclic ethoxyhemiketal directly through the protection reaction. During the analytical studies on the ethoxyhemiketal **5a**, it was observed that exposure to a strong vacuum can lead to expulsion of ethanol to give the free ketone **5**. This suggests, that the Boc protection, Dieckmann-type cyclisation to a ketal and subsequent liberation of a free ketone can be achieved in a one-pot synthesis with the right conditions and subsequent work-up (Fig. 5.16). It should be mentioned, that these experiments were conducted in September '19 and could not be further explored so far.

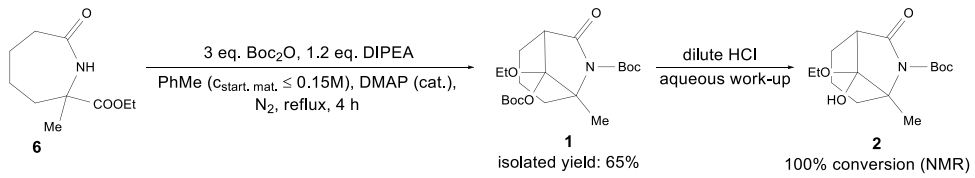

*Fig. 5.16 By increasing the reaction concentration to 0.15M, the Boc protection and cyclisation of **6** to give **1** can be carried out as a one-pot reaction. An aqueous work-up with dilute HCl should then readily give the bicyclic lactam **2**.*

NMR studies on ketalisation

During the herein described experiments, a multitude of different compounds were characterised by NMR experiments. One sample, that caught interest, was the product mixture of the desired bicyclic ketone and an ethoxy hemiketal.

This mixture could not be separated by simple column chromatography, as already mentioned. However, the fact that such a hemiketalic species was obtained after aqueous, slightly acidic work-up and subsequent column chromatography raised the question of its stability. To test out, whether the formation of such ketalic species was reproducible, the free bicyclic ketone was dissolved in CD_3OD and analysed through ^1H and ^{13}C NMR experiments. All recorded spectra using $CDCl_3$ as a solvent had given clear and well-resolved spectra. However, CD_3OD as a solvent gave spectra with extensive line broadening (Fig. 5.17).

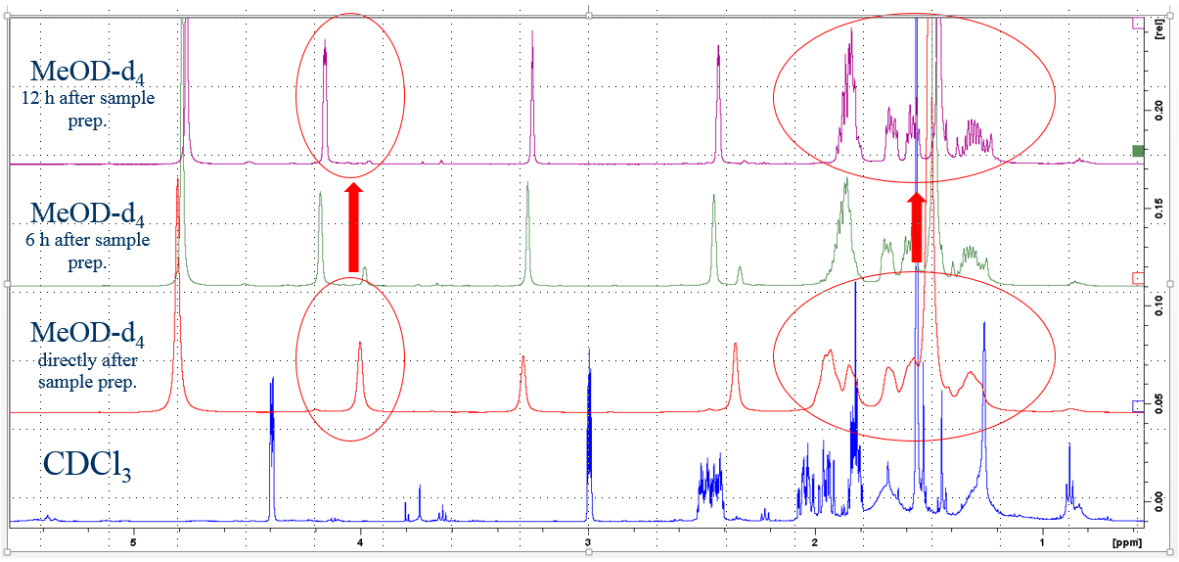

*Fig. 5.17 ^{1}H-NMR experiments of ketone **5** in MeOD-d$_4$ showed that measurements directly after sample preparation show extensive line broadening. Measuring the same sample after 6 and 12 h, peaks showed good resolution and two individual signals dissappeared, whilst two new signals appeared.*

The experiment was repeated with the same sample after roughly six hours. The newly recorded proton spectrum however was not only much better resolved, but also showed that two new signals had appeared. Two other signals with similar shift had equally decreased in their respective integral. Furthermore, another experiment after 12 hours showed that the newly formed signals had increased in their integral, the initial signals had almost disappeared. These signals had been attributed to the bridgehead atoms in $CDCl_3$. A ^{13}C-NMR experiment of the same sample was then carried out and revealed, that no signal in the typical range for ketones around 200 ppm could be found. Instead, a signal around 100 ppm was found. This had already been attributed to the bridging carbon in the hemiketalic, bicyclic side product.

To test whether such spectra could be reproduced and to investigate the process on a time scale, a free sample of ketone **5** was dissolved in CD_3OD and several proton spectra were recorded at different times. The first spectrum that had been measured and that had shown extensive line broadening had been measured only minutes after sample preparation. For this time-scaled experiment, the first spectrum was recorded about 7 minutes after sample preparation and did not show overly extensive line broadening. The following experiments were carried out after 30 mins, 1 h, 2 h, 3 h, 6 h and 12 h.

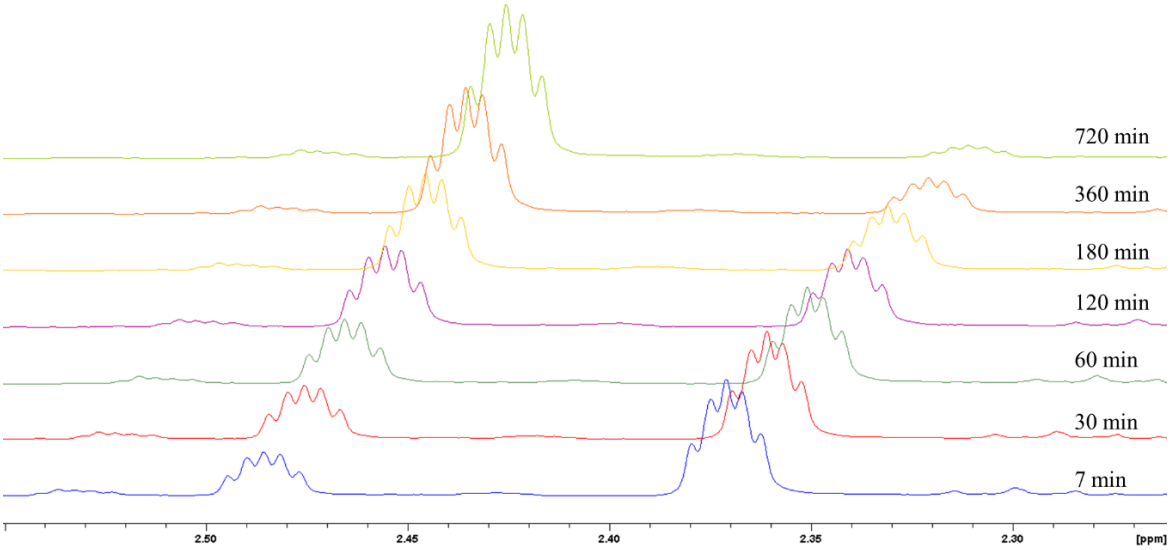

*Fig. 5.18 Time-dependent proton spectra of ketone **5** showed a significant transition for the bridgehead signals around 2.40 ppm. The transition is attributed to the change from a ketone into hemiketalic or ketalic species.*

Fig. 5.18 shows the stacked cut-outs of the recorded proton spectra between ~2.25 ppm and 2.55 ppm. Comparison with NMR experiments in $CDCl_3$ concluded that the signal at 2.37 ppm represents the α-lactam bridgehead proton. The initial signal for that proton decreases in integral units over time and a second, slightly downshifted signal appears and increases. The same change can also be observed for the other, as the second bridgehead identified signal. To support these observed changes, another analysis method was needed. However, because ^{13}C NMR experiments are much more time consuming due to the low relative abundance of ^{13}C nuclei, this could not be used to follow this process. A ^{13}C NMR experiment was conducted after the last ^{1}H spectrum (about 720 min, measurement time about 60 min) was recorded and is displayed in figure 5.19.

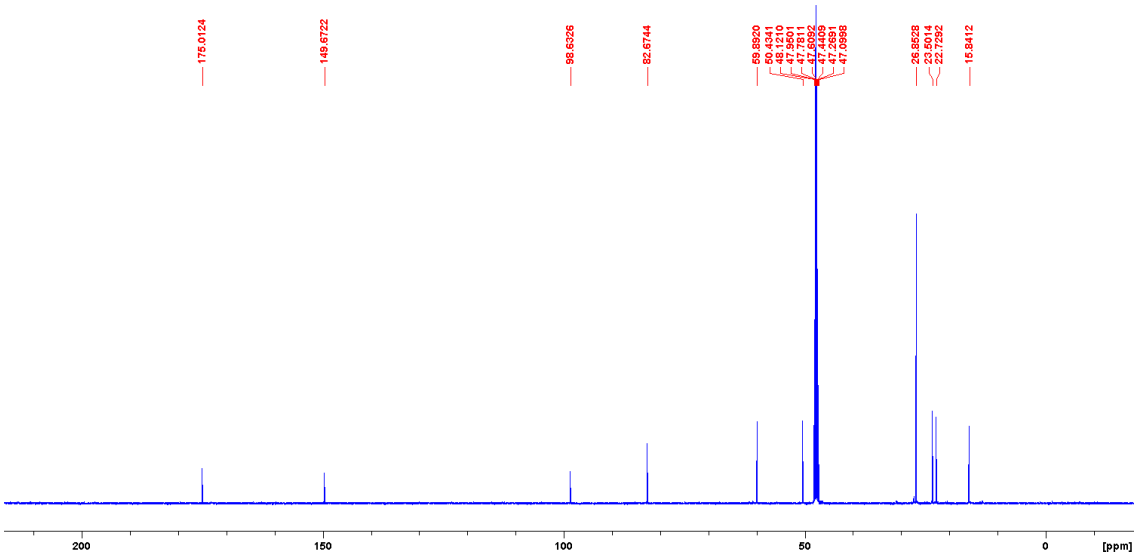

*Fig. 5.19 A recorded ^{13}C spectrum of ketone **5** after about 720 min shows that no signal in typical ketone shifts can be found. Instead, a signal at 98.6 ppm is found, suggesting the formation of a ketal.*

The corresponding ^{13}C spectrum, recorded about 12 h after ketone **5** was dissolved in MeOD-d_4, no signal in the typical keton carbonyl range can be found. Instead, a signal in the already mentioned range of ketals can be found at 98.6 ppm. This led to the conclusion, that the ketone **5** must be undergoing a change that only happens in methanol as a solvent, not chloroform. Considering that an ethoxyhemiketal had already been found, this change appears to come from the formation of a ketalic species in methanol (Fig. 5.20).

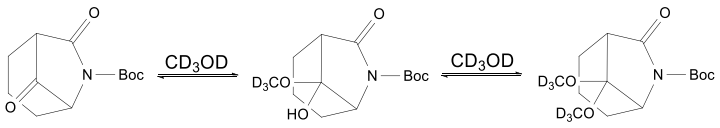

*Fig. 5.20 Dissolving ketone **5** in d_4-methanol appears to form an equilibrium with hemiketalic and/or ketalic species.*

The formation of such ketals (or acetals) is not unknown. Similar reactions between ketones/aldehydes and 1,2- or 1,3-dialcohols are common protection group strategies for carbonyl functionalities. Furthermore, the ready formation of carbonyls with simple alcohols and even water are known as well. However, these commonly referred to as hydrate species (in case of aqueous solutions) are often unstable and can usually not be isolated apart from few exceptions. This is known as the *Erlenmeyer rule*, which states that carbon atoms with more than one hydroxyl group tend to eliminate water to form the respective carbonyl. Following this theory, a reaction of the bicyclic ketone with methanol would allow two different species, a monomethoxy hemiketal and a dimethoxy ketal. The recorded spectra did not give conclusive evidence on which of these species is dominating is solution. It could be assumed that the hemiketal dominates considering that a seemingly stable ethoxy hemiketal was already identified. However, according to the mechanism of Dieckmann condensations, a hemikelic species could be reaction product itself and does not necessarily reflect the most stable/preferred species in solution.

The previously described spectra were recorded in MeOD-d_4, which apart from traces, does not contain any water. To see, if a geminal diol could be formed and found, NMR experiments in D_2O were planned. Unfortunately, bicyclic ketone **5** does not dissolve in pure D_2O enough to record meaningful proton spectra and a 1:1 mixture of CD_3OD:D_2O had to be used. The acquired ^1H NMR spectra from these experiments were found to show several signals in the region between 2.5 ppm – 3.00 ppm. Time dependent scans directly after sample prep., after 6 h and after 12 h do not show any significant change. Any transformation seemed to have already been completed after about 7 mins between the first contact of the ketone and the solvent. However, perhaps more conclusive was a ^{13}C-NMR experiment after 24 h (Fig. 5.21).

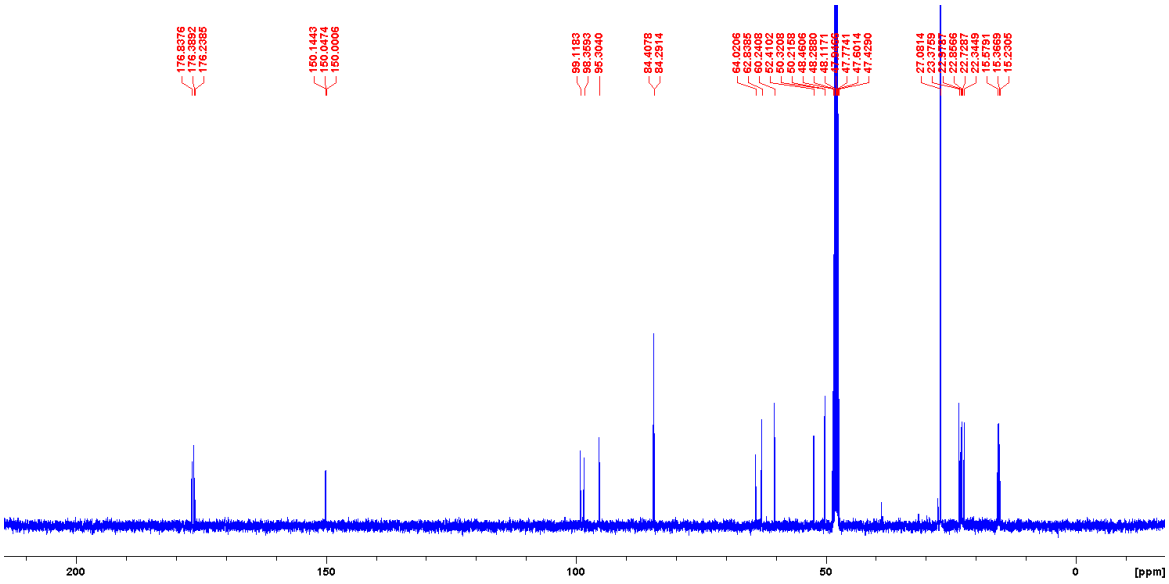

*Fig. 5.21 A ^{13}C experiments with ketone **5** in a mixture of CD_3OD and D_2O showed most signals in triplicates, which indicated three distinct species. Since no ketone signal was found, all three can be attributed to ketalic/diolic species.*

The recorded carbon spectrum shows, that for example for the lactam carbonyl signal around 176 ppm, three signals instead of one is found. No ketone signal was found, but three distinct signals around 100 ppm can be seen. This clearly indicates that three species of geminal -OR structure are formed when a MeOD-d_4:D_2O mixture is used as a solvent. A simple explanation here is an equilibrium between a ketal, a hemiketal and a free geminal diol. Integration of the presumed bridgehead proton signals shows that a ratio of roughly 1.0:1.1:0.8 between the three species is formed (Fig. 5.22).

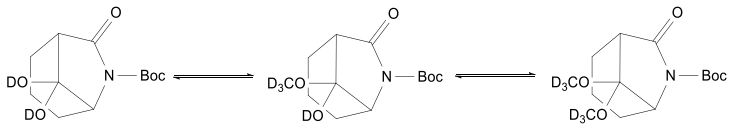

*Fig. 5.22 Dissolving ketone **5** in a mixture of MeOD-d_4 and D_2O gives three distinct species, likely to be a free geminal diol, a methoxy hemiketal and a dimethoxy ketal.*

To further investigate the presumed formation of such species, ketone **5** was dissolved in $CDCl_3$ for further NMR experiments. The sample was then added with five equivalents of non-deuterated methanol to examine changes in the spectra, both instantaneously and after the same time intervals as with pure MeOD-d_4.

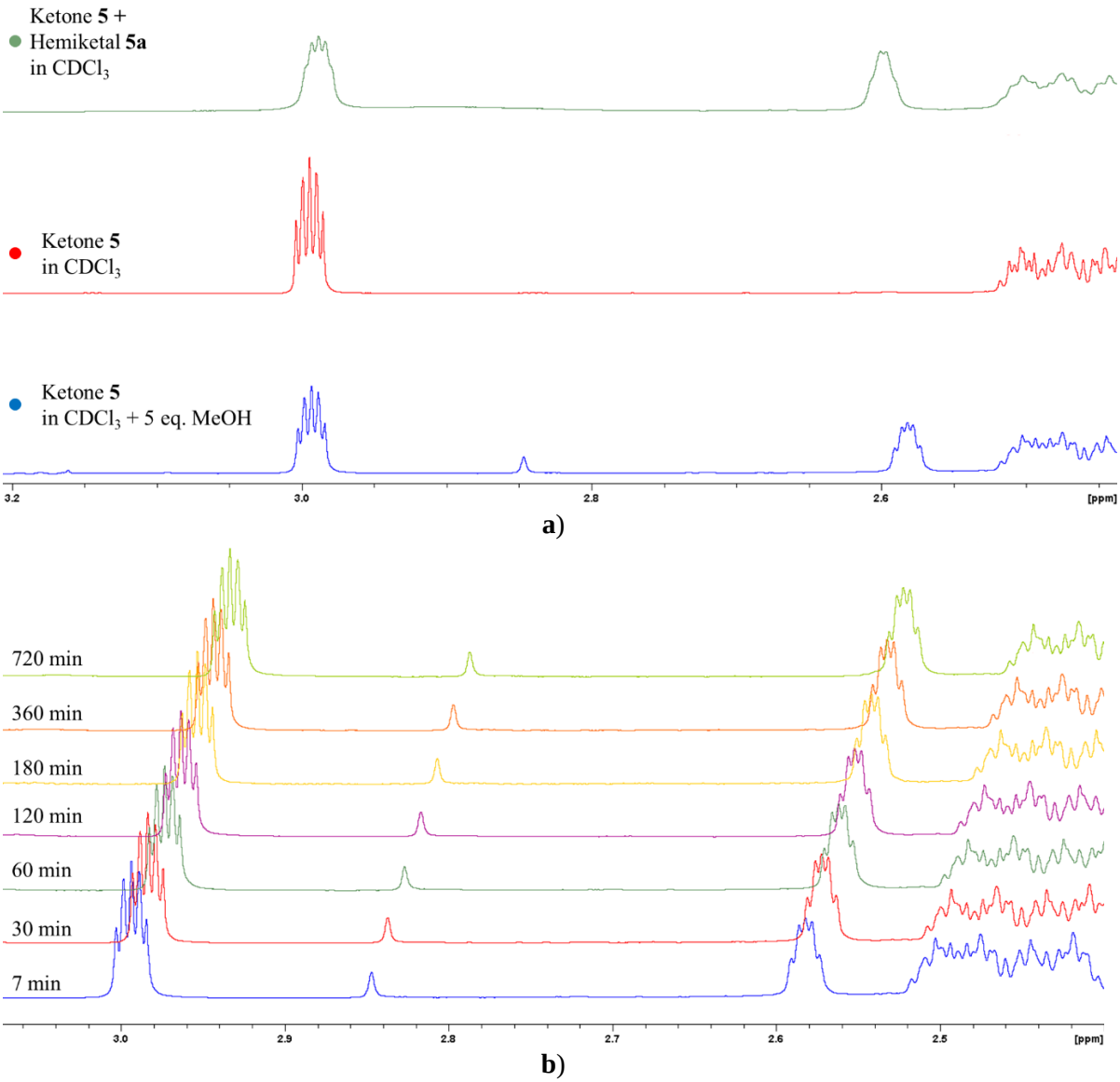

Fig. 5.23 ***a****) Comparison of* ^{1}*H-NMR spectra of ketone* ***5*** *in* $CDCl_3$ *(blue), in MeOD-*d_4 *(red) and of* ***5*** *and hemiketal* ***5a*** *(green).* ***b****) The addition of 5 eq. of MeOH to a solution of ketone* ***5*** *in* $CDCl_3$ *did not show any changes between 7 and 720 min.*

Fig 5.23**a** displays a direct comparison of the region between ~2.4 ppm to 3.2 ppm for proton NMR spectra of ketone **5** and hemiketal **5a** ($CDCl_3$, green), ketone **5** ($CDCl_3$, red) and ketone **5** ($CDCl_3$+5 eq. MeOH, blue after 7 min). Fig. 5.23**b** shows the stacked cut-outs of the recorded proton spectra between ~2.25 ppm and 2.55 ppm for the $CDCl_3$ / 5 eq. MeOH experiments. Firstly, the direct comparison of the mixture of ketone and ethoxyhemiketal shows that the newly formed signal has a strikingly similar chemical shift as the ethoxy hemiketal. Secondly, the spectra show that the addition of 5 eq. of MeOH results in a new signal at just below 2.6 ppm, but the original signal remains. Time-dependent experiments also show, that neither the initial signal, nor the new signal change in intensity over time.

This allows three general conclusions:

- Even if methanol is presented in excess, ketone **5** does not fully transform into hemiketal/ketal
- Ketone **5** most likely transforms into hemiketal in the presence of 5 equivalents of methanol
- Assuming that the transformation forms an equilibrium between ketone and other species, the equilibrium is either reached within only 7 minutes with a five-fold excess of methanol
  OR the equilibriums rates are so slow that the differences are not distinguishable within 12 h

The time-dependent experiments in MeOD-d_4:D_2O and in $CDCl_3$ with MeOH addition suggested that an equilibrium is reached within less than seven minutes. They also outline that more than one species is present under both respective conditions. However, the studies conducted in pure MeOD-d_4 showed that an equivalent transformation seems to take significantly longer to reach an equilibrium.

Fig. 5.24 shows the amount of residual ketone as a fraction plotted against the time, detected with ^{1}H NMR experiments. Coincidently, the spectrum recorded after 120 min shows that for **5** about 50% of the ketone is left. This could suggest a value for a half-life $t_{1/2}$ but further mathematical analysis revealed that the transformation does not follow the kinetics of either a 0th, first or second order reaction. The same time-dependent experiment in MeOD-d_4 was conducted using the methylated ketone **8**. The arguably most significant finding is the stark difference in the transformation speed. Ketone **8** undergoes transformation much faster and seems to reach a more or less stable equilibrium after about 3 h to 6 h. In contrast, ketone **5** transforms slower and does not seem to reach an equilibrium. However, it does show, that if MeOD-d_4 is presented as a solvent, an equilibrium is not reached as quickly as with the other tested solvents.

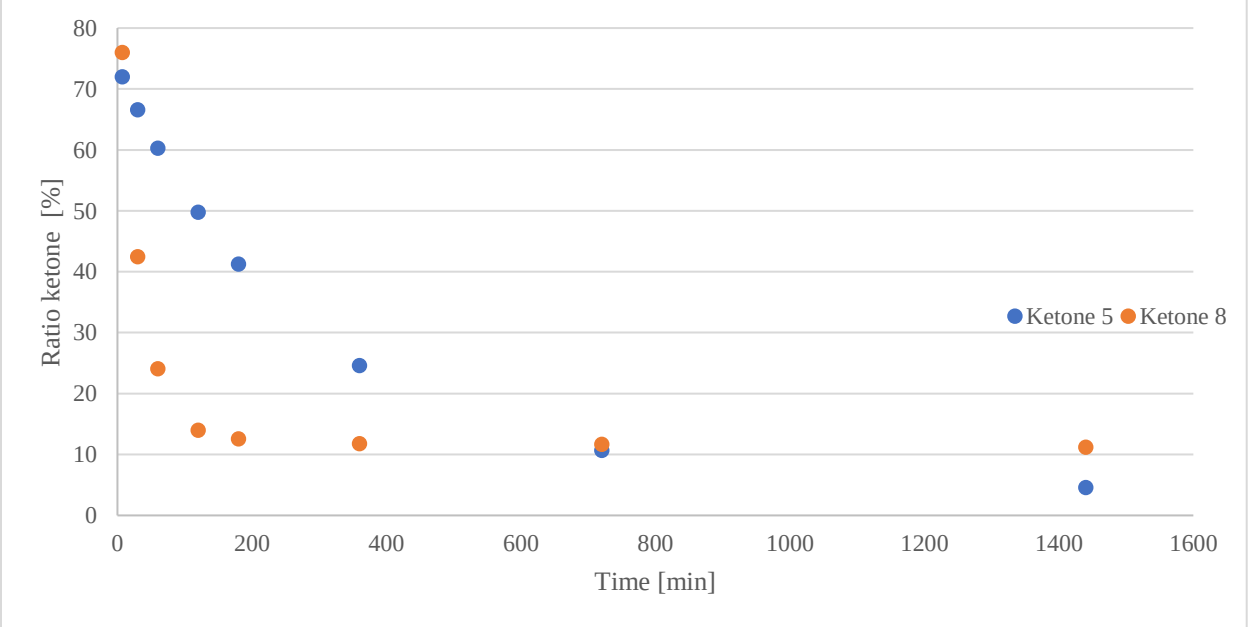

*Fig. 5.24 The transformation of ketones **5** and **8** to ketalic species, the ratio of residual ketone is plotted (determined by ^{1}H-NMR experiments.*

NMR studies on the obtained ethoxyhemiketal suffered from the fact that it was not possible to isolate it from the ketone through column chromatography. Because the behaviour of the free ketone was now studied, the mixture of ketone and hemiketal was used. Samples of this mixture were therefore dissolved in the same solvent systems as for the isolated ketone. To analysis the respective compounds individually, the bridgehead proton signals were used because of their comparatively clear distinction. For all the experiments, the ketone transformed in the mixture as it had as an isolate. The hemiketal on the other hand did not show any signs of any transformation. Neither a signal shift nor a change in integrals was observed for any of the conducted experiments.

Another question that arose was whether the free ketone could be recovered after the transformation into a hemiketal. The respective solvents of the samples used for the NMR experiments were therefore removed under a mild vacuum. After the solvent removal, the samples were re-dissolved in $CDCl_3$ and studied with ^1H NMR again. All recovered samples contained free ketone apart from the samples used for MeOD-d_4:D_2O mixtures. The respective samples showed signals identified as water with considerable integrals. The sample mixtures of ketone and hemiketal showed that the ethoxyhemiketal was still present, in roughly the same amount as in the original mixture. It appears as if the ethoxyhemiketal is particularly stable. However, subjecting the ethoxyhemiketal to a strong vacuum overnight will give the respective ketone. The NMR experiments indicate that no exchange between the ethoxy with a methoxy group takes place. Further experiments will have to elucidated whether this is exclusive to the ethoxy hemiketal, whether the methoxy hemiketal is particularly unstable or whether this is an isolated phenomenon.

The formation and seemingly stability of these hemiketalic species led to the question why such an unusual transformation occurs. Structurally, ketone **5** does not contain any uncommon functional groups or arrangements that would easily explain the observed behaviour. However, as for many polycyclic systems, ring strain effects are likely to influence the physicochemical properties. It had already been argued, that the ring strain of these systems plays one particular role in the bicyclisation reaction. It seems plausible that the formation of a bridge only increases ring strains, rather than decrease them. All the observed experimental results on the transformation of the bridging ketone group had one principle in common: the change from a sp^2 hybridised carbon (ketone) to sp^3 hybridisation (hemiketals, ketals, hydrates). It shall therefore be concluded, that the change from sp^2 to sp^3 hybridisation seems to be driven by the release of ring strain in the system. It can be argued that this has direct impact on synthetic application of these systems but will require further experiments to solidify this theory and the extend to which it affects further work.

5.5) Proposition of a comprehensive reaction mechanism

To summarise all findings on the Dieckmann-type cyclisation, a comprehensive reaction mechanism shall be proposed. The first important step is the deprotonation of the correct position. If the α-lactam position is deprotonated, the reaction may proceed. This deprotonation will compete with an acidic α-ester position. If said α-ester is deprotonated, the ring closure becomes impossible, but the resulting intermediate is stable under the applied conditions and can be recovered through aqueous work-up. Since the ester group is a necessity for the subsequent ring closure, only introduction of further substituents in α-ester position was found to prohibit this competing pathway. This deprotonation does not require overly strong bases. The free amine base DIPEA was found to promote the cyclisation sufficiently.

Once the correct enolate has formed, all following steps are dependent on the position of the ester group for two reasons:

1) The ester group is required to adopt an axial position to be close to the formed enolate
2) The second ring closure increases the ring strain of the system significantly. Structural modifications that force the caprolactam in a conformation that relieves some of the ring strain will facilitate the ring closure

The first reason becomes apparent when crystal structures of both axial and equatorial positioned lactam esters are taken under consideration. The argument of ring strain is less apparent but has drastic consequences on the mechanism. The Dieckmann cyclised intermediate is most likely formed in an equilibrium with the starting materials. In the case the N_α-disubstituted caprolactam **7**, the ester group is forced into an axial position through the steric clash with the Boc group. This now favoured conformation releases some of the ring strain, allowing the equilibrium to shift towards the bicyclic products. However, if a second N_α-substituent is not present, the equilibrium remains primarily in favour of the starting materials. This difference is manifested in the possibility to synthesis bicyclic products directly from the free caprolactam **6** in one-pot. The free lactam **6** is Boc protected in a first step, then undergoes Dieckmann-type cyclisation and the formed hemiketalic hydroxylate reacts with the excess of Boc_2O to give a stable bicyclic product. Its N_α-monosubstituted analogue forms the bicyclic product as well but needs much harsher conditions for the equilibrium to shift towards the products. This ultimately results in the need for the separation of the Boc protection step and the Dieckmann-type cyclisation step for the monosubstituted lactams.

Nevertheless, both N_α-mono- and -disubstituted Boc protected caprolactams, will then follow the same mechanism if strong bases like LiHMDS or LDA are applied. A lactam enolate, once formed, will stabilise through coordination of the counterion with the Boc protection group. Some stabilisation/chelation seems essential for the ring closure to occur here which was shown by experiments with a protection group that could not chelate a counter ion. The reaction solvent does not

seem to play a determining role in this. The enolate will then attack the required ester group intramolecularly. Once the enolate has attacked the ester carbonyl group, the hemiketalic intermediate is formed. This hemiketal seems to be unstable and reacts further, unless an electrophile is present to stabilise. This can be achieved through larger counterions like Na^+ and/or K^+, which can bridge between the chelating lactam carbonyl, the Boc carbamate and the free hemiketal hydroxylate group. Again, this hemiketalic species can then either react back under ring opening or form the ketone. The difference between mono and disubstituted lactams becomes apparent for this step as well. Optimisation attempts for lactam **5** only gave a maximum yield of 32%. On the other hand, **6** underwent the cyclisation much more readily, with better yields and under less selective conditions.

5.6) Observation of a possible rearrangement reaction

During the experiments to elucidate the reaction mechanism behind this Dieckmann-type cyclisation, a multitude of different compounds and side product were obtained. The vast majority of these side products could not be characterised despite all efforts to do so. Here, we would like to present two compounds that have been characterised, but that cannot be easily explained due to conflicting information.

Experiments with NaHMDS and KHMDS for the Dieckmann-type cyclisation had shown to give both a bicyclic ketone and an ethoxyhemiketal. Apart from these two products, and recovered starting material, another compound was obtained that gave the following NMR spectra (Fig. 5.25, 5.26).

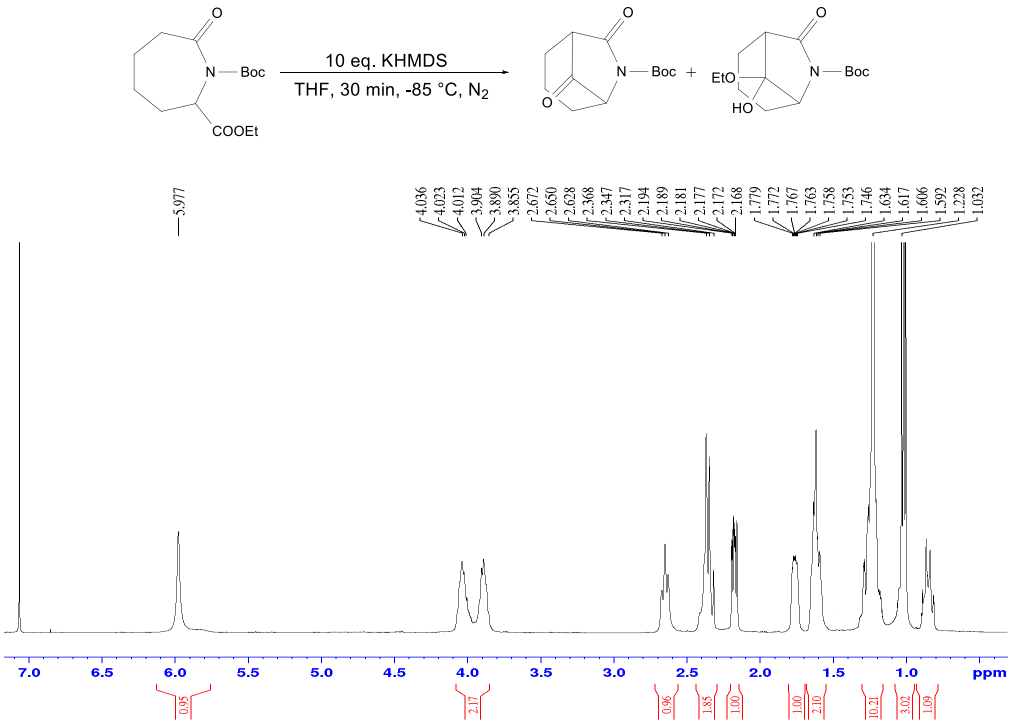

Fig. 5.25 ^{1}H-NMR of a newly found side product from the cyclisation reaction of the Boc protected caprolactam ethyl ester with 10 eq. of KHMDS.

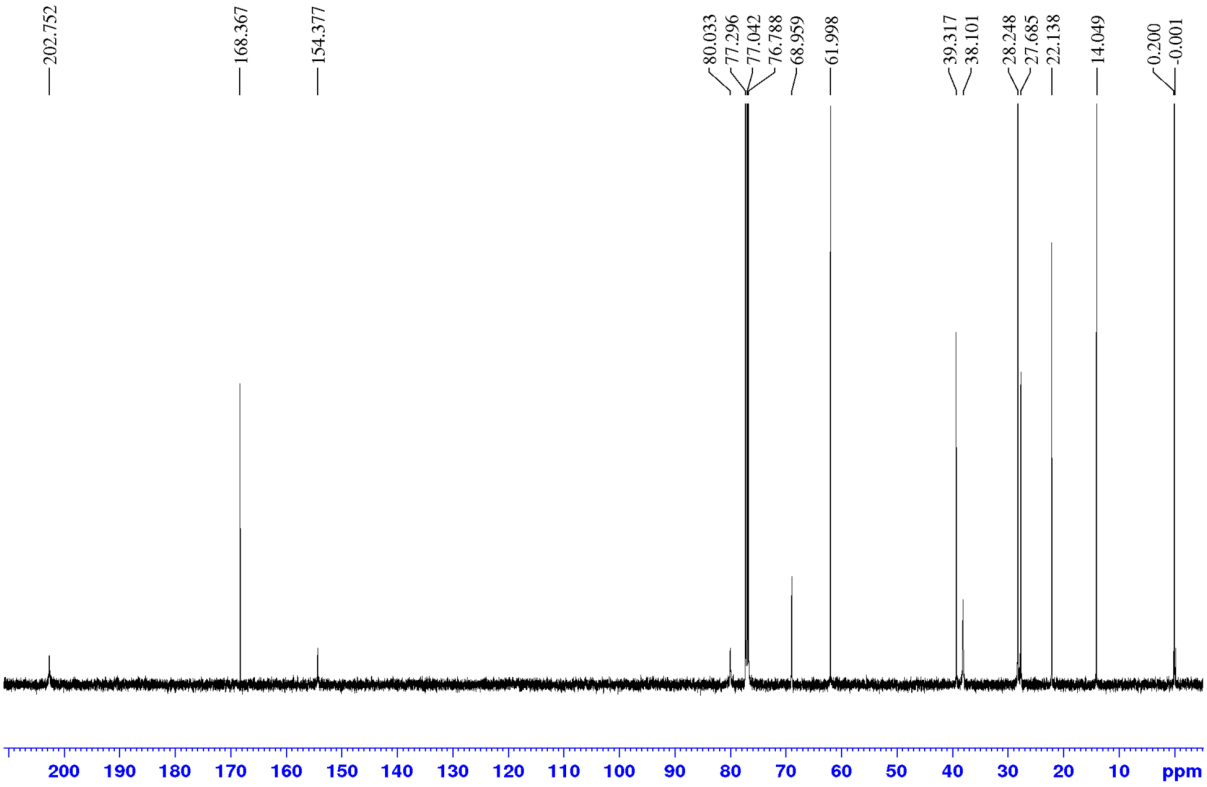

Fig. 5.26 ^{13}C-NMR of a newly found side product from the cyclisation reaction of the Boc protected caprolactam ethyl ester with 10 eq. of KHMDS.

The following pieces of information were extracted from the recorded spectra:

- The broad signal around 5.98 ppm (^{1}H) indicates a free amide NH
- The combination of the signals around 4.00 ppm and 0.85 ppm (both ^{1}H) indicate that an ethyl ester group is present; this is further supported by the signals at 168.4 ppm, 62.0 ppm and 14.0 ppm (^{13}C)
- The singulet at 1.23 ppm (^{1}H) indicates a Boc group; this is further supported by the signals at 154.4 ppm, 80.0 ppm and 28.2 ppm (^{13}C)
- Direct comparison of the chemical shifts and the signal integrals from around 2.70 ppm to 1.00 ppm (^{1}H) and between 69.0 ppm and 22.1 ppm (^{13}C) show high similarities with previously recorded spectra of caprolactams
- The signal at 202.8 ppm (^{13}C) indicates a carbonyl within the typical range of ketones and aldehydes
- The signals (^{1}H) are comparatively broad; previously recorded spectra of caprolactams with confirmed structures gave much better resolved spectra
- The signals at 202.8 ppm, 154.4 ppm and 80.0 ppm (^{13}C) show very low intensity; most likely stemming from extensive signal broadening

During the investigation of the possibility to cyclise the corresponding enantholactam, another compound was obtained that gave highly similar spectra. The excerpted information led to the following proposed structures (Fig. 5.27):

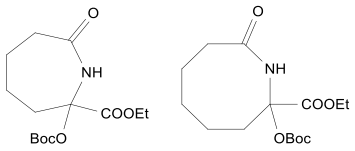

Fig. 5.27 Proposed structures of possible rearrangement products from Dieckmann-type cyclisations of capro- and enantholactams. However, the underlying mechanism could not be fully elucidated yet.

It seems that the Boc protection group has not only been rearranged from the lactam nitrogen to the N_{α}-position, but also that an additional oxygen atom is found. This is supported by the signal at 154.4 ppm and 154.6 ppm for the capro- and enantholactam respectively. Analysis of the 2D-NMR spectra also supports this. Spectra recorded using *heteronuclear multiple-bond correlation spectroscopy* (HMBC) experiments do not show any coupling from C3 protons to any of the presumed Boc group carbonyl. However, equivalent correlation can be found for the ethyl ester carbonyl carbon. The position of the proposed carbonic acid ester group can be determined by the missing of the corresponding proton signal of the now quaternary C2 carbon. However, mass spectrometry experiments for each respective sample could not solidify the proposed structures. No molecular ion peak could be found for a large number of different species such as simple protonated species $[M+H]^+$, with alkali ions $[M+Na/K]^+$ or more complex aggregates $[n_1\ M+n_2\ H/Na/K+n_3\ MeOH]^{n2+}$. *Infrared spectroscopy* (IR) experiments showed three peaks in the typical range of carbonyl peaks but could not deliver unequivocal proof.

What remains debatable is the origin of the comparatively far downfield shifted signals around 200 ppm. 2D-NMR spectra clearly indicate ^3J-correlation, as well as what can easily be interpreted as ^2J and/or ^4J correlations to protons from a presumed ring structure. These correlations, the integral of the presumed NH signal of about 1 and the fact that the chiral C2 was found to be quaternary all lead to the proposition of a cyclic over a ring opened structure.

A similar rearrangement phenomenon has been described on pyroglutamate esters using LiHMDS. A study presented by Dieltiens *et. al.* has proposed an intramolecular, nucleophilic attack of the deprotonated N_{α}-position as responsible for their observed Boc protection group migration. Their findings would suggest that the rearrangement should lead to a carboxylic acid ester rather than a carbonic acid ester. However, their study was conducted using the significantly smaller butyrolactams, rather than capro or enantholactams. Taken into account, that the ring size can impact reaction mechanisms significantly, it is possible that the herein presented carbonic acid ester formed through an altered mechanism.

Crystallography

During the earlier synthetic studies for LiHMDS induced cyclisations, a compound of about 3 mg was obtained. NMR analysis showed that the sample contained impurities and could not be identified at that moment. However, the sample was left to stand and was found to crystallise after several months. The crystalline material was suitable for SC-XRD analysis and was successfully characterised. To our surprise, a bicyclic carbonic acid ester was found (Fig. 5.28).

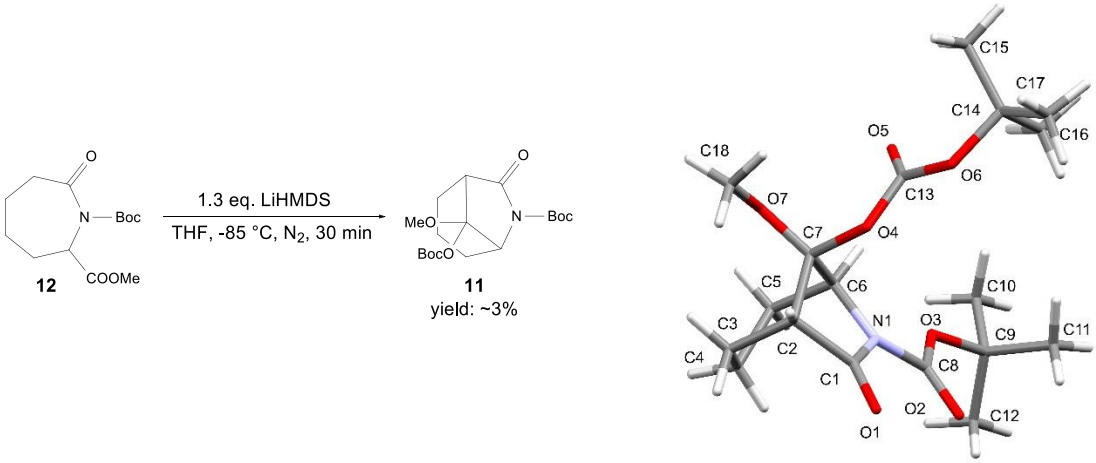

*Fig. 5.28 During the cyclisation experiments of methyl ester **12**, a bicyclic methoxy ketal was found.*

Carboxylate **1** was found after a bicyclisation experiment using caprolactam **12** as a starting material using LiHDMS as base. It was initially thought that this compound was formed during the Dieckmann-type cyclisation, but that the mechanism remained unknown. However, it seems most likely that this ketal was formed during the Boc protection reaction. As later experiments have shown, the bicyclic *tert*-butyl carbonate **11** shows strikingly similar R_f values to the monocyclic caprolactam **12**. The most likely explanation therefore seems that this product was formed during the protection step, was not separated from the main product and was subjected to the bicyclisation conditions without undergoing any transformation itself.

12 was found to crystallise in the monoclinic space group *C2/c* with one molecule in the asymmetric unit. The five-membered ring is found in the typical envelope conformation, the seven-membered ring in a boat conformation and therefore *endo*-positioned to the five-membered ring. The two Boc groups are found in a *syn* position to each other. Comparison of all bond lengths and angles shows, that similar to the other investigated Boc protected lactams, the C-N bond is found to be longer than for free lactams with a distance of 1.409 Å. The amide bond is also close to co-planarity with a torsion angle of 0.65 ° between C6-N1-C1-C2. Due to the lack of strong hydrogen bond donors, the structure has to rely on weak interactions. Three comparatively long C-H···O contacts are found, with the lactam and the carbamate carbonyls being the respective acceptors. The combination of these three possible interactions connects the molecules to layered structures along the crystallographic *b,c* plane.

The single layers are arranged in a bilayer in which the *tert*-butyl groups from the respective single layers form a connection through hydrophobic interactions. The bilayers are connected between each other through further hydrophobic interactions (Fig. 5.29).

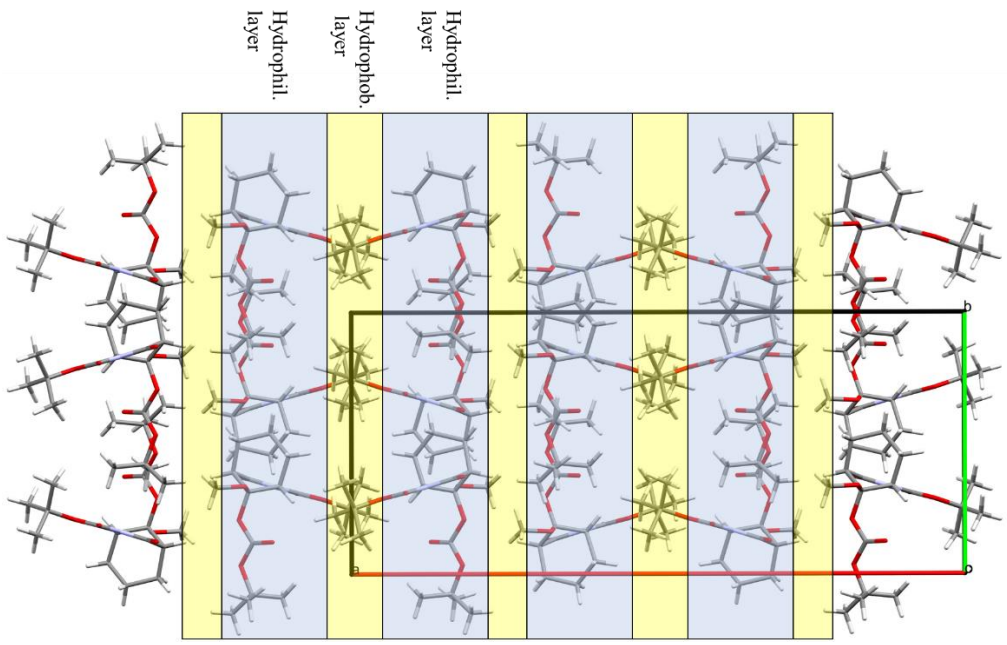

*Fig. 5.29 The crystal packing of carbonate **11** showed layered structures in which an alternating motif of hydrophilic and hydrophobic sheets is found.*

The compound was kindly purified through preparative HPLC by Dr Anish Parmar and the purified compound was then characterised by NMR and HR-MS.

---

[112] M. Hesse, H. Meier, B. Zeeh, *Spektroskopische Methoden in der organischen Chemie* 7th edition, Georg Thieme Verlag, Stuttgart, **2002**.
[113] E.L. Eliel, V.S. Rao, K.M. Pietrusiewicz, *Magn. Reson. Chem.* **2011**, *39*, 657-671.
[114] E. Riedel, *Anorganische Chemie*, 7th edition, de Gruyter, Berlin, **2007**.
[115] A) J. Bredt, *Ann*. **1924**, *437*, 1-13.; B) P.M. Warner, *Chem. Rev.* **1989**, *89*, 1067-1093.; C) J.Y.W. Mak, R.H. Pouwer, C.M. Williams, *Angew. Chem. Int. Ed.* **2014**, *53*, 2-27.
[116] N. Azizi, M.R. Saidi, *Organometallics* **2004**, *23*, 1457-1458.

Chapter 6 – Further synthetic efforts towards 7,8-dioxo-6-azabicyclo[3.2.1]octane derivatives

6.1) Abstract

The previous chapters have discussed the theoretical considerations on different aspects and their implementation into a new, promisingly versatile one-pot synthesis of 7,8-dioxo-6-azabicyclo[3.2.1]octanes, starting from a simple caprolactam. This chapter will discuss experiments towards a viable deprotection protocol for the Boc protected bicyclic scaffold. Acidolysis with neither Brønstedt nor Lewis acids gave the deprotected product in yields that would allow for major further synthetic advances. However, a thermal deprotection procedure is presented that allows for convenient conversion of two Boc protected bicyclic lactams into their respective free lactams in good yields. Additionally, further synthetic efforts towards the introduction of a sulfactam group through nucleophilic substitution, in an effort to mimic Avibactam's sulfate group, is presented. Preliminary experiments towards the introduction of a carboxylic acid group as an alternative are discussed as well.

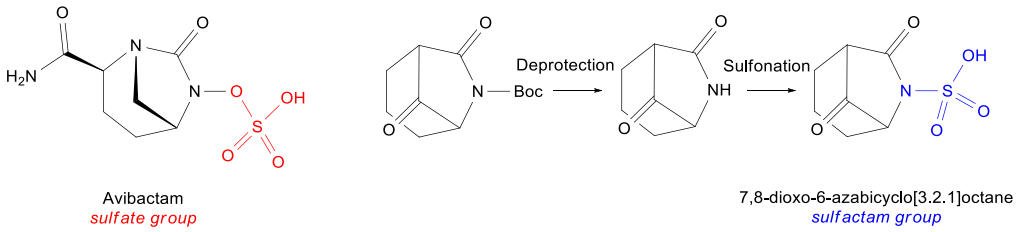

Fig. 6.1 Further synthetic advances were focused on the development of a deprotection and a subsequent sulfonation procedure to pave the way towards Avibactam analogues.

6.2) Introduction

The previous Chapters have outlined the synthetic advances in the establishment of a convenient approach to 7,8-dioxo-6-azabicyclo[3.2.1]octanes. The focus of these synthetic efforts remained on the development of the bicyclic scaffold and certain physicochemical aspects. The following descriptions shall now focus on further, undertaken experiments towards possible derivatisation. As this project was designed to lay the groundworks towards an analogue of the bicyclic urea Avibactam, the synthetic efforts were tailored towards Avibactam's functionalisation.

Avibactam only carries two functional groups besides the core urea structure: a carbamoyl-group and a sulfonamide group, attached to one of its urea nitrogens. This sulfonamide is thought to impact Avibactams efficacy in two ways: through strategically placed hydrogen bonds in the biological target and through an electron withdrawing effect on the urea group. To mimic such effects, an equivalent group was to be introduced into the, in this project presented, azabicyclooctane.

In contrast to Avibactam, the here presented 7,8-dioxo-6-azabicyclo[3.2.1]octane does not contain a nitrogen-oxygen bond, which could be used for an equivalent sulfonation. Instead, a nitrogen-sulfur bond was to be formed, similarly to the sulfactam group found in the monobactam antibiotic aztreonam.

The previously described syntheses resulted in *N*-Boc protected lactams, which had to be deprotected before such a sulfactam group could be introduced. During the work of this project, it was found that the Boc deprotection of this bicyclic lactam system was not as straightforward as for many other substrates. The deprotection of *tert*-butyloxycarbonyl (Boc) protected amines and amides has been described numerous times in literature. The probably most common method is acidolysis with Brønstedt acids, but the use of Lewis acids in more niche examples (Fig. 6.2) has been described as well. Chapter 1 has a described few general approaches that have been found to cleave Boc group efficiently using different protocols.

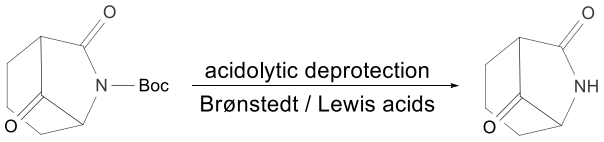

Fig. 6.2 Boc protection groups can be deprotected through acidolytic conditions for many substrates, both for Brønstedt and Lewis acids.

6.3) Results and Discussion

Because the acidolysis of Boc groups can often be done conveniently with very common Brønstedt-acids, first experiments focused on the use of such. A common procedure for Boc deprotection is the use of trifluoroacetic acid (TFA) in dichloromethane (Fig. 6.3). Bicyclic lactam **3** was therefore treated with a 0.2M solution of trifluoroacetic acid in dichloromethane, but no product formation was detected. The starting material could be recovered in roughly 60%, but analysis of the crude reaction mixture could not identify side products or degradation products formed.

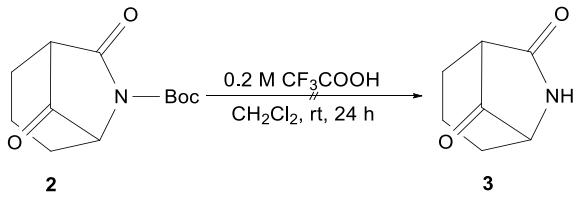

*Fig. 6.3 The deprotection of lactam **2** using a 0.2 molar solution of trifluoroacetic acid in dichloromethane did not show any indication of product formation after 24 h of stirring at room temperature.*

Another fairly convenient deprotection protocol is the use of aqueous HCl solutions at room temperature. Because bicyclic lactam **2** does not dissolve in water, a 1.5M HCl in H_2O:MeOH was chosen. However, no product formation was detected for this approach after basic work-up either.

Because bicyclic **2** lactam had been shown to undergo transformations in aqueous and alcohol containing solvents, it was thought that such transformations could possibly interfere with the deprotection reaction. For that reason, another water- and alcohol-free approach was chosen, and lactam **2** was dissolved in a 4M HCl solution in 1,4-dioxane (Fig. 6.4). TLC analysis indicated the formation of a new compound, which was then isolated through aqueous work-up, liquid-liquid extraction and column chromatography. NMR spectroscopic analysis of this new compound revealed that the desired deprotected lactam **3** had been formed but was only obtained with an unsatisfying yield of 17%. This allowed for a first spectroscopic analysis, but was not considered appropriate for further synthetic experiments and further experiments were undertaken.

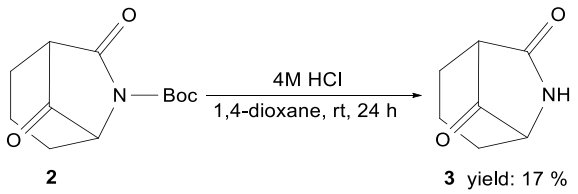

*Fig. 6.4 The deprotection of lactam **2** with a 4M solution of HCl in 1,4-dioxane showed first success in the formation of the deprotected product **3** with a poor yield of 17%.*

Because the experiments using Brønstedt acids for the deprotection had remained largely unsuccessful or only yielded unsatisfying yields, a different approach was envisaged. Such a different approach to the deprotection of Boc groups is the use of the strongly oxophilic trialkylsilyl triflates. As mentioned in Chapter 1, several of these silyl triflates have been used in the past for Boc deprotection. The use of the perhaps simplest, trimethylsilyl triflate (TMSOTf) has been reported to suffer from possible side reactions with other functionalities. Because the bridging carbonyl group was thought to potentially be susceptible to transformations and ring opening could not be excluded as a possibility, *tert*-butyldimethylsilyl triflate (TBDMSOTf) was chosen for a first experiment (Fig. 6.5).

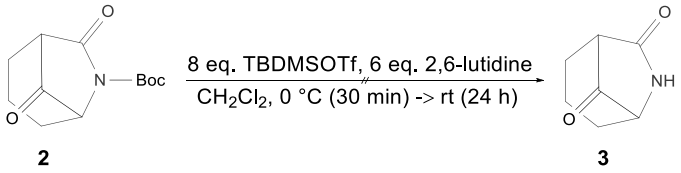

Fig. 6.5 The combination of the use of TBDMSOTf and 2,6-lutidine in dichloromethane had been described for Boc deprotection. In an effort to suppress side reactions, the reaction temperature was lowered to 0 °C but was allowed to rise to room temperature after no product formation was observed.

TLC analysis indicated that no product had formed, and that the starting material had remained unchanged after 24 h. NMR experiments of the worked-up crude mixture further supported that the Boc group had been retained and only starting material was recovered. A repeat of this experiment solely at room temperature gave the same analytical results and the TBDMSOTf deprotection was therefore declared as unsuitable and no further experiments were conducted.

To test, whether a more reactive silyl triflate could accomplish the deprotonation, TMSOTf was applied. In order to keep possible side reactions to a minimum, the starting material was dissolved in dichloromethane first, the solution was then cooled to -50 °C, before 8 eq. of TMSOTf were introduced. After 2 h of stirring at -50 °C, no sign of product formation was found, and the mixture was allowed to warm to room temperature. The mixture was stirred for another 24 h at room temperature, but no sign of product formation was found either. The experiment was repeated again at only room temperature to eliminate the possibility that the decreased temperatures could have supressed a successful deprotonation. However, the repetition at room temperature did not give any indication of product formation either.

A different approach that had been considered before but was thought to be challenging in terms of product detection was using neat formic acid[117]. Unfortunately, neither the starting material, nor the product can be visually detected under an ultraviolet light source and detection required TLC staining techniques. The most reliable staining was found to be a potassium permanganate stain and subsequent heating, but TLC analysis of formic acid solutions would suffer from overloading. However, because other deprotection procedures had failed, it was decided that formic acid should be investigated. The starting material was therefore dissolved in neat formic acid and stirred for 2 h but no product formation was detected after aqueous work-up of samples of the crude mixture. The same reaction mixture was subsequently heated to reflux, to investigate whether elevated temperatures could accomplish the deprotection, but no product was found after the aqueous work-up either. However, the worked-up samples showed no sign of any related compound, neither product, nor starting material or side products.

Because the samples after aqueous work-up had shown nothing through TLC analysis, suspicion was raised that the work-up might be responsible. However, TLC analysis of the crude product mixture was unreliably because the amount of HCOOH transferred onto the TLC plates contaminated the overloaded the plates and overshadowed any other possible compound. To dispose of the HCOOH from the plates, the plates were gently heated to evaporate all HCOOH after transfer of a sample. The so heated plates were then run normally, and a first sign of a product was found. Comparison with the starting material and a product sample from the HCl/dioxane experiments supported that product formation was observed.

This led to two possible explanations:

1) Formic acid could accomplish the deprotection whereas the other applied Brønsted acids could not
2) Heating the starting material solution had triggered the deprotection

Table. 6.1 The applied acidolytic conditions include both Brønstedt and Lewis acids. Product formation was only observed for 4M HCl in 1,4-dioxane, the experiments using formic acid gave product but it is unclear whether the acid took part in the deprotection

Acid	Solvent	Additional reagents	Short description of procedure
TFA	CH_2Cl_2	-	0.2M, room temperature, 24 h No product detected
HCl	H_2O:MeOH	-	1.5M, room temperature, 24 h No product detected
HCl	1,4-dioxane	-	4M, room temperature, 24 h 17% product yield
HCOOH	HCOOH	-	Neat, room temperature for 2 h, then reflux for several hours, product detected
TBDMSOTf	CH_2Cl_2	2,6-lutidine	0 °C for 30 min, room temperature for 24 h No product detected
TMSOTf	CH_2Cl_2	2,6-lutidine	-50 °C for 2 h, room temperature for 24 h, No product detected

The previous GC-MS analysis of bicyclic lactam **2** had indicated a decomposition process of some sort. To evaporate as much sample in as little time as possible, the injectors of GC-MS machines are routinely set to temperatures above 250 °C, much higher than the boiling point of formic acid of 100.8 °C. Because of these observations, a simple experiment was carried out by transferring a sample of **2** onto a TLC plate followed by gentle heating and subsequent routine TLC analysis. Comparison with both the starting material and the product then confirmed, that heat could be used for successful deprotection.

This simple experiment was carried out directly on a SiO_2 TLC plate. Silicon dioxide is known to exhibit a certain acidic character and it was thought that this might have been necessary for the deprotection. To investigate, whether the combination of heat and SiO_2 could form the basis of a viable synthetic procedure, the starting material was suspended in the high-boiling solvent *p*-cymene in the presence of SiO_2 used for column chromatography (Fig. 6.6).

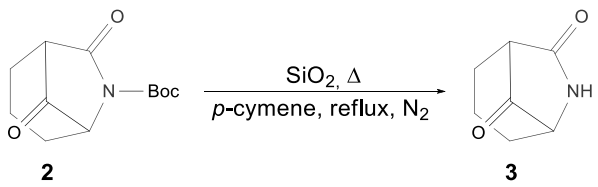

2 **3**

*Fig. 6.6 The first successful deprotection procedure with moderate product yields was found to be a solution of the protected lactam **2** in refluxing p-cymene in the presence of silica.*

Refluxing this solution for 4 h gave the deprotected product **3** with a moderate yield of 45%. *p*-Cymene was used as a solvent because of its high boiling point of 171-173 °C but was thought to fulfil a second role. The deprotection of Boc groups leads to the generation of *tert*-butyl cations which are known to form side protects with substrates, sensitive to electrophiles. This can be avoided using cation scavengers, like 1,3-dimethoxybenzene[118]. Aromatic solvents like *p*-cymene are not as effective as scavenger but the excess of solvent molecules was thought to act effectively.

Because the deprotection could be accomplished without the use of a dissolved Brønstedt acidic reagent, a number of experiments were undertaken to test whether the product yield could be improved by altering the conditions. These experiments are summarised below in table 6.2.

Table 6.2 After the deprotection was found to be successful in refluxing p-cymene with a moderate yield of 45%, it was thought that tailoring the reaction conditions could improve the yield further

Solvent (*p*-cymene)	SiO_2 added	Temp	Time	Yield
✓	✓	171 °C (reflux)	4 h	45 %
X	✓	170 °C	4 h	61 %
X	X	170 °C	4 h	67 %
X	X	150 °C	4 h	64 %
X	X	150 °C	15 min	83 %

To our surprise, the best yield was achieved when lactam **2** is neatly heated to ~150 °C for only 15 min without the addition of any secondary compound (Fig. 6.7). As mentioned, the decomposition of Boc protected species at elevated temperatures had been described before[119], but the vast majority of Boc protected substrates are not tested for their suitability for thermal deprotection because of possible decomposition. NMR-analysis of the crude product without any further purification showed indications of slight impurity, but the so obtained product could be used for further synthetic purposes as was.

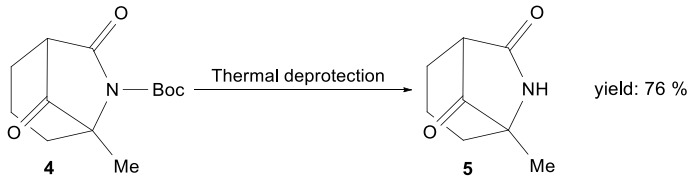

*Fig. 6.7 After the thermal deprotection had been found to be a successful procedure for bicyclic lactam **2**, the same protocol was used to effectively deprotect the methylated, bicyclic lactam **4** as well with a good yield of 76%.*

This deprotection protocol was developed alongside the synthetic optimisations discussed in the previous chapter. Methyl bicycle **4** was then subjected to the same reaction conditions to obtain the respective free lactam **5**. During the determination of the melting point of **5**, it was observed that the samples started to sublime at a temperature of around 92 °C. The experimental set up was therefore slightly adjuste. Additionally, best results were observed when the reaction vessel was heated rapidly. Rapid heating, followed by recollection of all sublimed components, followed by triplicate repetition gave a good yield of 76% of the deprotected lactam **5**.

The disadvantage of this unusual synthetic approach is that even after additional heating cycles, the product still contained starting material which had to be separated. However, the practical ease justified this approach and no further optimisation of this procedure was thought to be necessary at this point. It should be noted that this approach might not be suitable for other substrates.

Both of the obtained, bicyclic lactams **3** and **5** were found to be soluble in water to some extent. This is of particular importance for bioavailability and biological activity. The most likely explanation is the ready formation of the *geminal* diol bridge and the possibility to form interactions between water and the deprotected amide group.

Crystallography of deprotected lactam **3**

The recrystallisation of lactam **3** from ethyl acetate:methanol (10:1) gave suitable crystalline material for SC-XRD analysis. The successful acquisition of a full data set revealed that a *geminal* diol was crystallised instead of ketone **3**. Considering the conclusions drawn in Chapter 6, it seems plausible that this formation occurs readily in the presence of humidity. A decrease in ring strain seems to be the most likely explanation why *geminal* diol **3a** is stable as an isolated compound (Fig. 6.8).

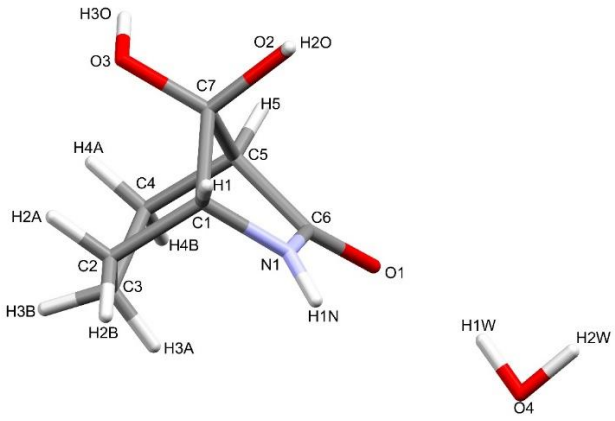

*Fig. 6.8 The SC-XRD of a crystallised sample of **3** showed that the free ketone was not obtained, but the respective geminal diol **3a** as a hydrate.*

Diol **3a** was found to crystallise in the monoclinic space group $P2_1/n$. The asymmetric unit contains one molecule of **3a** and an additional molecule of water. For the sake of clarity, this shall be referred to as a hydrate under the crystallographic definition of a crystal structure containing water. None of the bond lengths or angles showed unexpected values but shall be compared to the two other obtained SC-XRD data set for bicyclic lactams in table 6.3.

*Table 6.3 Comparison of the bond lengths and angles of lactams **2a**, **6**, and **3a** shows that the five-membered lactam ring in the deprotected lactam **3a** is quite similar to the five-membered parent lactam*

	2a	**6**	**3a**	2-pyrrolidine (CSD entry: NILYAY)
a	1.486 Å	1.480 Å	1.467 Å	1.460 Å
b	1.521 Å	1.534 Å	1.542 Å	1.534 Å
c	1.528 Å	1.529 Å	1.534 Å	1.527 Å
d	1.517 Å	1.520 Å	1.524 Å	1.518 Å
e	1.395 Å	1.409 Å	1.326 Å	1.335 Å
α	99.9 °	99.8 °	99.4 °	103.1 °
β	100.4 °	100.5 °	99.5 °	104.3 °
γ	101.5 °	100.9 °	99.7 °	104.4 °
δ	106.5 °	106.0 °	108.1 °	108.5 °

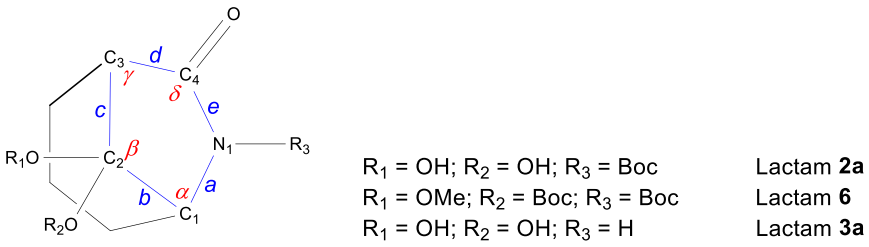

*Fig. 6.8 The comparison of selected bond lengths and angles showed that the deprotected, bicyclic lactam **3a** resembles more the parent butyrolactam, rather than Boc protected bicyclic lactams **2a** and **6**.*

One length, that was already examined in detail in chapter 4, is the amide bond length, bond *e* in figure 6.8. As already discussed, the Boc protected lactams show a significantly elongated amide bond compared to the corresponding free amides. Lactam **3a** displays strikingly similar bond lengths compared to γ-butyrolactam (CSD entry: NILYAY), with the bonds *a*-*d* being only slightly longer. Bond *e* on the other hand is slightly shorter. Furthermore, all bond angles within the butyrolactam ring are exclusively smaller for the bicyclic system than for free γ-butyrolactam. The decreased angles are likely to be a direct result from the increased ring strain, which forces the sp^3 hybridised carbons to adopt angles smaller than in the parent lactam. The fact, that the amide bond of **3a** is much closer and even slightly shorter than in the parent lactam suggests that the ring strain has little or no effect on the amide bond length. Unfortunately, the presented data cannot be compared to the lengths and angles in the corresponding ketones, which could further support this.

A look into the hydrogen bonding patterns in lactam **3a** shows two major, overarching patterns. The first motif involves the formation of hydrogen bonds between the lactam functionalities and the water molecules. The lactam carbonyl is found to form the O4-H1W···O1 contact, instead of forming lactam-lactam interactions. The respective water molecule than forms the O4-H2W···O3 contact to one of the bridging *gem.* diol groups of a neighbouring lactam with the same OH group than forming the O3-H3O···O4. As figure 6.9 shows, these interactions are symmetry related through an inversion centre to another lactam and water molecule each, which gives the graph set descriptor $R_4^4(8)$.

This gives the appearance of a rectangular-shaped formation of two water molecules and two lactam molecules. Furthermore, each respective water molecule is involved in a heterotrimeric interaction between two lactam molecules and itself. The two lactam molecules are connected through the interaction N1-H1N···O2, which is completed through the already mentioned O3-H3O···O4 and O4-H1W···O1 interactions.

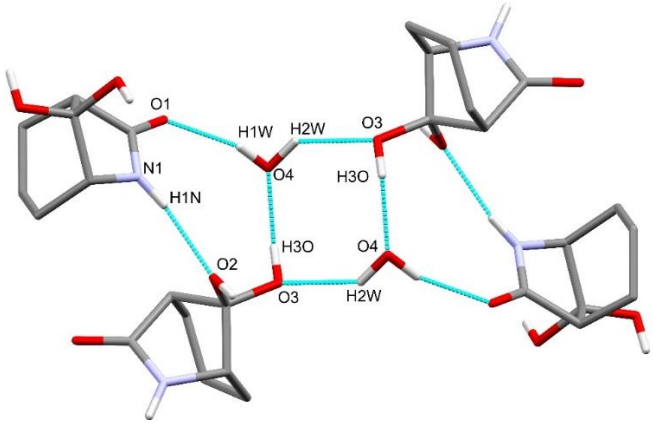

Fig. 6.9 The rectangular-shaped interactions connect two water and two lactam molecules. The respective water-diol interaction is further involved in a set of heterotrimeric amide-diol-water interactions. Carbon-bound protons are hidden for clarity.

Additional to the formation of this cyclic structure, a bifurcated interaction between O2-H2O···O1 and the weaker C1-H1···O1 can be found. These interactions between the lactam carbonyls, one of the diolic OH groups and the stereocenter carbon form C(6)-chains (Fig. 6.10).

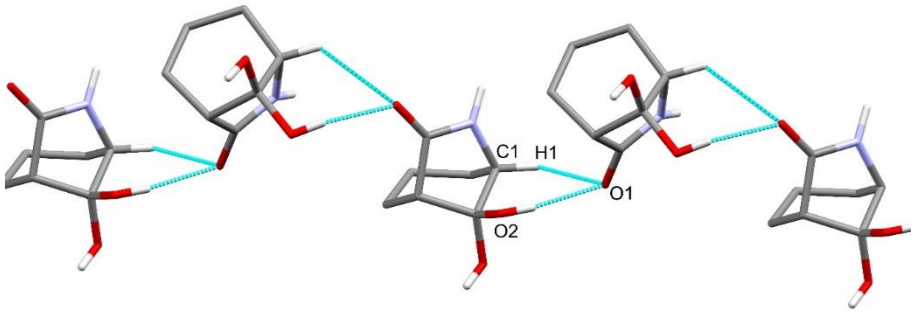

Fig. 6.10 The combination of the stereocenter-lactam carbonyl and the diol-lactam carbonyl interactions connect the lactam molecules in C(7)-chains.

Further weak CH-O interactions can be found, but only seem to stabilise the established main hydrogen bonding patterns. The combination of all interactions forms a three-dimensional network (Fig. 6.11).

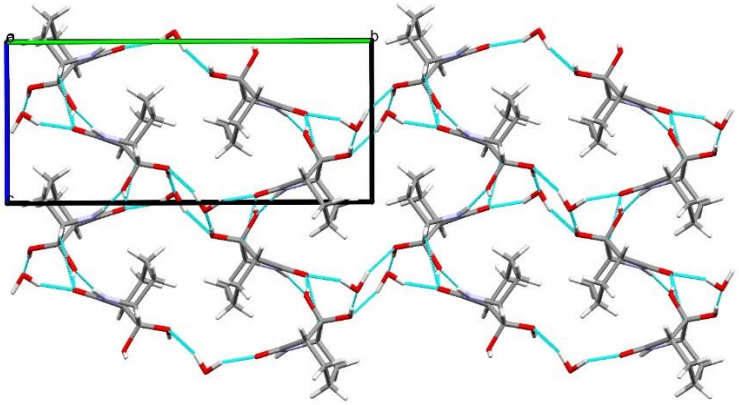

*Fig. 6.11 The combination of all interactions in the crystal structure of gem. diol **3a** forms a three-dimensional network with the water molecule embedded.*

Sulfonation

The next synthetic step was the introduction of a sulfactam group on the lactam nitrogen. To find a suitable sulfonation strategy and to avoid the loss of precious bicyclic product, the adaption of published approaches was carried out using commercially available ε-caprolactam first. Several sulfonations of lactam nitrogens have been described, mostly on β-lactam systems in close relation to the monobactam antibiotic *aztreonam*. A distinct difference between aztreonam and avibactam is the sulfur group attached to the lactam nitrogen in aztreonam. The introduction of a sulfactam group was chosen as an alternative to the sulfonate group found in avibactam (Fig. 6.12).

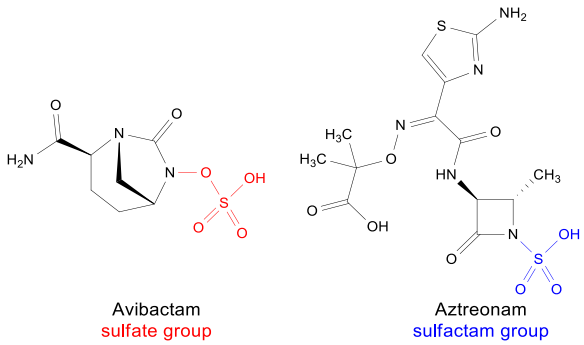

*Fig. 6.12 Because bicyclic lactam **3** does not contain a N-O bond, which is synthetically challenging to establish, the sulfactam group as seen in aztreonam was envisaged.*

Table 6.5 summarises the synthetic procedures applied to ε-caprolactam as a model system (Fig. 6.13). Literature procedures for the sulfonation of aztreonam-type β-lactams often utilise the easy-to-handle SO_3·pyridine complex in either pyridine or dimethylformamide (DMF)[120]. The main difference in these procedures is the applied temperature and the order in which the solvent is heated, and the reagents are added. For that reason, a number of slightly altered protocols were experimented with.

Table 6.5 3 Seven different synthetic protocols were tried. The alterations included different sulfonating reagents, solvents and temperature amongst others.

Sulfonating agent	Solvent	Alteration	Short description of procedure
SO_3·pyridine	pyridine	-	caprolactam dissolved in solvent, reagent added, heated to 80 °C, stirred for 3 h, worked-up
SO_3·pyridine	DMF	changed solvent	caprolactam dissolved in solvent, reagent added, heated to 80 °C, stirred for 3 h, worked-up
SO_3·pyridine	pyridine	changed addition order	solvent heated to 80 °C, reagent added, caprolactam added, stirred for 3 h, worked-up
SO_3·pyridine	pyridine	+ 4 eq. DIPEA	solvent heated to 80 °C, reagents added, caprolactam added, stirred for 3 h, worked-up
$ClSO_3H$	CH_2Cl_2	-	caprolactam dissolved in solvent, solution cooled to -78 °C, reagent added, stirred for 24 h, worked up
$ClSO_3H$	CH_2Cl_2	room temperature	caprolactam dissolved in solvent, reagent added, stirred for 24 h, worked up
$ClSO_3H$	CH_2Cl_2	reflux	caprolactam dissolved in solvent, reagent added, stirred for 24 h, worked up

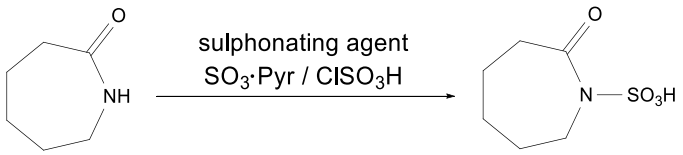

Fig. 6.13 The sulfonation of caprolactam was used as a model system for the bicyclic lactams.

Analysis of the crude product mixtures before and after aqueous work-up showed no indication of sulfonated caprolactam. In fact, the starting material was recovered for all experiments. Because the use of SO_3·Pyr had not been successful, another method was investigated. The introduction of the sulfactam group was thought to involve the nucleophilic attack of the nitrogen on sulfur, which would not require a leaving group for SO_3. A similar overall mechanism was thought to be possible using chlorosulfuric acid $ClSO_3H$, which would then involve a nucleophilic attack as well, but would result in a chloride ion leaving. Unfortunately, none of the used protocols showed any sign of product formation and only starting material was recovered.

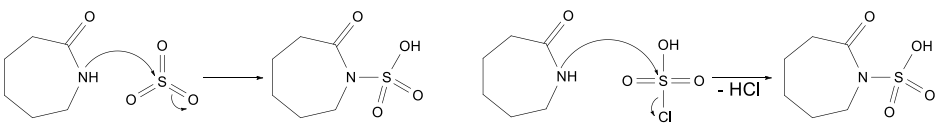

Fig. 6.14 The nucleophilic attack of the lactam nitrogen on sulfur was thought to be mechanistically related for both SO_3 and $ClSO_3H$, but using $ClSO_3H$ with Cl^- as a leaving group was thought to be an alternative.

Because none of the above mentioned sulfonation reactions was found to be successful, an alternative to the sulfonamide group was desired. Apart from the electronic effects caused by the strongly electron withdrawing SO_3H group, it was thought to increase water solubility. The carbon-based analogues of sulfonamides are carbamic acid, which are known to decarboxylate readily. It was therefore decided to introduce an alkyl acetate instead of a formate, followed by saponification of the introduced ester group (Fig. 6.15).

Tab. 6.6 A summary of the applied reagents and reaction conditions is listed. The combination of NaH, in refluxing THF for 6 h gave the desired product in a yield of 82%.

Base	Solvent	Time	Temperature	Obtained compound
NaH	DMF	2.5 h	-20 °C	Starting material
NaH	DMF	24 h	rt	Starting material
DIPEA	PhMe	6 h	60 °C	Starting material
DIPEA	PhMe	18 h	reflux	Starting material
NaH	THF	6 h	reflux	Desired product

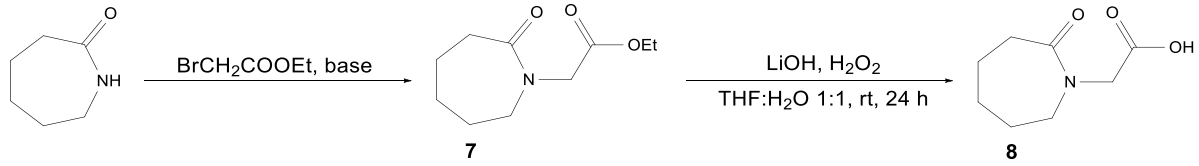

Fig. 6.15 Introduction of an ethyl ester group for subsequent saponification was chosen as alternative for the sulfonamide group to increase the water solubility.

The initial experiment was based on common procedures for alkylation reagents with alkyl bromides, but the starting material was recovered, and no indication of product formation was observed. The combination of DIPEA in toluene was chosen as it forms the basis for the Boc protection strategy for caprolactam precursors, but did not succeed either. However, the combination of NaH in refluxing THF converted ε-caprolactam into the *N*-alkylated ester **7** in a good yield of 82% (Tab. 6.6).

For the next synthetic step, the ester was to be saponified without hydrolysis of the amide bond. The $LiOH/H_2O_2$ protocol had already shown success in related system and was chosen again. This straightforward approach gave the desired free acid in a good yield of 76%.

The successful preparation of free acid **8** led to a first synthetic effort towards an analogue bicyclic system. The outline of the specific reaction conditions is given in figure 6.16. The reaction was monitored using TLC analysis, which indicated that all starting material was used up after about 2 h.

However, in contrast to the unsubstituted caprolactam model system, several side products were found, but could not be fully identified. Please note, the described sulfonation and alkylation experiments were conducted in Sept. ’19 and could not be further developed and analysed.

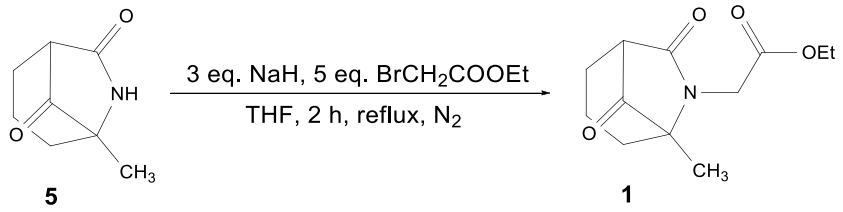

*Fig. 6.16 The introduction of a carboxylic acid group instead of a sulfactam group was thought to be a potential alternative. Unfortunately, the desired product was not found, but analysis and optimisation should lead to bicyclic product **1** in the future.*

6.5) Summary and Conclusion

After several unsuccessful Boc deprotection experiments using acidolysis, a simple thermal deprotection was developed that allows for a convenient deprotection to give the free 7,8-dioxo-6-azabicyclo[3.2.1]octane scaffold **1** in a good yield of 83%. A slightly altered procedure found use in the preparation of the methylated analogue **2** with a similarly good yield of 76%. The SC-XRD structure of the stable *geminal* diol **3a** as a hydrate was successfully acquired. Comparison with bicyclic precursors **3** and **5**, and with free γ-butyrolactam has shown that the bond lengths and angles within the five-membered ring of **3a** are much more similar to the parent lactam. It was concluded that the additional ring strain does not seem to influence the character of the amide bond, which should be of particular interest to potential chemical and medicinal applications. Furthermore, synthetic efforts towards the introduction of a sulfactam group using SO_3·pyridine and chlorosulfuric acid have been described. None of the conducted experiments had shown success on ε-caprolactam as a model system and similar outcomes are expected for equivalent experiments on bicyclic lactams. The introduction of a carboxylic acid group was envisaged instead. After some modification, an ethyl 2-carboxyethyl group was successfully introduced on the model system, subsequent saponification gave the respective free acid with a good yield of 63% over two steps. The introduction of the same group on the free, bicyclic lactam **2** was attempted, but could not be brought to completion as of today.

---

[117] R.B. Hamed, J. Mecinovic, C. Ducho, T.D.W. Claridge, C.J. Schofield, *Chem. Comm.* **2010**, *46*, 1413-1415.
[118] U. Schmidt, A. Lieberknecht, H. Bökens, H. Griesser, *J. Org. Chem.* **1983**, *48*, 2680-2685.
[119] K.E. Krakowiak, J.S. Bradshaw, *Synth. Comm.* **2006**, *26*, 3999-4004.
[120] A) W.V. Curran, A.A. Ross, V.J. Lee, *The Journal of Antibiotics* **1988**, 1418-1429.; B) K. Ikeda, K. Achiwa, M. Sekiya, *Chem. Pharm. Bull*. **1989**, *37*, 1179-1184.; C) L. Banfi, G. Cascio, G. Guanti, E. Manghisi, E. Narisano, R. Riva, *Tetrahedron* **1994**, *50*, 11967-11982.

Summary, Conclusion and Future work

The main objective of this project was the development of a convenient synthesis of the 7,8-dioxo-6-azabicyclo[3.2.1]octane scaffold *via* Dieckmann-type cyclisation from simple caprolactams. The initial cyclisation protocol gave poor product yields of only 8-15%, depending on the starting material, not including the synthetic efforts required for the respective precursors. First experiments and preparations of these bicyclic lactams through base induced cyclisation of N_α-substituted caprolactams had revealed that simple modification of the cyclisation protocol could influence the product yield but could not give satisfying outcomes to application-based standards. Parameters like the reaction solvent, temperature, concentration, reaction time, counter-ion of the base, the protection group and the conformational situation of the caprolactam precursors appeared to have significant impact, but had also revealed a lack of fundamental understanding of such N_α-esters. This triggered efforts into the investigation of crucial aspects of the physicochemical behaviour of the general compound class of lactams. It was possible to acquire the first ever published data-set of a SC-XRD structure of δ-valerolactam without secondary components. Amide bond parameters of the acquired δ-valerolactam structure revealed discrepancies with theoretical calculations, which had calculated torsion angles of -25.0 ° and -17.8 ° for the amide bond. The presented structure on the other hand revealed a torsion angle of only -2.8 °. The importance of this finding is reflected in the theories around the abnormally fast hydrolysis of δ-valerolactam. The theoretical calculations had supported a weakened amide bond as the explanation, whereas our findings support the argument of facilitated nucleophilic attack through the conformational situation in δ-valerolactam. It was also possible to compare physicochemical aspects of the homologous series of lactams, without the interference of secondary compounds in the SC-XRD data available.

These findings were then brought into a wider context, by studying the solid-state behaviour of N_α-esters and carboxylic acids of lactams. To complement the available data, a number of new lactams were synthesised, and crystallisation experiments led to nine new structures to be implemented into the existing literature. It was found that the position of N_α-esters will change, depending on their size: smaller ester will adopt an equatorial position, larger esters an axial. This also supports the general concept of the equatorial position being the energetically favoured conformation for this substitution pattern. Introduction of *N*-protection groups will lead to axial conformations, most likely due to a steric clash between the groups. The eight-membered enantholactams appear to be exempt from these general trends, as their larger ring size and their conformational flexibility allows for equatorially positioned N_α-esters, even in the presence of *N*-protection. It was also found that the size of N_α-esters and the ring size impact the dominating amide bonding pattern. Smaller rings and smaller esters allow for the somewhat preferred formation of $R_2^2(8)$ amide dimers, larger esters and larger rings will resort to C(4)-chains as their preferred bonding motif. The introduction of carboxylic acid groups will change these trends as they appear to dominate the crystal packing over amide bondings. Furthermore, it was found that the

introduction of the electron withdrawing Boc protection group impacts the amide bond in that it appears to decrease the bond strength. This was supported by a hydrolysis experiment on a Boc protected caprolactam ester which led to hydrolytic ring opening as well as saponification of the esters. This had not been observed for any of the other lactam esters studied and might have been a result of a potentially decreased partial double bond character of Boc protected lactams.

The implementation of these findings into a synthetic background led to further experiments on Dieckmann-type cyclisations on such lactam esters. It was found that N_α-esters of valerolactams and enantholactams are unlikely to give bicyclic products, which was thought to be a result of the increased ring strain for valerolactams and the unique conformational situation in enantholactams. It was also found that Boc protection appears to be necessary for these Dieckmann-type cyclisations to occur. It was discussed, that the possible chelation of counter-ions through the additional carbamate group and the electron withdrawing effect of it appear to be essential for successful cyclisation. Despite all efforts, it was not possible to increase the product yield of bicyclic lactams above 32% for N_α-monosubstituted caprolactam esters. However, the experiments regarding the cyclisation of a N_α-disubstituted caprolactam led to the development of a convenient one-pot procedure for the respective bicyclic lactam, without the need for a separate Boc protection step, in good yields of 65%. The success of this procedure is thought to be a direct result of the manipulated conformational situation of the N_α-disubstituted caprolactam. It appears as if the key was the balance between the concentration of the respective precursor and Boc_2O as an electrophile, which is thought to scavenge a hemiketalic intermediate, to drive the reaction equilibrium towards its products. The summary of all conducted experiments resulted in a proposed reaction mechanism of this Dieckmann-type condensation which included the discussion about a number of reactions parameters. During the synthetic experiments, it was observed that the newly synthesised bicyclic lactams tends to form stable *geminal* diols. The combination of NMR experiments and SC-XRD data acquired, suggest that the stability of these diols is a direct result of the transition from sp^2 to sp^3 hybridised bridging carbons and the resulting decrease in ring strain. This somewhat unusual behaviour could influence their biological activity and biochemical aspects profoundly, but it is impossible to forecast to what extent this might be. Additionally to the development of this convenient synthesis, first efforts were made towards the effective deprotection and derivatisation of the presented bicyclic lactams. It was found that acidolysis does not seem to be effective in the Boc deprotection of these systems, but thermal cleavage gave the deprotected lactams in good yields of up to 83%. Unfortunately, efforts to introduce the desirable sulfactam group remained unsuccessful and will require further investigation.

Future work should be aimed towards the exploration of the possibility to utilise this Dieckmann-type cyclisation for other substrates. Considering the conditions of the here presented one-pot synthesis of the 7,8-dioxo-6-azabicyclo[3.2.1]octane, this approach should tolerate a wide variety of substrates. Of particular interest could be the possible synthesis of Avibactam analogous compounds. Such synthesis

could start from either cyclohexenones through selective functionalisation of through phenols *via* hydrogenation. This is complemented by the fact that the ring expansion from cyclohexanones to caprolactams through the use of Schmidt reaction conditions is thought to retain stereocentres, which could allow asymmetric synthesis of relevant precursors. It should be noted, that the hazardous nature of the Schmidt reaction leaves room for further improvement and could be reinvestigated for the purpose of scaling-up. In the context of synthesising a variety of analogues, the developed deprotection procedure may require further investigation as well, as thermal deprotection might not tolerate as many substrates. As Avibactams sulfate group has been found to be essential to its efficacy, the introduction of a sulfactam group should also be revisited. However, the respective free lactams are not necessarily limited to the use as potential β-lactamase inhibitors and could also find widespread application in other areas of medicial chemistry. Experiments concerning bioactivity are of great interest and this interesting bicyclic scaffold could hold the key to many other challenges in modern medicine, additionally to antibiotic resistances.

Part II – Experimental

Materials and Methods

Melting points were determined on a Zeiss Axio Vision microscope, fitted with a Linkam THMS600 stage. Temperature-controlled crystallisation experiments were performed on the same. Infrared spectra were recorded on a PerkinElmer Spectrum 100 FT-IR spectrometer. All wave numbers are given in cm^{-1}. Mass spectra were recorded on a TSQ Endura Mass Spectrometer. High-resolution mass spectra were recorded on a Thermo Exactive Plus Orbitrap Mass Spectrometer with a Dionex UltiMate 3000 Quaternary RSLCnano System. Proton (^{1}H, 500 MHz) and carbon (^{13}C, 125 MHz) nuclear magnetic resonance experiments were performed on a Bruker instrument at 27 °C and 20 °C, respectively. NMR samples were prepared in $CDCl_3$, MeOD-d_4, TMS was used as an internal chemical shift standard, unless otherwise indicated. Reactions were followed with TLC (254 µm SiO_2 60-F), visualization accomplished by $KMnO_4$-staining. Column chromatography was performed using SiO_2 (230-400 mesh, 0.063-0.040 mm). All reactions that required water free reaction conditions were performed under a nitrogen atmosphere. Dry solvents were purified over activated aluminium oxide. Commercially available starting materials were used as received by Fluorochem, Acros Organics or Sigma Aldrich.

Crystallography

Single crystal X-ray diffraction was performed at 173 K with a Bruker D8 Venture diffractometer, using a Cu K_α source. Structure solution was carried out with shelxs, and structure refinement with shelxl was finished using ShelXle software.

Slow-solvent evaporation crystallisation

Solvent-evaporation crystallisation experiments were carried out by dissolving a small amount of the respective compound (>100 mg) in a suitable solvent in a test tube. The test tube was left to stand without disturbances, until enough solvent evaporated to afford single crystalline material, suitable for single-crystal structural determination.

Vapor-diffusion crystallisation

A vial, containing a small amount of the respective compound (>100 mg), dissolved in a suitable solvent A of high polarity was placed in a sealed vessel, together with a second vial, containing a solvent B, of lower polarity and lower boiling point than solvent A. The sealed vessel was left to stand without disturbances, until single crystalline material, suitable for single crystal structural determination was formed.

Temperature-controlled crystallisation

Under a microscope with temperature-control stage, a small amount of sample (>5 mg) were placed between two glass slides and heated until the solid sample started to melt. The melting process was slowed done through temperature control until only few crystallites were left after which the temperature was lowered by 0.1 $K \cdot min^{-1}$ until the sample had fully solidified. The process was repeated until single crystalline material, suitable for single crystal structural determination could be harvested.

Experiment descriptions Chapter 2

Synthesis of Dimethyl-2-aminopimelate (13)

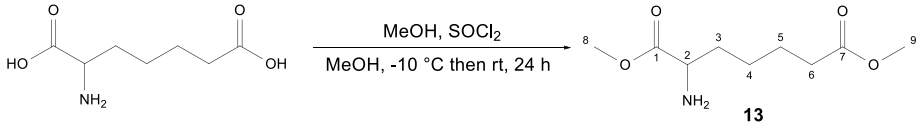

13

A three-necked round bottom flask, equipped with a drying tube, a thermometer and a septum is charged with 200 ml of methanol. The solvent is cooled below -10 °C with an ice-NaCl mixture before 15 ml (0.206 mol) of thionyl chloride are added dropwise so that the temperature did not exceed -5 °C. The mixture was stirred for 10 min before 1.0 g (0.0571 mol) of 2-aminopimelic acid are quickly added. The mixture is allowed to warm to room temperature and stirred vigorously for 24 h. The solvent is distilled of under reduced pressure, the residue is treated with an aqueous, saturated $NaHCO_3$ sol. until no more gas develops and the pH is above 7. The aqueous phase is extracted with 50 ml of ethyl acetate five times, the combined organic phases are dried over $MgSO_4$, the drying agent is filtered off and the solvent is removed *in vacuo*. The residual yellow oil crystallised after several days at room temperature to give the desired product. Yield: 93% (0.99 g); m.p.: 106 °C; Lit: 106 °C[121]; ^{1}H NMR (500 MHz, $CDCl_3$, δ [ppm]) 3.65 (s, 3H, *H8*); 3.60 (s, 3H, *H9*); 3.38 (t, 1H, ^3J = 6 Hz, *H2*); 2.25 (t, 2H, ^3J = 8 Hz, *H6*); 1.67-1.48 (m, 6H, *H3*, *H4*, *H5*); 1.35 (m, 2H, NH_2);^{13}C NMR (125 MHz, $CDCl_3$, δ [ppm]) 176. (*C1*); 173.9 (*C7*); 54.2 (*C2*); 51.9 (*C8*); 51.5 (*C9*); 34.4, 33.8 (*C3*, *C6*); 25.1, 24.6 (*C4*, *C5*); IR (ATR) ν: 2932, 2868, 1730, 1582, 1556, 1513, 1435, 1364, 1294, 1269, 1238, 1177, 1134, 1108, 1061, 1026, 997, 984, 944, 886, 862, 828, 767, 740, 633, 600, 554, 487, 424

Synthesis of Methyl-7-oxoazepane-2-carboxylate (2)

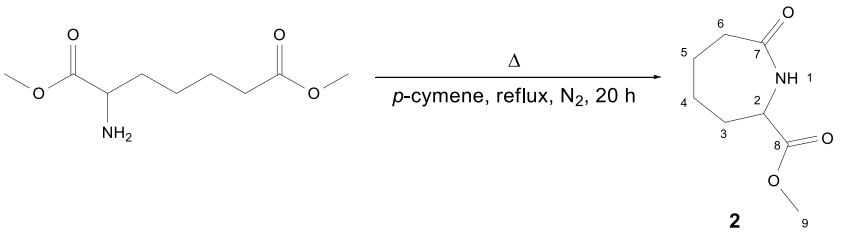

1.00 g (4.94 mmol) of Dimethyl-2-aminopimelate are dissolve in 250 ml of *p*-cymene. The colorless solution is refluxed for 20 h under a nitrogen atmosphere, the solution turned intensily orange. The solvent is removed *in vacuo* and the residue is purified with twofold column chromatography [SiO_2; ethyl acetate:cyclohexane; 1:4 → ethyl acetate] to give the desired product as colorless needles. Yield: 69% (0.58 g); m.p.: 74 °C; ^{1}H NMR (500 MHz, $CDCl_3$, δ [ppm]) 6.42 (br s, 1H, *NH*); 4.12-4.11 (m, 1H, *H2*); 3.80 (s, 3H, *H9*); 2.55-2.50 (m, 1H, *H3*); 2.44-2.38 (m, 1H, *H6*); 2.10-2.05 (m, 1H, *H3'*); 1.92-1.86 (m, 1H, *H5*); 1.72-1.55 (m, 3H, *H4*, *H5'*, *H6*'); ^{13}C NMR (125 MHz, $CDCl_3$, δ [ppm]) 176.1 (*C7*); 171.9 (*C8*); 55.9 (*C2*); 53.0 (*C9*); 37.0 (*C6*); 33.9 (*C3*); 29.7 (*C4*); 22.9 (*C5*); IR (ATR) ν: 3268, 2978, 2949, 2918, 2850, 1739, 1644, 1469, 1436, 1401, 1343, 1312, 1298, 1265, 1242, 1212, 1183, 1136, 1089, 1012, 965, 933, 874, 850, 809, 732, 685, 587, 517, 482, 420. GC-MS: calculated: 171.09 $[M]^+$, found: 171

Synthesis of 7-oxoazepane-2-carboxylic acid (14)

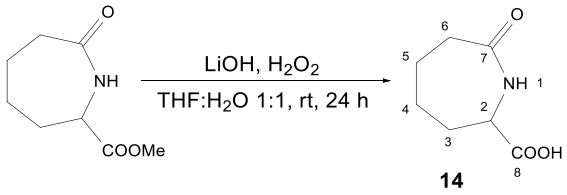

0.195 g (8.18 mmol) of LiOH monohydrate are dissolved in a mixture of 15 ml THF and 15 ml of H_2O, the mixture is stirred and 0.35 g (2.04 mmol) of starting material are added to the solution. 2.1 ml of an aqueous H_2O_2-sol. (30% w/v, 2.06 mmol) are added to the solution, which is stirred for 24 h. The pH of the aqueous phase is adjusted to 3 with 0.5M HCl, stirred for another 30 min and extracted with 20 ml ethyl acetate five times. The combined organic phases are dried over $MgSO_4$, the solvent is removed *in vacuo* to give the product as a white solid. Yield: 70% (0.22 g); m.p.: 159 °C; Lit: 160-162 °C[122]; ^{1}H-NMR: (500 MHz, MeOD-d_4, δ [ppm]) 4.21-4.15 (m, 1H, *H2*); 2.58-2.53 (m, 1H, *H6*); 2.44-2.39 (m, 1H, *H6'*); 2.21-2.17 (m, 1H, *H3*); 2.01-1.90 (m, 1H, *H4*); 1.89-1.63 (m, 3H, *H3'*, *H4'*, *H5*); 1.60-1.53 (m, 1H, *H5'*); ^{13}C-NMR: (125 MHz, MeOD-d_4, δ[ppm]) 178.5 (*C7*); 173.0 (*C8*); 55.3 (*C2*); 36.2 (*C6*); 32.8 (*C3*); 28.7 (*C4*); 22.7 (*C5*)

General procedure for syntheses of *tert*-butyl-7-oxoazepane-1,2-dicarboxylate esters

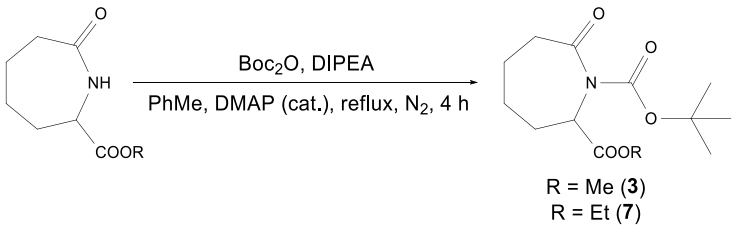

A three-necked round bottom flask, equipped with a reflux condenser, a tap and a stopper is charged with 0.5 g of the starting material under a nitrogen atmosphere. 50 ml of dry toluene, 200 mg of DMAP, 3 eq. of Boc_2O and 1.2 eq. of DIPEA are added and the solution is refluxed for 4 h. The reaction mixture is allowed to cool to room temperature, 15 ml of water are added and the reaction is stirred for another 90 min. Another 100 ml H_2O are added to the biphasic mixture and the aqueous phase is extracted with 50 ml of toluene five times. The combined organic layers are dried over $MgSO_4$, the drying agent is filtered off and the solvent is removed *in vacuo*. The residue is purified with column chromatography [SiO_2; ethyl acetate:cyclohexane; 1:10 → 1:4] to give the desired products.

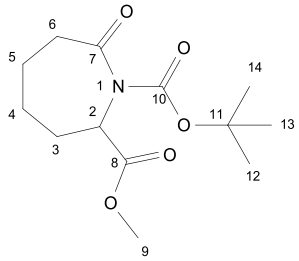

Yield (**3**): 77 %; m.p.: 69-71 °C; R_f: 0.43 (ethyl acetate:cyclohexane 1:4); ^{1}H-NMR: (500 MHz, $CDCl_3$, δ [ppm]) 5.26 (dd, J_d = 3 Hz, J_{dd} = 6 Hz, 1H, *H2*); 3.79 (s, 3H, *H9*); 2.71-2.66 (m, 1H, *H6*); 2.52-2.48 (m, 1H, *H3*); 2.42-2.37 (m, 1H, *H6'*); 1.84-1.79 (m, 3H, *H3'*, *H4*, *H5*); 1.55-1.47 (m, 2H, *H4'*, *H5'*); 1.51 (m, 9H, *H12*, *H13*, *H14*); ^{13}C-NMR: (125 MHz, $CDCl_3$, δ[ppm]) 175.8 (*C8*); 170.9 (*C7*); 153.5 (*C10*); 83.3 (*C11*); 56.6 (*C2*); 52.4 (*C9*); 39.6 (*C6*); 29.9 (*C3*); 27.9 (*C12*, *C13*, *C14*); 25.6 (*C4*); 22.7 (*C5*); IR (ATR) ν = 2940, 1740, 1482, 1461, 1442, 1365, 1334, 1301, 1286, 1240, 1199, 1153, 1083, 1046, 991, 954, 904, 880, 849, 798, 786, 762, 672, 648, 613, 578, 552, 481, 435; ESI-MS: calculated: 294.0 $[M+Na]^+$; found: 294.0

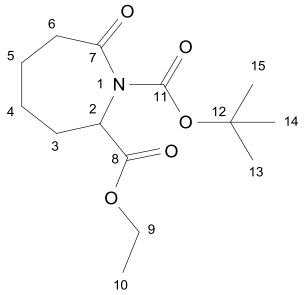

Yield (**7**): 64 %; R_f: 0.52 (ethyl acetate:cyclohexane 1:3); ^{1}H-NMR: (500 MHz, $CDCl_3$, δ[ppm]) 5.32 (dd, J_d = 3 Hz, J_{dd} = 6 Hz, 1H, *H2*); 4.26-4.16 (m, 2H, *H10*); 2.67-2.54 (m, 2H, *H6*); 2.12-2.07 (m, 1H, *H3*); 1.89-1.65 (m, 5H, *H3', H4*, *H5*); 1.62 (s, 3H, *H8*); 1.46 (s, 9H, *H14, H15*, *H16*); 1.28 (t, ^3J = 7.1 Hz, 3H, *H11*); ^{13}C-NMR: (125 MHz, $CDCl_3$, δ[ppm]) 178.6 (C*7*); 173.5 (*C9*); 153.4 (*C12*); 82.5 (*C13*); 62.9 (*C2*); 61.5 (*C10*); 38.1 (*C5*); 36.0 (*C3*); 27.9 (*C14, C15, C16*); 23.1 (*C5*); 22.9 (*C8*); 21.8 (*C4*); 14.1 (*C11*); IR (ATR) ν = 2981, 2940, 1783, 1713, 1665, 1455, 1367, 1301, 1247, 1214, 155, 1117, 1065, 978, 915, 849, 822, 788, 756, 746, 710; HRMS: Calculated: 308.1474 $[M+MeOH+Na]^+$, found 308.1462

General Procedure for Dieckmann-type cyclisations of caprolactam esters:

A three-necked round bottom flask, equipped with a thermometer, a tap and a septum is charged with 1 eq. of the respective lactam before 50 ml of dry THF are added. The solution is stirred and cooled, using dry-ice (-78 °C), ethyl acetate – liquid nitrogen mixtures (-85 °C) or ethyl acetate/toluene – liquid nitrogen mixtures (-100 °C). A 1M solution of base (MHMDS; Li, Na, K) in THF/toluene/ethyl benzene is added slowly so that the temperature does not increase above -70 °C. The reaction mixture is stirred for 30 min before 15 ml of aqueous, saturated NH_4Cl-sol. is added, the biphasic mixture is then allowed to warm to room temperature. 50 ml of water are added and the aqueous phase is extracted with 30 ml ethyl acetate five times. The combined organic layers are dried over $MgSO_4$, the drying agent is filtered off and the solvent is revomed *in vacuo*. The residue is purified with column chromatography [SiO_2; ethyl acetate:cyclohexane; 1:6 → 1:4] to give the bicyclic product.

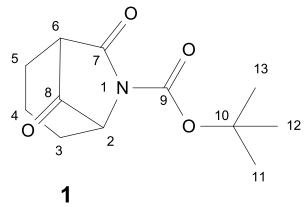

1

R_f = 0.30 [SiO_2; ethyl acetate:*n*-hexane; 1:1]; m.p.: 93-94 °C; ^{1}H NMR (500 MHz, $CDCl_3$, δ [ppm]) 4.39 (ddd, ^3J = 1 Hz, ^3J = 2 Hz, ^4J = 5 Hz, 1H, *H2*); 3.00 (ddd, ^3J = 1 Hz, ^3J = 2 Hz, ^4J = 5 Hz, 1H, *H6*); 2.52-2.46 (m, 1H, *H5*); 2.45-2.40 (m, 1H, *H3*); 2.08-2.00 (m, 1H, *H3'*); 1.99-1.92 (m, 1H, *H5'*); 1.86-1.80 (m, 2H, *H4*); 1.56 (s, 9H, *H11*, *H12*, *H13*); ^{13}C NMR (125 MHz, $CDCl_3$, δ [ppm]) 207.3 (*C8*); 168.9 (*C7*); 148.4 (*C9*); 84.1 (*C10*); 64.9 (*C6*); 55.0 (*C2*); 33.2 (*C3*); 32.8 (*C4*); 28.0 (*C11*, *C12*, *C13*); 17.1 (*C5*); IR (ATR) ν: 3315, 2977, 2942, 2867, 1714, 1442, 1392, 1365, 1340, 1306, 1259, 1223, 1137, 1114, 1081, 1054, 997, 952, 907, 875, 855, 766, 711, 641, 586, 515, 470, 433, 409. GC-MS: calculated: 238.12 $[M-H]^+$, found: 238.11

Synthesis of Methyl-6-oxoazinane-2-carboxylate (9)

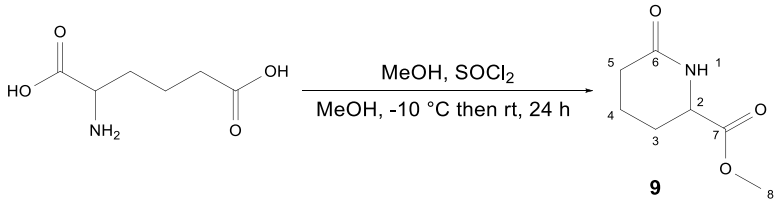

9

A three-necked round bottom flask equipped with a thermometer, a drying tube and a septum was charged with 40 ml of methanol. The solvent is cooled below -10 °C with an ice-NaCl mixture and 3.4 ml (2.07 g, 0.0174 mol) of thionyl chloride are added dropwise to the solvent, so that the temperature did not exceed -5 °C. The mixture is stirred for 10 min, before 2.50 g (0.0155 mol) of 2-aminoadipic acid are added quickly to the solution. The mixture is then allowed to warm to room temperature and stirred for 24 h. The solvent is distilled of under reduced pressure and the residue was treated with aqueous, saturated $NaHCO_3$ solution until no more gas develops and the pH of the solution is adjusted to above 7. The aqueous phase is extracted with 20 ml ethyl acetate five times and the combined organic phases are dried over $MgSO_4$. The drying agent is filtered off, the solvent is removed *in vacuo* and the residue is left to crystallise to give the product as colorless crystals. Yield: 58% (1.41 g); R_f = 0.23 [SiO_2; ethyl acetate]; m.p.: 65 °C; ^{1}H NMR (500 MHz, $CDCl_3$, δ [ppm]) 6.55 (br s, 1H, *NH*); 4.12-4.10 (m, 1H, *H2*); 3.78 (s, 3H, *H8*); 2.44-2.31 (m, 2H, *H5*); 2.21-2.16 (m, 1H, *H3*); 1.91-1.77 (m, 3H, *H3'*, *H4*); ^{13}C NMR (125 MHz, $CDCl_3$, δ [ppm]) 171.7 (*C7*); 171.5 (*C6*); 54.7 (*C2*); 52.7 (*C8*); 31.1 (*C5*); 25.5 (*C3*); 19.5 (*C4*); IR (ATR) ν: 3279, 2976, 2930, 2833, 1765, 1636, 1469, 1410, 1366, 1320, 1278, 1265, 1242, 1212, 1136, 1089, 1012, 965, 933, 874, 850, 822, 740, 670, 587, 517, 482. GC-MS: calculated: 157.1 $[M]^+$; found: 157

Synthesis of 6-oxoazinane-2-carboxylic acid (10)

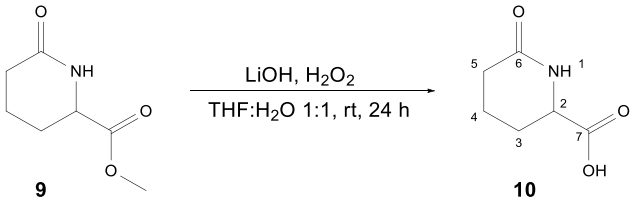

0.3 g (1.91 mmol) of methyl ester **9** are dissolved in a mixture of THF (15 ml) and water (15 ml). Subsequently, 183 mg (7.64 mmol) LiOH monohydrate are added, followed by 65 µl (2.10 mml) of a 30% aqueous H_2O_2 solution. The mixture is stirred for 24 h and then the pH adjusted to 3 with 0.5M aqueous HCl and extracted five times with ethyl acetate. The combined organic layers are dried over $MgSO_4$ and the solvent is removed *in vacuo* to give a viscous, colorless oil, which crystallised after several hours to give the crystalline product. Yield: 79% (0.22 g); R_f = 0.35 [SiO_2; ethyl acetate:cyclohexane; 1:4]; m.p.: 178 °C; Lit: 178-179 °C[123]; ^{1}H NMR (500 MHz, $CDCl_3$, δ [ppm]) 4.72-4.70 (m, 1H, *H2*); 3.77 (s, 3H, *H8*); 2.61-2.56 (m, 1H, *H5*); 2.52-2.45 (m, 1H, *H5'*); 2.19-2.15 (m, 1H, *H3*); 2.09-2.02 (m, 1H, *H3'*); 1.82-1.71 (m, 2H, *H4*); ^{13}C NMR (125 MHz, $CDCl_3$, δ [ppm]) 172.1 (*C7*); 170.2 (*C6*); 83.6 (*C10*); 58.5 (*C2*); 52.5 (*C8*); 34.6 (*C5*); 27.9 (*C11*, *C12*, *C13*); IR (ATR) ν: 3202, 2933, 1720, 1642, 1582, 1489, 1453, 1372, 1297, 1246, 1222, 1172, 1098, 1036, 940, 873, 799, 765, 737, 710, 620, 538, 495; HR-MS: calculate: 144.0655 $[M+H]^+$; found: 144.0643

Synthesis of *tert*-butyl-2-methyl-6-oxoazinane-1,2-dicarboxylate (5)

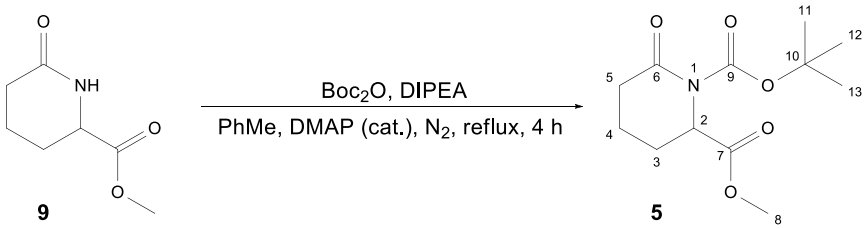

A two-necked round bottom flask, equipped with a reflux condenser and a stopper is charged with 0.5 g (3.18 mmol) of lactam **9** and 100 mg of DMAP under an inert atmosphere. The solids are dissolved in 50 ml of dry toluene and 2.04 ml (2.08 g, 9.55 mml) of di-*tert*-butyl decarbonate (Boc_2O) and 0.7 ml (0.53 g, 4.13 mmol) of diisopropylethylamine are added dropwise. The solution is refluxed for 6 h, allowed to cool to room temperature and quenched with 15 ml water. The biphasic mixture is stirred for another 90 min before another 100 ml of water are added and the aqueous phase is extracted with 20 ml of toluene five times. The combined organic phases are dried over $MgSO_4$, the drying agent is filtered off and the solvent is removed *in vacuo*. The residue is purified *via* column chromatography [SiO_2; ethyl acetate:cyclohexane; 1:6 → 1:4] to give the product as a colorless oil.

Yield: 81% (0.66 g); R_f = 0.35 [SiO_2; ethyl acetate:cyclohexane; 1:4]; ^{1}H NMR (500 MHz, $CDCl_3$, δ [ppm]) 4.72-4.70 (m, 1H, *H2*); 3.77 (s, 3H, *H8*); 2.61-2.56 (m, 1H, *H5*); 2.52-2.45 (m, 1H, *H5'*); 2.19-2.15 (m, 1H, *H3*); 2.09-2.02 (m, 1H, *H3'*); 1.82-1.71 (m, 2H, *H4*); ^{13}C NMR (125 MHz, $CDCl_3$, δ [ppm]) 172.1 (*C7*); 170.2 (*C6*); 83.6 (*C10*); 58.5 (*C2*); 52.5 (*C8*); 34.6 (*C5*); 27.9 (*C11*, *C12*, *C13*); IR (ATR) ν: 2930, 1738, 1700, 1467, 1463, 1400, 1366, 1321, 1268, 1244, 1199, 1142, 1123, 1080, 1046, 954, 900, 855, 786, 712, 672, 648, 600, 578, 487. GC-MS: calculated: 257.1 $[M]^+$; found: 157 $[M\text{-}Boc]^+$

Synthesis of Methyl-1-benzyl-7-oxoazepane-2-carboxylate (4)

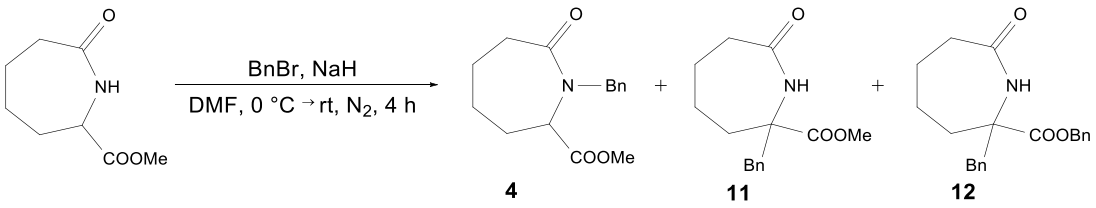

A three-necked round bottom flask, equipped with a thermometer, a tap and a septum, is charged with 0.5 g (2.9 mmol) of the starting material under a nitrogen atmosphere. 50 ml of dry DMF are added and the solution was cooled down to 0 °C. 3.9 ml (2.71 g, 0.0158 mol) of benzyl bromide and 131 mg (78.4 mg pure NaH, 3.3 mmol) of NaH (60% suspension in mineral oil) are added. The solution is stirred at 0 °C for 30 min, the reaction mixture is allowed to warm to room temperature and the mixture is stirred for another 4 h. 15 ml of water are added to the mixture before 150 ml of aqueous, saturated NaCl-sol. are added and the aqueous phase is extracted with 50 ml of ethyl acetate five times. The combined organic layers are dried over $MgSO_4$, filtered off and the solvent is removed *in vacuo*. The residue is purified with column chromatography [SiO_2; ethyl acetate:cyclohexane; 1:4 → 1:1] to give the desired product **4**, as well as side-products **11** and **12**.

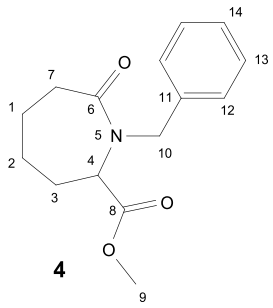

Yield (**4**): 65 % (0.49 g); R_f: 0.43 (ethyl acetate:*n*-hexane 1:1); ^{1}H-NMR: (500 MHz, $CDCl_3$, δ [ppm]) 7.33-7.26 (m, 5H, *H12*, *H13*, *H14*); 5.22 (d, ^2J = 14.8 Hz, 1H, *H10*); 4.11-4.06 (m, 2H, *H10'*, *H2*); 3.72 (s, 3H, *H9*); 2.75-2.70 (m, 1H, *H6*); 2.39-2.34 (m, 1H, *H6'*); 2.31-2.28 (m, 1H, *H3*); 1.81-1.78 (m, 2H, *H4*, *H5*); 1.51-1.46 (m, 3H, *H3'*, *H4'*, *H5'*); ^{13}C-NMR: (125 MHz, $CDCl_3$, δ [ppm])=176.0 (*C7*); 171.2 (*C8*); 137.2 (*C11*); 128.6 (*C13*); 128.5 (*C12*); 127.6 (*C14*); 59.9 (*C2*); 52.5 (*C10*); 52.4 (*C9*); 37.0 (*C6*); 30.7 (*C3*); 25.9 (*C4*); 22.7 (*C5*); IR (ATR) ν = 3119, 2978, 2936, 2868, 1715 (C=O), 1681 (C=O), 1442, 1391, 1365, 1207, 1259, 1233, 1137, 1125, 1054, 1026, 997, 952, 906, 875, 855, 780, 766, 736, 641, 586, 515, 469; HRMS: calculated: 261.3163 $[M]^+$; found: 261.3157

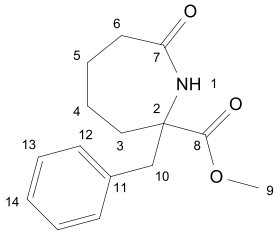

11

Yield (**11**): 22 % (0.17 g); R_f: 0.17 (ethyl acetate:*n*-hexane 1:1); ^{1}H-NMR: (500 MHz, $CDCl_3$, δ [ppm]) 7.32-7.27 (m, 3H, *H13*, *H14*); 7.09-7.07 (m, 2H, *H12*); 5.88 (br s, 1H, *NH*); 3.74 (s, 3H, *H9*); 3.21 (d, ^2J = 13.7 Hz, 1H, *H10*); 2.96 (d, ^2J = 13.7 Hz, 1H, *H10'*); 2.58-2.53 (m, 1H, *H6*); 2.41-2.32 (m, 2H, *H6'*, *H3*); 1.98-1.93 (m, 1H, *H4*); 1.89-1.84 (m, 1H, *H3'*); 1.76-1.71 (m, 1H, *H5*); 1.63-1.55 (m, 2H, *H4'*, *H5'*); ^{13}C-NMR: (125 MHz, $CDCl_3$, δ[ppm]) 177.2 (*C7*); 173.2 (*C2*); 134.2 (*C11*); 129.7 (*C13*); 129.0 (*C12*); 127.9 (*C14*); 63.8 (*C2*); 52.5 (*C9*); 46.4 (*C10*); 38.9 (*C3*); 37.7 (*C6*); 26.0 (*C4*); 22.8 (*C5*); IR (ATR) ν = 3298, 3078, 2975, 1707 (C=O), 1624 (C=O), 1463, 1441, 1366, 1308, 1204, 1154, 1114, 1081, 1054, 1027, 998, 974, 953, 876, 856, 831, 759, 727, 695, 641, 573, 545, 494, 467; HRMS: calculated: 284.12629 $[M+Na]^+$, found: 284.1257

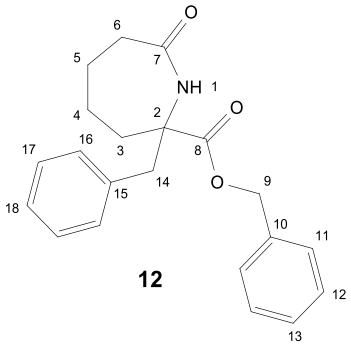

12

Yield (**12**): 7 % (68 mg); R_f: 0.28 (ethyl acetate:*n*-hexane 1:1); ^{1}H-NMR: (500 MHz, $CDCl_3$, δ[ppm]) 7.39-7.30 (m, 5H, *H11*, *H12*, *H18*); 7.28-7.21 (m, 3H, *H17*, *H13*); 7.01-6.98 (m, 2H, *H16*); 5.87 (br s, 1H, *NH*); 5.18 (q, ^2J = 11.2 Hz, 2H, *H9*); 3.21 (d, ^2J = 13.8 Hz, 1H, *H14*); 2.92 (d, ^2J = 13.8 Hz, 1H, *H14*); 2.52-2.48 (m, 1H, *H6*); 2.41-2.36 (m, 1H, *H3*); 2.33-2.26 (m, 1H, *H6'*); 1.94-1.82 (m, 2H, *H3'*, *H4*); 1.72-1.67 (m, 1H, *H5*); 1.62-1.51 (m, 2H, *H4'*, *H5'*); ^{13}C-NMR: (125 MHz, $CDCl_3$, δ[ppm]) 177.2 (*C7*); 172.6 (*C2*); 134.9 (*C10*); 134.0 (*C15*); 129.8 (*C16*); 129.0 (*C13*); 128.9 (*C11*); 128.7 (*C12*); 128.6 (*C17*); 127.8 (*C18*); IR (ATR) ν = 3196, 3066, 2946, 2861, 1733(C=O), 1661 (C=O), 1498, 1440, 1415, 1361, 1341, 1287, 1240, 1215, 1198, 1176, 1139, 1093, 1074, 1011, 956, 921, 875, 854, 795, 780, 735, 636, 585, 572, 549, 513, 465; HRMS: calculated: $[M+Na]^+$ 344.12628 found: 344.1257

[121] E. Atherton, C.J. Logan, R.C. Sheppard, *J. Chem. Soc., Perkin Trans 1* **1981**, 538-546.
[122] E. Perrotti, N. Palladino. M. Greco, M. De Malde *Ann. Chim.* **1966**, *56*, 1358-1372.
[123] M.F. Shostakovskii, M.S. Rabinovich, E.V. Preobrazhenskaya, G.N. Zykova *Zhurnal Obchchei Khimii* **1960**, *30*, 67-71.

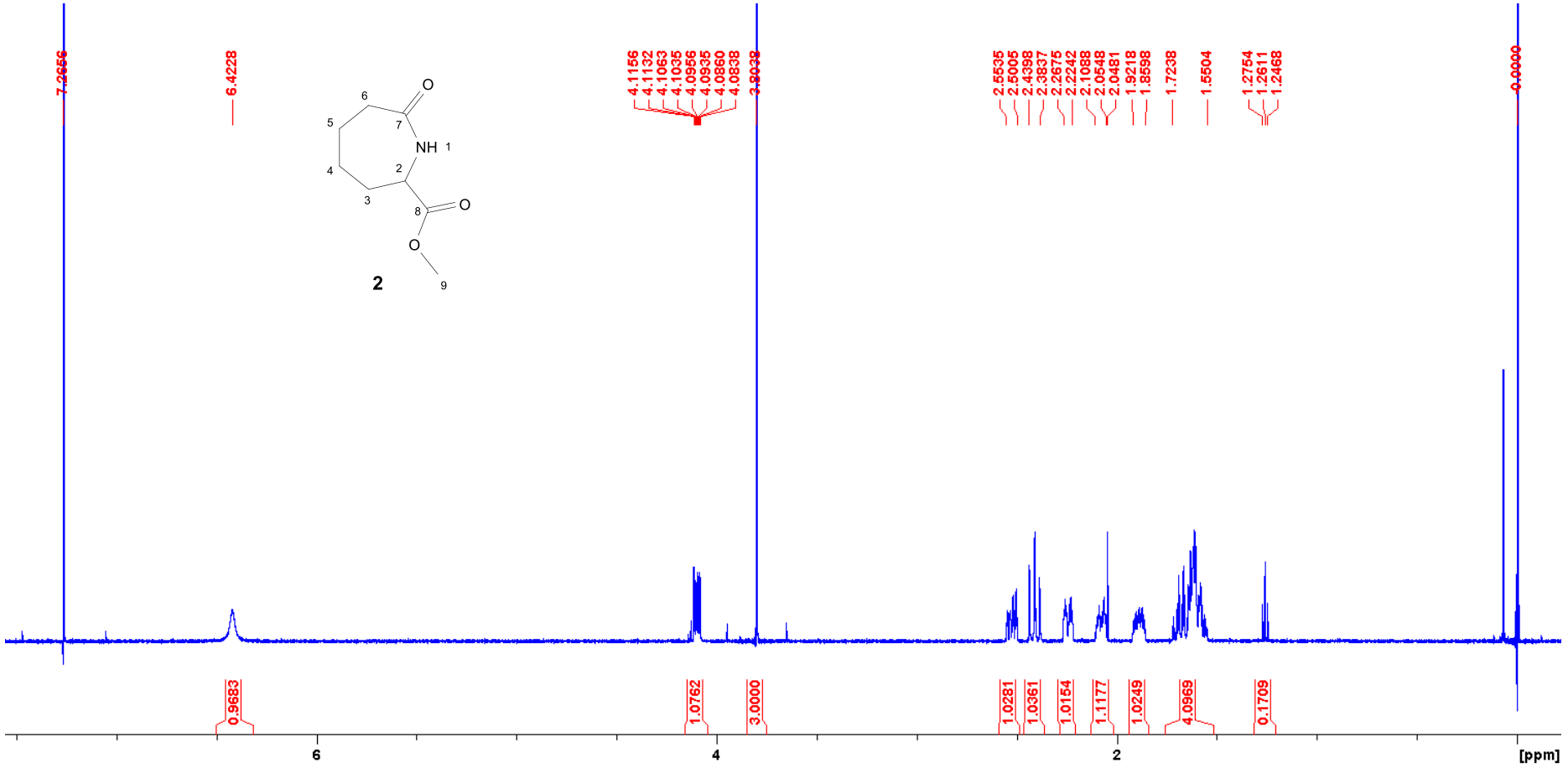
7.2656
6.4228
4.1156
4.1132
4.1063
4.1035
4.0956
4.0935
4.0860
4.0838
3.8038
2.5535
2.5005
2.4398
2.3837
2.2675
2.2242
2.1088
2.0548
2.0481
1.9218
1.8598
1.7238
1.5504
1.2754
1.2611
1.2468
0.0000
NH
O
O
O
1
2
3
4
5
6
7
8
9
2
0.9683
1.0762
3.0000
1.0281
1.0361
1.0154
1.1177
1.0249
4.0969
0.1709
6
4
2
[ppm]

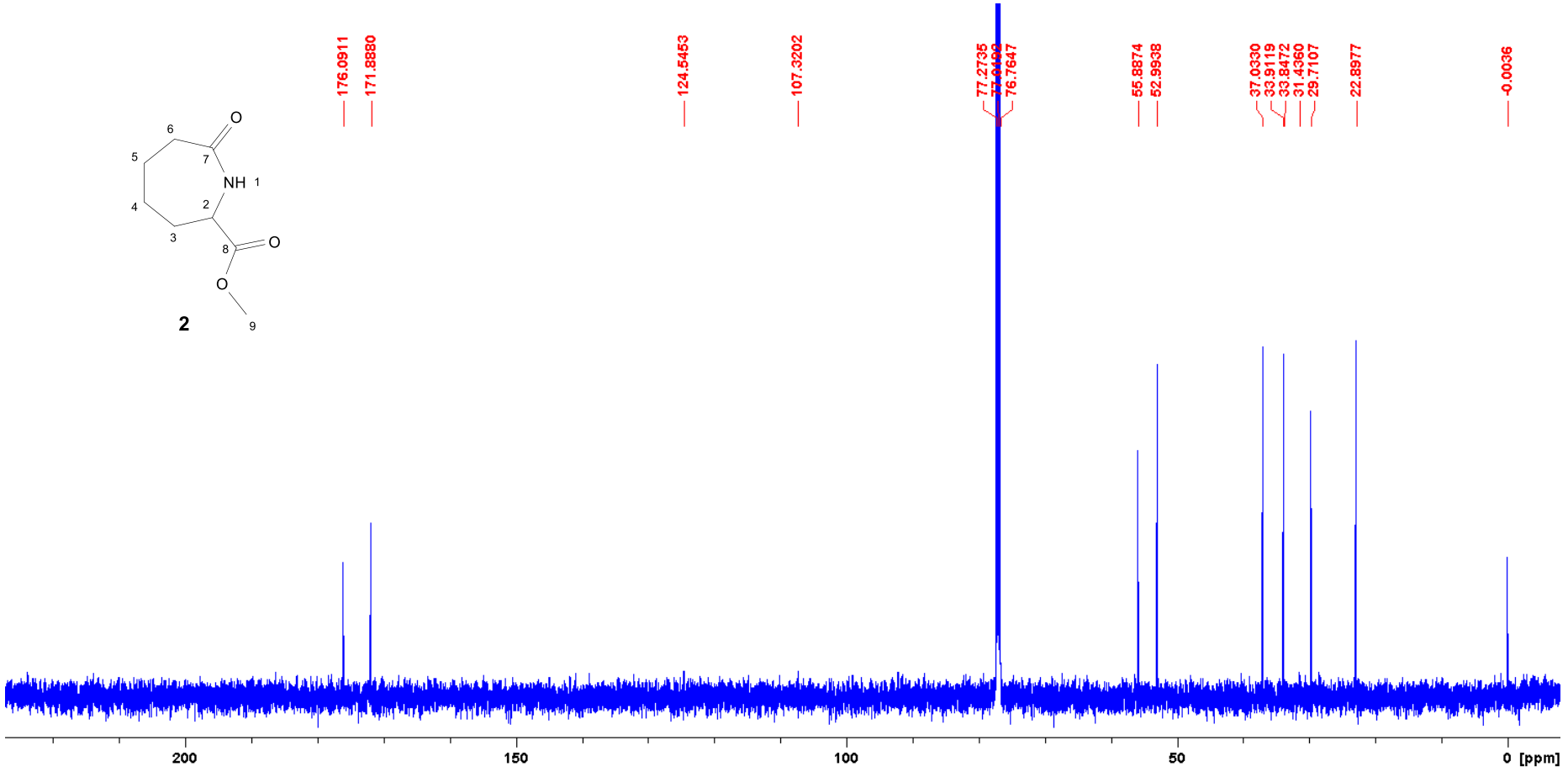
176.0911
171.8880
124.5453
107.3202
77.2735
77.0183
76.7647
55.8874
52.9938
37.0330
33.9119
33.8472
31.4360
29.7107
22.8977
-0.0036
O
6
5
7
NH 1
4
2
3
8
O
O
9
2
200
150
100
50
0 [ppm]

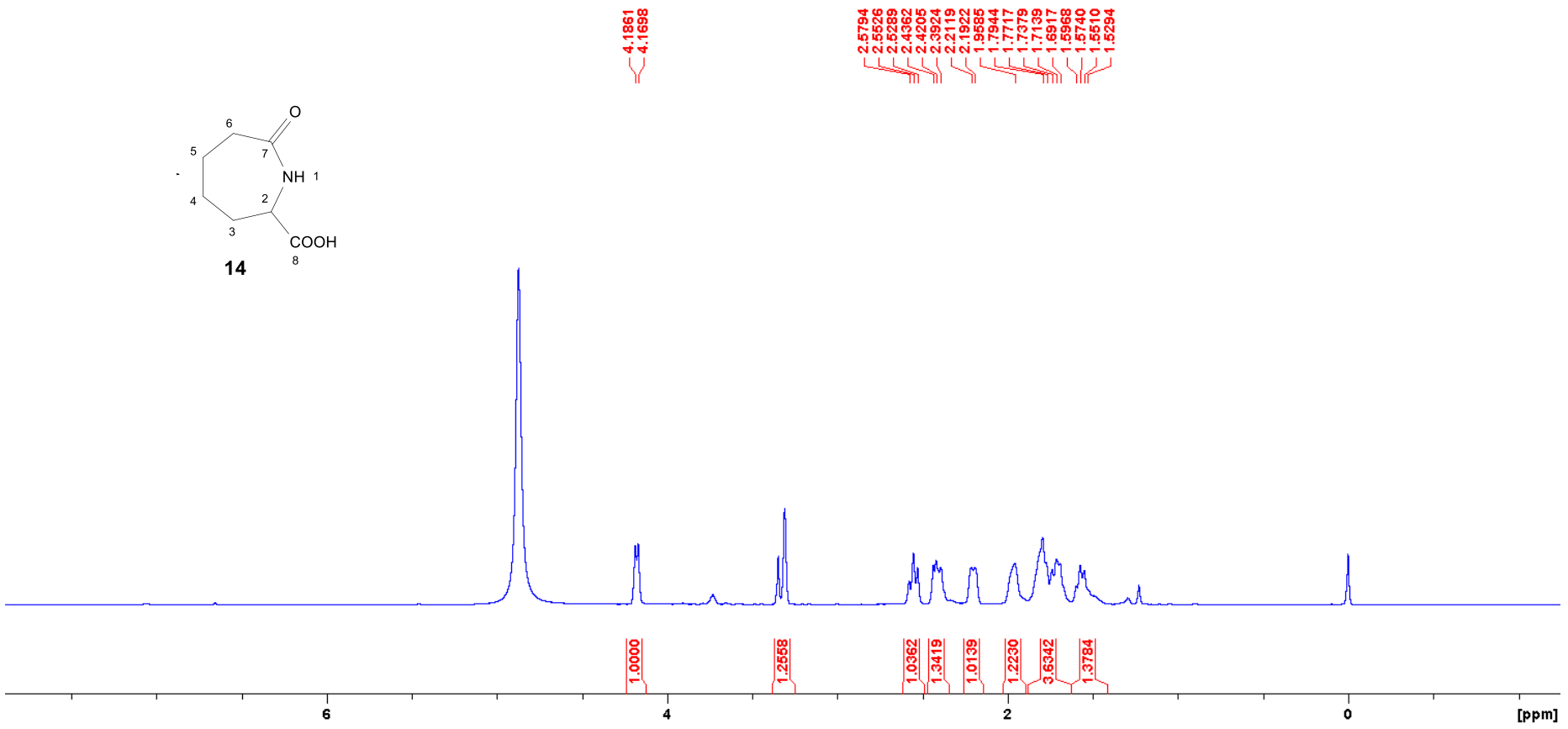
4.1861
4.1698
2.5794
2.5526
2.5289
2.4362
2.4205
2.3924
2.2119
2.1922
1.9585
1.7944
1.7717
1.7379
1.7139
1.6917
1.5968
1.5740
1.5510
1.5294
O
6
7
5
NH 1
4
2
3
COOH
8
14
1.0000
1.2558
1.0362
1.3419
1.0139
1.2230
3.6342
1.3784
6
4
2
0
[ppm]

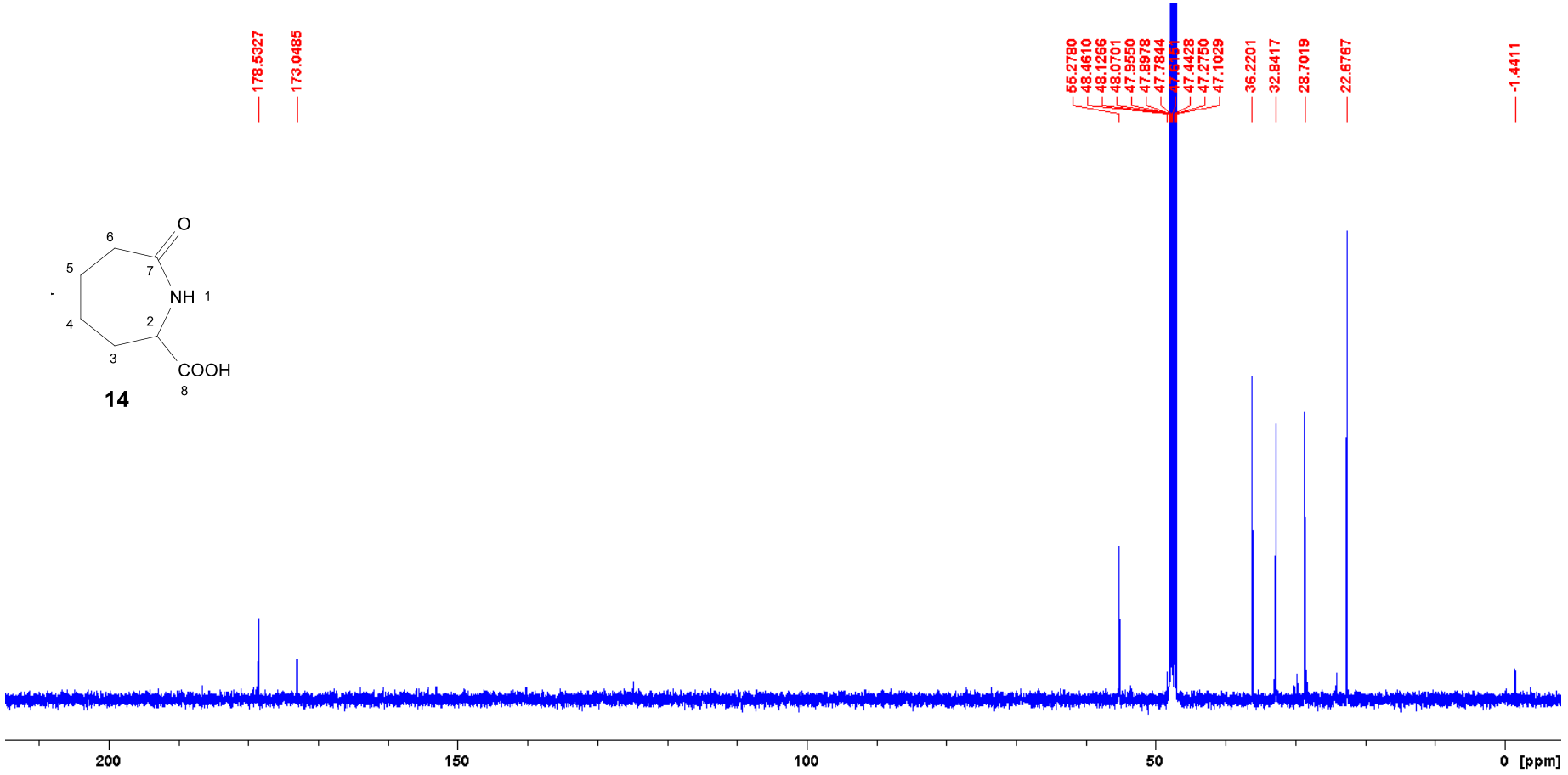
178.5327
173.0485
55.2780
48.4610
48.1266
48.0701
47.9550
47.8978
47.7844
47.4428
47.2750
47.1029
36.2201
32.8417
28.7019
22.6767
-1.4411
O
NH
COOH
1
2
3
4
5
6
7
8
200
150
100
50
0 [ppm]

14

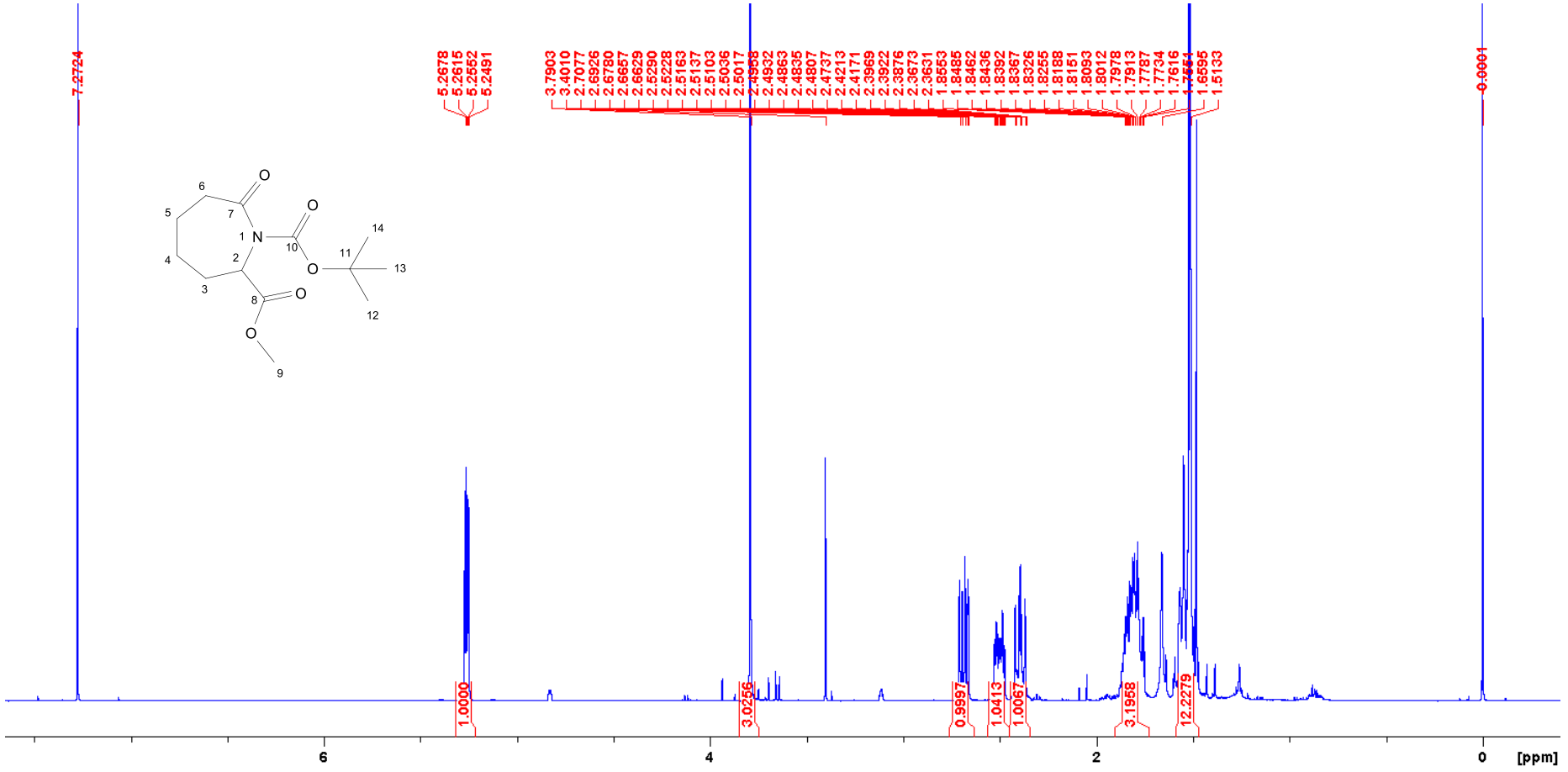
7.2724
5.2678
5.2615
5.2562
5.2491
3.7903
3.4010
2.7077
2.6926
2.6780
2.6657
2.6629
2.5290
2.5228
2.5163
2.5137
2.5103
2.5036
2.5017
2.4958
2.4932
2.4863
2.4835
2.4807
2.4737
2.4213
2.4171
2.3969
2.3922
2.3876
2.3673
2.3631
1.8553
1.8485
1.8462
1.8436
1.8392
1.8367
1.8326
1.8255
1.8188
1.8151
1.8093
1.8012
1.7978
1.7913
1.7787
1.7734
1.7616
1.6595
1.5133
0.0001
1.0000
3.0256
0.9997
1.0413
1.0067
3.1958
12.2279
6
4
2
0
[ppm]

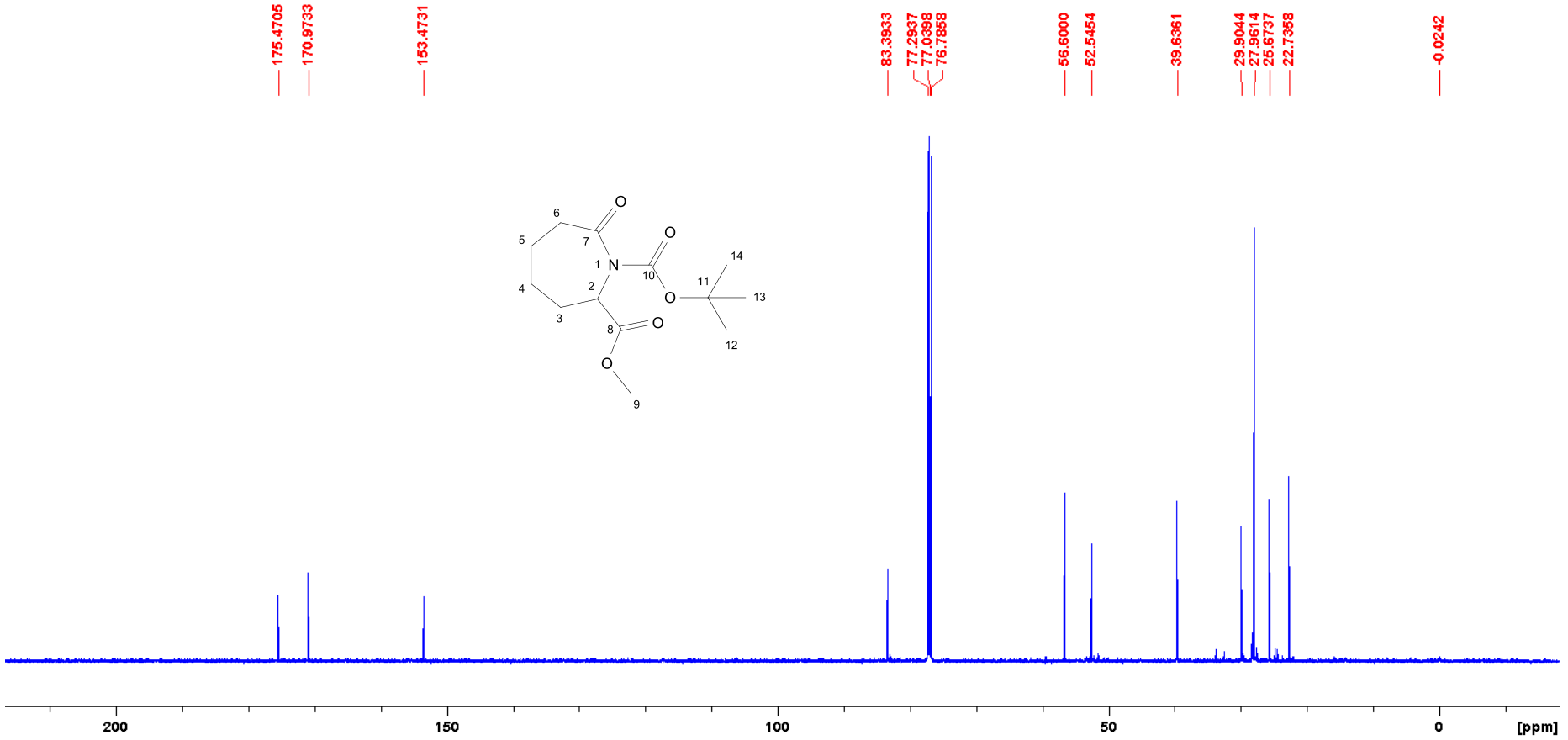
175.4705
170.9733
153.4731
83.3933
77.2937
77.0398
76.7858
56.6000
52.5454
39.6361
29.9044
27.9614
25.6737
22.7358
-0.0242
O
6
7
5
1
N
10
O
O
14
11
13
4
2
3
8
O
O
12
O
9
200
150
100
50
0
[ppm]

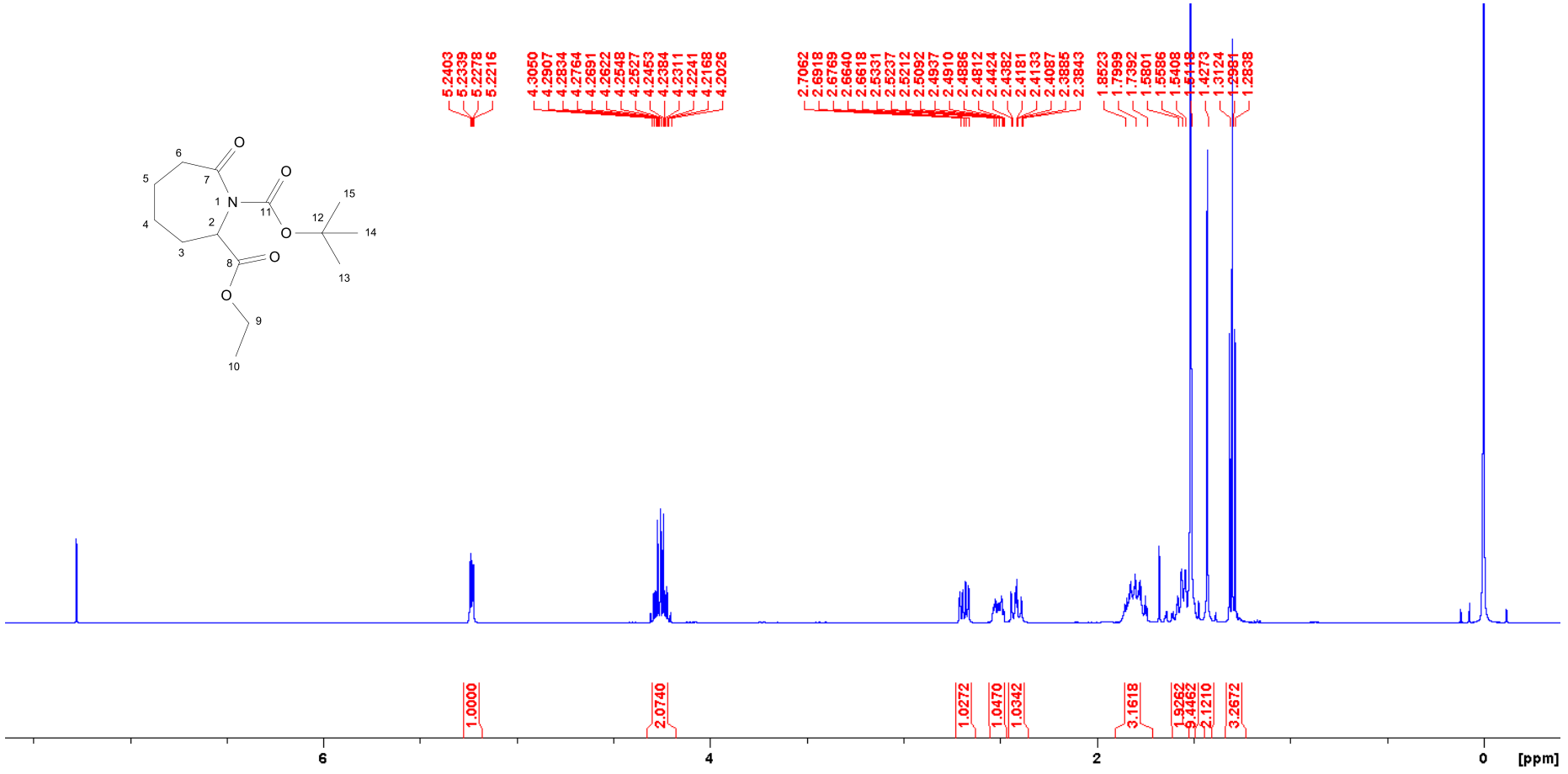
5.2403
5.2339
5.2278
5.2216
4.3050
4.2907
4.2834
4.2764
4.2691
4.2622
4.2548
4.2527
4.2453
4.2384
4.2311
4.2241
4.2168
4.2026
2.7062
2.6918
2.6769
2.6640
2.6618
2.5331
2.5237
2.5212
2.5092
2.4937
2.4910
2.4886
2.4812
2.4424
2.4382
2.4181
2.4133
2.4087
2.3885
2.3843
1.8523
1.7999
1.7392
1.5801
1.5586
1.5408
1.4273
1.3124
1.2981
1.2838
1.0000
2.0740
1.0272
1.0470
1.0342
3.1618
1.9262
9.4462
2.1210
3.2672
6
4
2
0
[ppm]

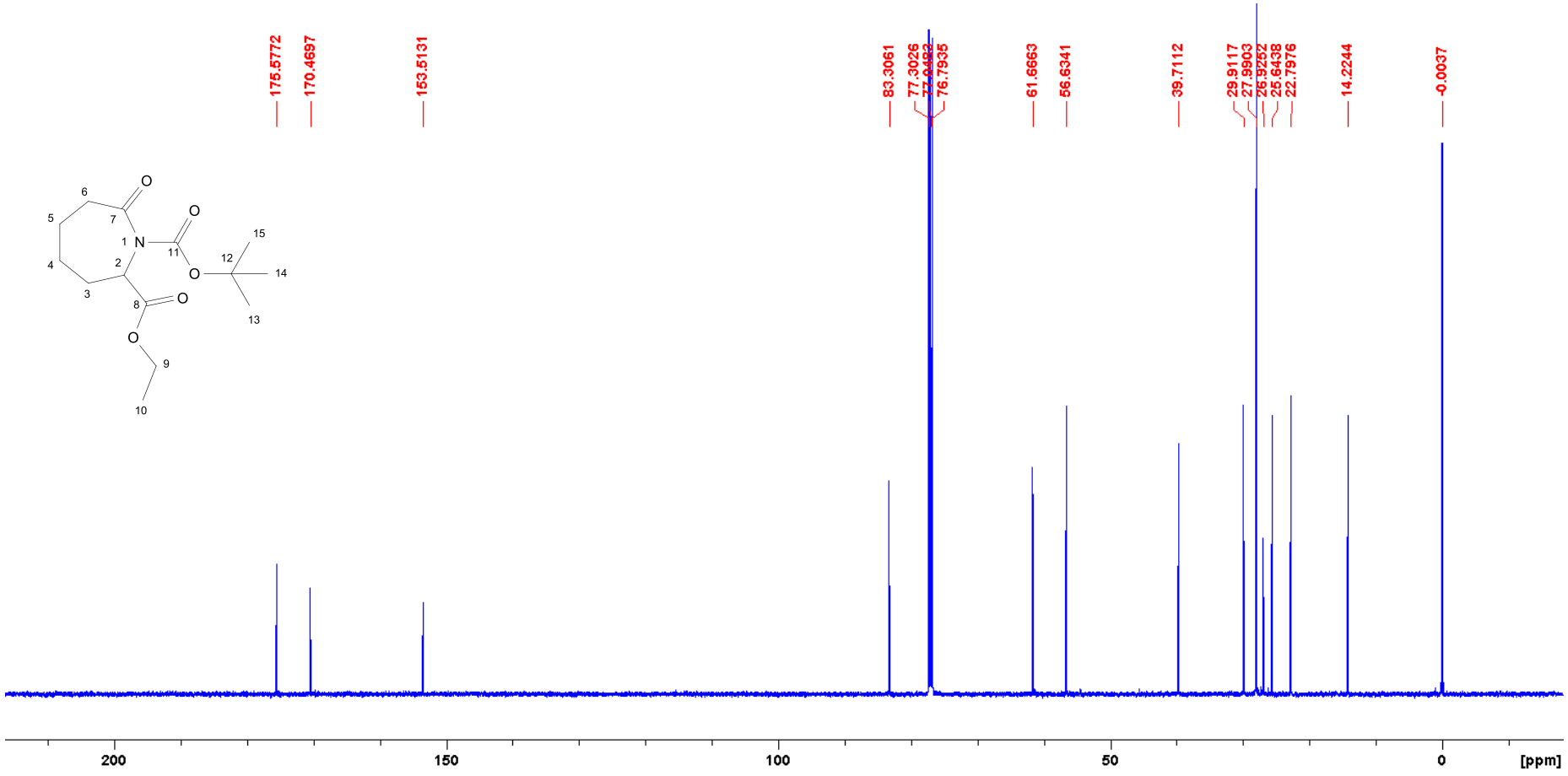
175.5772
170.4697
153.5131
83.3061
77.3026
77.0483
76.7935
61.6663
56.6341
39.7112
29.9117
27.9903
26.9252
25.6438
22.7976
14.2244
-0.0037
200
150
100
50
0
[ppm]

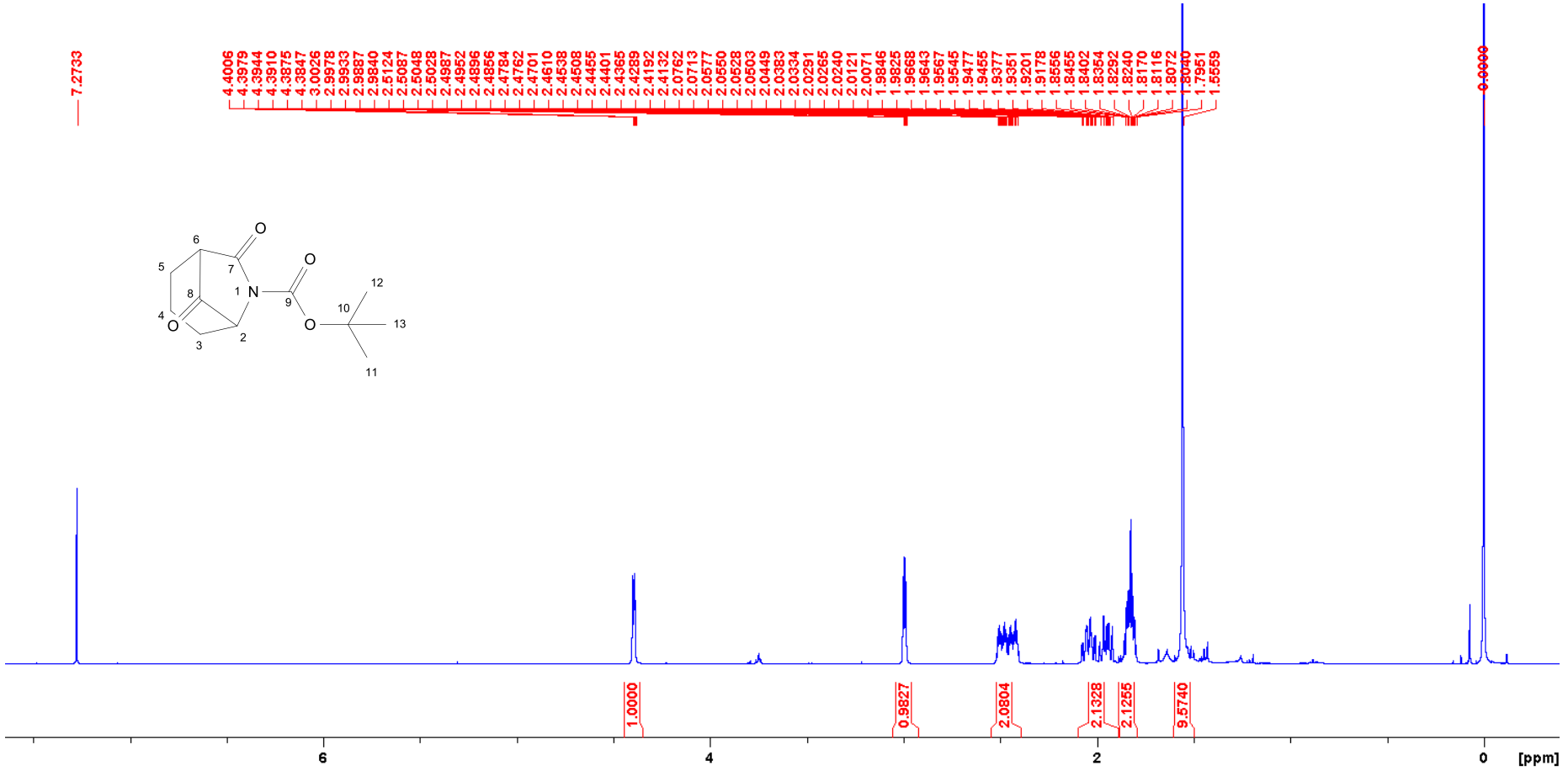
7.2733
4.4006
4.3979
4.3944
4.3910
4.3875
4.3847
3.0026
2.9978
2.9933
2.9887
2.9840
2.5124
2.5087
2.5048
2.5028
2.4987
2.4952
2.4896
2.4856
2.4784
2.4762
2.4701
2.4610
2.4538
2.4508
2.4455
2.4401
2.4365
2.4289
2.4192
2.4132
2.0762
2.0713
2.0577
2.0550
2.0528
2.0503
2.0449
2.0383
2.0334
2.0291
2.0265
2.0240
2.0121
2.0071
1.9846
1.9825
1.9668
1.9643
1.9567
1.9545
1.9477
1.9455
1.9377
1.9351
1.9201
1.9178
1.8556
1.8455
1.8402
1.8354
1.8292
1.8240
1.8170
1.8116
1.8072
1.8040
1.7951
1.5569
0.0000
1.0000
0.9827
2.0804
2.1328
2.1255
9.5740
6
4
2
0
[ppm]

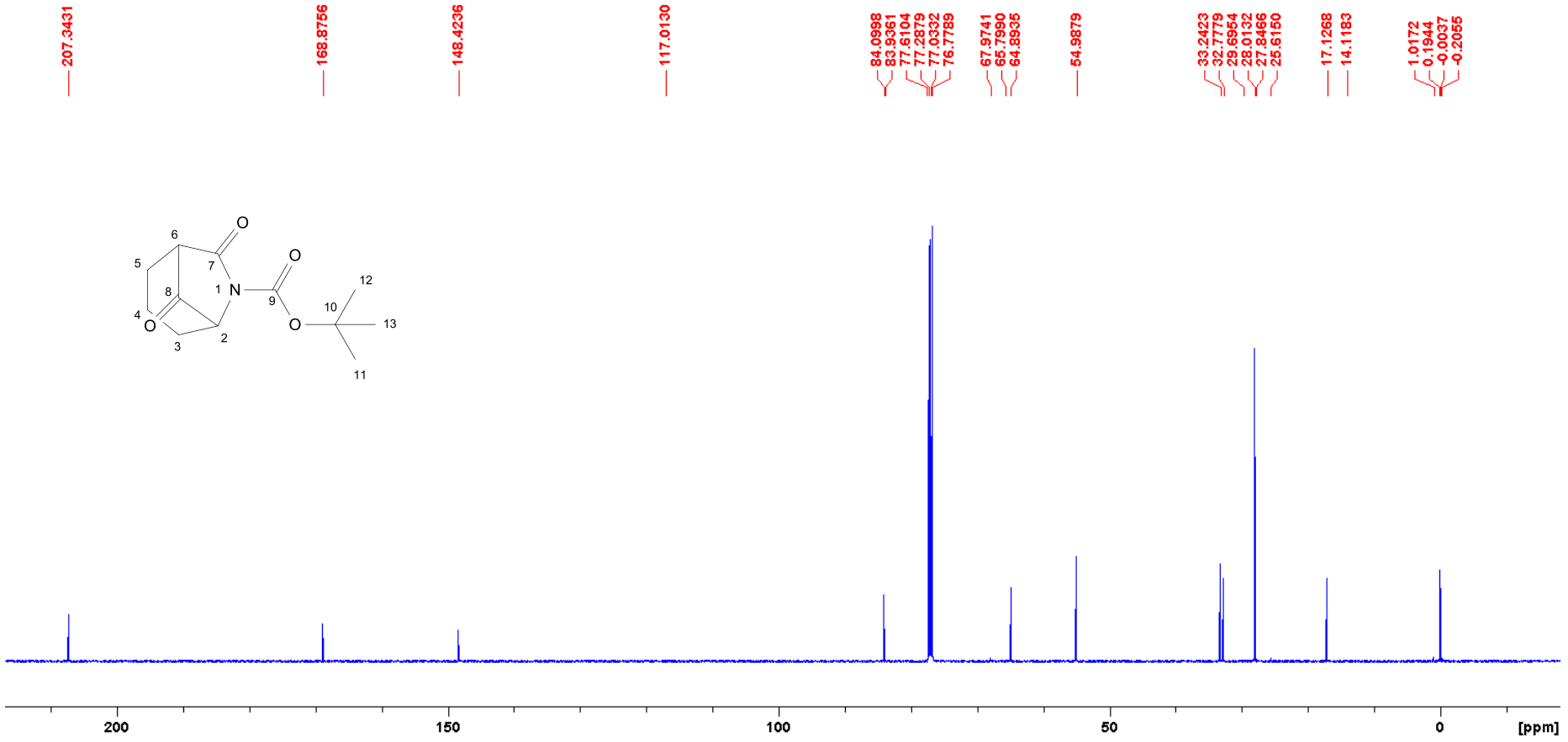
207.3431
168.8756
148.4236
117.0130
84.0998
83.9361
77.6104
77.2879
77.0332
76.7789
67.9741
65.7990
64.8935
54.9879
33.2423
32.7779
29.6954
28.0132
27.8466
25.6150
17.1268
14.1183
1.0172
0.1944
-0.0037
-0.2055
O
6
5
7
O
8
1
N
9
O
4
O
10
12
13
3
2
11
200
150
100
50
0
[ppm]

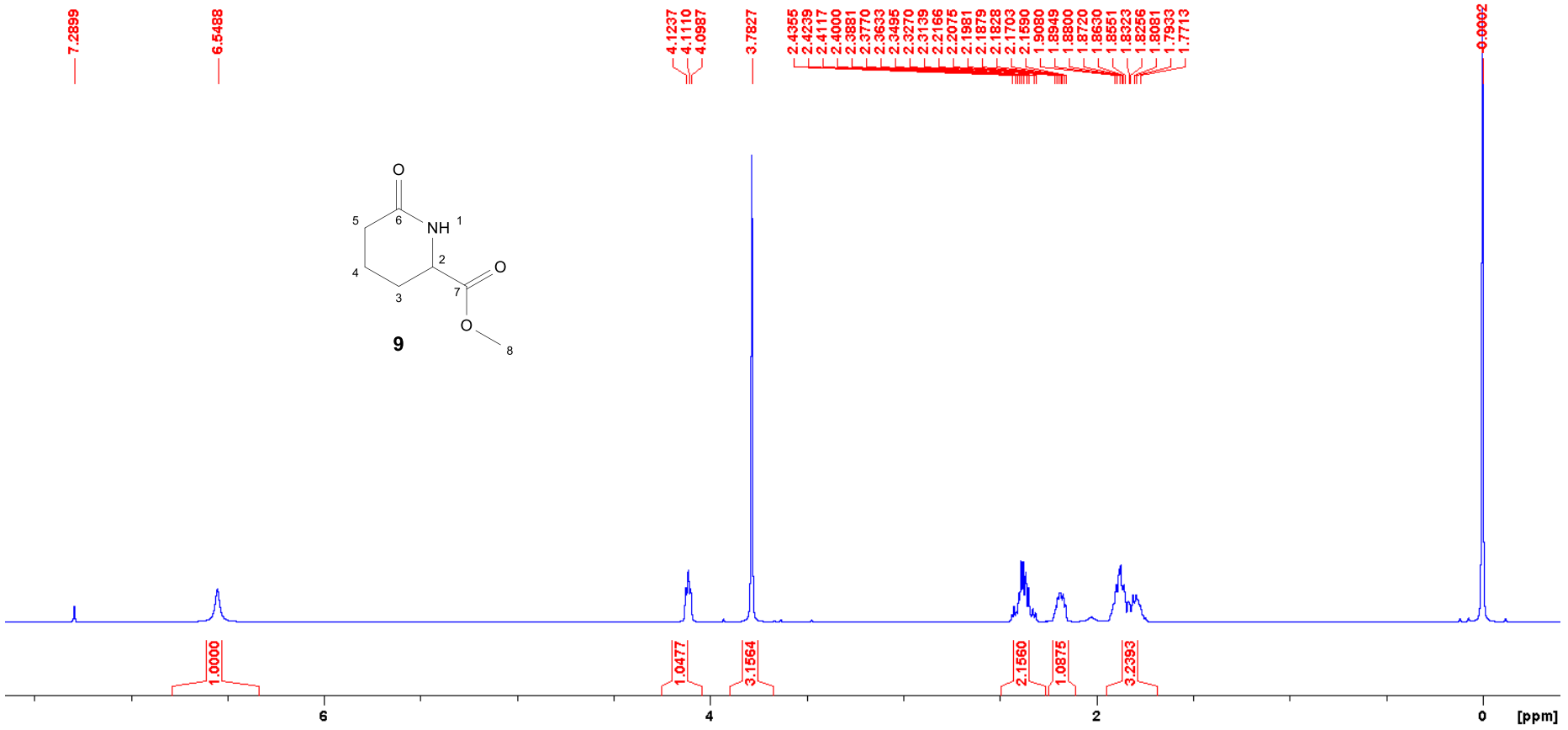
7.2899
6.5488
4.1237
4.1110
4.0987
3.7827
2.4355
2.4239
2.4117
2.4000
2.3881
2.3770
2.3633
2.3495
2.3270
2.3139
2.2166
2.2075
2.1981
2.1879
2.1828
2.1703
2.1590
1.9080
1.8949
1.8800
1.8720
1.8630
1.8551
1.8323
1.8256
1.8081
1.7933
1.7713
0.0002
O
NH
O
O
1
2
3
4
5
6
7
8
9
1.0000
1.0477
3.1564
2.1560
1.0875
3.2393
6
4
2
0
[ppm]

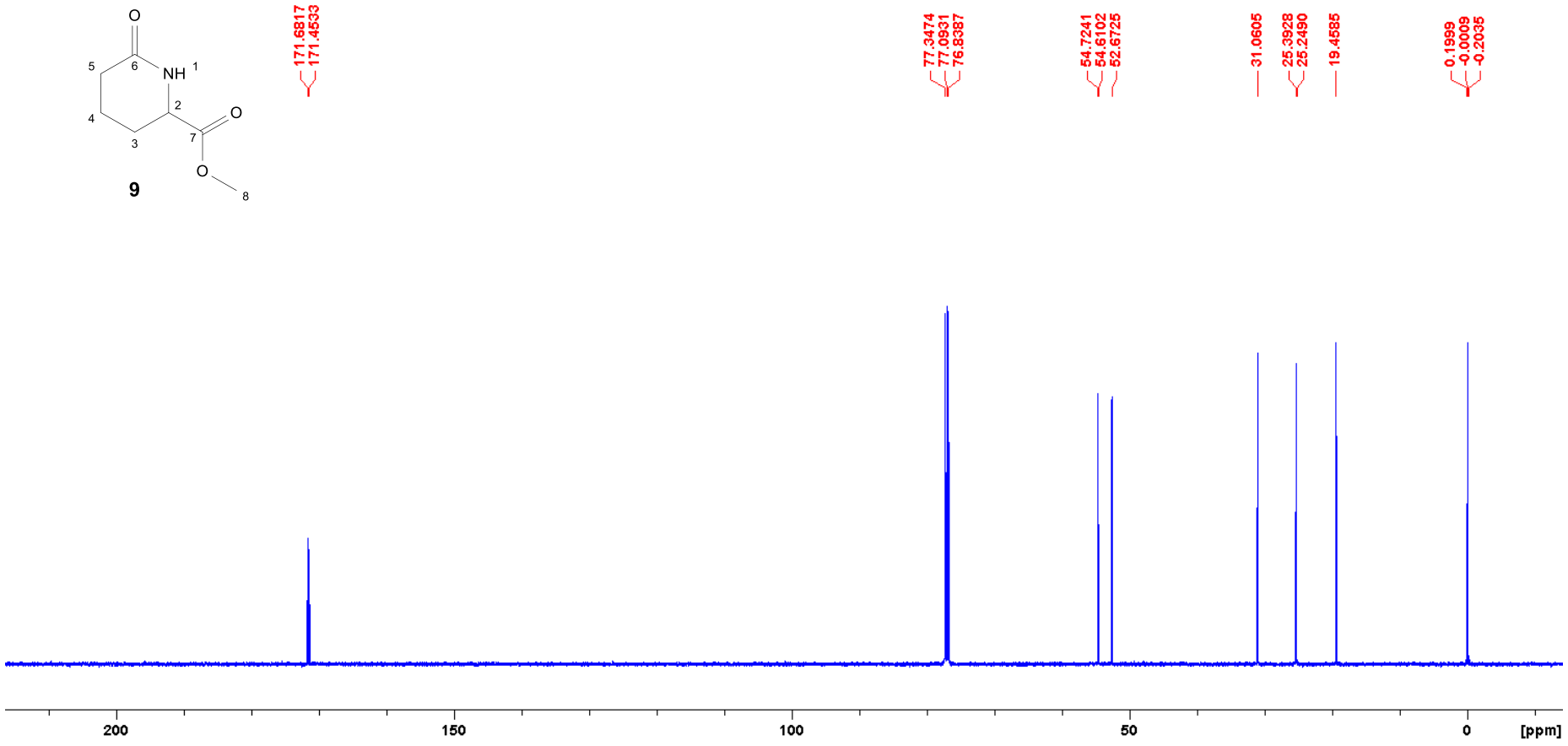
O
NH
O
O
1
2
3
4
5
6
7
8
9
171.6817
171.4533
77.3474
77.0931
76.8387
54.7241
54.6102
52.6725
31.0605
25.3928
25.2490
19.4585
0.1999
-0.0009
-0.2035
200
150
100
50
0
[ppm]

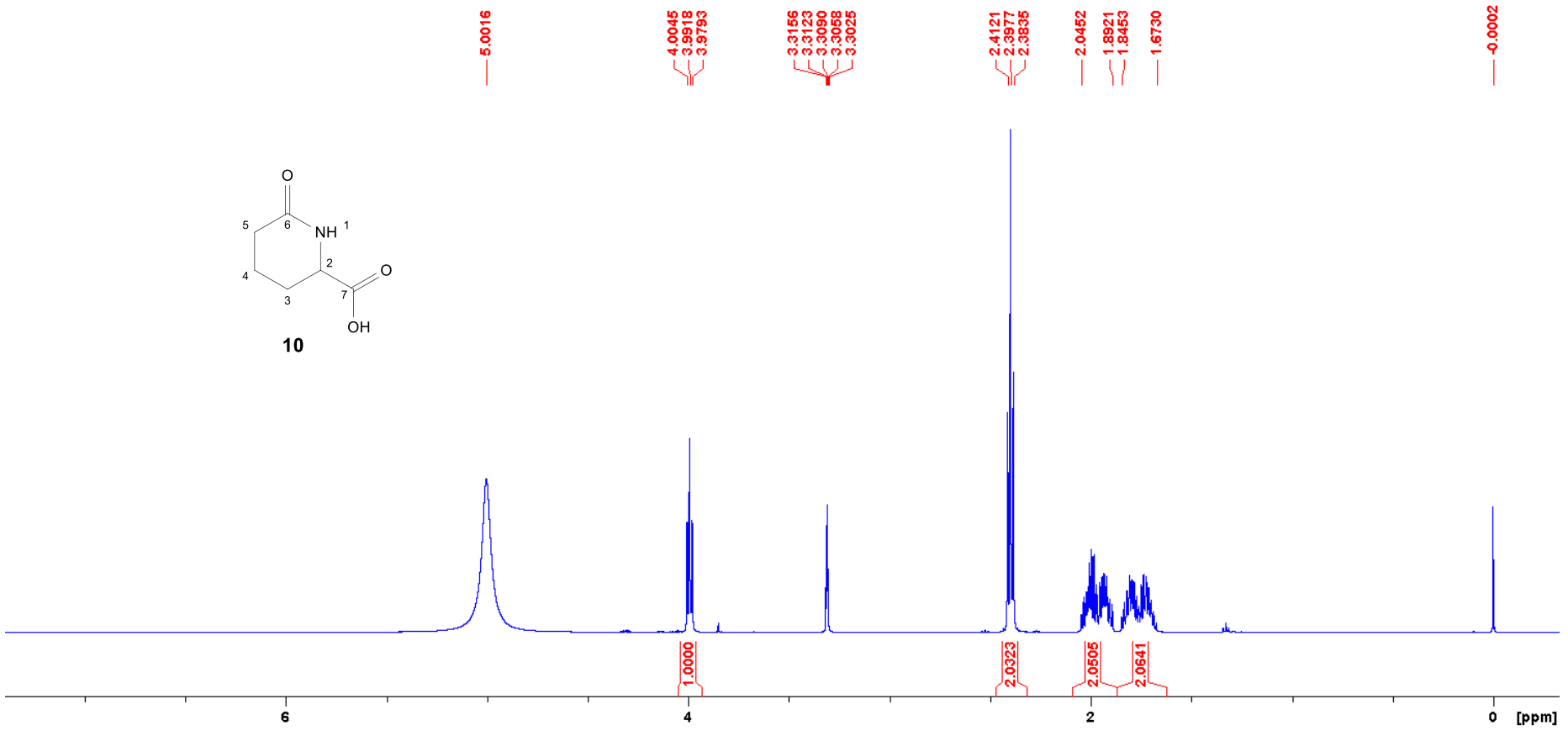
5.0016
4.0045
3.9918
3.9793
3.3156
3.3123
3.3090
3.3058
3.3025
2.4121
2.3977
2.3835
2.0452
1.8921
1.8453
1.6730
-0.0002
O
NH
O
OH
1
2
3
4
5
6
7
10
1.0000
2.0323
2.0505
2.0641
6
4
2
0
[ppm]

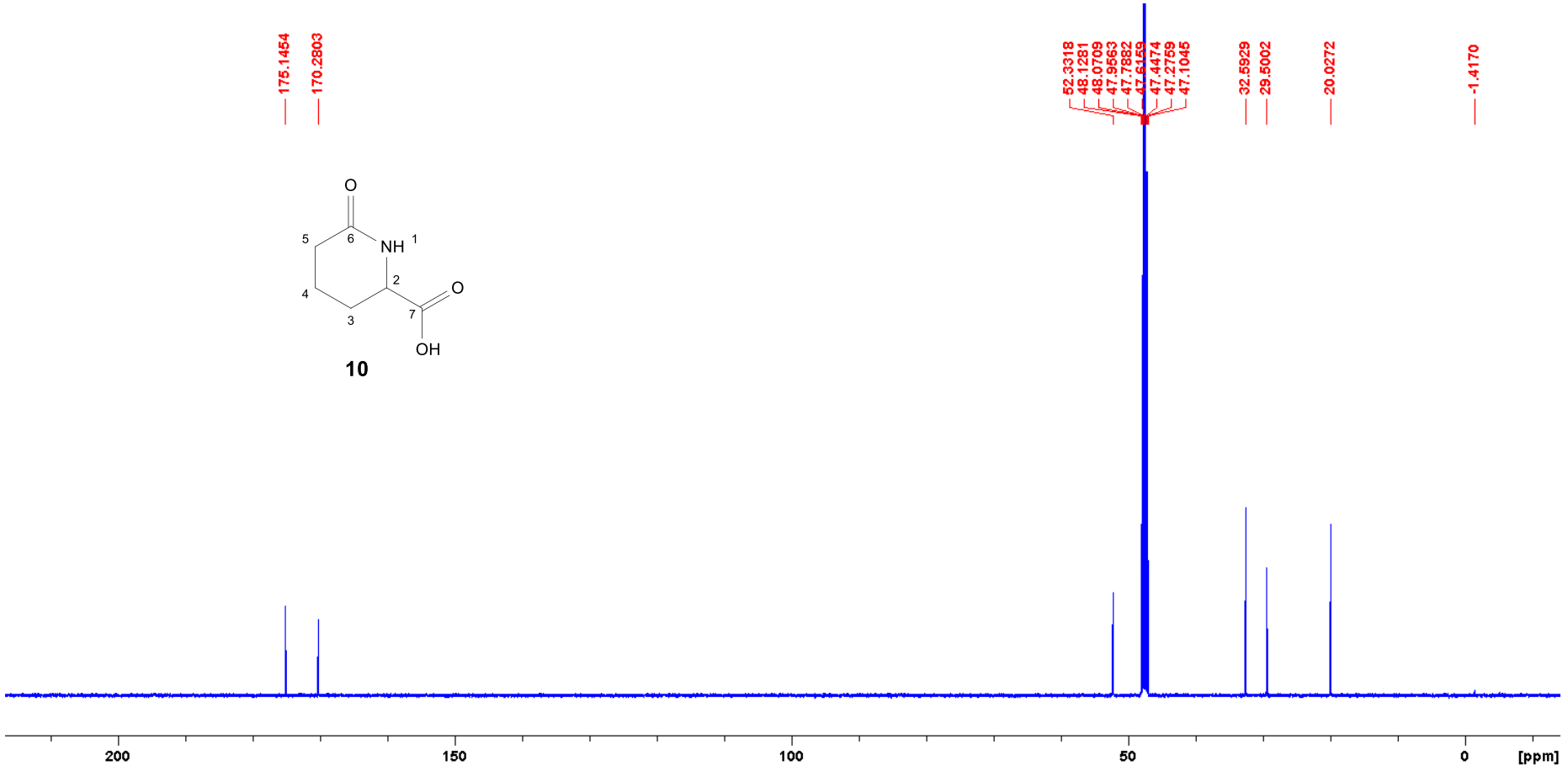
175.1454
170.2803
52.3318
48.1281
48.0709
47.9563
47.7882
47.6153
47.4474
47.2759
47.1045
32.5929
29.5002
20.0272
-1.4170
O
NH
OH
1
2
3
4
5
6
7
200
150
100
50
0
[ppm]

10

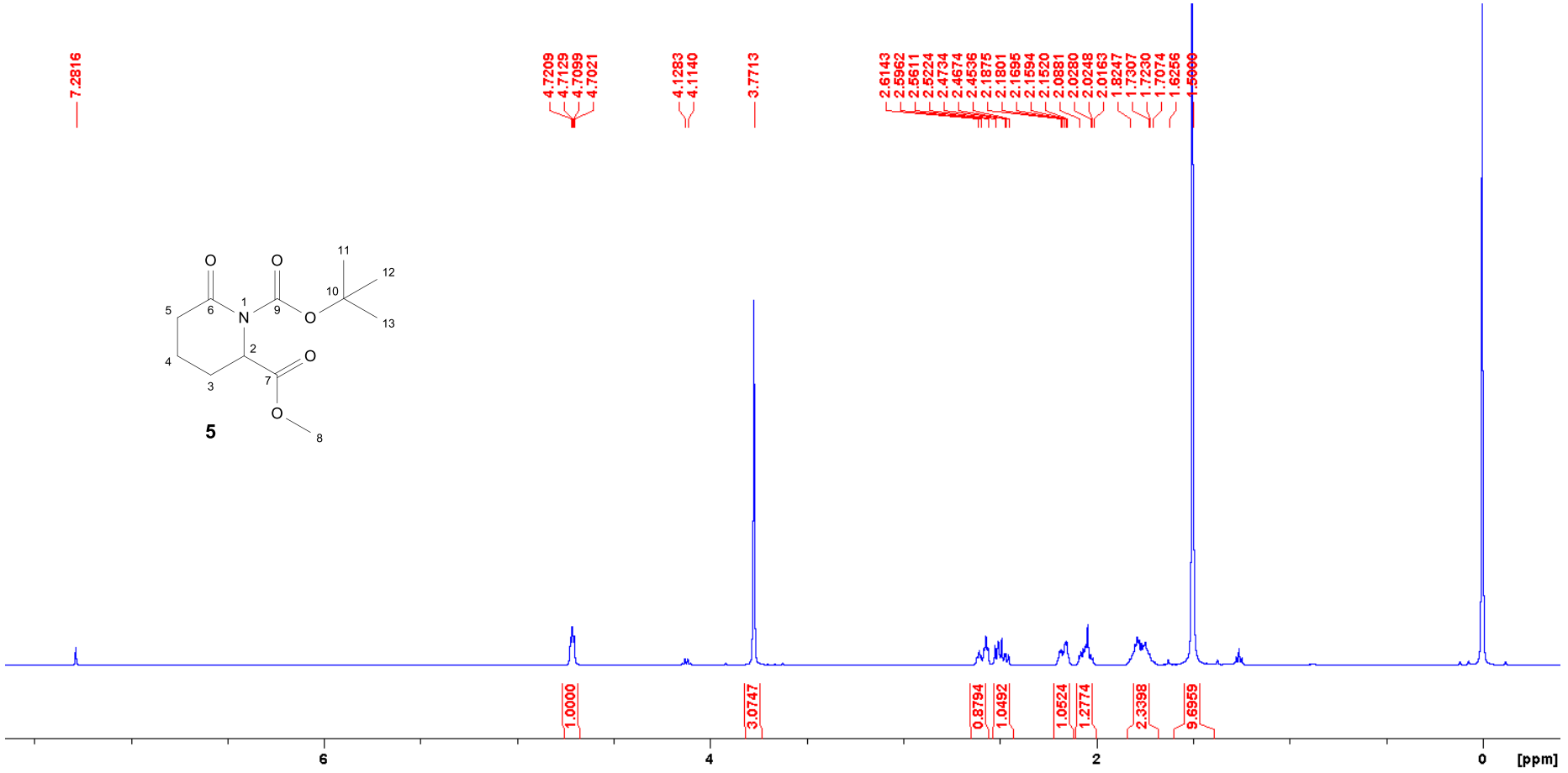
7.2816
4.7209
4.7129
4.7099
4.7021
4.1283
4.1140
3.7713
2.6143
2.5962
2.5611
2.5224
2.4734
2.4674
2.4536
2.1875
2.1801
2.1695
2.1594
2.1520
2.0881
2.0280
2.0248
2.0163
1.8247
1.7307
1.7230
1.7074
1.6256
1.5000
1.0000
3.0747
0.8794
1.0492
1.0524
1.2774
2.3398
9.6959
6
4
2
0
[ppm]

5

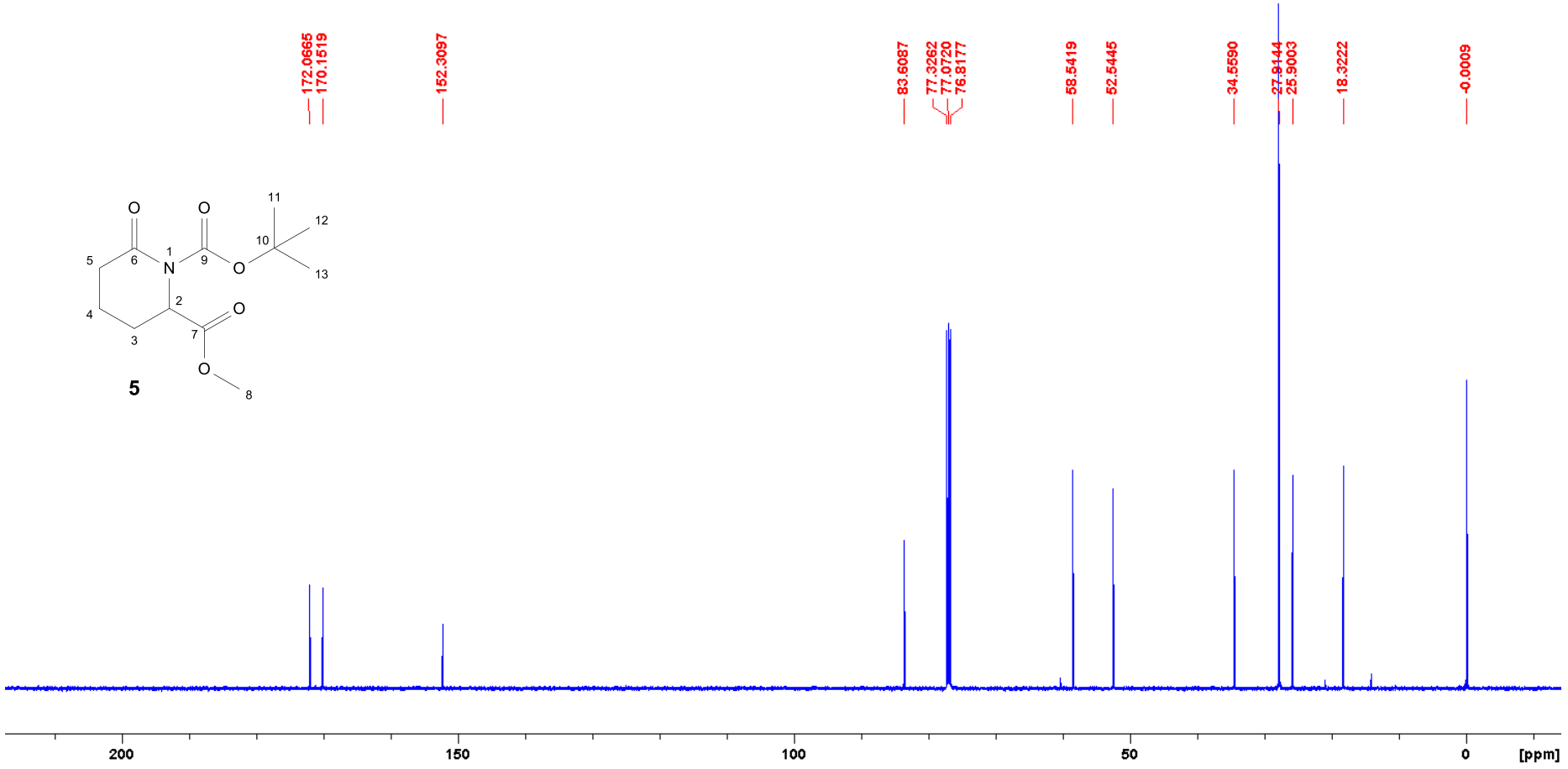
172.0665
170.1519
152.3097
83.6087
77.3262
77.0720
76.8177
58.5419
52.5445
34.5590
27.8144
25.9003
18.3222
-0.0009
O
O
11
12
10
5
6
1
N
9
O
13
4
2
O
3
7
O
8
5
200
150
100
50
0
[ppm]

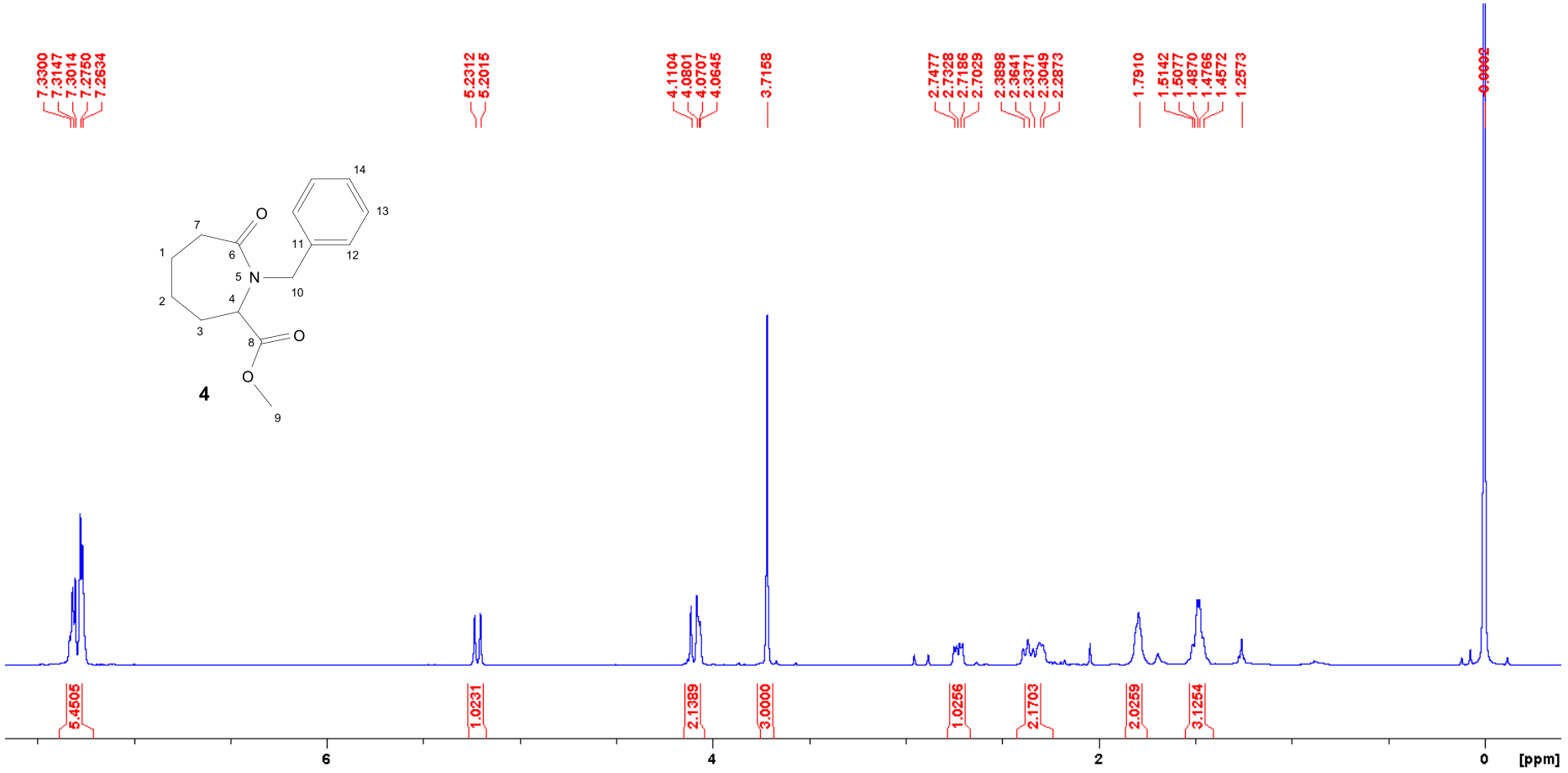
7.3300
7.3147
7.3014
7.2750
7.2634
5.2312
5.2015
4.1104
4.0801
4.0707
4.0645
3.7158
2.7477
2.7328
2.7186
2.7029
2.3898
2.3641
2.3371
2.3049
2.2873
1.7910
1.5142
1.5077
1.4870
1.4766
1.4572
1.2573
0.0000
14
13
12
11
10
9
8
7
6
5
4
3
2
1
O
O
O
N
4
5.4505
1.0231
2.1389
3.0000
1.0256
2.1703
2.0259
3.1254
6
4
2
0
[ppm]

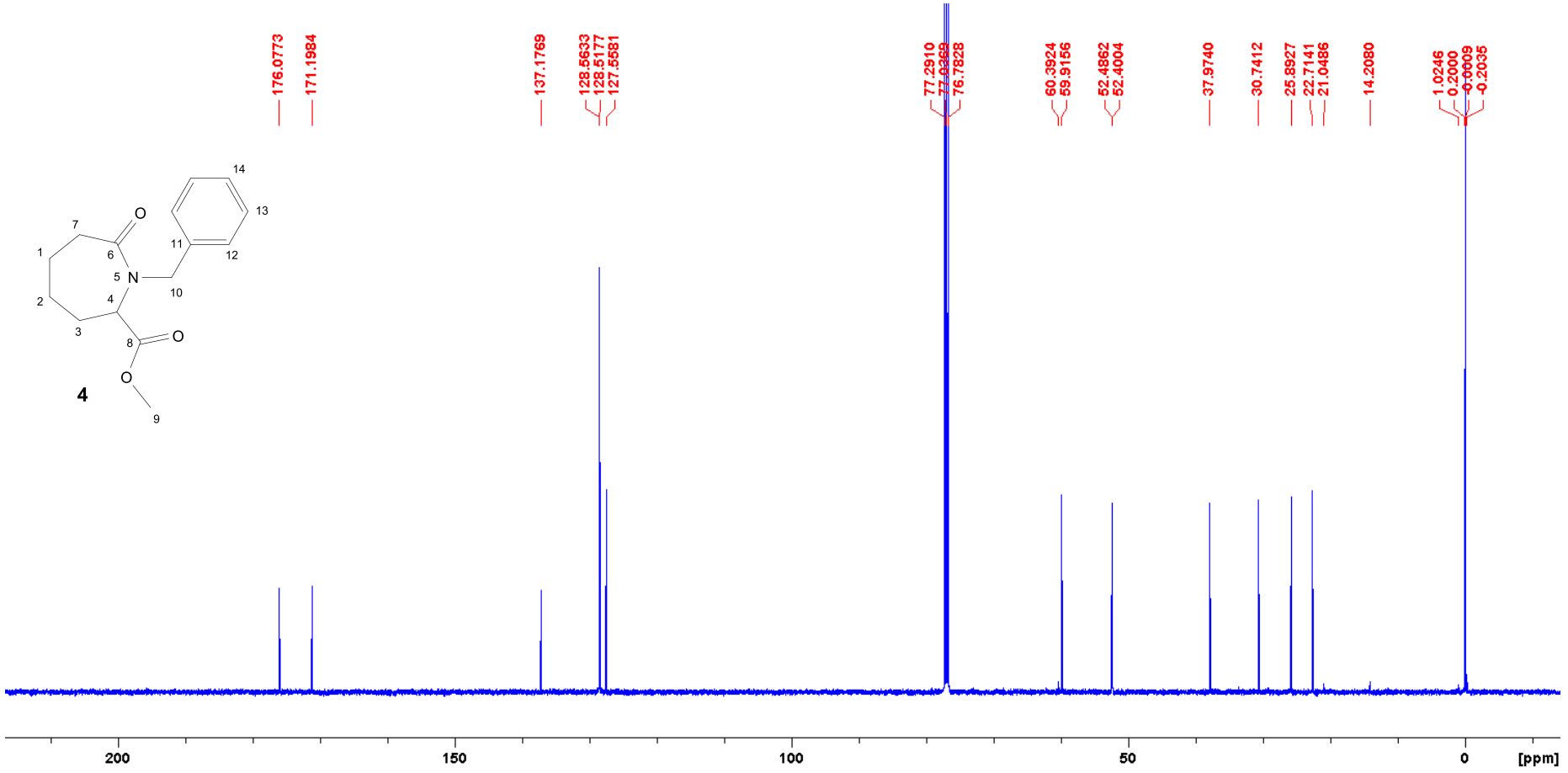
176.0773
171.1984
137.1769
128.5633
128.5177
127.5581
77.2910
77.0369
76.7828
60.3924
59.9156
52.4862
52.4004
37.9740
30.7412
25.8927
22.7141
21.0486
14.2080
1.0246
0.2000
0.0000
-0.0009
-0.2035
4
200
150
100
50
0
[ppm]

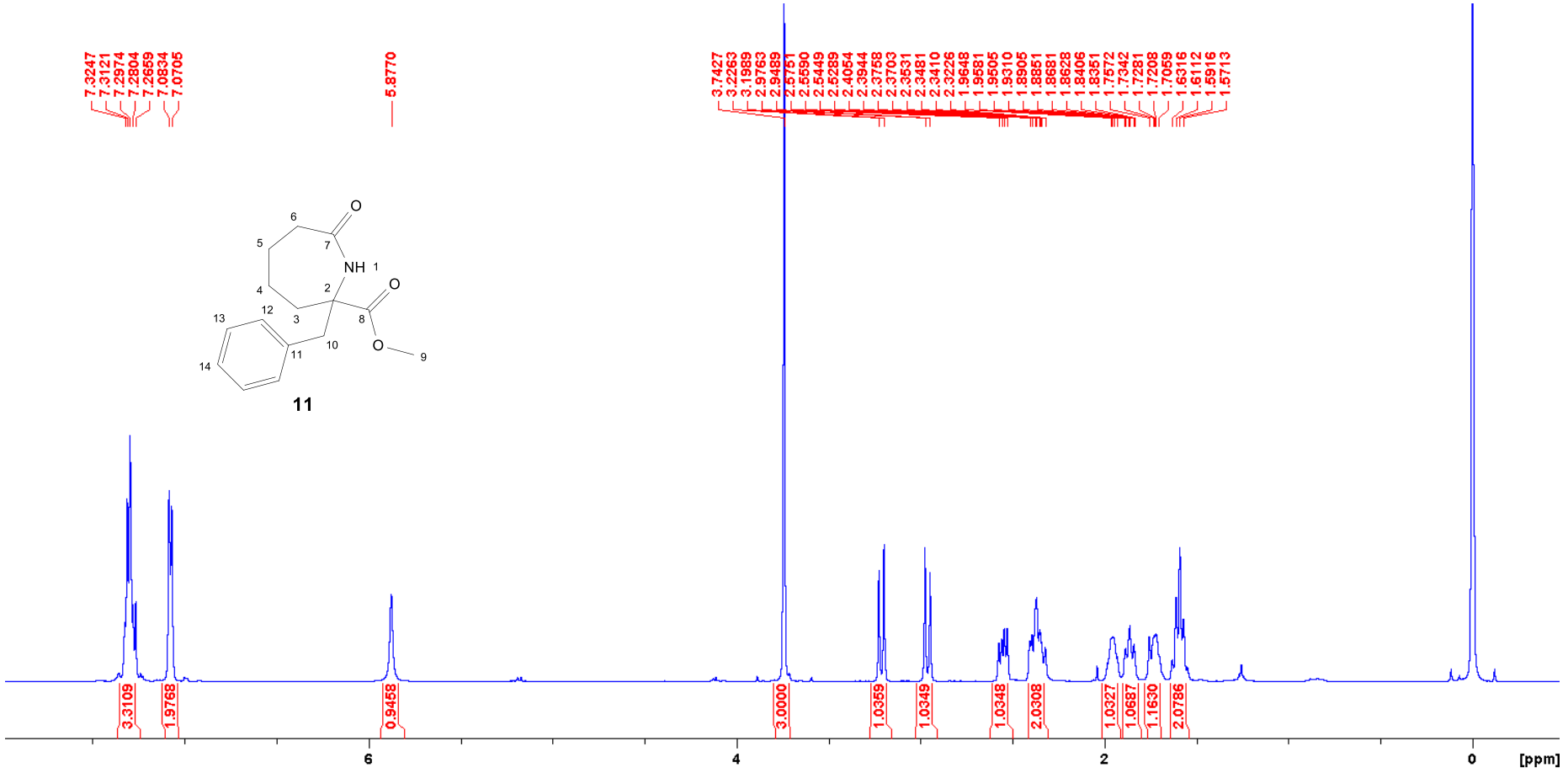
7.3247
7.3121
7.2974
7.2804
7.2659
7.0834
7.0705
5.8770
3.7427
3.2263
3.1989
2.9763
2.9489
2.5751
2.5590
2.5449
2.5289
2.4054
2.3944
2.3758
2.3703
2.3531
2.3481
2.3410
2.3226
1.9648
1.9581
1.9505
1.9310
1.8905
1.8851
1.8681
1.8628
1.8406
1.8351
1.7572
1.7342
1.7281
1.7208
1.7059
1.6316
1.6112
1.5916
1.5713
O
NH
O
O
1
2
3
4
5
6
7
8
9
10
11
12
13
14
11
3.3109
1.9768
0.9458
3.0000
1.0359
1.0349
1.0348
2.0308
1.0327
1.0687
1.1630
2.0786
6
4
2
0
[ppm]

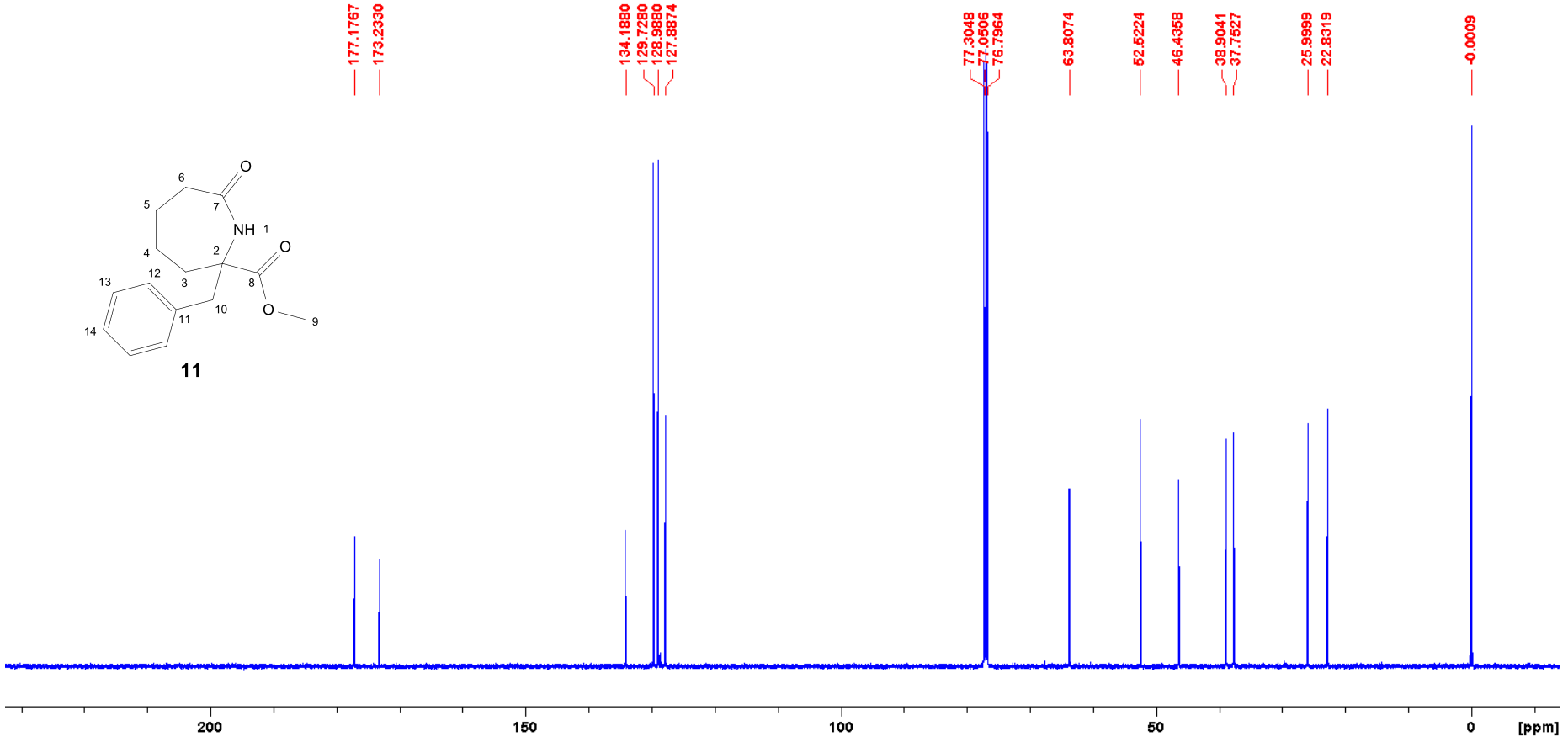
177.1767
173.2330
134.1880
129.7280
128.9880
127.8874
77.3048
77.0506
76.7964
63.8074
52.5224
46.4358
38.9041
37.7527
25.9999
22.8319
-0.0009
O
6
5
7
NH 1
4
2
O
12
3
8
13
10
O
11
9
14
200
150
100
50
0
[ppm]

11

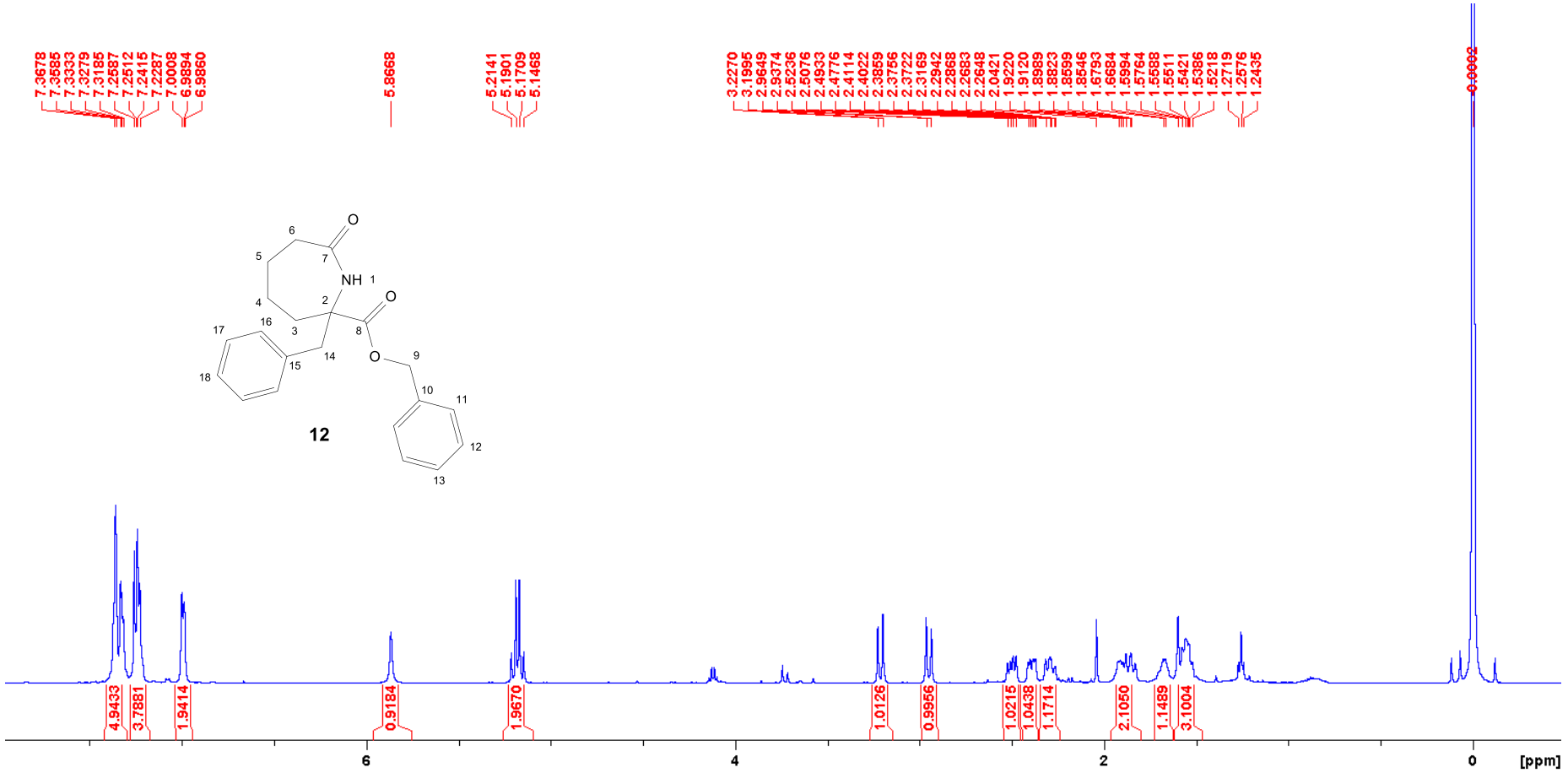
7.3678
7.3585
7.3333
7.3279
7.3185
7.2587
7.2512
7.2415
7.2287
7.0008
6.9894
6.9860
5.8668
5.2141
5.1901
5.1709
5.1468
3.2270
3.1995
2.9649
2.9374
2.5236
2.5076
2.4933
2.4776
2.4114
2.4022
2.3859
2.3756
2.3722
2.3169
2.2942
2.2868
2.2683
2.2648
2.0421
1.9220
1.9120
1.8989
1.8823
1.8599
1.8546
1.6793
1.6684
1.5994
1.5764
1.5588
1.5511
1.5421
1.5386
1.5218
1.2719
1.2576
1.2435
0.0000
NH
O
O
O
12
4.9433
3.7881
1.9414
0.9184
1.9670
1.0126
0.9956
1.0215
1.0438
1.1714
2.1050
1.1489
3.1004
6
4
2
0
[ppm]

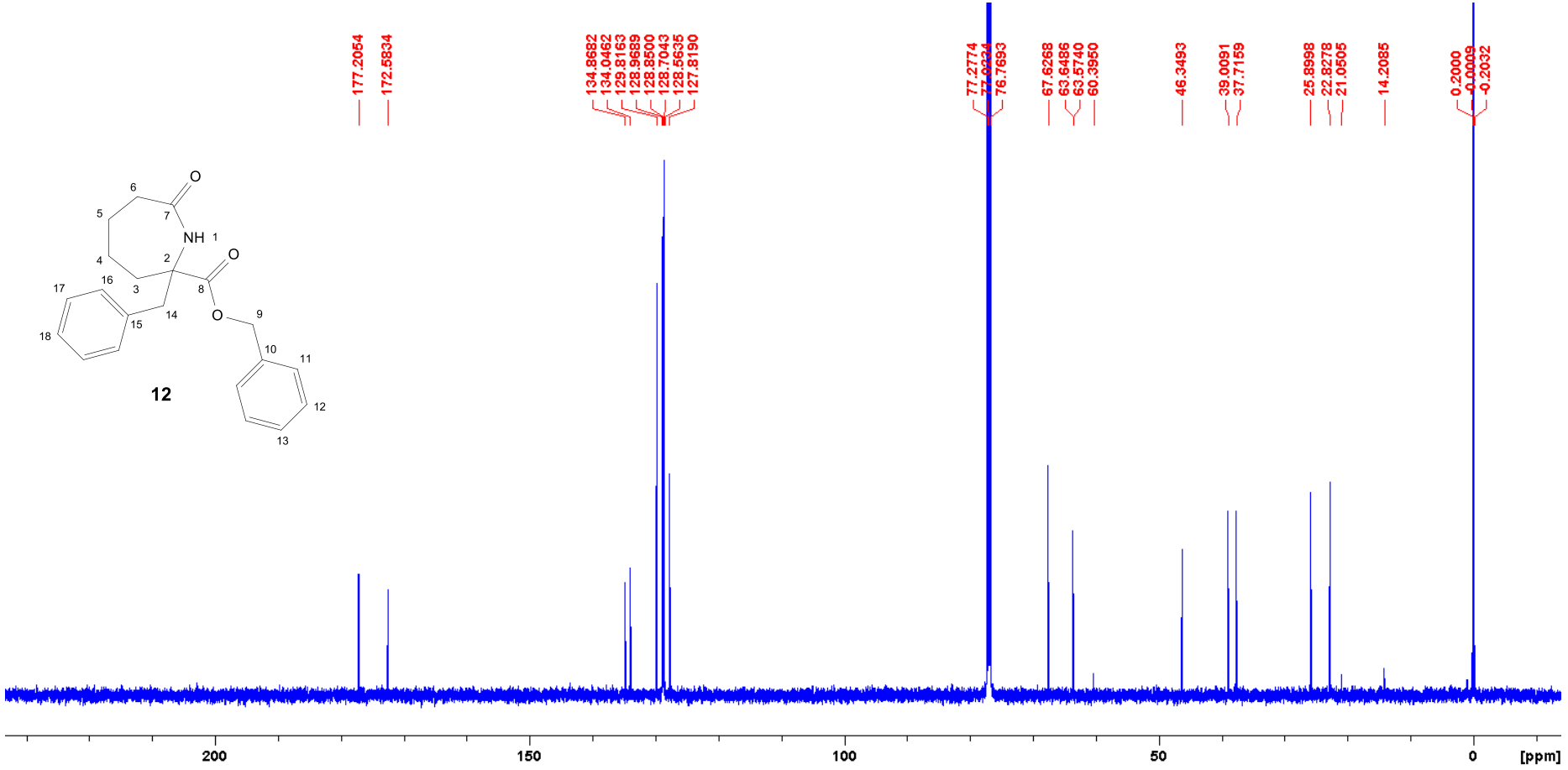
177.2054
172.5834
134.8682
134.0462
129.8163
128.9689
128.8500
128.7043
128.5635
127.8190
77.2774
77.0224
76.7693
67.6268
63.6486
63.5740
60.3950
46.3493
39.0091
37.7159
25.8998
22.8278
21.0505
14.2085
0.2000
-0.0009
-0.2032
200
150
100
50
0
[ppm]
12

Synthesis of pyroglutamate ester *via* alcohol/thionyl chloride

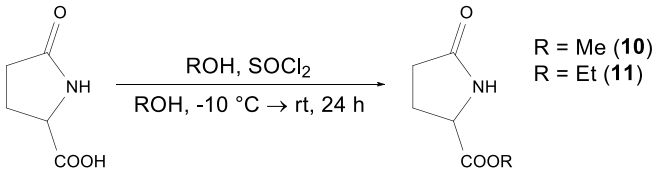

A three-necked round bottom flask, equipped with a drying tube, a thermometer and a septum is charged with 50 ml of the respective alcohol. The solvent is cooled with an ice-NaCl mixture below -10 °C, before 2.81 ml (4.61 g, 0.039 mmol) of thionyl chloride are added dropwise so that the temperature does not exceed -5 °C. The mixture is stirred for 10 min before 2.00 g (0.016 mol) of pyroglutamic acid are added quickly. The mixture is allowed to warm to room temperature and stirred for 24 h. The solvent is removed *in vacuo*, the residue is treated with aqueous, saturated $NaHCO_3$-sol. until no more gas develops and the pH is above 7. 20 ml of water are added and the mixture is extracted with 20 ml ethyl acetate five times. The combined organic phases are dried over $MgSO_4$, the drying agent is filtered off and the solvent is removed *in vacuo*.

Synthesis of pyroglutamate esters *via* Steglich Esterification

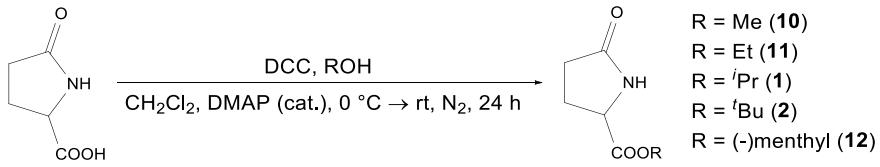

A three-necked round bottom flask, equipped with a thermometer, a tap and a septum is charged with 1.0 g (7.74 mmol) of pyroglutamic acid. 10 ml of dry dichloromethane are added and the 100 mg of DMAP and 3 eq. of the respective alcohol are added under vigorous stirring. The solution is cooled below 0 °C, before 1.6 g (7.75 mmol) of dicyclohexyl carbodiimide is added, the mixture is stirred for 30 min before being allowed to warm to room temperature and stirred for another 24 h. The resulting suspension is filtered, washed with dichloromethane several times, the filtrate's solvent is removed *in vacuo* and the residue resuspended in 15 ml dichloromethane and filtered again. The organic phase is washed with 0.5M aqueous HCl two times, with aqueous, saturated $NaHCO_3$-sol. two times and once more with water. The organic phase is dried over $MgSO_4$, the drying agent is filtered off and the solvent removed *in vacuo*. The residue is purified with column chromatography twice [SiO_2; ethyl acetate:cyclohexane; 1:2 → ethyl acetate] to give the desired products.

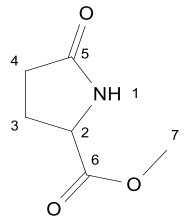

Yield (**10**): 15.2 % R_f: 0.18 (ethyl acetate); ^{1}H-NMR: (500 MHz, $CDCl_3$, δ[ppm]) 6.46 (br s, 1H, *NH*); 4.27 (dd, J_d = 5 Hz, J_{dd} = 9 Hz, 1H, *H2*); 3.78 (s, 3H, *H7*); 2.52-2.31 (m, 4H, *H2*, *H3*); ^{13}C-NMR: (125 MHz, $CDCl_3$, δ[ppm]) 177.9 (*C5*); 172.5 (*C6*); 55.9 (*C2*); 52.6 (*C7*); 29.2 (*C3*); 24.8 (*C4*)

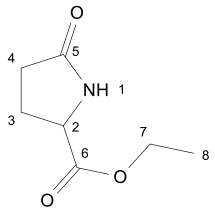

Yield (**11**): 23 % R_f: 0.23 (ethyl acetate); ^{1}H-NMR: (500 MHz, $CDCl_3$, δ[ppm]) 6.63 (br s, 1H, *NH*); 4.26-4.20 (m, 3H, *H2*, *H7*), 2.52-2.31 (m, 4H, *H3*, *H4*); 2.25-2.19 (m, 1H, *H3'*); 1.20 (t, ^3J = 7 Hz, 3H, *H8*); ^{13}C-NMR: (125 MHz, $CDCl_3$, δ[ppm]) 1780.0 (*C5*); 172.1 (*C6*); 61.7 (*C7*); 55.5 (*C2*); 29.3 (*C3*); 24.8 (*C4*); 14.1 (*C8*)

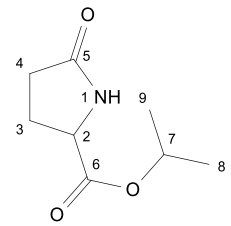

Yield (**1**): 68 % R_f: 0.31 (ethyl acetate); m.p.: 86 °C; ^{1}H-NMR: (500 MHz, $CDCl_3$, δ[ppm]) 6.60 (br s, 1H, *NH*); 5.07 (sep., 1H, *H7*); 4.21 (dd, J_d = 5 Hz, J_{dd} = 8 Hz, 1H, *H2*); 2.51-2.30 (m, 3H *H3*, *H4*); 2.23-2.16 (m, 1H, *H3'*); 1.27 (d, ^3J = 6 Hz, 6H, *H8*, *H9*); ^{13}C-NMR: (125 MHz, $CDCl_3$, δ[ppm]) 178.0 (*C5*); 171.6 (*C6*); 69.3 (*C7*); 55.6 (*C2*); 29.3 (*C3*); 24.8 (*C4*); 21.7 (*C8*, *C9*)

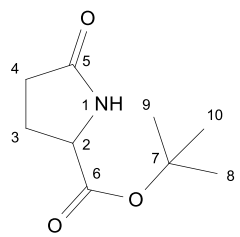

Yield (**1**): 8 % R_f: 0.26 (ethyl acetate); m.p.: 97 °C; Lit: 93 °C[124]; ^{1}H-NMR: (500 MHz, $CDCl_3$, δ[ppm]) 6.15 (br s, 1H, *NH*); 4.11 (dd, J_d = 8 Hz, J_{dd} = 6 Hz, 1H, *H2*); 2.45-2.27 (m, 3H, *H4*, *H3*); 2.21-2.14 (m, 1H, *H3'*); 1.48 (s, 9H, *H8*, *H9*, *H10*); ^{13}C-NMR: (125 MHz, $CDCl_3$, δ[ppm]) 177.7 (*C5*); 171.1 (*C6*); 82.4 (*C7*); 56.1 (*C2*); 29.3 (*C3*); 28.0 (*C8*, *C9*, *C10*); 24.9 (*C4*)

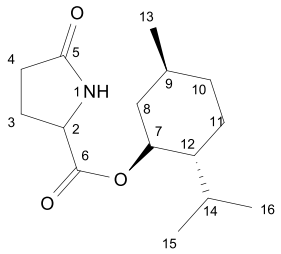

Yield (**12**): 71 % R_f: 0.41 (ethyl acetate); m.p.: 124 °C (decomp.); ^{1}H-NMR: (500 MHz, $CDCl_3$, δ[ppm]) 6.12 (br s, 1H, *NH*); 4.75 (m, 1H, *H7*); 4.24-4.21 (m, 1H, *H2*); 2.53-2.45 (m, 1H, *H4*); 2.41-2.33 (m, 2H, *H3*); 2.24-2.17 (m, 1H, *H4*); 2.00-1.96 (m, 1H, *H8*); 1.84-1.79 (m, 1H, *H14*); 1.73-1.69 (m, 3H, *H10*, *H11*); 1.51-1.47 (m, 1H, *H9*); 1.45-1.39 (m, 1H, *H12*); 1.10-1.05 (m, 1H, *H10'*); 1.03-0.96 (m, 1H, *H8'*); 0.92-0.89 (m, 7H, *H11*, *H13*, *H15*, *H16*); 0.77-075 (m, 3H, *H15'*, *H16*'); ^{13}C-NMR: (125 MHz, $CDCl_3$, δ[ppm]) 177.6 (*C5*); 171.5 (*C6*); 75.8 (*C7*); 55.6 (*C2*); 46.9 (*C12*); 40.7 (*C8*); 34.1 (*C11*); 31.1 (*C9*); 29.3 (*C3*); 26.4 (*C14*); 25.0 (*C4*); 23.4 (*C10*); 22.0 (*C13*); 20.8, 16.3 (*C15*, *C16*)

General Procedure for cyclic β-keto esters from cycloketones

A three-necked flask, equipped with a reflux condenser and a stopper and a dropping funnel is charged with 3 eq of NaH (60%-suspension in mineral oil) under a nitrogen atmosphere. 200 ml of dry toluene are added, the slurry is stirred vigorously and 2 eq. of dialkyl carbonate are added. The mixture is gently refluxed before 5.0 g (1 eq.) of the respective cycloketone, dissolved in 100 ml of dry toluene are added dropwise so that the reaction mixture does not overheat. The mixture is stirred for 4 h, before being allowed to cool to room temperature. 0.5 M aqueous HCl is added dropwise under ice cooling until no more gas develops and the pH is below 7. 200 ml of water are added and the aqueous phase is extracted with 50 ml toluene five times. The combined organic phases are dried over $MgSO_4$, the drying agent is filtered off and the solvent is removed *in vacuo*. The residue is purified using column chromatography [SiO_2; ethyl acetate:cyclohexane; 1:20 → 1:10] to give the desired products as colorless oils.

General Procedure for Schmidt reaction for lactams

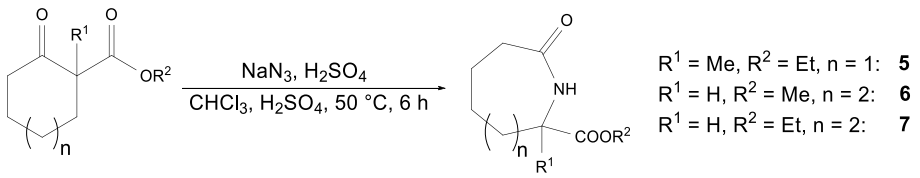

A two-necked flask, equipped with a reflux condenser and a stopper, is charged 1 eq (not more than 0.5 g) of the respective ketone and 30 ml of $CHCl_3$ and 15 ml of conc. H_2SO_4 are added. 1.2 eq of NaN_3 are added slowly, so that the formation of foam does not cover the surface of the solvent. The mixture is gently stirred and warmed to 50 °C for 6 h. The mixture is allowed to cool to room temperature and is poured onto 200 g of crushed ice and aqueous, concentrated NH_3-sol. is added dropwise until the aqueous phase is adjusted to pH above 7. The layers are separated, and the aqueous layer is extracted with 50 ml chloroform three times. The combined organic phases are dried over $MgSO_4$, the drying agent is filtered off and the solvent is removed *in vacuo*. The residue is purified with column chromatography [SiO_2: ethyl acetate] to give the desired lactams.

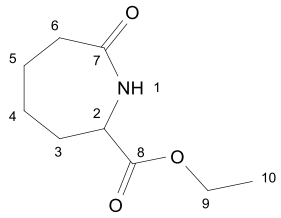

Yield (**17**): 44 % R_f: 0.21 (ethyl acetate); m.p.: 73-74 °C; ^{1}H-NMR: (500 MHz, $CDCl_3$, δ[ppm]) 6.45 (br s, 1H, *NH*); 4.25 (q, ^3J = 7 Hz, 2H, *H9*); 4.02 (ddd, J_d = 1 Hz, J_{dd} = 5 Hz, J_{ddd} = 10 Hz, 1H, *H2*); 2.55-2.49 (m, 1H, *H3*); 2.27-2.22 (m, 1H, *H6*); 2.10-2.04 (m, 1H, *H3'*); 1.92-1.86 (m, 1H, *H4*); 1.71-1.55 (m, 3H, *H4', H5*); 1.30 (td, J_d = 1 Hz, J_{td} = 10 Hz, 3H, *H10*); ^{13}C-NMR: (125 MHz, $CDCl_3$, δ[ppm]) 176.1 (*C7*); 171.4 (*C8*); 62.3 (*C9*); 56.0 (*C2*); 37.1 (*C6*); 33.9 (*C3*); 29.7 (*C4*); 22.9 (*C5*)

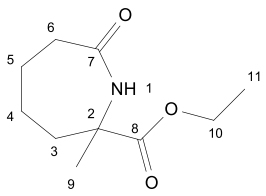

Yield (**5**): 74 % R_f: 0.28 (ethyl acetate); m.p.: 96 °C; ^{1}H-NMR: (500 MHz, $CDCl_3$, δ[ppm]) 6.13 (br s, 1H, *NH*); 4.25 (q, ^3J = 7 Hz, 2H, *H9*); 2.55-2.50 (m, 1H, *H3*); 2.37-2.26 (m, 2H, *H6*, *H3*); 1.92-1.87 (m, 1H, *H4*); 1.76-1.68 (m, 2H, *H5*, *H6'*); 1.61-1.54 (m, 2H, *H4'*, *H5'*); 1.49 (s, 3H, *H11*); 1.31 (t, ^3J = 7 Hz, 2H, *H10*); ^{13}C-NMR: (125 MHz, $CDCl_3$, δ[ppm]) 177.6 (*C2*); 173.8 (*C8*); 61.8 (*C9*); 59.7 (*C7*); 39.1 (*C6*); 37.6 (*C3*); 28.3 (*C11*); 26.4 (*C5*); 22.9 (*C4*); 14.2 (*C10*); IR (ATR) ν = 3198, 3087, 2974, 2936, 2859, 1730, 1661, 1579, 1456, 1411, 1382, 1360, 1343, 1311, 1290, 1261, 1215, 1174, 1152, 1121, 1093, 1057, 1038, 1006, 954, 889, 879, 837, 803, 769, 757, 735, 718, 693, 656, 620, 576, 547, 510, 462; HRMS: calculated: 200.1286 $[M+H]^+$ found: 200.1264

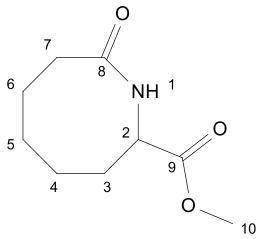

Yield (**6**): 35 % R_f: 0.37 (ethyl acetate); m.p.: 89 °C; Lit: 80-82 °C[125]; ^{1}H-NMR: (500 MHz, $CDCl_3$, δ[ppm]) 6.05 (br d, 1H, *NH*); 4.31-4.26 (m, 1H, *H8*); 3.79 (s, 3H, *H10*); 2.44-2.35 (m, 2H, *H3*); 2.05-1.99 (m, 1H, *H7*); 1.92-1.72 (m, 4H, *H4*, *H5*, *H6*); 1.57-1.42 (m, 2H, *H5', H6'*); ^{13}C-NMR: (125 MHz, $CDCl_3$, δ[ppm]) 175.3 (*C2*); 172.1 (*C9*); 54.9 (*C10*); 52.7 (*C8*); 36.2 (*C3*); 33.6 (*C7*); 27.9 (*C4*); 25.8 (*C5*); 24.2 (*C6*); IR (ATR) ν = 3365, 2922, 2856, 1732, 1650, 1488, 1429, 1397, 1362, 1334, 1309, 1256, 1216, 1158, 1030, 981, 951, 911, 887, 873, 822, 791, 765, 747, 720, 677, 638, 570, 516; HRMS: calculated: 186.1130 $[M+H]^+$ found: 186.1110

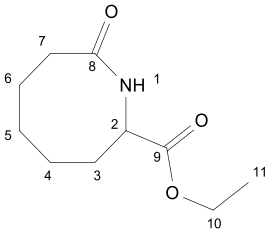

Yield (**7**): 54% R_f: 0.23 (ethyl acetate); m.p.: 91 °C; ^{1}H-NMR: (500 MHz, $CDCl_3$, δ[ppm]) 6.02 (br d, 1H, *NH*); 4.28-4.22 (m, 3H, *H1*, *H9*); 2.4-2.38 (m, 2H, *H6*); 2.02-2.00 (m, 1H, *H2*); 1.88-1.75 (m, 4H, *H3*, *H4*, *H5*); 1.64-1.47 (m, 3H, *H2', H3', H4'*); 1.30 (t, ^3J = 7 Hz, 3H, *H10*); ^{13}C-NMR: (125 MHz, $CDCl_3$, δ[ppm]) 175.3 (*C7*); 171.6 (*C8*); 61.9 (*C9*); 55.0 (*C1*); 36.3 (*C6*); 33.6 (*C2*); 27.9 (*C5*); 25.8 (*C3*); 14.1 (*C10*); IR (ATR) ν = 3311, 2937, 2867, 1730, 1614, 1467, 1447, 1362, 1350, 1322, 1289, 1260, 1242, 1221, 1184, 1160, 1095, 1061, 1017, 947, 915, 800, 770, 753, 713, 654, 572, 513, 502; HRMS: calculated: 200.1281 $[M+H]^+$ found: 200.1281

Synthesis of 1-*tert*-butyl-2-ethyl-8-oxoazocane-1,2-dicarboxylate (8)

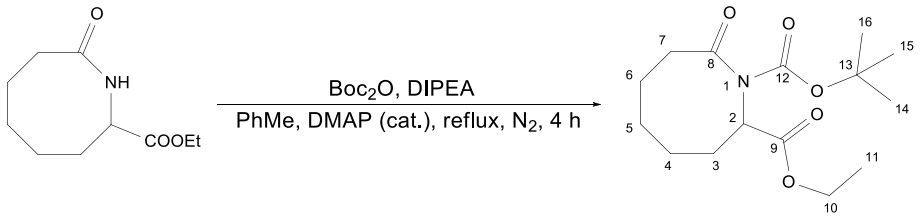

A three-necked round bottom flask, equipped with a reflux condenser, a tap and a septum is charged with 0.5 g (2.5 mmol) of enatholactam **7** under a nitrogen atmosphere. 50 ml of dry toluene are added,

followed by 200 mg DMAP, 1.64 g (7.5 mmol) Boc_2O and 0.61 ml (3.5 mmol) DIPEA and the mixture is gently refluxed for 4 h. The reaction mixture is allowed to cool to room temperature and 15 ml of water are added, the biphasic mixture is stirred for another 90 min. 100 ml of water are added and the aqueous layer is extracted with 50 ml toluene three times. The combined organic layers are dried over $MgSO_4$, the drying agent is filtered off and the solvent is removed *in vacuo*. The residue is purified with column chromatography [SiO_2; ethyl acetate:cyclohexane; 1:4] to give the desired lactam as a viscous oil that crystallised after several days. Yield (**8**): 83% (0.62 g) R_f: 0.16 (ethyl acetate); m.p.: 98 °C; ^{1}H-NMR: (500 MHz, $CDCl_3$, δ[ppm]) 4.58 (dd, J_d = 5 Hz, J_{dd} = 12 Hz, 1H, *H1*); 4.21 (qq, ^2J_d = 7 Hz, $^3J_{dd}$ = 21 Hz, 2H, *H9*); 2.79-2.73 (m, 1H, *H6*); 2.58-2.53 (m, 1H, *H6'*); 2.25-2.18 (m, 1H, *H2*); 2.08-2.00 (m, 1H, *H2'*); 1.96-1.90 (m, 1H, *H5*); 1.83-1.67 (m, 3H, *H3*, *H4*, *H5*); 1.51 (s, 9H, *H13*, *H14*, *H15*); 1.45-1.37 (m, 2H, *H3'*, *H4'*); 1.28 (t, ^3J = 7 Hz, 3H, *H10*); ^{13}C-NMR: (125 MHz, $CDCl_3$, δ[ppm]) 177.0 (*C7*); 170.3 (*C8*); 151.9 (*C11*); 83.4 (*C12*); 61.5 (*C9*); 58.3 (*C1*); 38.1 (*C6*); 30.8 (*C2*); 29.1 (*C5*), 28.0 (*C13*, *C14*, *C15*); 27.1 (*C4*); 24.2 (*C3*); 14.1 (*C10*); IR (ATR) ν = 2980, 2942, 2865, 2334, 1745, 1713, 1699, 1464, 1448, 1394, 1367, 1354, 1331, 1315, 1293, 1279, 1260, 1200, 1149, 1125, 1109, 1083, 1047, 1022, 988, 955, 932, 897, 850, 818, 766, 743, 708, 674, 592, 549, 526, 476; HRMS: calculated: 322.1630 $[M+Na]^+$ found: 322.1623

Synthesis of 2-[[(1,1-Dimethylethoxy)carbonyl]amino]heptanedioic acid (9)

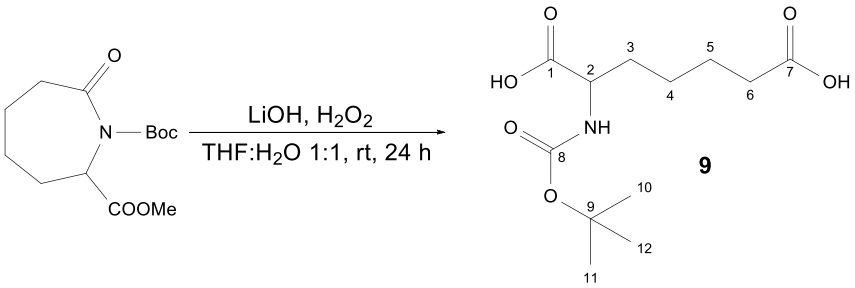

A round bottom flask is charged with 1.02 g (3.57 mmol) of 1-*tert*-butyl-2-methyl-7-oxoazepane-1,2-dicarboxylate (**17**). 25 ml of THF and 25 ml of H_2O are added, followed by 0.34 (14.2 mmol) LiOH monohydrate and 3.5 ml of H_2O_2 (30% in water) and the suspension is stirred for 24 h at room temperature. The pH is adjusted to 3 with 0.5M HCl and the aqueous solution is extracted with 50 ml ethyl acetate three times. The combined organic layers are dried over $MgSO_4$, the drying agent is filtered off and the solvent is removed *in vacuo* to give the hydrolysis product as a white crystalline solid. Yield (**9**): 83% (0.75 g); m.p.: 118 °C (decomp.) ^{1}H-NMR: (500 MHz, $CDCl_3$, δ[ppm]) 4.06 (dd, J_d = 5 Hz, J_{dd} = 9 Hz, 1H, *H2*); 2.30 (t, ^3J = 7 Hz, 2H, *H6*); 1.82-1.79 (m, 1H, *H3*); 1.65-1.62 (m, 3H, *H5*, *H3'*); 1.44-1.43 (m, 11H, *H4*, *H10*); ^{13}C-NMR: (125 MHz, $CDCl_3$, δ[ppm]) 176.0 (*C1*); 174.9 (*C7*); 156.8 (*C8*); 80.0 (*C9*); 53.5 (*C2*); 33.3, 31.2 (*C3*, *C6*); 27.3 (*C10*); 25.1, 24.2 (*C4*, *C5*); IR (ATR) ν = 3324, 2976, 2936, 2859, 1729, 1678, 1645, 1531, 1454, 1395, 1368, 1298, 1280, 1254, 1215, 1106, 1068,

1051, 1014, 886, 852, 819, 784, 762, 743, 684, 626, 579, 535, 459; HRMS: calculated: 276.1442 $[M+H]^+$ found: 276.1424

[124] E. Tascher, C. Wasielewski, J.F. Biernat, *Liebigs Ann.* **1961**, *646*, 119-122.
[125] L. Benati, D. Nanni, C. Sangiorgi, P. Spagnolo *J. Org. Chem.* **1999**, *64*, 7836-7841.

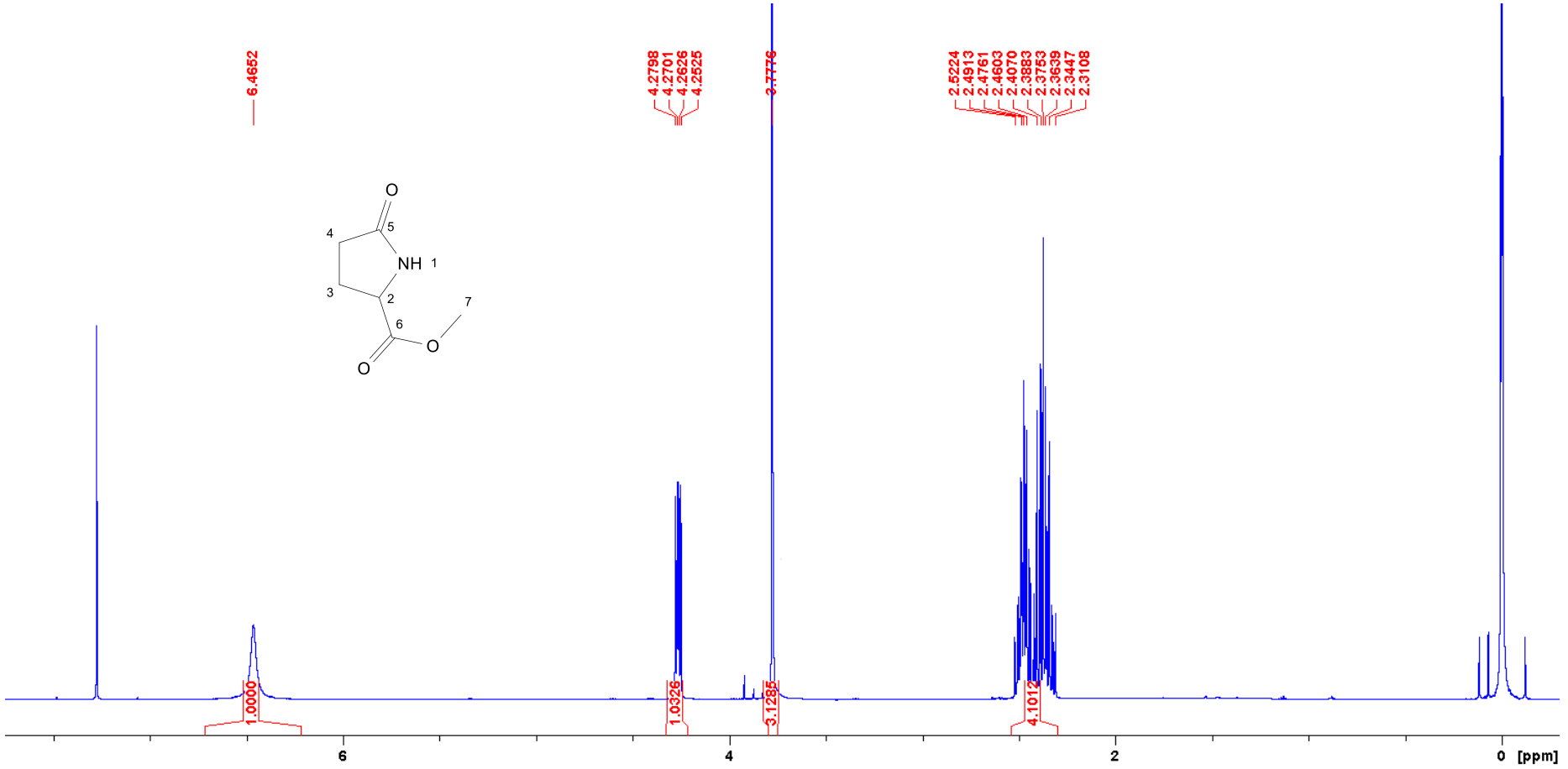
6.4652
4.2798
4.2701
4.2626
4.2525
3.7776
2.5224
2.4913
2.4761
2.4603
2.4070
2.3883
2.3753
2.3639
2.3447
2.3108
O
5
4
NH 1
3
2
7
6
O
O
1.0000
1.0326
3.1285
4.1012
6
4
2
0 [ppm]

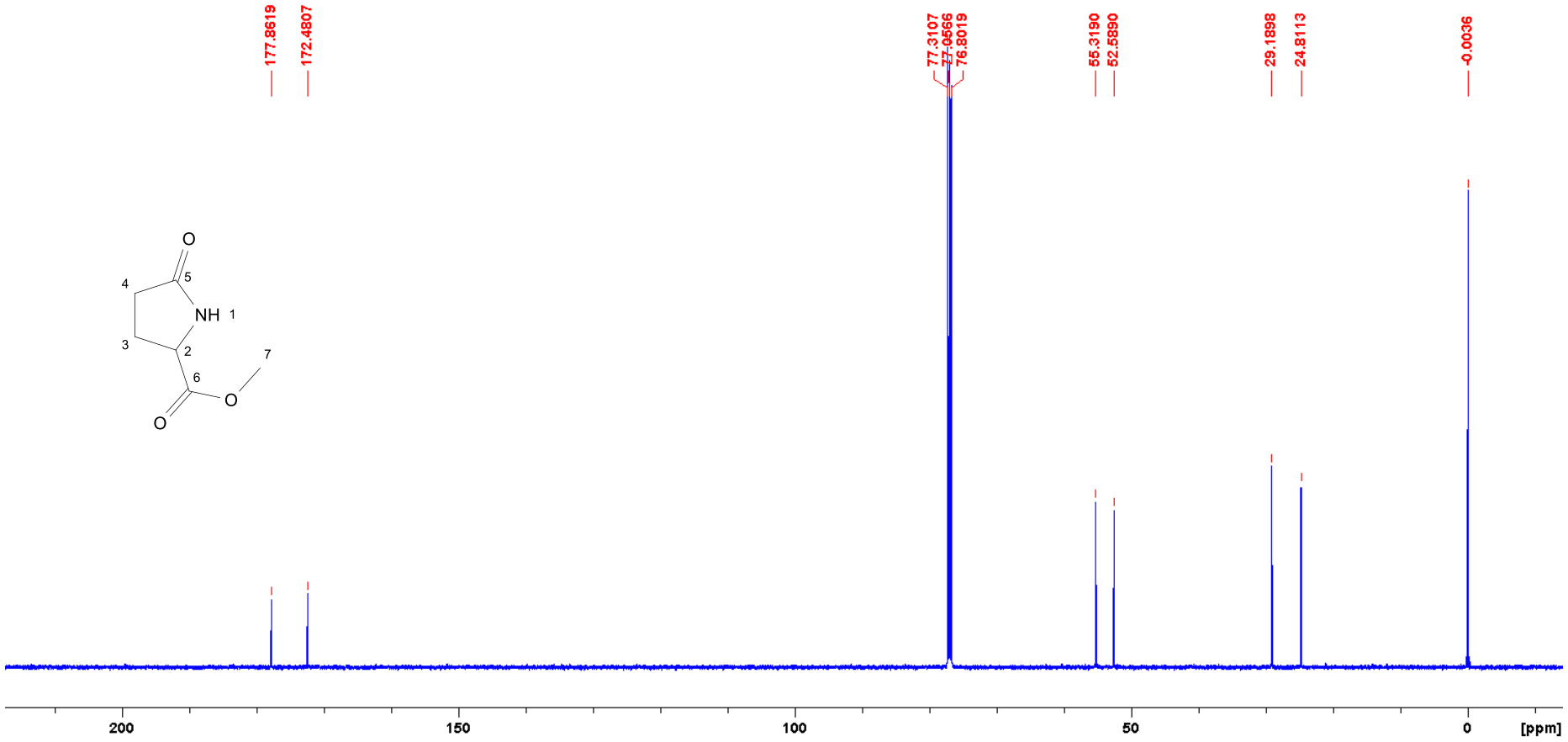
177.8619
172.4807
77.3107
77.0566
76.8019
55.3190
52.5890
29.1898
24.8113
-0.0036
O
5
4
NH 1
3
2
6
7
O
O
200
150
100
50
0
[ppm]

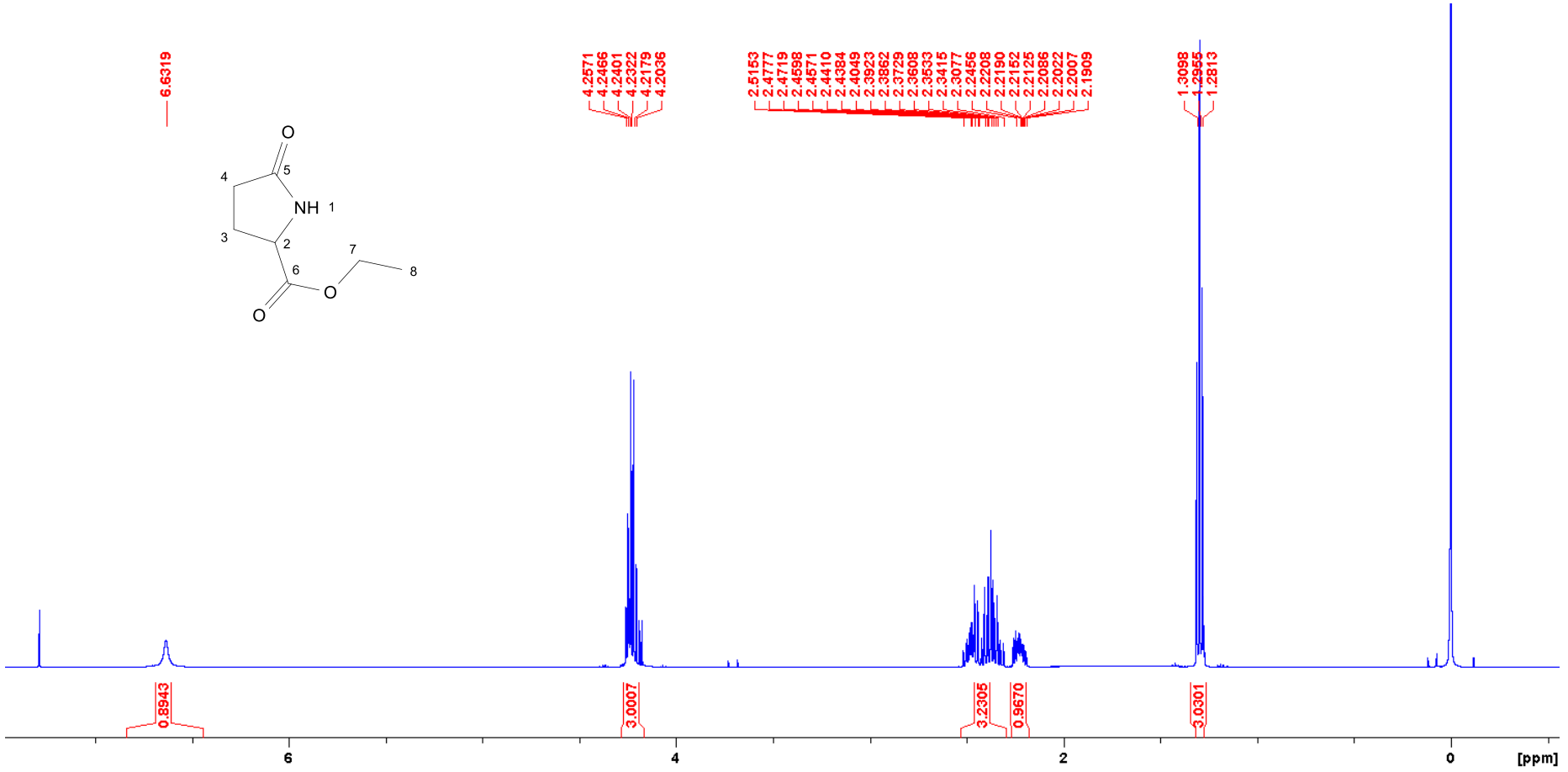
6.6319
4.2571
4.2466
4.2401
4.2322
4.2179
4.2036
2.5153
2.4777
2.4719
2.4598
2.4571
2.4410
2.4384
2.4049
2.3923
2.3862
2.3729
2.3608
2.3533
2.3415
2.3077
2.2456
2.2208
2.2190
2.2152
2.2125
2.2086
2.2022
2.2007
2.1909
1.3098
1.2956
1.2813
O
5
4
NH
1
3
2
7
8
6
O
O
0.8943
3.0007
3.2305
0.9670
3.0301
6
4
2
0
[ppm]

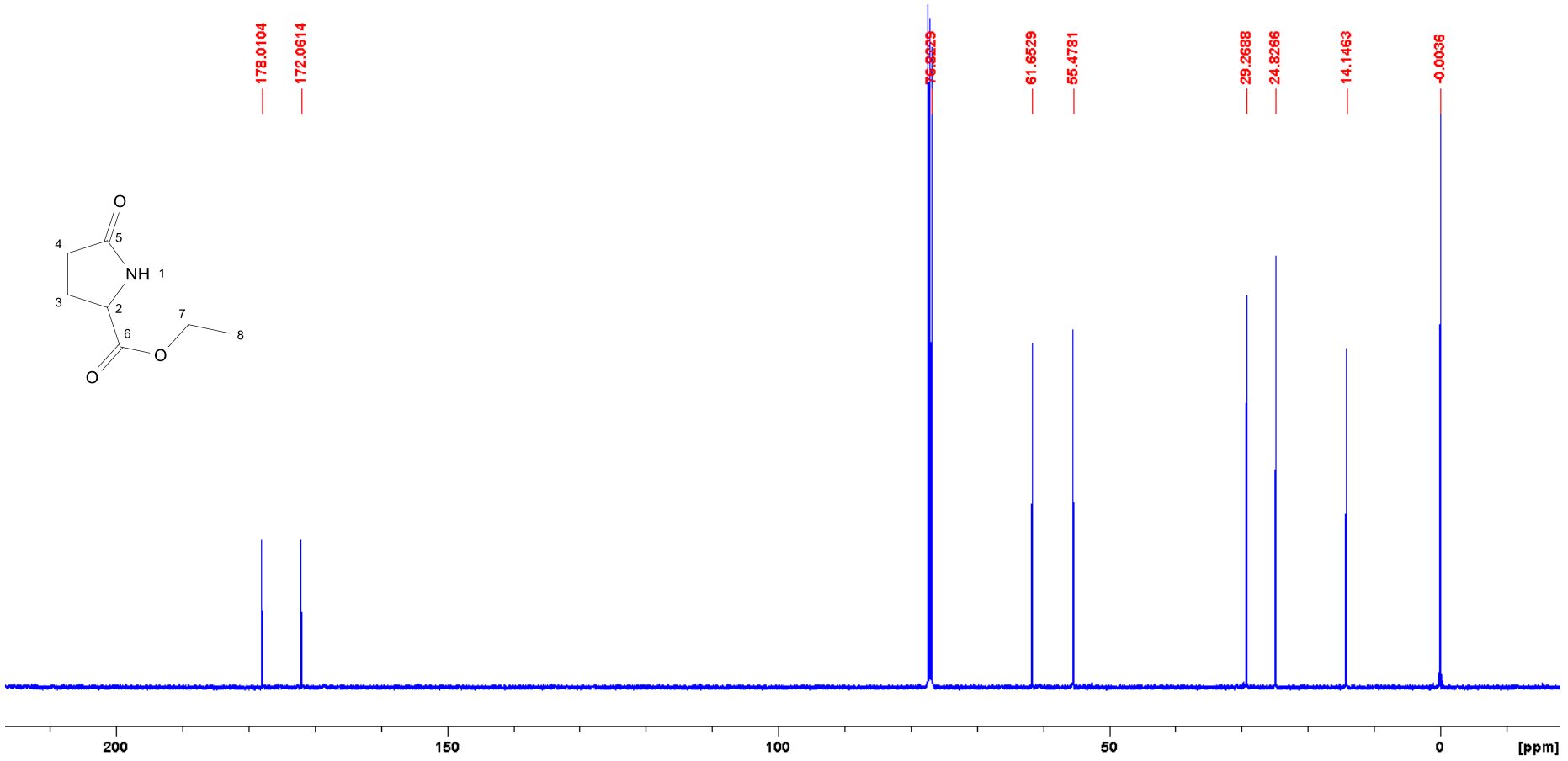
178.0104
172.0614
76.8229
61.6529
55.4781
29.2688
24.8266
14.1463
-0.0036
O
5
4
NH 1
3
2
7
8
6
O
O
200
150
100
50
0
[ppm]

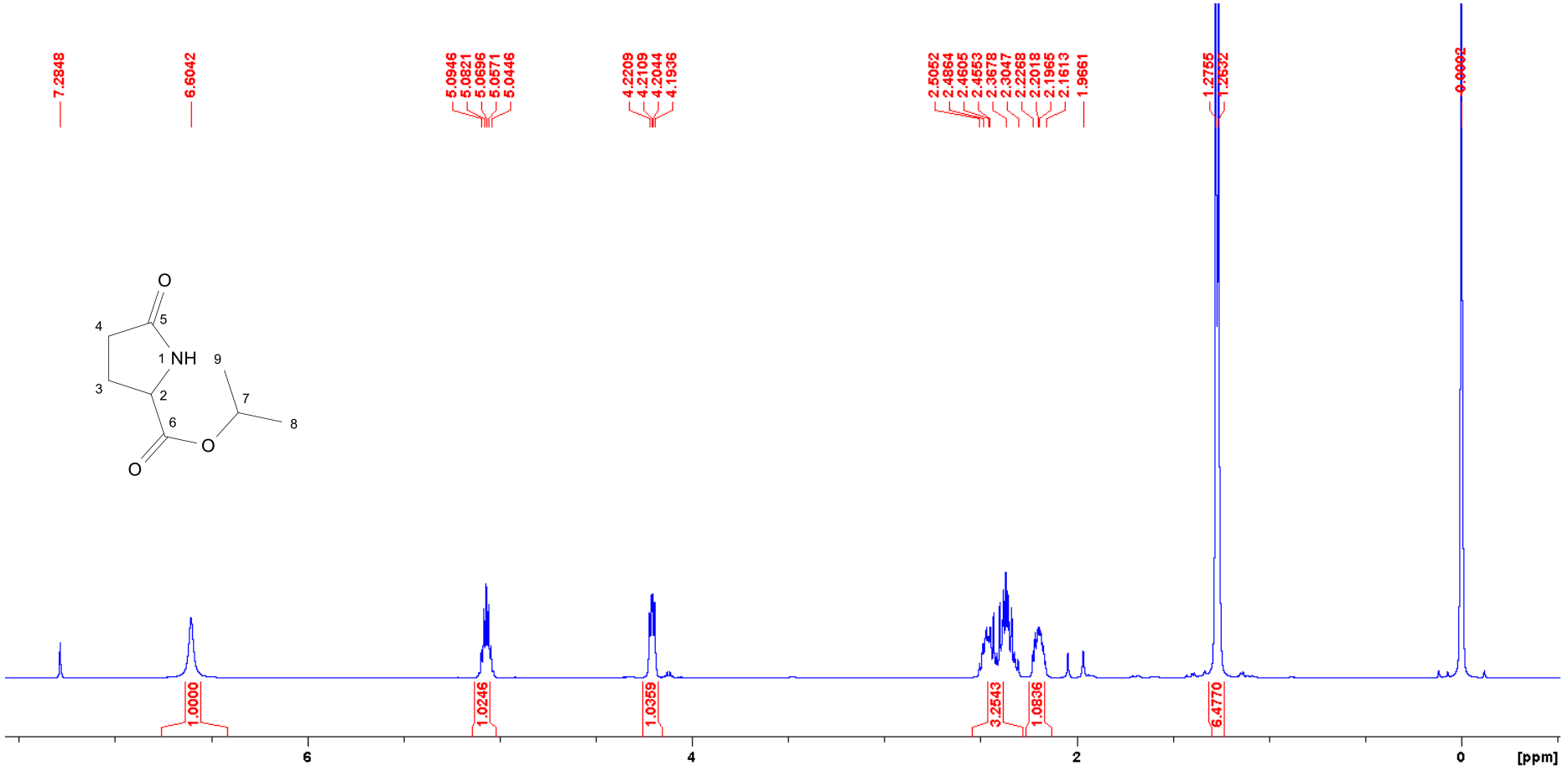
7.2848
6.6042
5.0946
5.0821
5.0696
5.0571
5.0446
4.2209
4.2109
4.2044
4.1936
2.5052
2.4864
2.4605
2.4553
2.3678
2.3047
2.2268
2.2018
2.1965
2.1613
1.9661
1.2755
1.2532
0.0002
O
5
4
1 NH
9
3
2
7
6
8
O
O
1.0000
1.0246
1.0359
3.2543
1.0836
6.4770
6
4
2
0
[ppm]

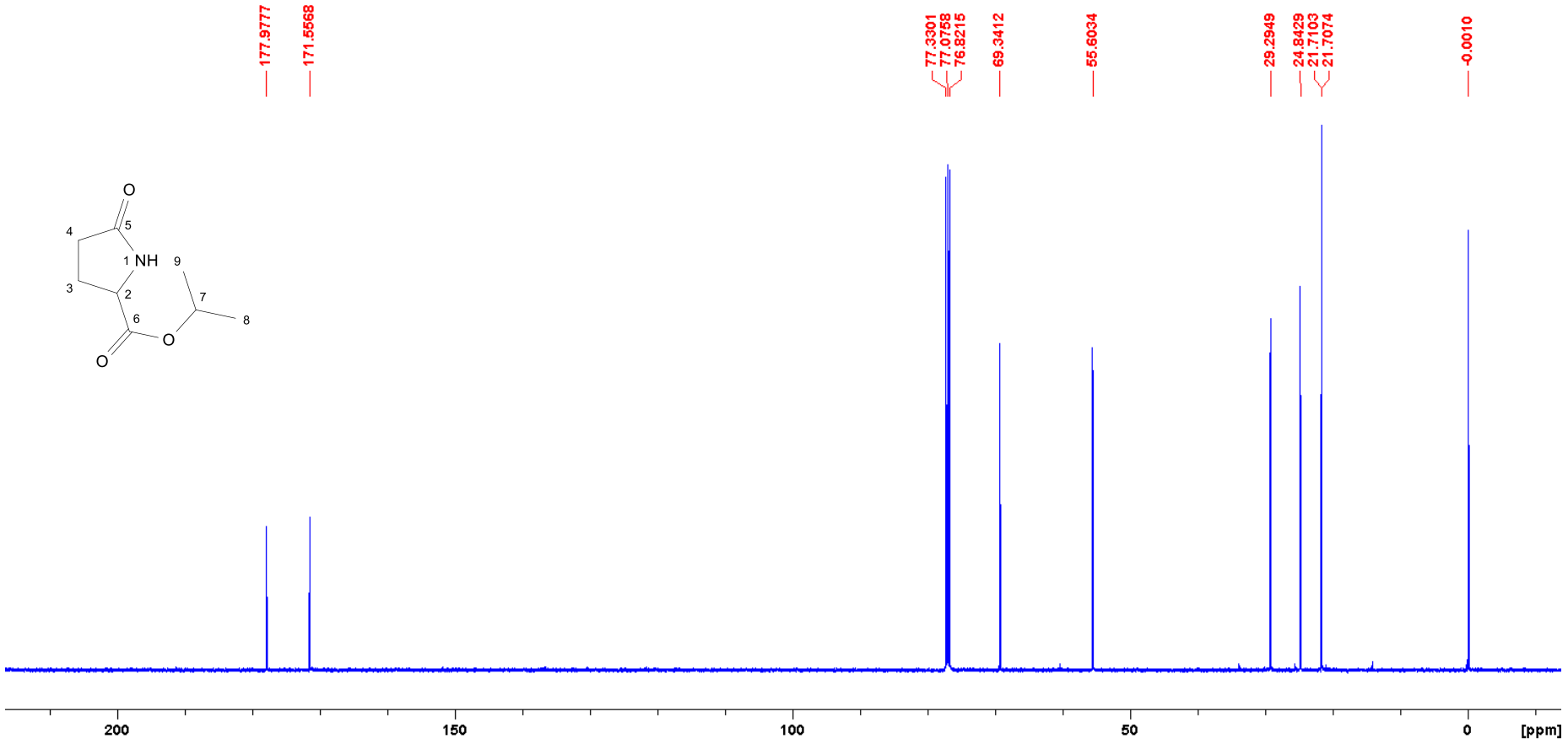
177.9777
171.5568
77.3301
77.0758
76.8215
69.3412
55.6034
29.2949
24.8429
21.7103
21.7074
-0.0010
O
5
4
1 NH
9
3
2
7
8
6
O
O
200
150
100
50
0
[ppm]

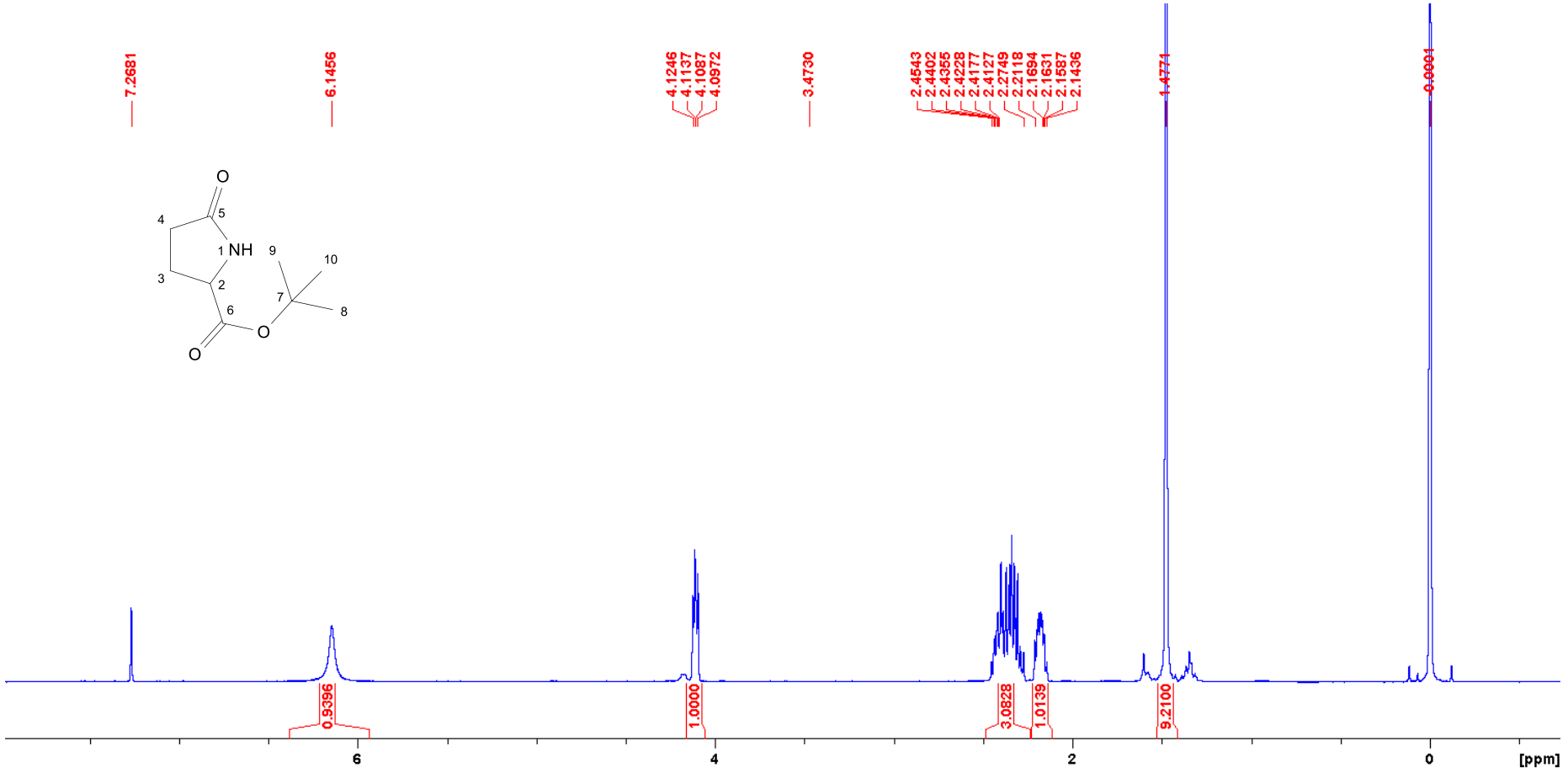
7.2681
6.1456
4.1246
4.1137
4.1087
4.0972
3.4730
2.4543
2.4402
2.4355
2.4228
2.4177
2.4127
2.2749
2.2118
2.1694
2.1631
2.1587
2.1436
1.4771
0.0001
O
5
4
1 NH
9
10
3
2
7
8
6
O
O
0.9396
1.0000
3.0828
1.0139
9.2100
6
4
2
0
[ppm]

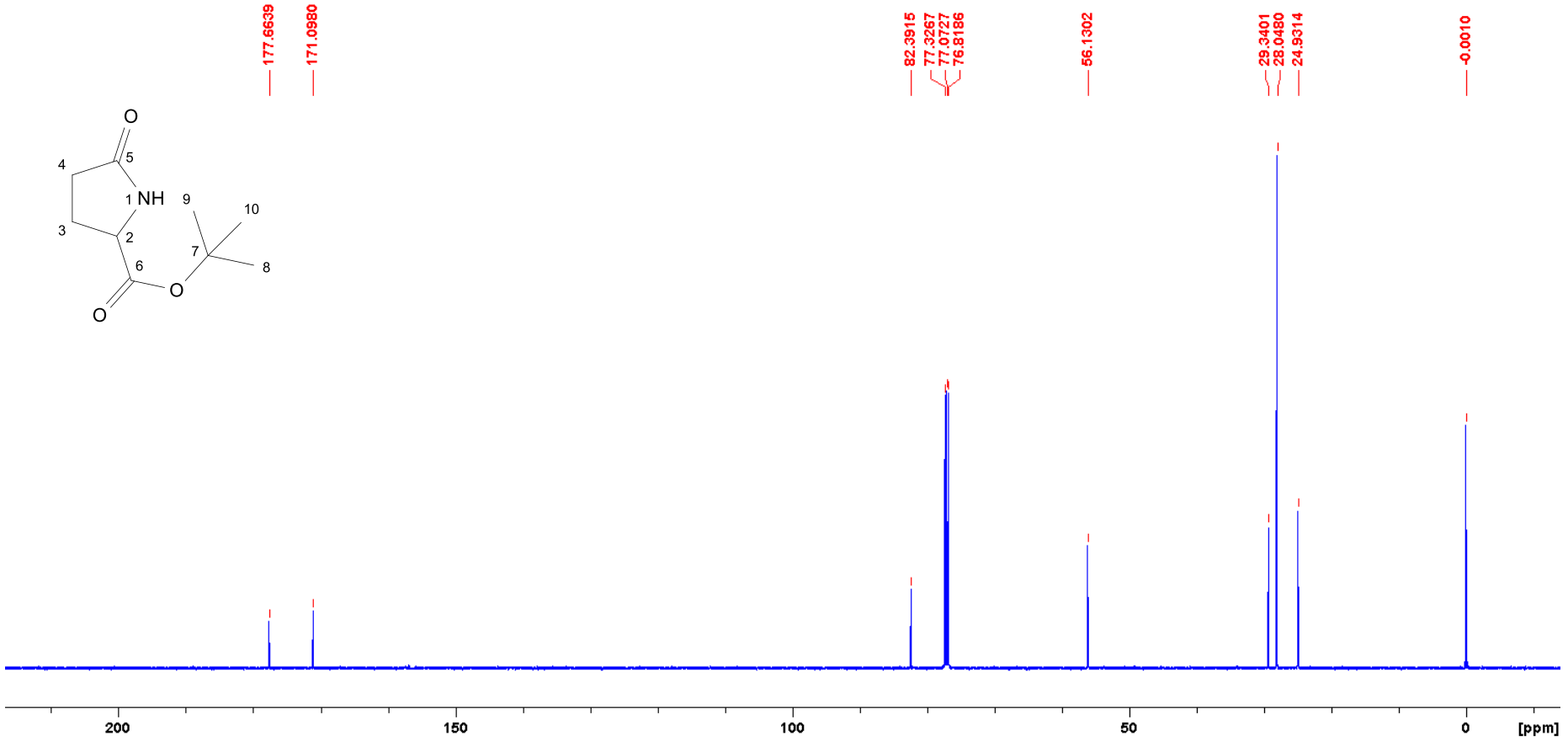
177.6639
171.0980
82.3915
77.3267
77.0727
76.8186
56.1302
29.3401
28.0480
24.9314
0.0010
O
5
4
NH
1
9
10
3
2
7
8
6
O
O
200
150
100
50
0
[ppm]

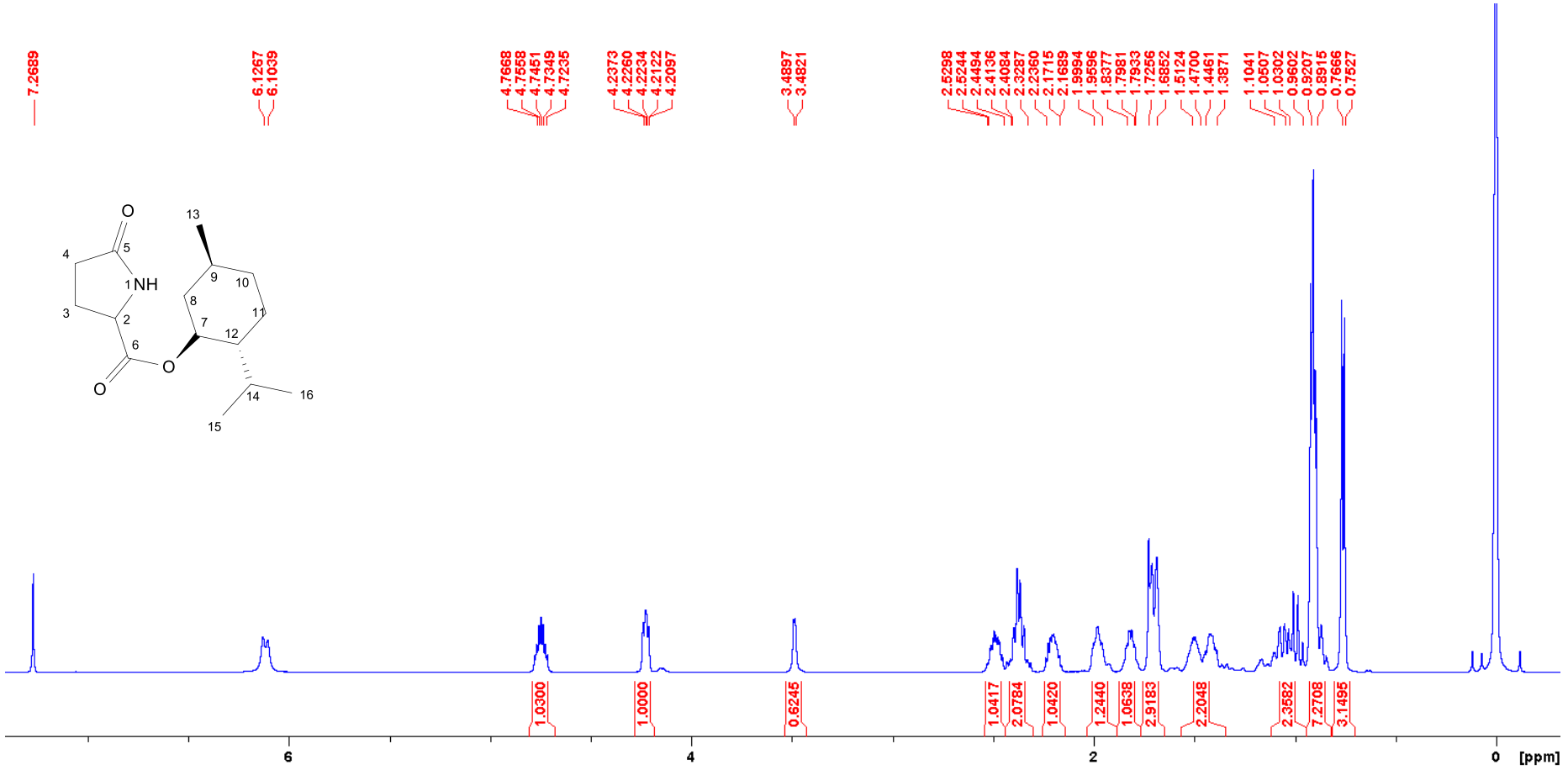
7.2689
6.1267
6.1039
4.7668
4.7558
4.7451
4.7349
4.7235
4.2373
4.2260
4.2234
4.2122
4.2097
3.4897
3.4821
2.5298
2.5244
2.4494
2.4136
2.4084
2.3287
2.2360
2.1715
2.1689
1.9994
1.9596
1.8377
1.7981
1.7933
1.7256
1.6852
1.5124
1.4700
1.4461
1.3871
1.1041
1.0507
1.0302
0.9602
0.9207
0.8915
0.7666
0.7527
O
5
4
NH
1
3
2
6
O
O
13
9
10
8
11
7
12
14
16
15
1.0300
1.0000
0.6245
1.0417
2.0784
1.0420
1.2440
1.0638
2.9183
2.2048
2.3582
7.2708
3.1495
6
4
2
0
[ppm]

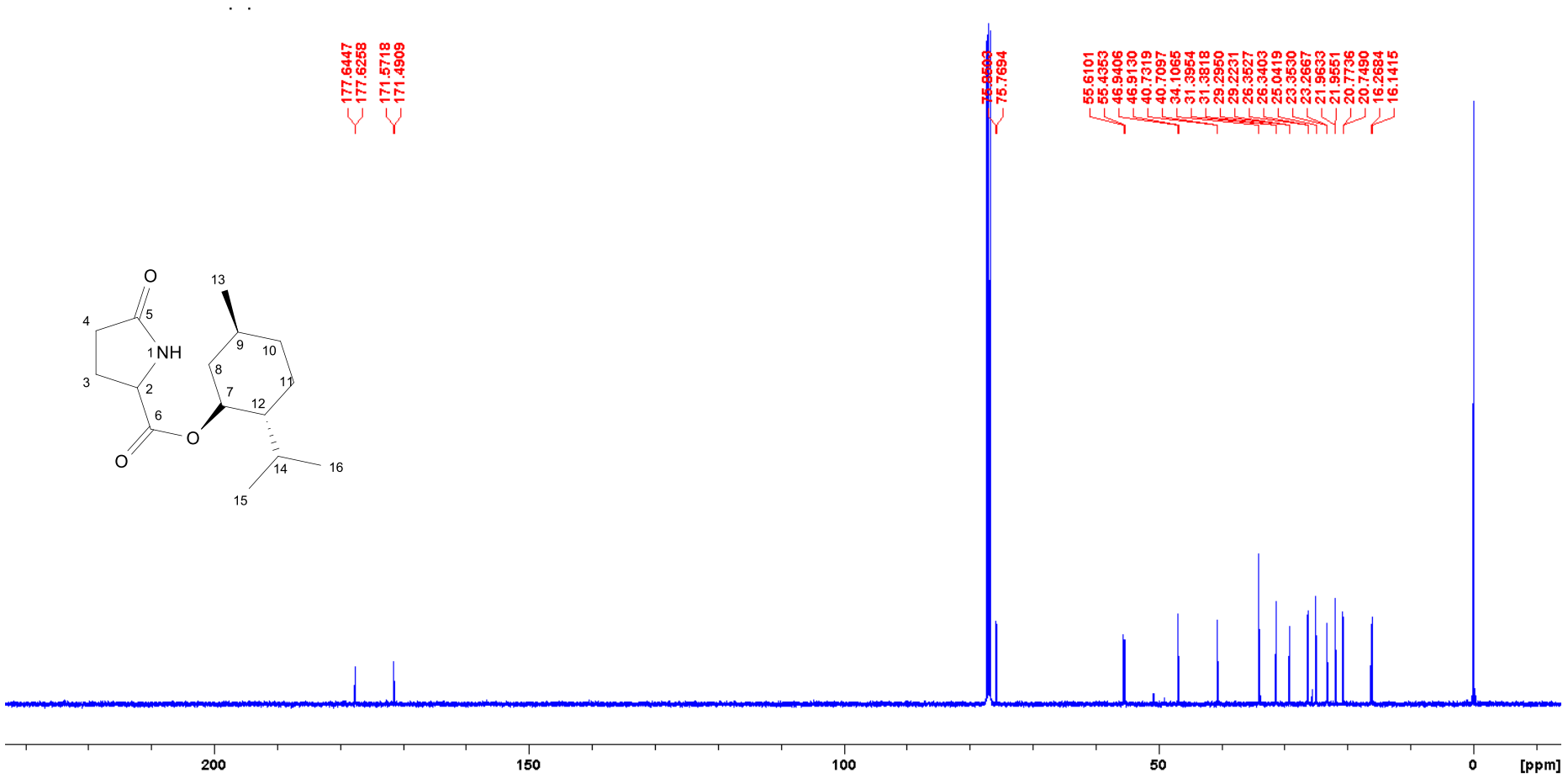
177.6447
177.5258
171.5718
171.4909
75.9593
75.7694
55.6101
55.4353
46.9406
46.9130
40.7319
40.7097
34.1065
31.3954
31.3818
29.2950
29.2231
26.3527
26.3403
25.0419
23.3530
23.2667
21.9633
21.9551
20.7736
20.7490
16.2684
16.1415
O
5
4
1 NH
3
2
6
O
O
13
9
10
8
11
7
12
14
16
15
200
150
100
50
0
[ppm]

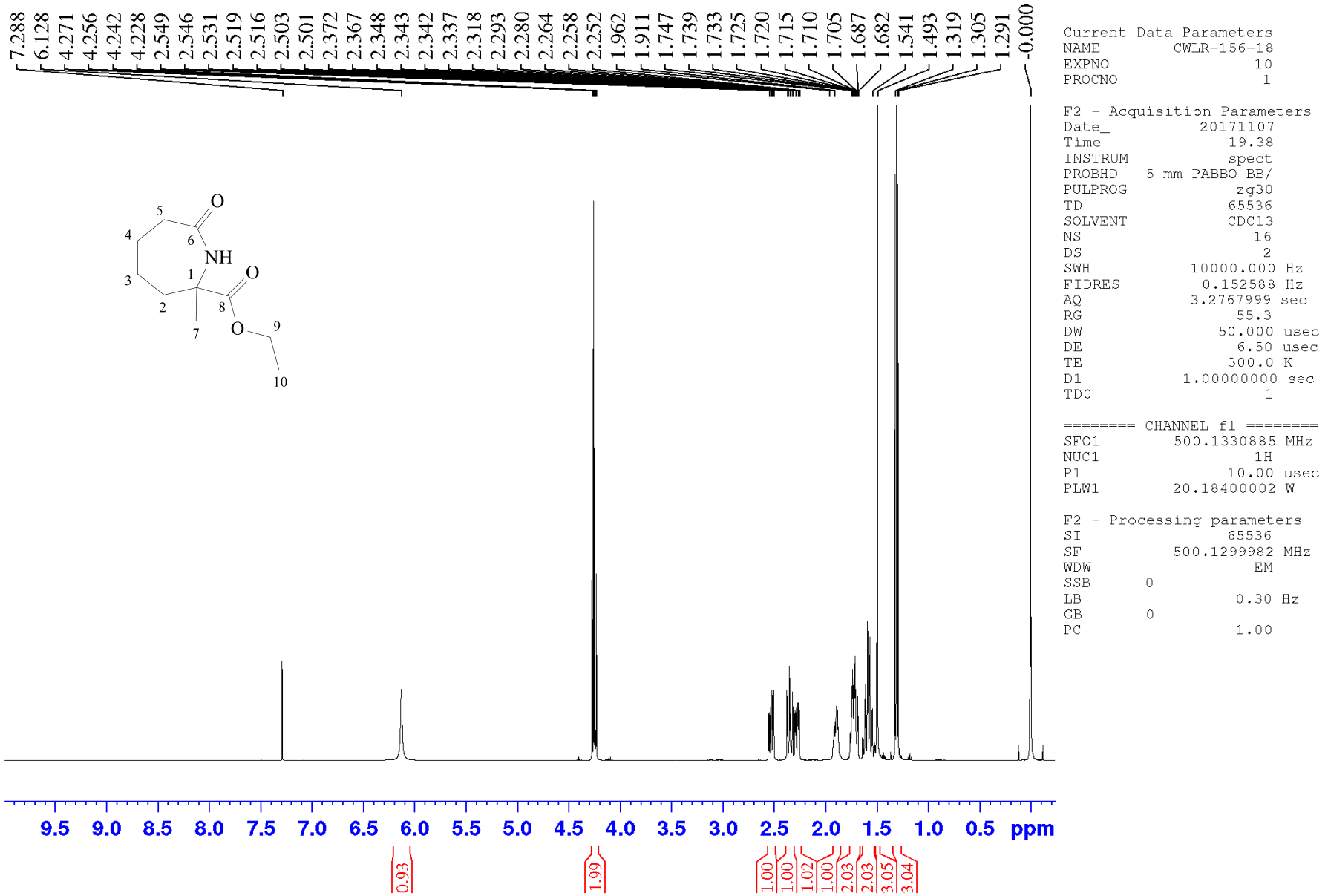


```
Current Data Parameters
NAME          CWLR-156-18
EXPNO                  10
PROCNO                  1

F2 - Acquisition Parameters
Date_           20171107
Time               19.38
INSTRUM            spect
PROBHD   5 mm PABBO BB/
PULPROG             zg30
TD                 65536
SOLVENT            CDCl3
NS                    16
DS                     2
SWH           10000.000 Hz
FIDRES         0.152588 Hz
AQ            3.2767999 sec
RG                  55.3
DW                50.000 usec
DE                 6.50 usec
TE                300.0 K
D1           1.00000000 sec
TD0                    1

======== CHANNEL f1 ========
SFO1         500.1330885 MHz
NUC1                1H
P1                10.00 usec
PLW1         20.18400002 W

F2 - Processing parameters
SI                 65536
SF           500.1299982 MHz
WDW                   EM
SSB       0
LB                 0.30 Hz
GB        0
PC                 1.00
```

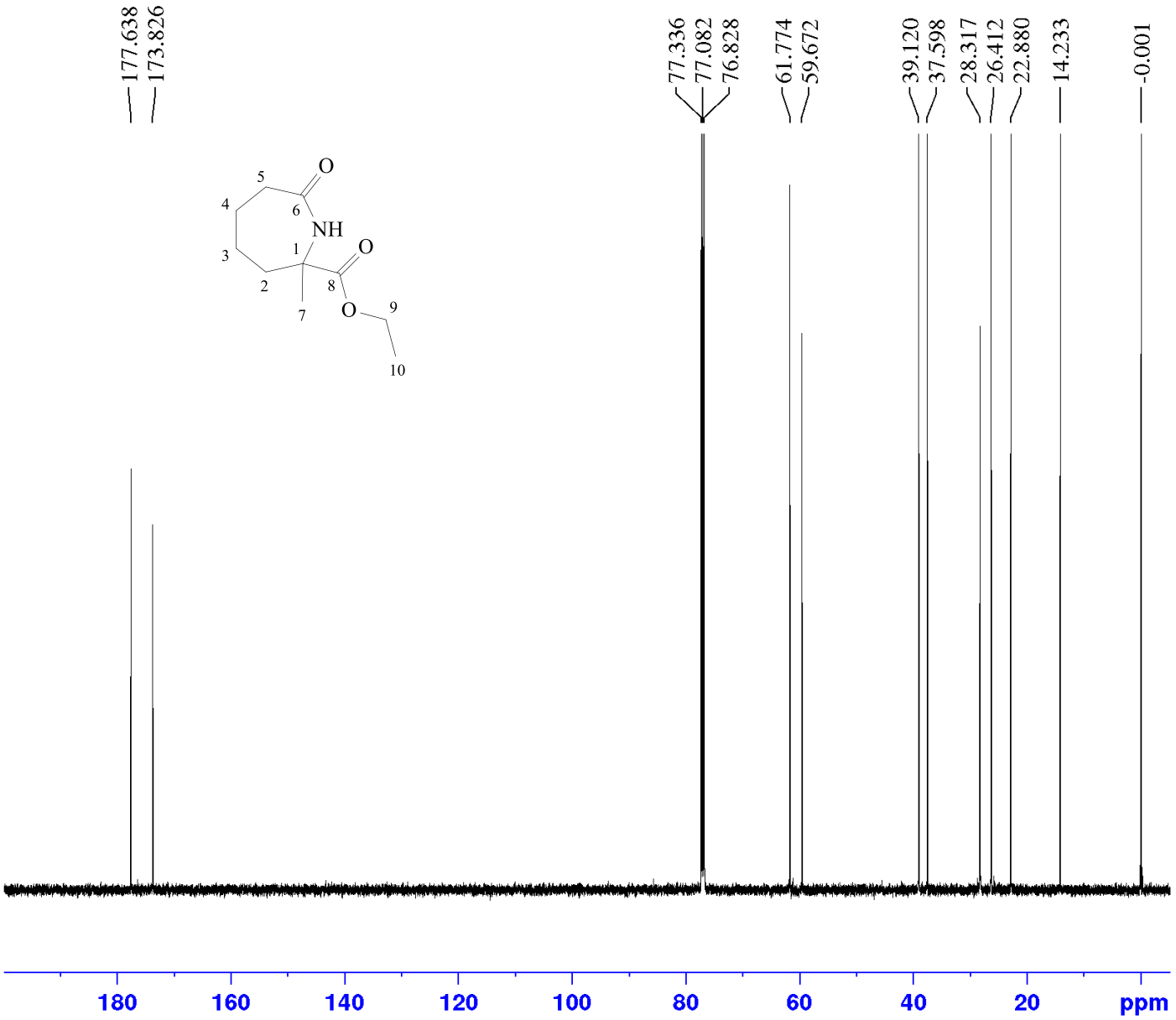


```
Current Data Parameters
NAME         CWLR-156-18
EXPNO                 11
PROCNO                 1

F2 - Acquisition Parameters
Date_           20171107
Time               21.09
INSTRUM            spect
PROBHD   5 mm PABBO BB/
PULPROG          zgpg30
TD                119044
SOLVENT             CDCl3
NS                    512
DS                      4
SWH           31250.000 Hz
FIDRES         0.262508 Hz
AQ            1.9047040 sec
RG               190.14
DW               16.000 usec
DE                7.87 usec
TE                300.0 K
D1           1.00000000 sec
D11          0.03000000 sec
TD0                    1

======== CHANNEL f1 ========
SFO1         125.7716202 MHz
NUC1                 13C
P1                10.00 usec
PLW1         67.00000000 W

======== CHANNEL f2 ========
SFO2         500.1320005 MHz
NUC2                 1H
CPDPRG[2          waltz64
PCPD2             80.00 usec
PLW2         20.18400002 W
PLW12         0.31536999 W
PLW13         0.15863000 W

F2 - Processing parameters
SI                 131072
SF           125.7577852 MHz
WDW                  EM
SSB       0
LB                1.00 Hz
GB        0
PC                1.40
```

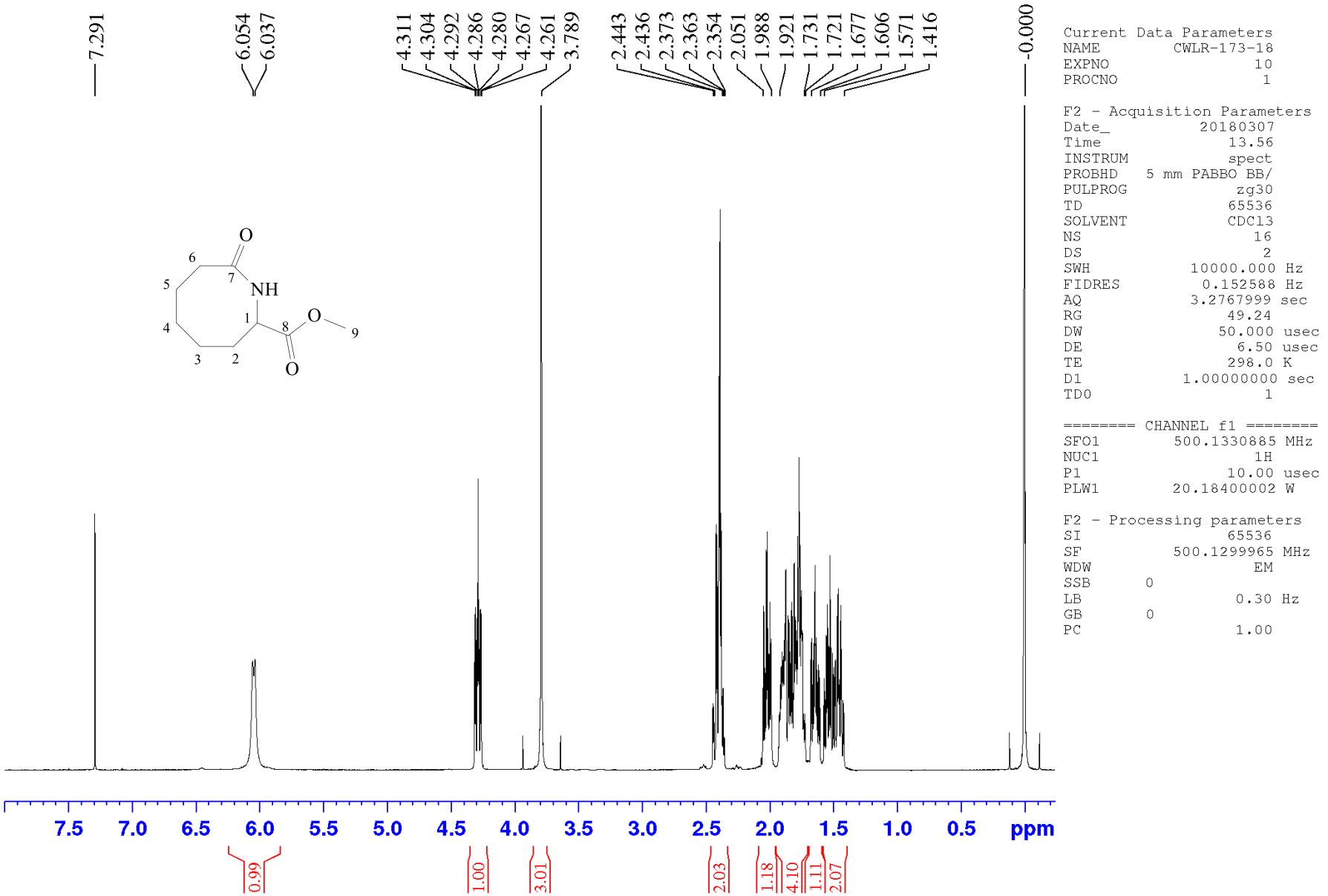


```
Current Data Parameters
NAME         CWLR-173-18
EXPNO                 10
PROCNO                 1

F2 - Acquisition Parameters
Date_           20180307
Time               13.56
INSTRUM            spect
PROBHD   5 mm PABBO BB/
PULPROG             zg30
TD                 65536
SOLVENT            CDCl3
NS                    16
DS                     2
SWH           10000.000 Hz
FIDRES         0.152588 Hz
AQ            3.2767999 sec
RG                 49.24
DW                50.000 usec
DE                 6.50 usec
TE                298.0 K
D1           1.00000000 sec
TD0                    1

======== CHANNEL f1 ========
SFO1         500.1330885 MHz
NUC1                  1H
P1                10.00 usec
PLW1         20.18400002 W

F2 - Processing parameters
SI                 65536
SF           500.1299965 MHz
WDW                   EM
SSB       0
LB                 0.30 Hz
GB        0
PC                 1.00
```

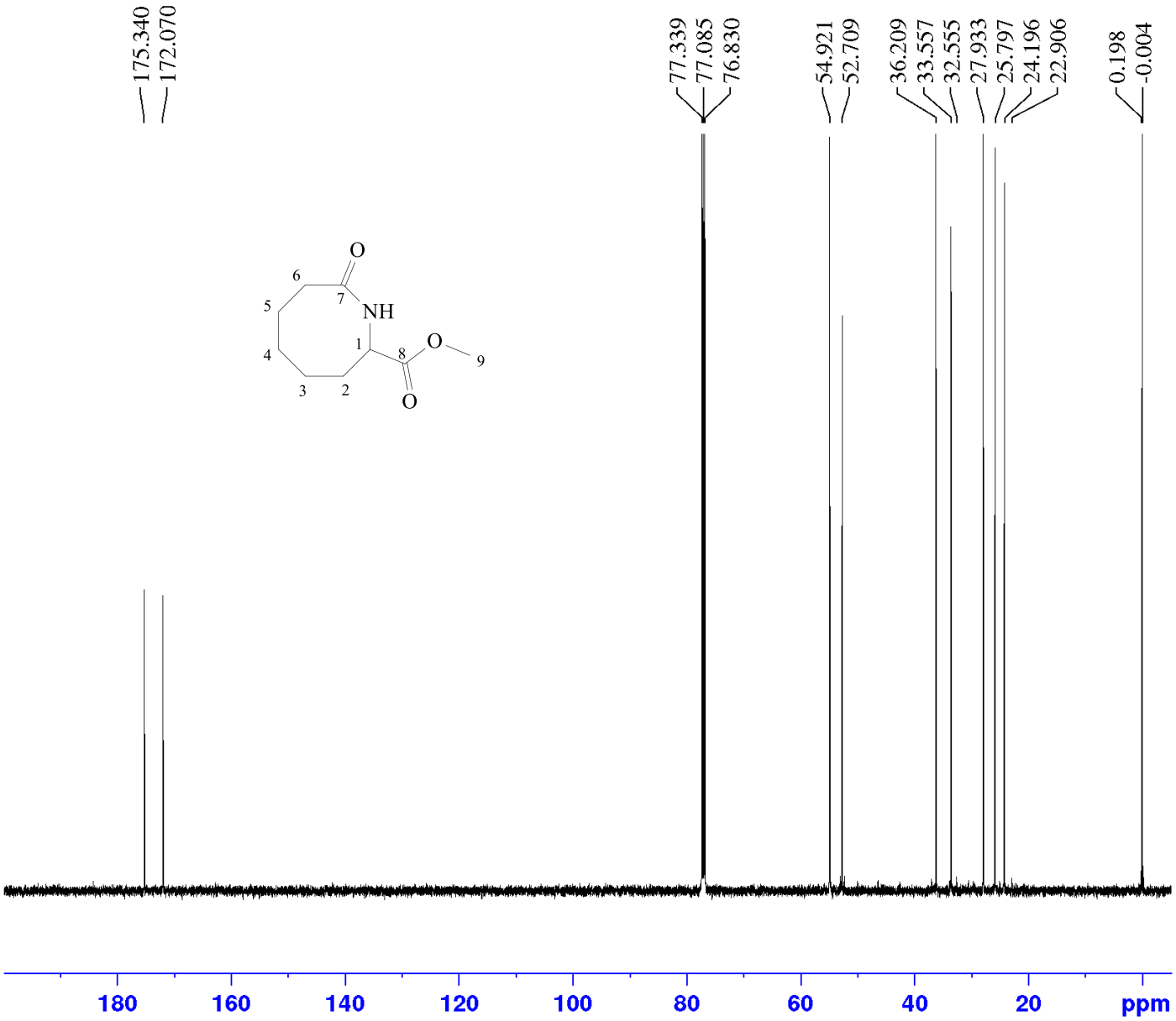


```
Current Data Parameters
NAME         CWLR-173-18
EXPNO                 11
PROCNO                 1

F2 - Acquisition Parameters
Date_           20180307
Time               14.29
INSTRUM            spect
PROBHD   5 mm PABBO BB/
PULPROG          zgpg30
TD                65536
SOLVENT           CDCl3
NS                  512
DS                    4
SWH           29761.904 Hz
FIDRES         0.454131 Hz
AQ             1.1010048 sec
RG                190.14
DW                16.800 usec
DE                 6.50 usec
TE                298.0 K
D1             2.00000000 sec
D11            0.03000000 sec
TD0                   1

======== CHANNEL f1 ========
SFO1         125.7703637 MHz
NUC1                13C
P1                10.00 usec
PLW1         67.00000000 W

======== CHANNEL f2 ========
SFO2         500.1320005 MHz
NUC2                1H
CPDPRG[2         waltz16
PCPD2             80.00 usec
PLW2         20.18400002 W
PLW12         0.31536999 W
PLW13         0.15863000 W

F2 - Processing parameters
SI                 32768
SF           125.7577861 MHz
WDW                  EM
SSB       0
LB                 1.00 Hz
GB        0
PC                 1.40
```

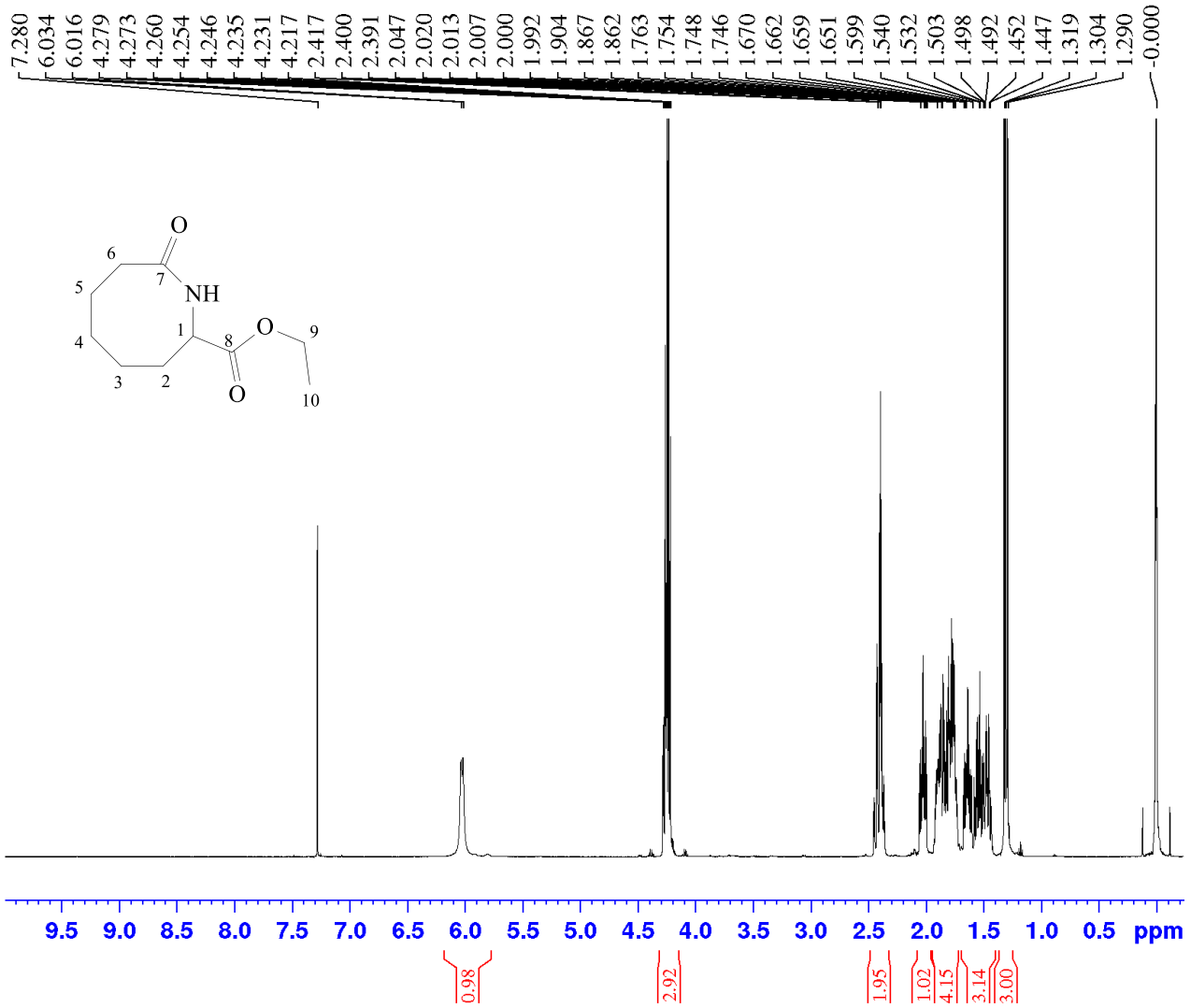


```
Current Data Parameters
NAME        CWLR-137-8-2
EXPNO                 20
PROCNO                 1

F2 - Acquisition Parameters
Date_           20180406
Time               13.35
INSTRUM            spect
PROBHD   5 mm PABBO BB/
PULPROG             zg30
TD                 65536
SOLVENT            CDCl3
NS                    16
DS                     2
SWH           10000.000 Hz
FIDRES         0.152588 Hz
AQ            3.2767999 sec
RG                 63.32
DW               50.000 usec
DE                6.50 usec
TE                298.0 K
D1           1.00000000 sec
TD0                    1

======== CHANNEL f1 ========
SFO1         500.1330885 MHz
NUC1                1H
P1                10.00 usec
PLW1         20.18400002 W

F2 - Processing parameters
SI                 65536
SF           500.1300021 MHz
WDW                   EM
SSB       0
LB                 0.30 Hz
GB        0
PC                 1.00
```

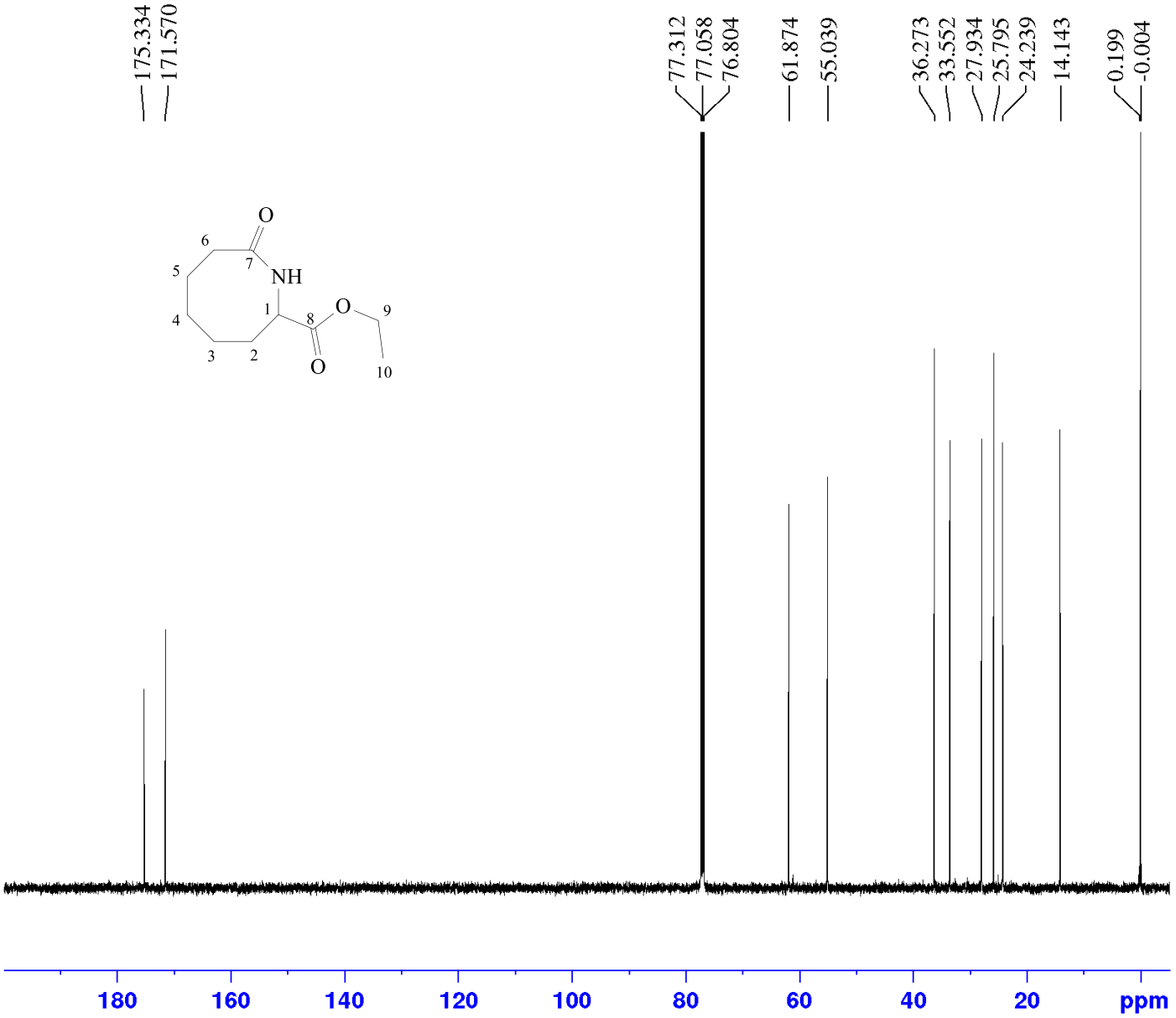


```
Current Data Parameters
NAME        CWLR-137-8-2
EXPNO                 21
PROCNO                 1

F2 - Acquisition Parameters
Date_           20180406
Time               14.09
INSTRUM            spect
PROBHD   5 mm PABBO BB/
PULPROG          zgpg30
TD                65536
SOLVENT           CDCl3
NS                  512
DS                    4
SWH           29761.904 Hz
FIDRES         0.454131 Hz
AQ            1.1010048 sec
RG               190.14
DW               16.800 usec
DE                6.50 usec
TE                298.0 K
D1           2.00000000 sec
D11          0.03000000 sec
TD0                   1

======== CHANNEL f1 ========
SFO1         125.7703637 MHz
NUC1                13C
P1                10.00 usec
PLW1         67.00000000 W

======== CHANNEL f2 ========
SFO2         500.1320005 MHz
NUC2                1H
CPDPRG[2         waltz16
PCPD2             80.00 usec
PLW2         20.18400002 W
PLW12         0.31536999 W
PLW13         0.15863000 W

F2 - Processing parameters
SI                 32768
SF           125.7577870 MHz
WDW                  EM
SSB       0
LB                1.00 Hz
GB        0
PC                1.40
```

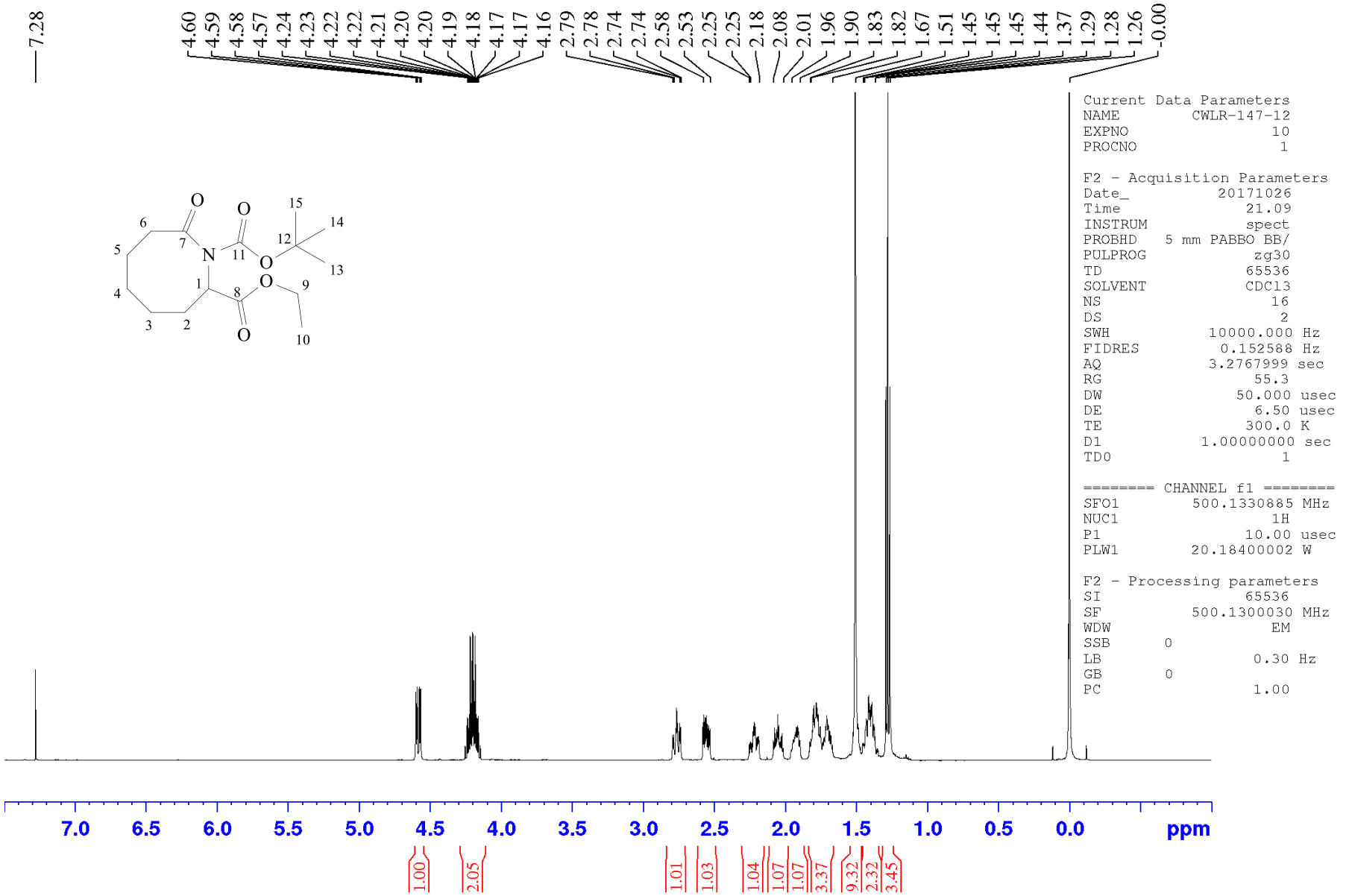
7.28
4.60 4.59 4.58 4.57 4.24 4.23 4.22 4.22 4.21 4.20 4.20 4.19 4.18 4.17 4.17 4.16
2.79 2.78 2.74 2.74 2.58 2.53 2.25 2.25 2.18 2.08 2.01 1.96 1.90 1.83 1.82 1.67 1.51 1.45 1.45 1.45 1.44 1.37 1.29 1.28 1.26 -0.00
Current Data Parameters
NAME CWLR-147-12
EXPNO 10
PROCNO 1
F2 - Acquisition Parameters
Date_ 20171026
Time 21.09
INSTRUM spect
PROBHD 5 mm PABBO BB/
PULPROG zg30
TD 65536
SOLVENT CDCl3
NS 16
DS 2
SWH 10000.000 Hz
FIDRES 0.152588 Hz
AQ 3.2767999 sec
RG 55.3
DW 50.000 usec
DE 6.50 usec
TE 300.0 K
D1 1.00000000 sec
TD0 1
======== CHANNEL f1 ========
SFO1 500.1330885 MHz
NUC1 1H
P1 10.00 usec
PLW1 20.18400002 W
F2 - Processing parameters
SI 65536
SF 500.1300030 MHz
WDW EM
SSB 0
LB 0.30 Hz
GB 0
PC 1.00
7.0 6.5 6.0 5.5 5.0 4.5 4.0 3.5 3.0 2.5 2.0 1.5 1.0 0.5 0.0 ppm
1.00 2.05 1.01 1.03 1.04 1.07 1.07 3.37 9.32 2.32 3.45

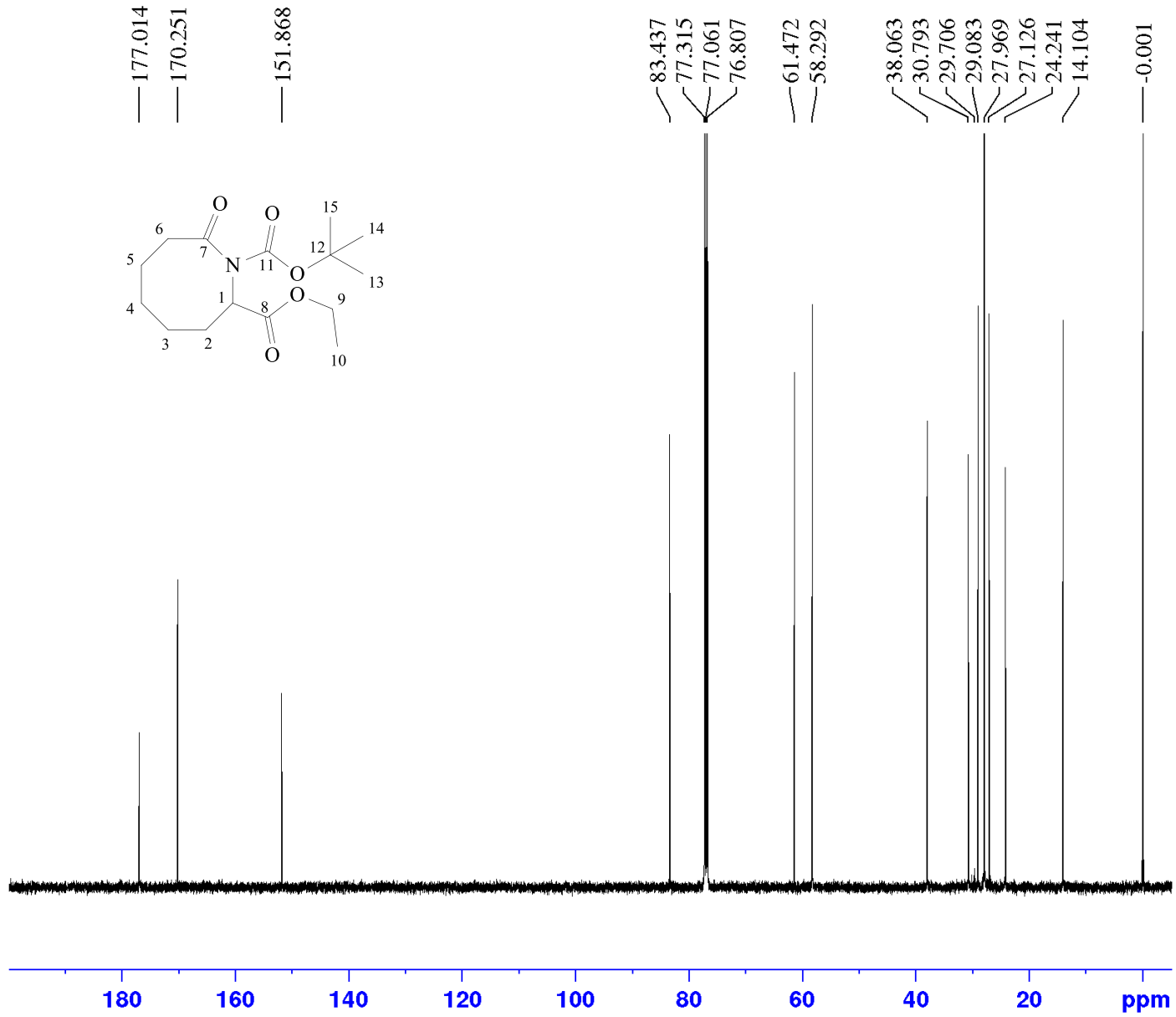


```
Current Data Parameters
NAME         CWLR-147-12
EXPNO                 11
PROCNO                 1

F2 - Acquisition Parameters
Date_           20171026
Time               21.40
INSTRUM            spect
PROBHD   5 mm PABBO BB/
PULPROG          zgpg30
TD                119044
SOLVENT             CDCl3
NS                    512
DS                      4
SWH           31250.000 Hz
FIDRES         0.262508 Hz
AQ            1.9047040 sec
RG               190.14
DW               16.000 usec
DE                7.87 usec
TE                300.0 K
D1           1.00000000 sec
D11          0.03000000 sec
TD0                    1

======== CHANNEL f1 ========
SFO1         125.7716202 MHz
NUC1                 13C
P1                10.00 usec
PLW1         67.00000000 W

======== CHANNEL f2 ========
SFO2         500.1320005 MHz
NUC2                 1H
CPDPRG[2          waltz64
PCPD2             80.00 usec
PLW2         20.18400002 W
PLW12         0.31536999 W
PLW13         0.15863000 W

F2 - Processing parameters
SI                 131072
SF           125.7577860 MHz
WDW                  EM
SSB       0
LB                1.00 Hz
GB        0
PC                1.40
```

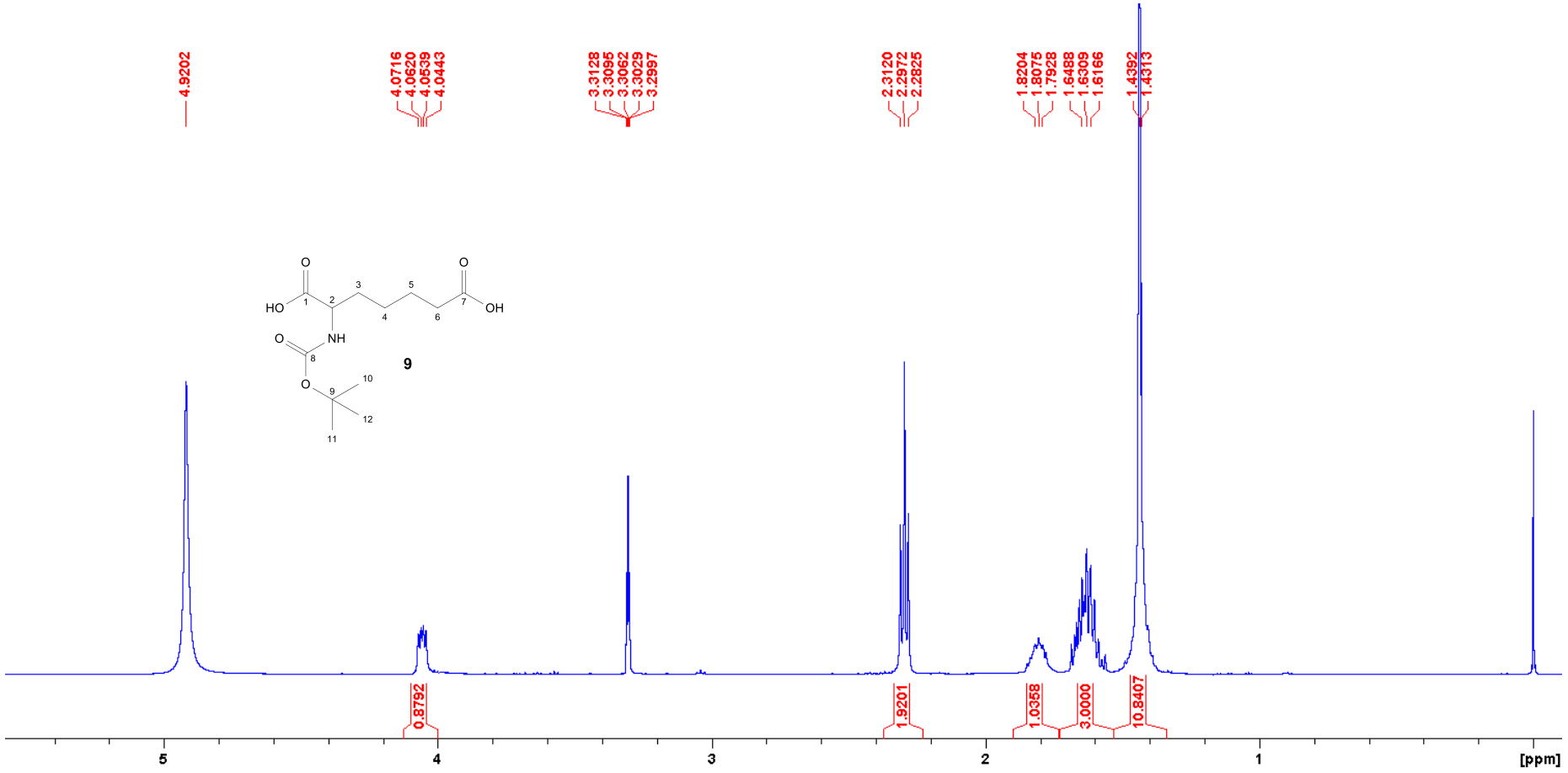
4.9202
4.0716
4.0620
4.0539
4.0443
3.3128
3.3095
3.3062
3.3029
3.2997
2.3120
2.2972
2.2825
1.8204
1.8075
1.7928
1.6488
1.6309
1.6166
1.4392
1.4313
HO
OH
NH
9
0.8792
1.9201
1.0358
3.0000
10.3407
5
4
3
2
1
[ppm]

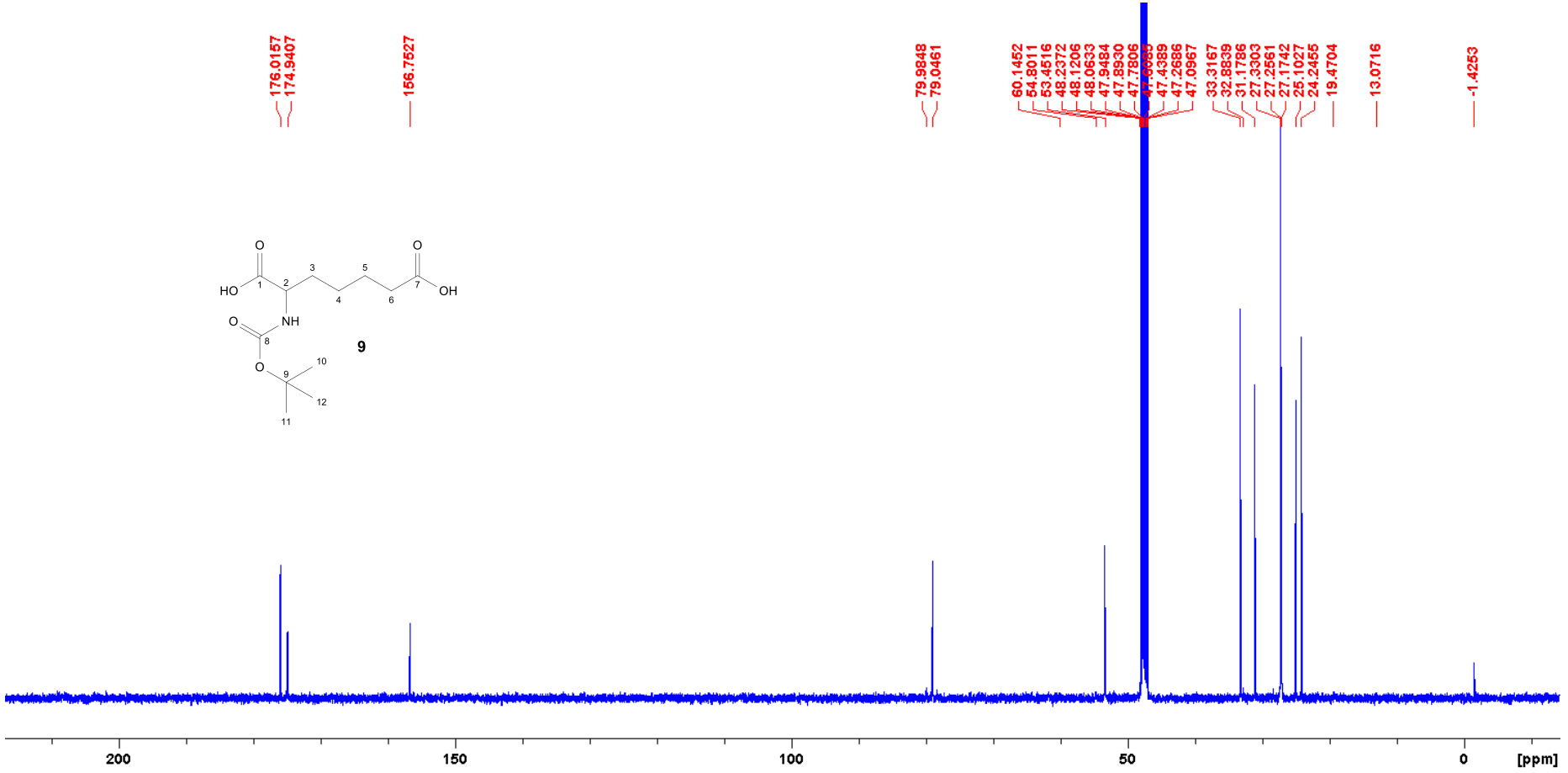
176.0157
174.9407
156.7527
79.9848
79.0461
60.1452
54.8011
53.4516
48.2372
48.1206
48.0633
47.9484
47.8930
47.7806
47.4389
47.2686
47.0967
33.3167
32.8839
31.1786
27.3303
27.2561
27.1742
25.1027
24.2455
19.4704
13.0716
-1.4253
HO
OH
NH
O
9
200
150
100
50
0
[ppm]

General procedure for the optimised Dieckmann-type cyclisation

A three-necked round bottom flask, equipped with a thermometer, a tap and a septum is charged with 1.0 eq. of the respective lactam before 50 ml of dry THF are added. The solution is stirred and cooled, using ethyl acetate – liquid nitrogen mixtures (-85 °C). A 2M solution of LDA (3.0 eq.) in THF/toluene/ethyl benzene is added slowly so that the temperature does not increase above -80 °C. The reaction mixture is stirred for 30 min before 15 ml of aqueous, saturated NH_4Cl-sol. is added, the biphasic mixture is then allowed to warm to room temperature. 50 ml of water are added and the aqueous phase is extracted with 30 ml ethyl acetate five times. The combined organic layers are dried over $MgSO_4$, the drying agent is filtered off and the solvent is revomed *in vacuo*. The residue is purified with column chromatography [SiO_2; ethyl acetate:cyclohexane; 1:6 → 1:2].

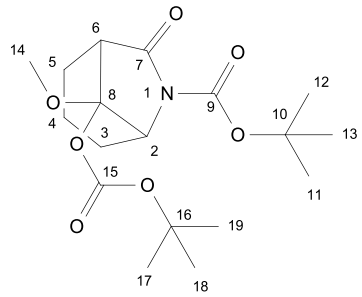

(**11**). The cyclization of the respective methylester yielded side product **11** as a colorless, viscous oil which crystallized after several weeks at room temperature. Yield: 2 %; R_f: 0.29 (ethyl acetate:cyclohexane; 1:4); ^{1}H-NMR: (500 MHz, $CDCl_3$; δ[ppm]) 4.83 (br s, 1H, *H2*); 3.40 (s, 3H, *H14*); 3.10 (br s, 1H, *H6*); 1.98-1.83 (m, 4H, *H3*, *H5*); 1.68-1.60 (m, 2H, *H4*); 1.52 (s, 9H, *H11*, *H12*, *H13*); 1.48 (s, 9H, *H17*, *H18*, *H19*); ^{13}C-NMR: (125 MHz, $CDCl_3$; δ [ppm]) 171.9 (*C7*); 150.3; 149.1 (*C9*, *C15*); 106.3 (*C8*); 83.1 (*C10*, *C16*); 59.5 (*C14*); 50.5 (*C2*); 48.6 (*C6*); 28.0 (*C11*, *C12*, *C13*); 27.6 (*C17*, *C18*, *C19*); 23.7 (*C3*); 22.8 (*C5*); 16.0 (*C4*). HRMS: Calculated: 394.1842 $[M+Na]^+$, found 394.1836

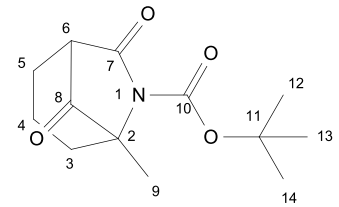

(**8**) starting from methyl lactam ester (**7**); white, crystalline solid. Product yield 76 %; R_f: 0.23 (ethyl acetate/cyclohexane; 1:4); ^{1}H-NMR: (500 MHz, $CDCl_3$, δ[ppm]) 2.98-2.96 (m, 1H, *H6*); 2.55-2.53 (m, 1H, *H3*); 2.42-2.39 (m, 1H, *H5*); 2.04-2.01 (m, 1H, *H5'*); 1.83-1.80 (m, 1H, *H4*); 1.76-1.69 (m, 2H, *H3'*, *H4'*); 1.57 (s, 9H, *H12*, *H13*, *H14*), 1.51 (s, 3H, *H9*); ^{13}C-NMR (125 MHz, $CDCl_3$, δ[ppm]) 208.6 (*C8*); 169.5 (C*7*); 148.8 (*C10*); 83.9 (*C11*); 70.3 (*C2*); 53.2 (*C6*); 38.6 (*C5*); 33.1 (*C3*); 28.1 (*C12*, *C13*, *C14*); 18.5 (*C4*); 16.6 (*C9*); IR (ATR) ν = 3367, 2876, 2845, 2811, 1790 (C=O), 1745 (C=O), 1704 (C=O),

1502, 1434, 1421, 1378, 1289, 1241, 1229, 1200, 1128, 1106, 1087, 1063, 1027, 906, 867, 834, 812, 742; HRMS: Calculated: 322.1631 $[M+Na]^+$, found 322.1622

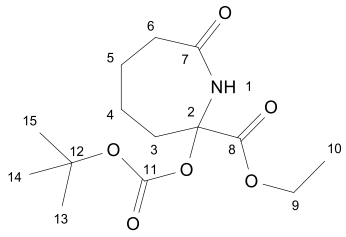

Rearrangement product (**9**)*;* starting from lactam ester (**4**) colorless, viscous oil. Product yield: 8 % ; R_f: 0.61 (ethyl acetate/cyclohexane 1:4); ^{1}H-NMR: (500 MHz, $CDCl_3$, δ[ppm]) 6.11 (br s, 1H, *NH*); 4.26-4.14 (m, 2H, *H9*); 3.10-3.08 (m, 1H, *H6*); 2.54-2.47 (m, 2H, *H5*); 2.24-2.22 (m, 1H, *H4*); 2.11-2.09 (m, 1H, *H3*); 1.79-1.64 (m, 3H, *H3', H4', H6'*); 1.43 (s, 9H, *H12, H13, H14*); 1.25 (t, 3H, ^3J = 7.2 Hz, *H9*); ^{13}C-NMR: (125 MHz, $CDCl_3$, δ[ppm]) 202.8 (*C7*); 168.4 (*C8*); 154.4 (*C11*); 80.0 (*C12*); 69.0 (*C2*); 60.0 (*C9*); 39.3 (*C6*); 38.1 (*C3*); 28.2 (*C13, C14, C15*); 27.7 (*C5*) ; 22.1 (*C4*); 14.0 (*C10*) IR (ATR) ν = 2940, 2920, 2877, 1773 (C=O), 1703 (C=O), 1690 (C=O), 1500, 1433, 1421, 1353, 1307, 1270, 1233, 1205, 1162, 1142, 1103, 970, 946, 905, 833, 801, 762, 720, 677, 635, 590, 532; HRMS: Calculated: 324.1428 $[M+Na]^+$, found 324.1204

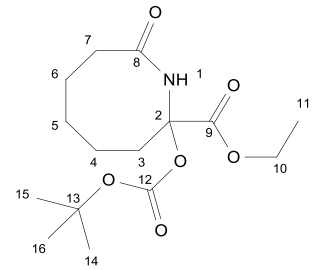

Rearrangement product (**10**); starting from lactam ester (**3**); colorless, viscous oil. Product yield: 14 %; R_f: 0.14 (ethyl acetate/cyclohexane 1:4); ^{1}H-NMR: (500 MHz, $CDCl_3$, δ[ppm]) 5.98 (br s, 1H, *NH*); 4.04-4.00 (m, 1H, *H10*); 3.90-3.89 (m, 1H, *H10'*); 2.67-2.63 (m, 1H, *H7*); 2.37-2.32 (m, 2H, *H3*); 2.19-2.17 (m, 1H, *H7'*); 1.78-1.75 (m, 1H, *H6*); 1.63-1.59 (m, 2H, *H4, H5*); 1.23 (s, 11H, *H4', H5', H14, H15, H16*), 1.02 (t, 3H, ^3J = 7.4 Hz, *H11*); 0.86-0.84 (m, 1H, *H5*'); ^{13}C-NMR: (125 MHz, $CDCl_3$, δ[ppm]) 204.3 (*C8*); 168.3 (*C9*); 154.6 (*C12*); 79.9 (*C13*); 73.1 (*C2*); 62.3 (*C10*); 38.4 (*C7*); 30.1 (*C3*); 28.3 (*C14, C15, C16*); 27.6 (*C6*); 23.1 (*C4*); 14.0 (*C5*); IR (ATR) ν = 2951, 2942, 2866, 1770 (C=O), 1732 (C=O), 1699 (C=O), 1453, 1430, 1382, 1315, 1271, 1222, 1156, 1103, 1079, 1030, 988, 955, 907, 803, 737, 719, 660, 632, 559, 505; HRMS: calculated: 338.1588 $[M+Na]^+$, found 338.1216

General procedure for One-pot Dieckmann cyclization

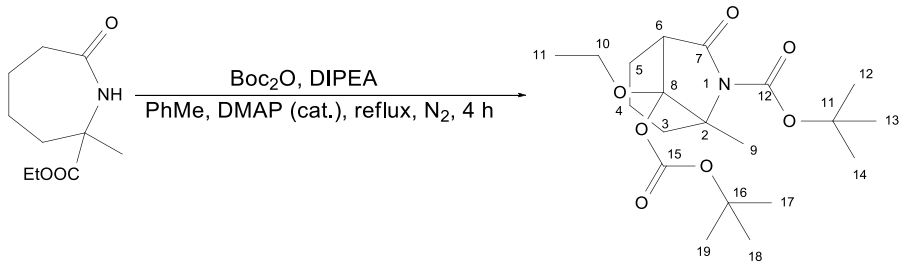

1.0 eq of Ethyl 2-methyl-7-oxoazepane-2-carboxylate (**15**) is dissolved in 50 ml of dry toluene, followed by the addition of 3.0 eq of Boc_2O, 1.2 eq of DIPEA and 200 mg of DMAP. The mixture is heated to reflux for 4 h before the mixture is allowed to cool to room temperature and 15 ml H_2O are added. The mixture is stirred for 90 mins, the aqueous layer is washed with 30 ml toluene three times and the combined organic phases dried over $MgSO_4$, filtered and the solvent removed *in vacuo*. The residue is purified by column chromatography [SiO_2; ethyl acetate : cyclohexane; 1:4] to give the desired product as a light yellow oil. (**1**). 1.5 g of starting material (**6**); Product yield 1.96 g (65%); R_f: 0.48 (ethyl acetate/cyclohexane 1:4); ^{1}H-NMR: (500 MHz, $CDCl_3$, δ[ppm]) 3.84-3.73 (m, 2H, *H10*); 3.66-3.65 (t, ^3J = 3.5 Hz, 1H, *H6*); 2.04-2.00 (m, 1H, *H3*); 1.91-1.82 (m, 3H, *H3'*, *H4*, *H5*); 1.66-1.61 (m, 2H, *H4'*, *H5*'); 1.55+1.54 (2s, 12H, *H9*, *H14*, *H15*, *H16*); 1.46 (s, 9H, *H19*, *H20*, *H21*); 1,24 (t, ^3J = 7 Hz, 3H, *H11*); ^{13}C-NMR (125 MHz, $CDCl_3$, δ[ppm]) 172.7 (C*7*); 151.1 (*C17*); 149.5 (*C12*); 107.2 (*C8*); 83.0 (*C18*); 82.4 (*C13*); 68.9 (*C6*); 61.0 (*C10*); 47.2 (*C2*); 30.6 (*C3*); 28.1 (*C19*, *C20*, *C21*); 27.6 (*C14*, *C15*, *C16*); 23.3 (*C5*); 18.1 (*C3*); 17.8 (*C4*); 15.4 (*C9*); IR (ATR) ν = 2979, 2939, 1759, 1713, 1653, 1457, 1393, 1367, 1332, 1249, 1225, 1166, 1134, 1089, 1030, 976, 878, 850, 760; HRMS: Calculated: 423.2233 $[M+H+Na]^+$, found: 423.2225

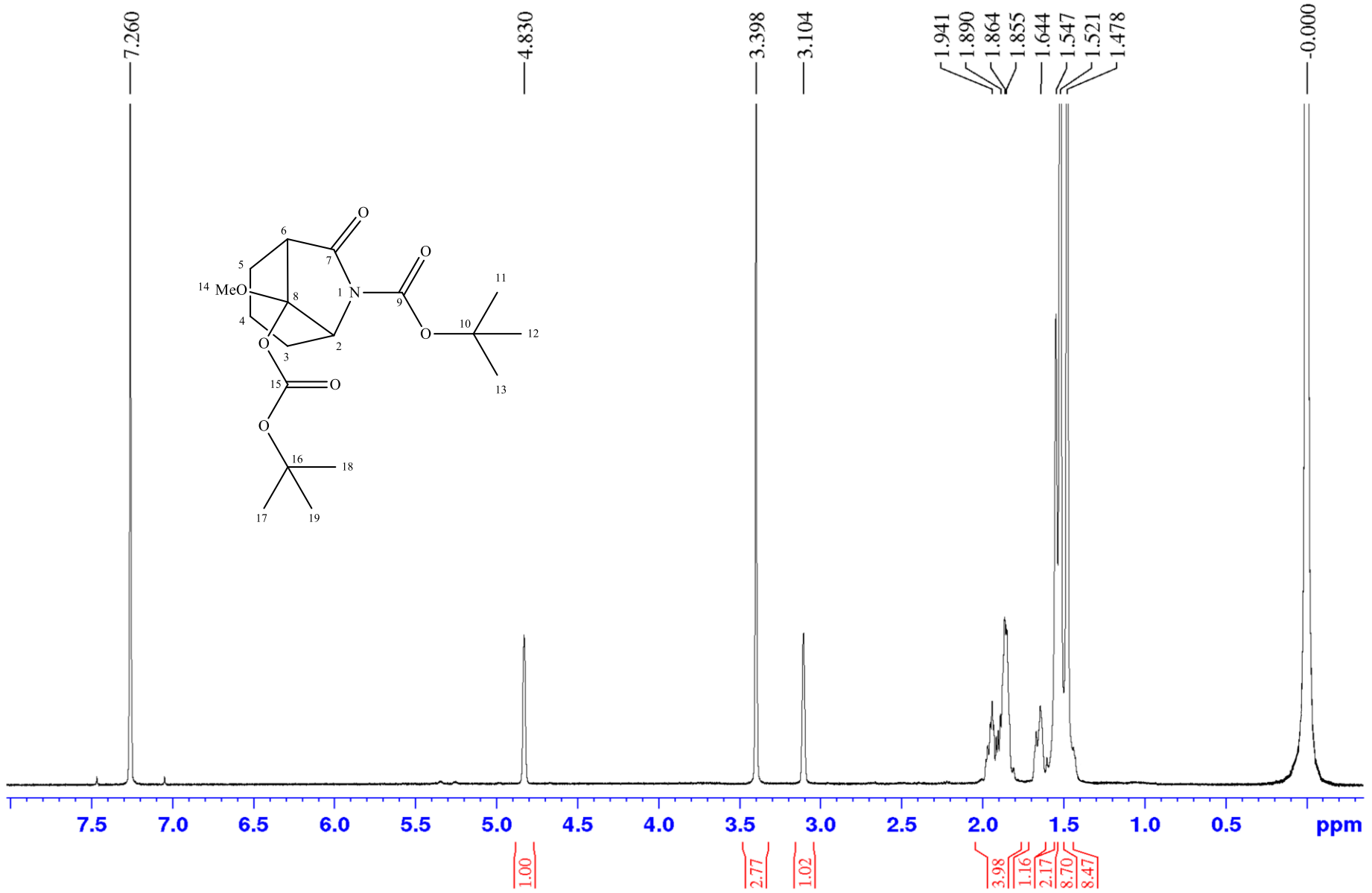
7.260
4.830
3.398
3.104
1.941
1.890
1.864
1.855
1.644
1.547
1.521
1.478
-0.000
MeO
N
O
7.5
7.0
6.5
6.0
5.5
5.0
4.5
4.0
3.5
3.0
2.5
2.0
1.5
1.0
0.5
ppm
1.00
2.77
1.02
3.98
1.16
2.17
8.70
8.47

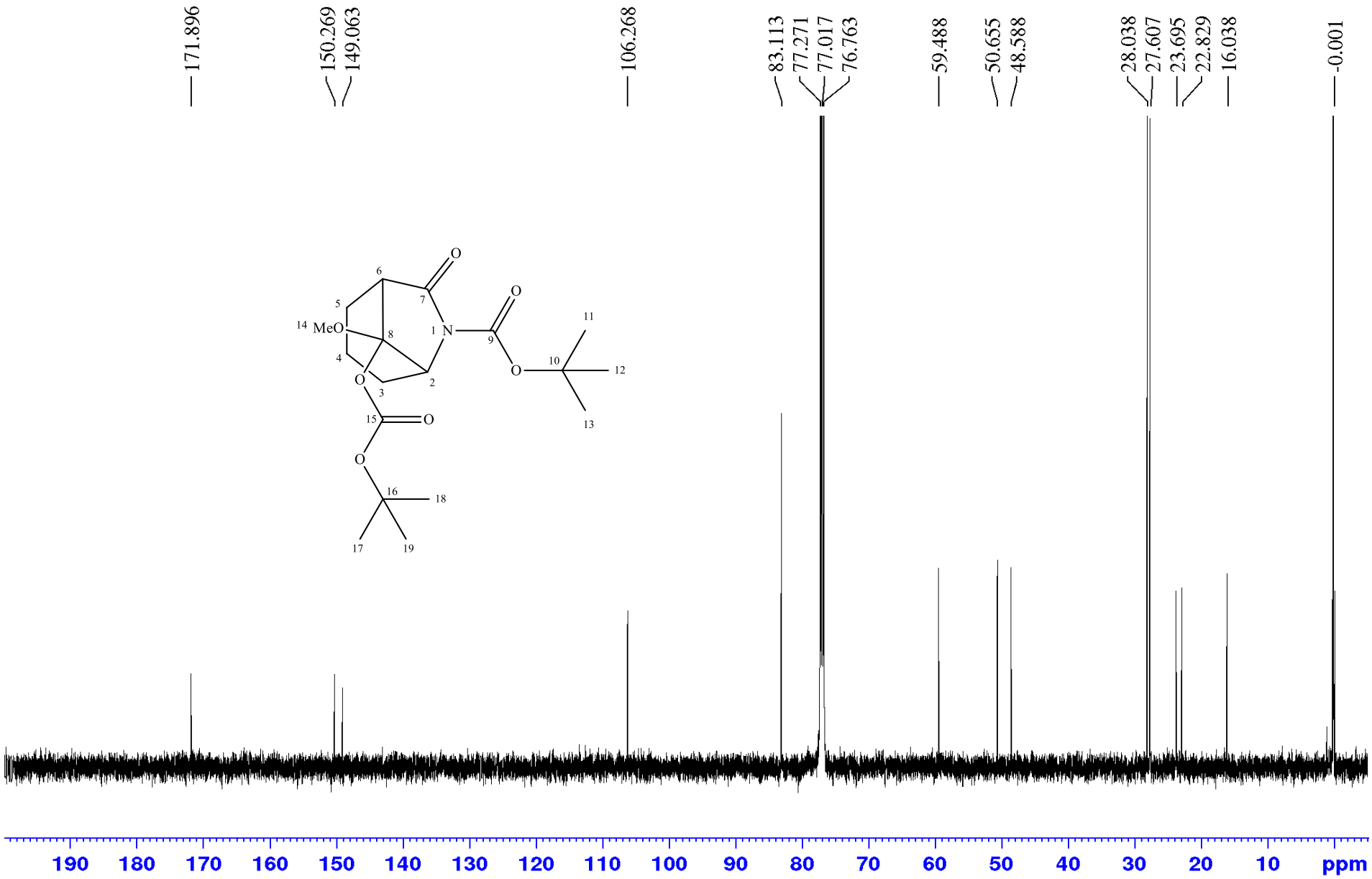
171.896
150.269
149.063
106.268
83.113
77.271
77.017
76.763
59.488
50.655
48.588
28.038
27.607
23.695
22.829
16.038
-0.001
MeO
N
O
190
180
170
160
150
140
130
120
110
100
90
80
70
60
50
40
30
20
10
ppm

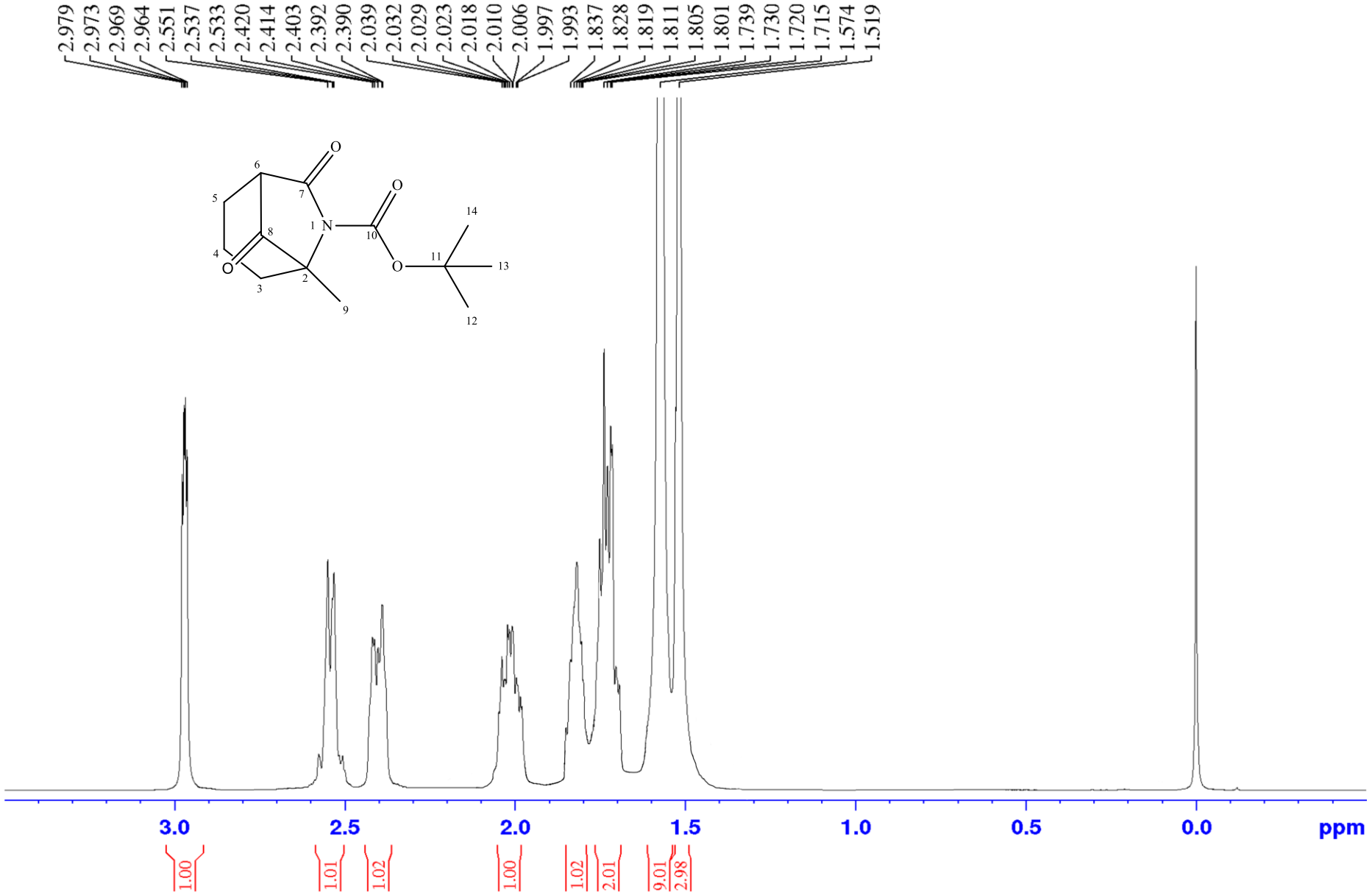
2.979
2.973
2.969
2.964
2.551
2.537
2.533
2.420
2.414
2.403
2.392
2.390
2.039
2.032
2.029
2.023
2.018
2.010
2.006
1.997
1.993
1.837
1.828
1.819
1.811
1.805
1.801
1.739
1.730
1.720
1.715
1.574
1.519
O
O
O
O
N
1
2
3
4
5
6
7
8
9
10
11
12
13
14
3.0
2.5
2.0
1.5
1.0
0.5
0.0
ppm
1.00
1.01
1.02
1.00
1.02
2.01
9.01
2.98

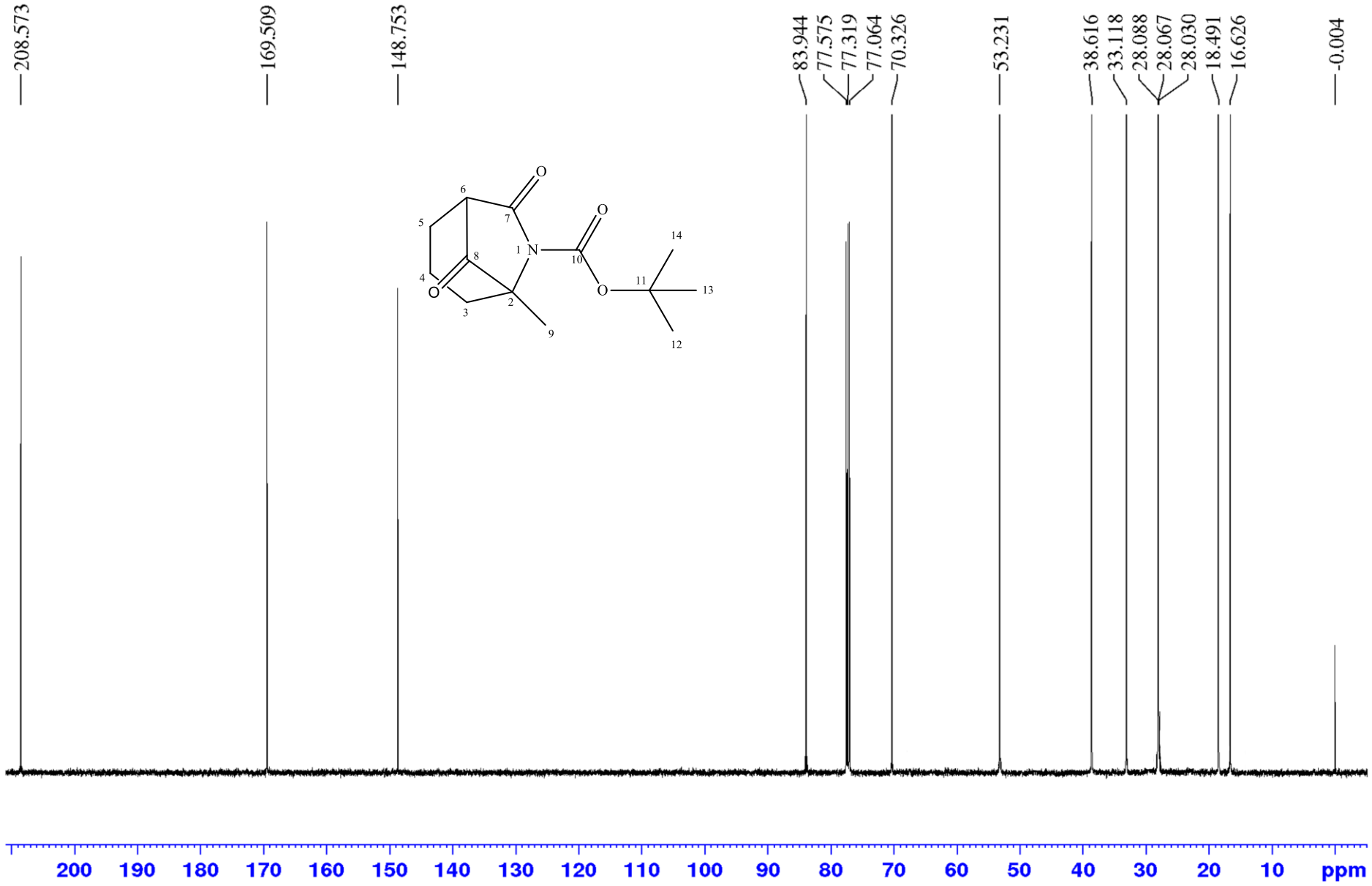
208.573
169.509
148.753
83.944
77.575
77.319
77.064
70.326
53.231
38.616
33.118
28.088
28.067
28.030
18.491
16.626
-0.004
O
6
7
5
1
N
10
O
14
8
4
O
11
13
2
3
9
12
200
190
180
170
160
150
140
130
120
110
100
90
80
70
60
50
40
30
20
10
ppm

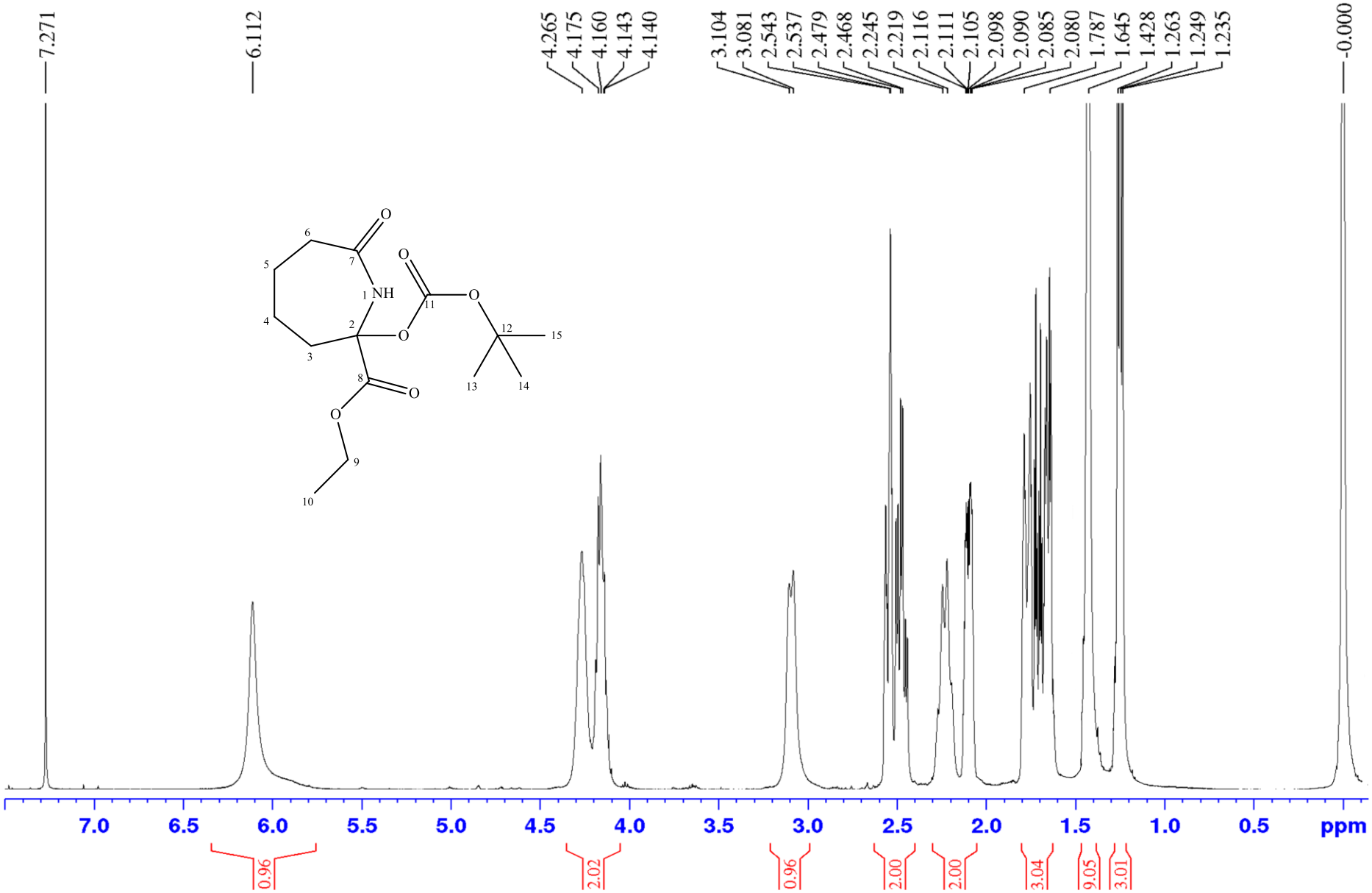
7.271
6.112
4.265
4.175
4.160
4.143
4.140
3.104
3.081
2.543
2.537
2.479
2.468
2.245
2.219
2.116
2.111
2.105
2.098
2.090
2.085
2.080
1.787
1.645
1.428
1.263
1.249
1.235
-0.000
NH
7.0
6.5
6.0
5.5
5.0
4.5
4.0
3.5
3.0
2.5
2.0
1.5
1.0
0.5
ppm
0.96
2.02
0.96
2.00
2.00
3.04
9.05
3.01

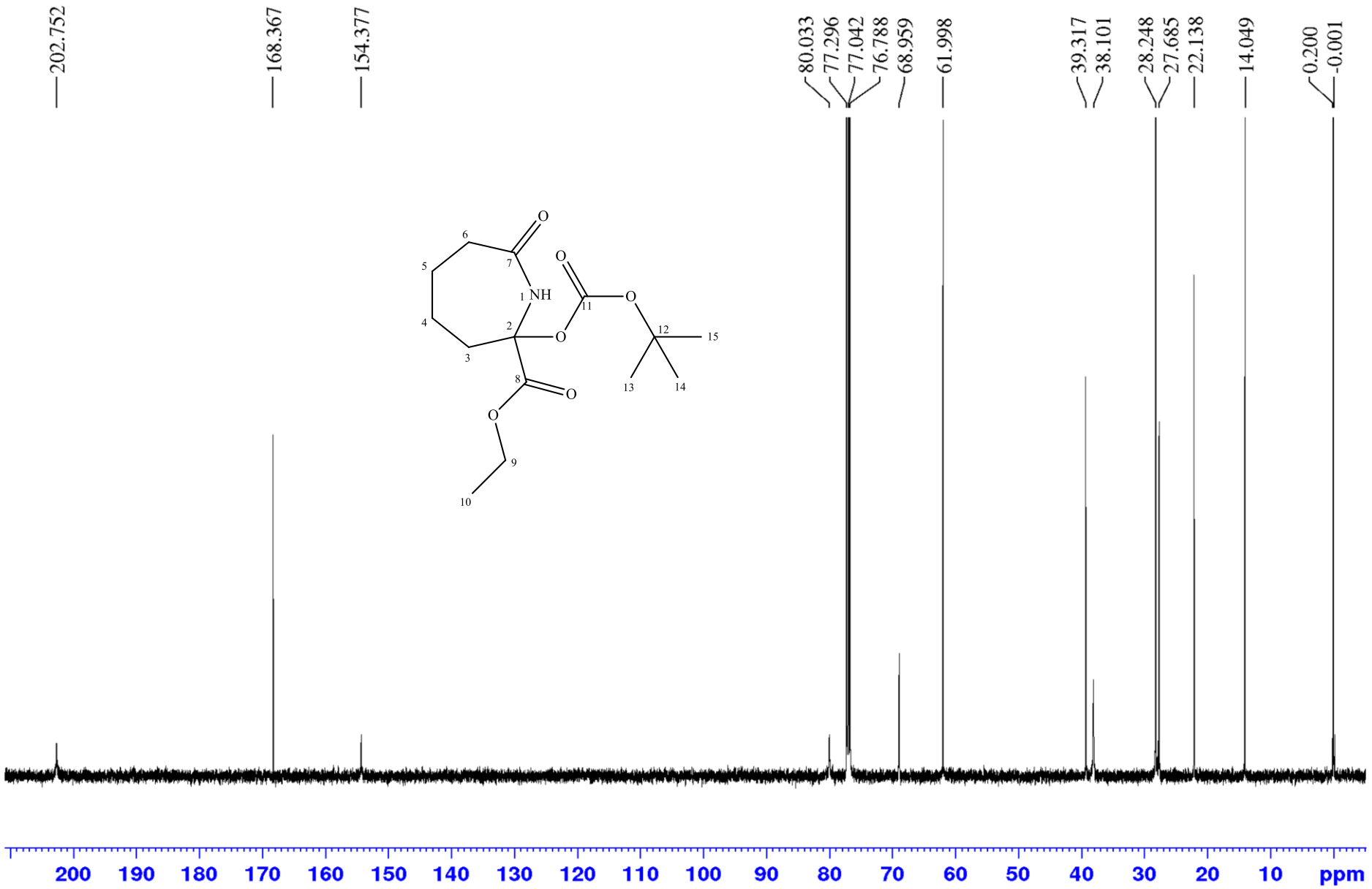
202.752
168.367
154.377
80.033
77.296
77.042
76.788
68.959
61.998
39.317
38.101
28.248
27.685
22.138
14.049
0.200
-0.001
NH
O
O
O
O
O
O
1
2
3
4
5
6
7
8
9
10
11
12
13
14
15
200
190
180
170
160
150
140
130
120
110
100
90
80
70
60
50
40
30
20
10
ppm

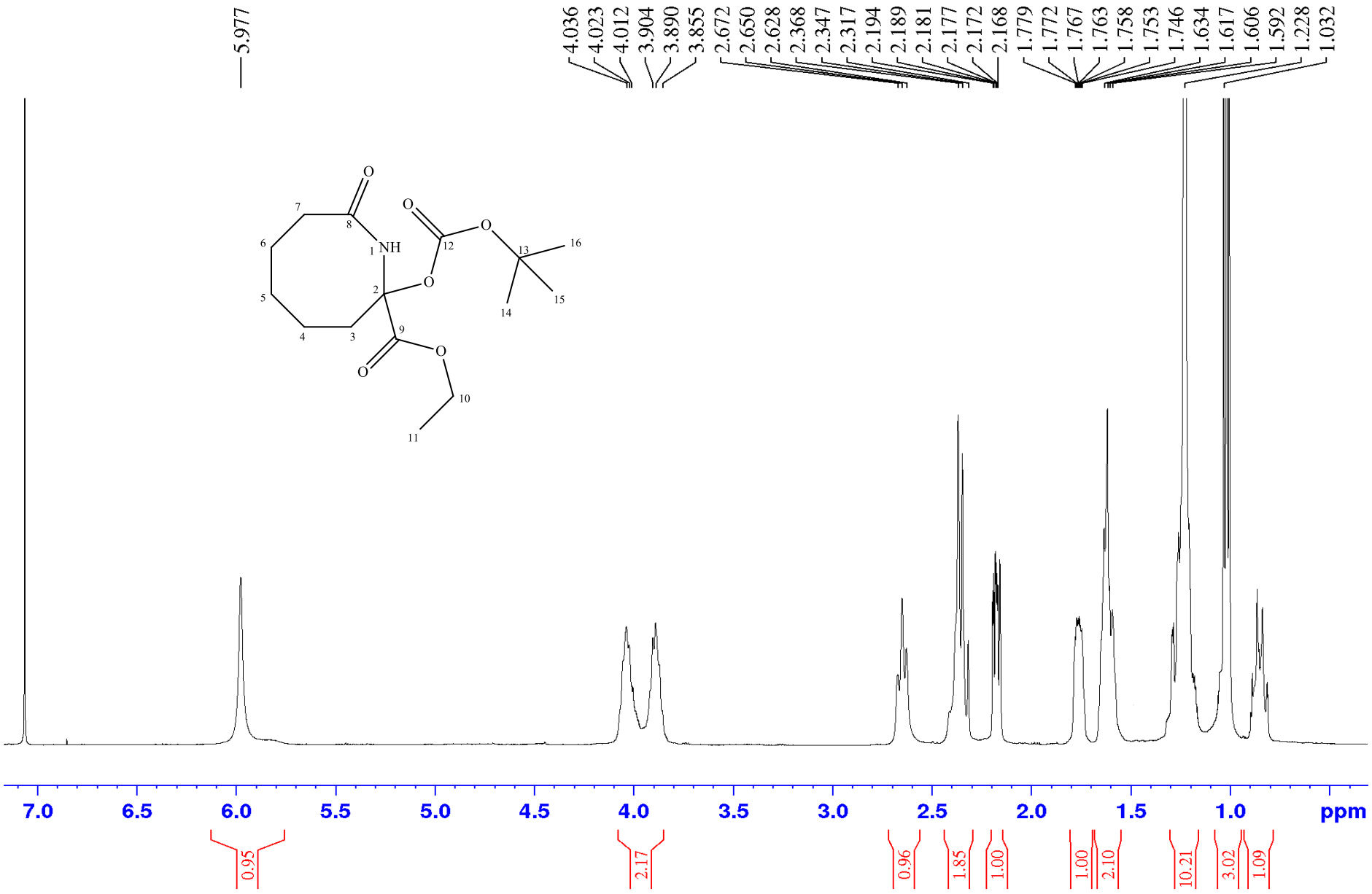
5.977
4.036
4.023
4.012
3.904
3.890
3.855
2.672
2.650
2.628
2.368
2.347
2.317
2.194
2.189
2.181
2.177
2.172
2.168
1.779
1.772
1.767
1.763
1.758
1.753
1.746
1.634
1.617
1.606
1.592
1.228
1.032
NH
7.0
6.5
6.0
5.5
5.0
4.5
4.0
3.5
3.0
2.5
2.0
1.5
1.0
ppm
0.95
2.17
0.96
1.85
1.00
1.00
2.10
10.21
3.02
1.09

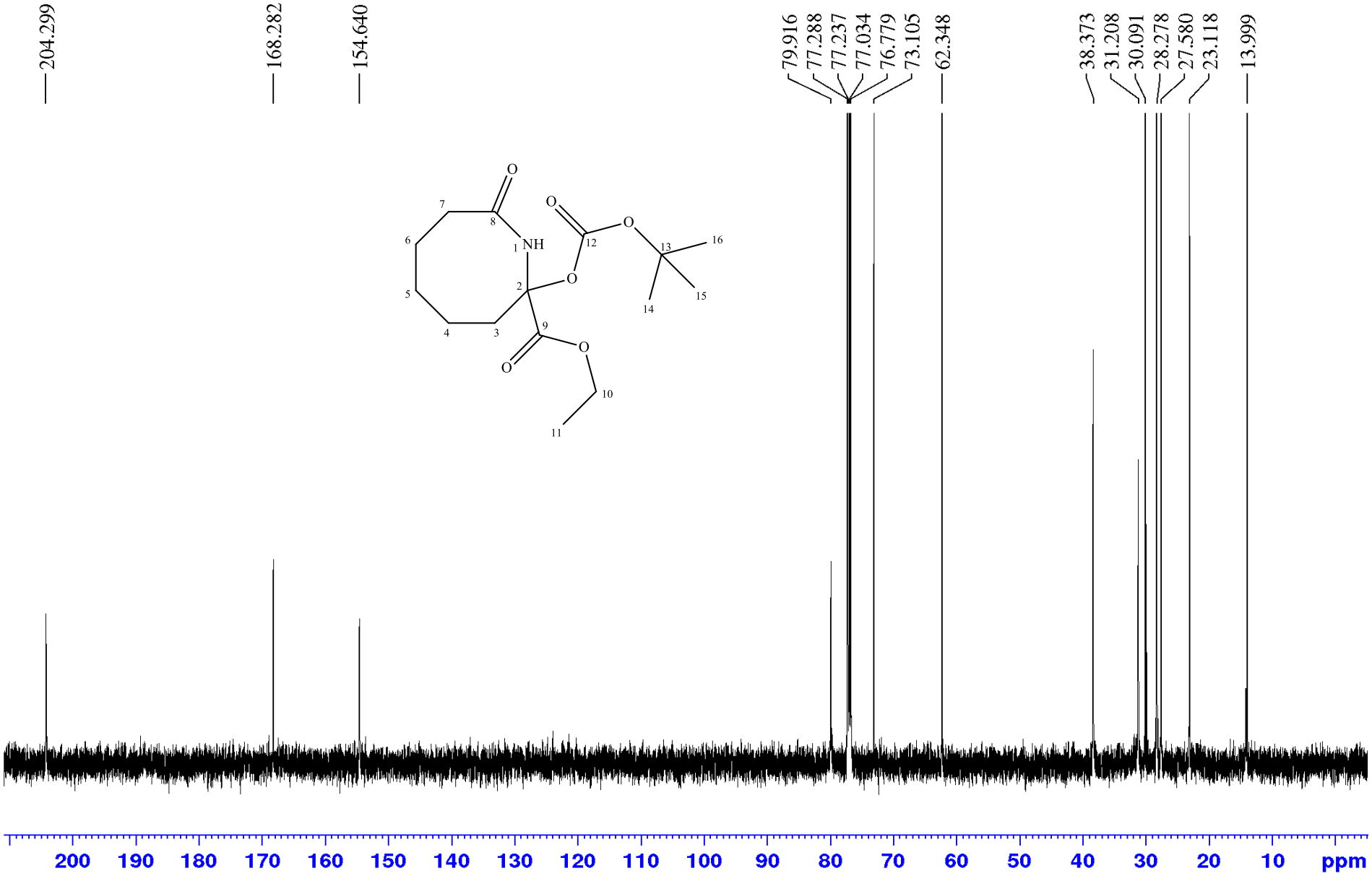
204.299
168.282
154.640
79.916
77.288
77.237
77.034
76.779
73.105
62.348
38.373
31.208
30.091
28.278
27.580
23.118
13.999
NH
200
190
180
170
160
150
140
130
120
110
100
90
80
70
60
50
40
30
20
10
ppm

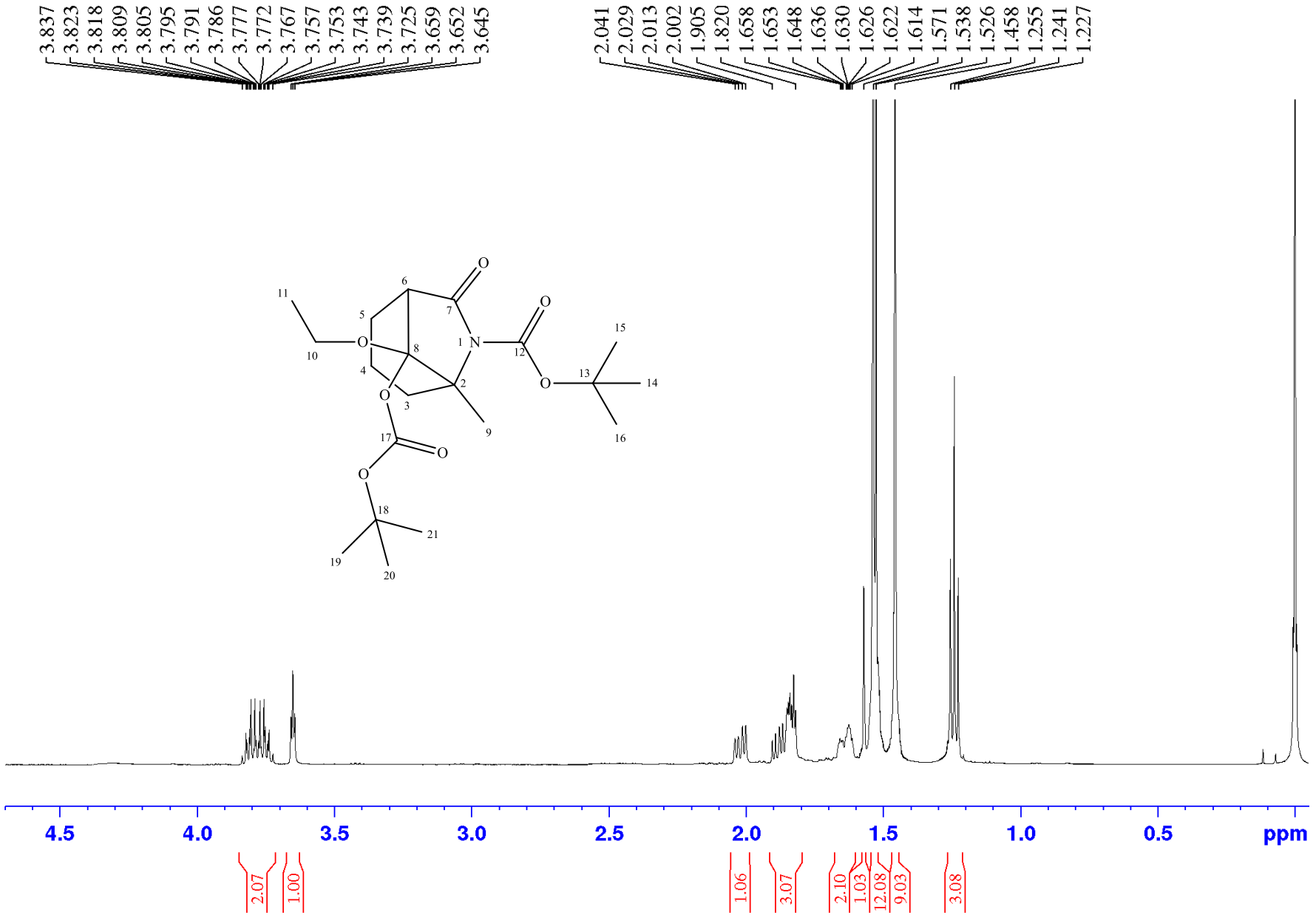
3.837
3.823
3.818
3.809
3.805
3.795
3.791
3.786
3.777
3.772
3.767
3.757
3.753
3.743
3.739
3.725
3.659
3.652
3.645
2.041
2.029
2.013
2.002
1.905
1.820
1.658
1.653
1.648
1.636
1.630
1.626
1.622
1.614
1.571
1.538
1.526
1.458
1.255
1.241
1.227
4.5
4.0
3.5
3.0
2.5
2.0
1.5
1.0
0.5
ppm
2.07
1.00
1.06
3.07
2.10
1.03
12.08
9.03
3.08

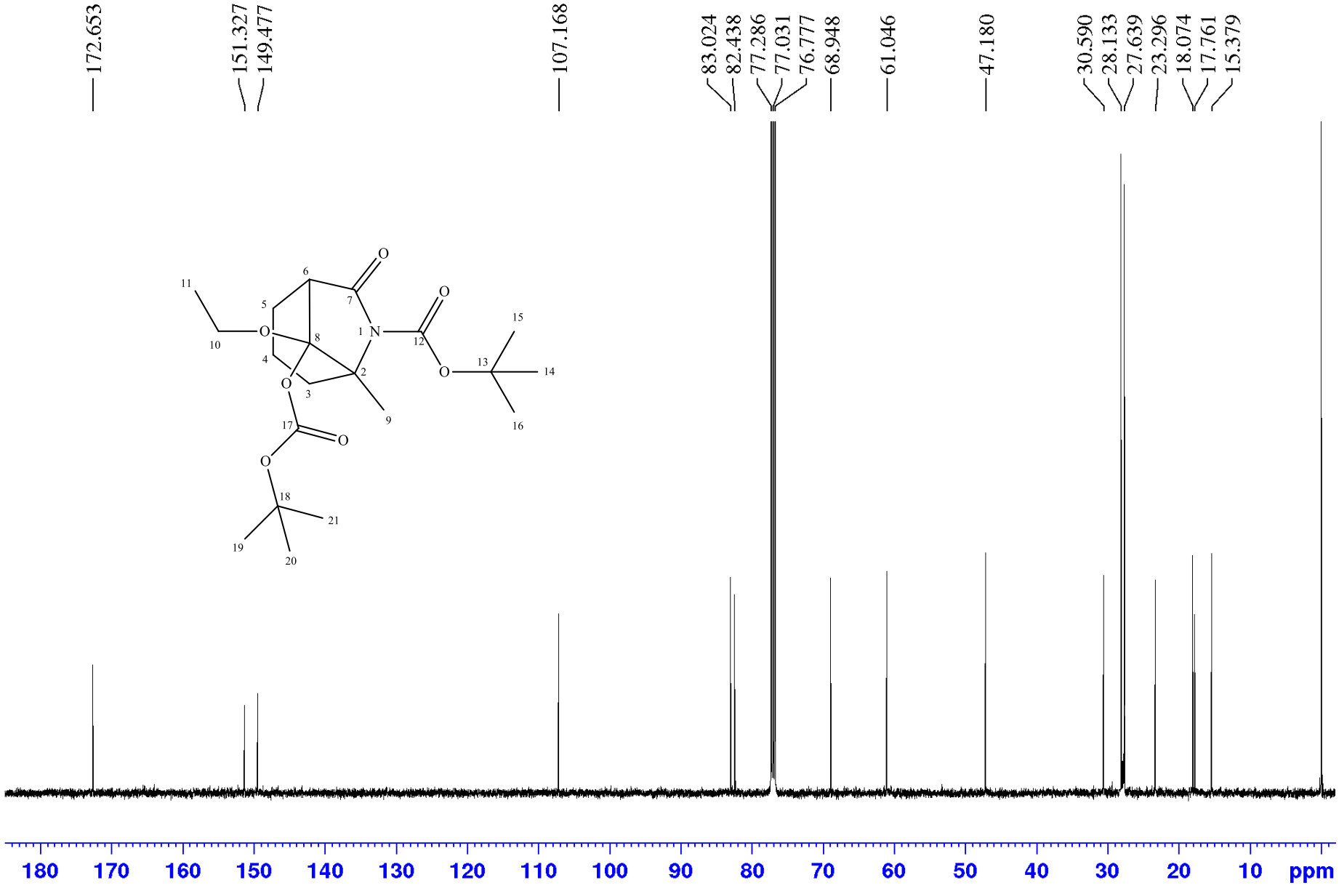
172.653
151.327
149.477
107.168
83.024
82.438
77.286
77.031
76.777
68.948
61.046
47.180
30.590
28.133
27.639
23.296
18.074
17.761
15.379
180
170
160
150
140
130
120
110
100
90
80
70
60
50
40
30
20
10
ppm

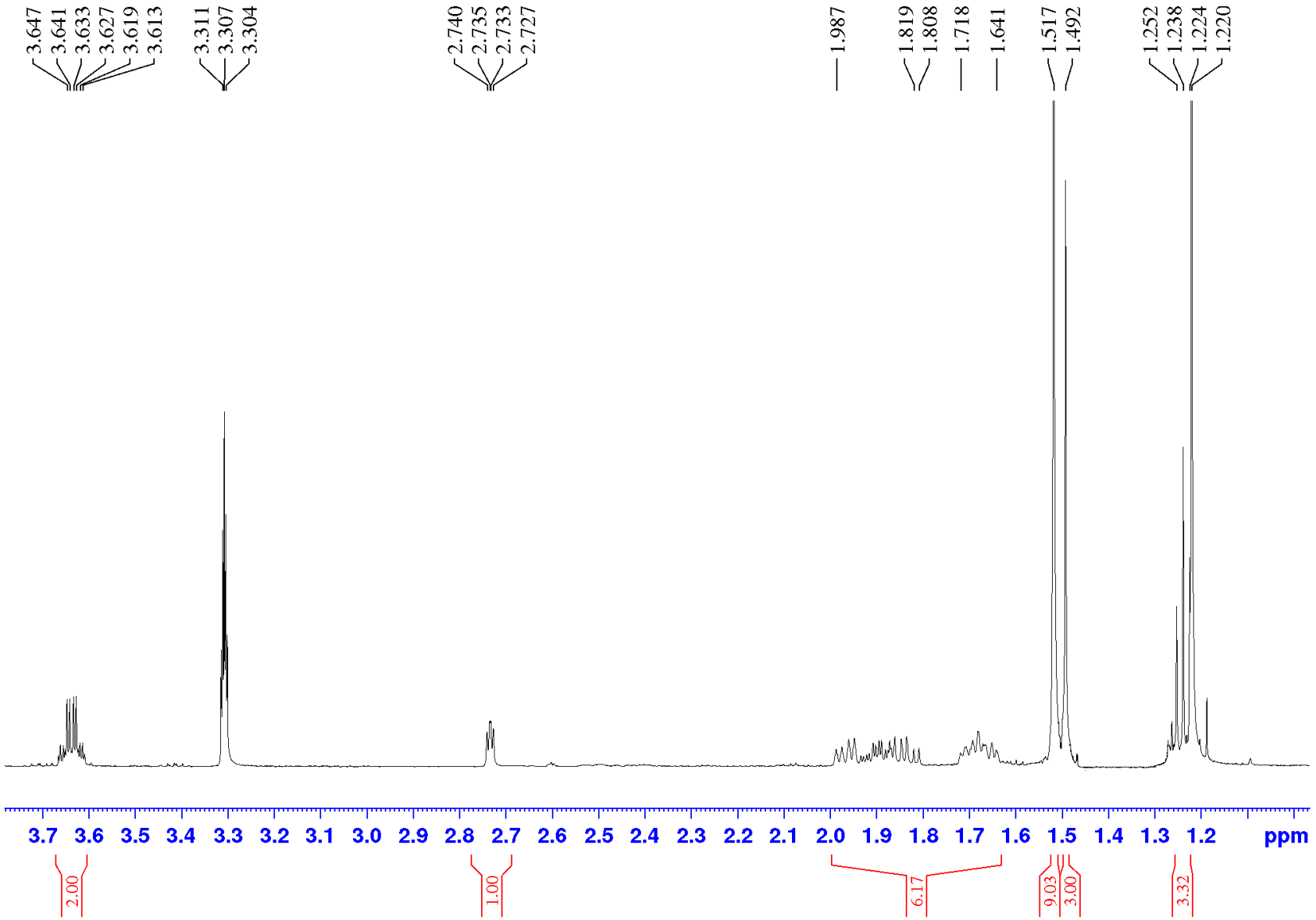
3.647
3.641
3.633
3.627
3.619
3.613
3.311
3.307
3.304
2.740
2.735
2.733
2.727
1.987
1.819
1.808
1.718
1.641
1.517
1.492
1.252
1.238
1.224
1.220
3.7 3.6 3.5 3.4 3.3 3.2 3.1 3.0 2.9 2.8 2.7 2.6 2.5 2.4 2.3 2.2 2.1 2.0 1.9 1.8 1.7 1.6 1.5 1.4 1.3 1.2 ppm
2.00
1.00
6.17
9.03
3.00
3.32

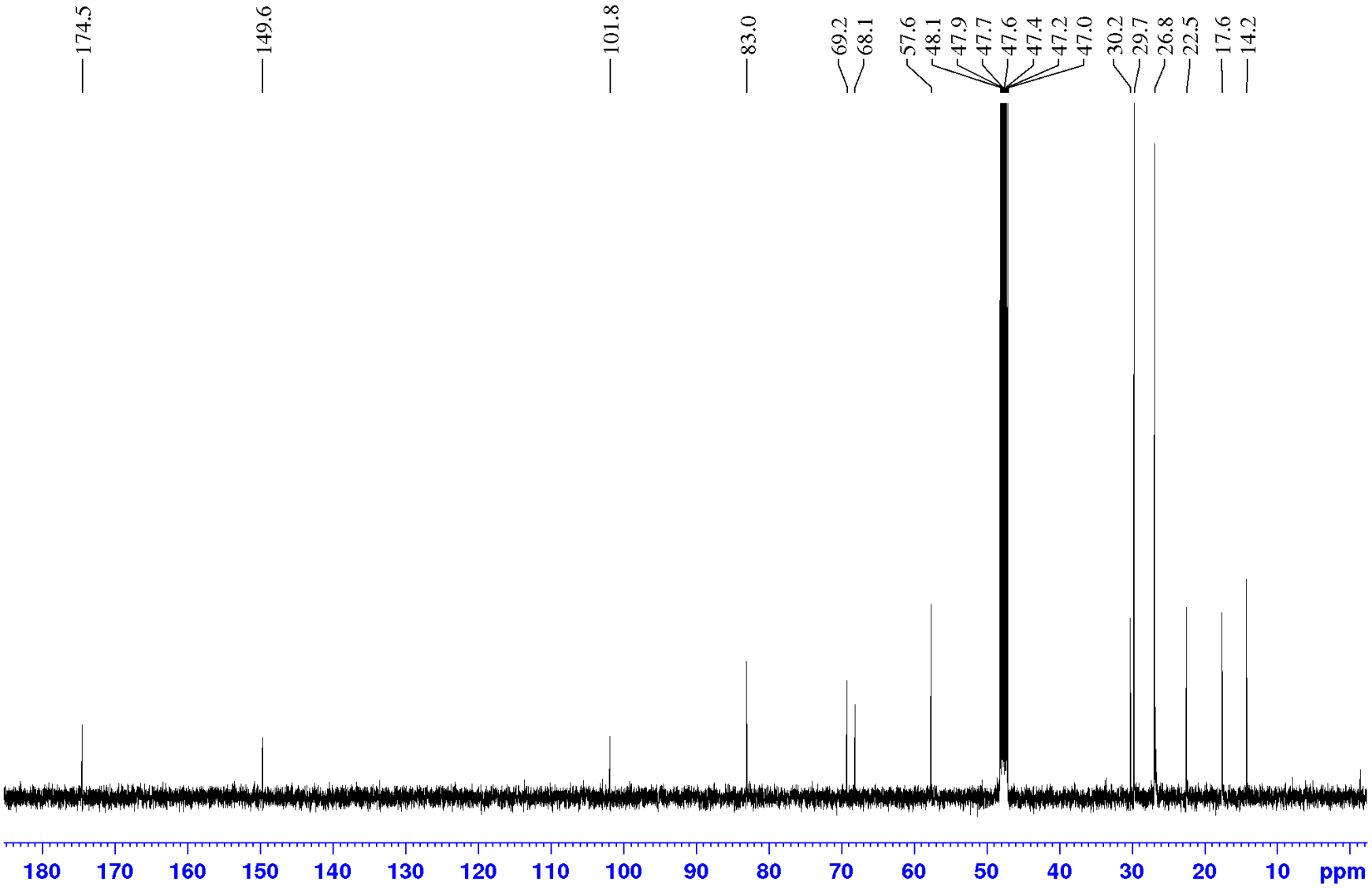
174.5
149.6
101.8
83.0
69.2
68.1
57.6
48.1
47.9
47.7
47.6
47.4
47.2
47.0
30.2
29.7
26.8
22.5
17.6
14.2
180
170
160
150
140
130
120
110
100
90
80
70
60
50
40
30
20
10
ppm

Synthesis of 7,8-dioxo-6-azabicyclo[3.2.1]octane

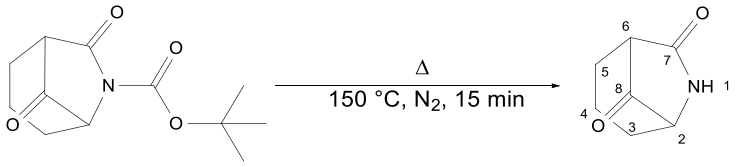

A vial, filled with 50 mg of the starting material is placed in a sand bath under a nitrogen atmosphere. The set up is quickly heated to 150 °C for 15 min, the vial is allowed to cool to room temperature to give the crystalline product. Yield (**1**): 83 % R_f: 0.21 (methanol:ethyl acetate; 1:10); ^{1}H-NMR: (500 MHz, MeOD-d_4, δ[ppm]) 3.55-3.54 (m), 3.45-3.44 (m, 1.3H, *H2*); 2.32 (m), 2.19-2.18 (m, 1.3H, *H6*); 1.93-1.72 (m, 3.5H); 1.59-1.29 (m, 6.9H)(*H3*, *H4*, *H5*); ^{13}C-NMR: (125 MHz, MeOD-d_4, δ[ppm]) 178.8, 178.3 (*C7*); 102.0, 101.2 (*C8*); 58.7, 55.6 (*C2*); 48.1 (*C6*); 26.9, 24.6, 24.2, 21.5, 15.8, 15.6 (*C3*, *C4*, *C5*); GC-MS: calculated: $[M]^+$ 139.1 found: 139

Synthesis of 5-Methyl-7,8-dioxo-6-azabicyclo[3.2.1]octane

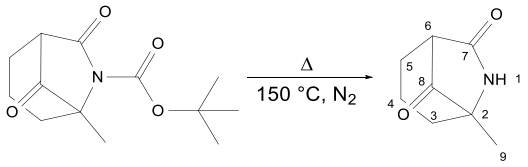

50 mg of the starting material are placed in a long-necked glass tube under an inert atmosphere and heated rapidly to 150 °C until all starting material is molten. The tube is allow to cool to room temperature, before all sublimed, crystalline material is rinsed with methanol, the solvent is evaporated *in vacuo*. This procedure is repeated three times and the crystalline residue is purified with column [SiO_2; methanol : ethyl acetate; 1:100 → 1:15] to give the desired product as white crystals. Yield (**2**): 76 % R_f: 0.34 (methanol:ethyl acetate; 1:15); ^{1}H-NMR: (500 MHz, MeOD-d_4, δ[ppm]) 7.02 (br s, 1H, *NH*); 2.87-2.86 (m, 1H, *H6*); 1.97-1.73 (m, 6H, *H3*, *H4*, *H5*); 1.33 (s, 3H, *H9*); ^{13}C-NMR: (125 MHz, MeOD-d_4, δ[ppm]) 210.8 (*C8*); 172.2 (*C7*); 65.5 (*C2*); 52.7 (*C6*); 39.9 (*C3*); 31.3 (*C5*); 18.4 (*C4*); 17.1 (*C9*); GC-MS: calculated: $[M]^+$ 153.1 found: 153

Synthesis of Ethyl-1-(2-carboxylethyl)-7-oxoazepane

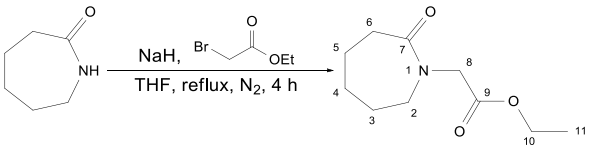

A two-necked round bottom flask, equipped with a reflux condenser and a septum, is charged with 1.00 g (8.38 mmol) of ε-caprolactam and 1.06 g (3 eq. 0.0265 mol NaH) of NaH-suspension in mineral oil (60%) under a nitrogen atmosphere. 30 ml of dry THF are added, and the slurry is stirred until no more gas develops. 4.9 ml (7.4 g, 5 eq., 0.0433 mol) of ethyl bromoacetate are added dropwise and the slurry is gently refluxed for 4 h. The mixture is allowed to cool to room temperature and 10 ml of water are added dropwise under ice cooling. Another 100 ml of water and 100 ml of ethyl acetate are added, the aqueous phase is extracted with 30 ml ethyl acetate three times and the combined organic phases are dried over $MgSO_4$. The drying agent is filtered off, the solvent is removed *in vacuo* and the residue is purified using column chromatography [SiO_2; ethyl acetate:cyclohexane; 1:4 → 1:1] to give the product as a viscous oil. Yield (**2**): 81 % R_f: 0.30 (ethyl acetate:cyclohexane; 1:1); ^{1}H-NMR: (500 MHz, MeOD-d_4, δ[ppm]) 4.18 (q, ^3J = 7 Hz, 2H, *H10*); 4.14 (s, 2H, *H8*); 3.41 (br s, 2H, *H2*); 2.59-2.57 (m, 2H, *H6*); 1.75-1.71 (m, 6H, *H3, H4, H5*); 1.28 (t, ^3J = 7 H, 3H, *H11*); ^{13}C-NMR: (125 MHz, MeOD-d_4, δ[ppm]) 176.3 (*C7*); 169.8 (*C9*); 61.1 (*C8*); 51.3 (*C2*); 50.5 (*C10*); 36.9 (*C6*); 30.0 (*C3*); 28.0 (*C5*); 23.2 (*C4*); 14.2 (*C11*); GC-MS: calculated: $[M]^+$ 199.1 found: 199

Synthesis of 1-(carboxyethyl)-7-oxoazepane

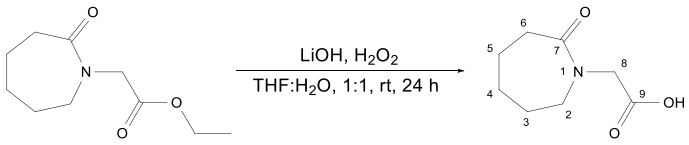

A round bottom flask is charged with 0.3 g (1.75 mmol) of ethyl-1-(2-carboxylethyl)-7-oxoazepane (**7**). 25 ml of THF and 25 ml of H_2O are added, followed by 0.34 (14.2 mmol) LiOH monohydrate and 3.5 ml of H_2O_2 (30% in water) and the suspension is stirred for 24 h at room temperature. The pH is adjusted to 3 with 0.5M HCl and the aqueous solution is extracted with 50 ml ethyl acetate three times. The combined organic layers are dried over $MgSO_4$, the drying agent is filtered off and the solvent is removed *in vacuo* to give the hydrolysis product as a white crystalline solid. Yield (**8**): 68%; ^{1}H-NMR: (500 MHz, MeOD-d_4, δ[ppm]) 4.12 (s, 2H, *H8*); 3.50-3.48 (m, 2H, *H2*); 2.58-2.56 (m, 2H, *H6*); 1.77-1.76 (m, 4H, *H3, H5*); 1.70-1.68 (m, 2H, *H4*); ^{13}C-NMR: (125 MHz, MeOD-d_4, δ[ppm]) 177.7 (*C7*); 171.4 (*C9*); 51.1 (*C2*); 50.0 (*C8*); 36.1 (*C6*); 29.5 (*C3*); 27.4 (*C5*); 22.9 (*C4*)

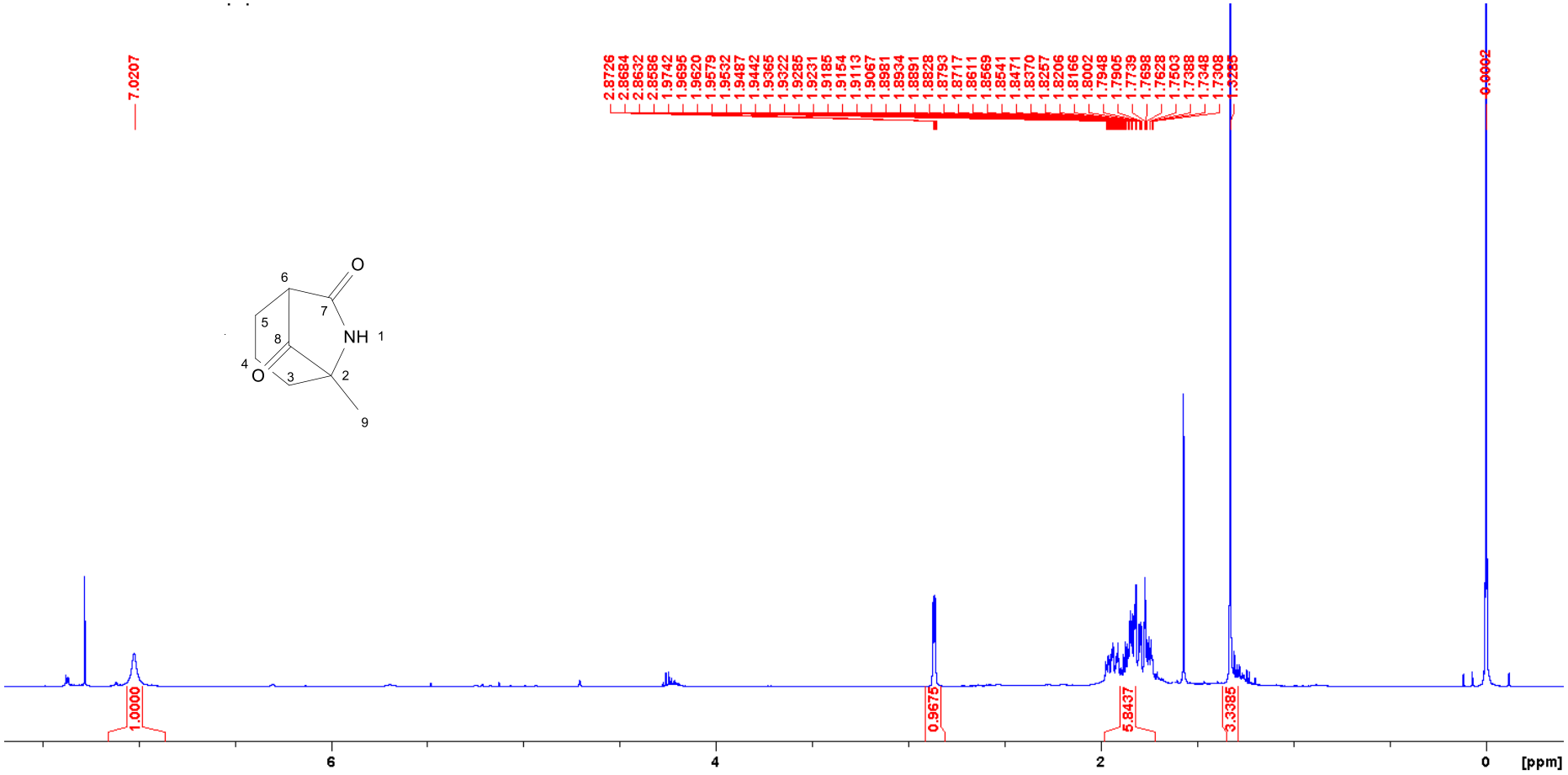
7.0207
2.8726
2.8684
2.8632
2.8586
1.9742
1.9695
1.9620
1.9579
1.9532
1.9487
1.9442
1.9365
1.9322
1.9285
1.9231
1.9185
1.9154
1.9113
1.9067
1.8981
1.8934
1.8891
1.8828
1.8793
1.8717
1.8611
1.8569
1.8541
1.8471
1.8370
1.8257
1.8206
1.8166
1.8002
1.7948
1.7905
1.7739
1.7698
1.7628
1.7503
1.7388
1.7348
1.7308
1.3285
0.0002
O
6
7
5
8
NH
1
4
O
3
2
9
1.0000
0.9676
5.8437
3.3385
6
4
2
0
[ppm]

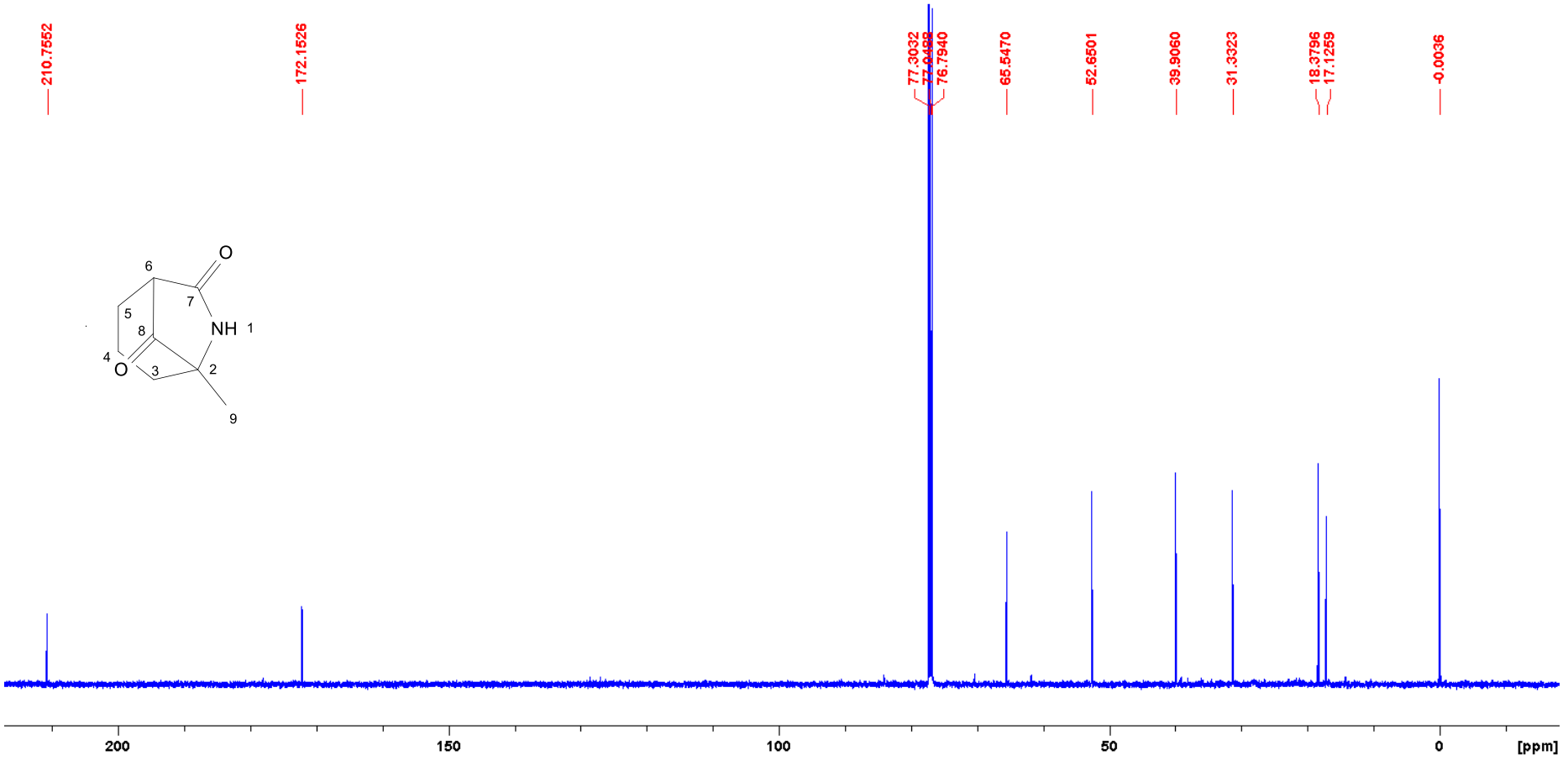
210.7552
172.1526
77.3032
77.0488
76.7940
65.5470
52.6501
39.9060
31.3323
18.3796
17.1259
-0.0036
O
6
7
5
8
NH
1
4
O
3
2
9
200
150
100
50
0
[ppm]

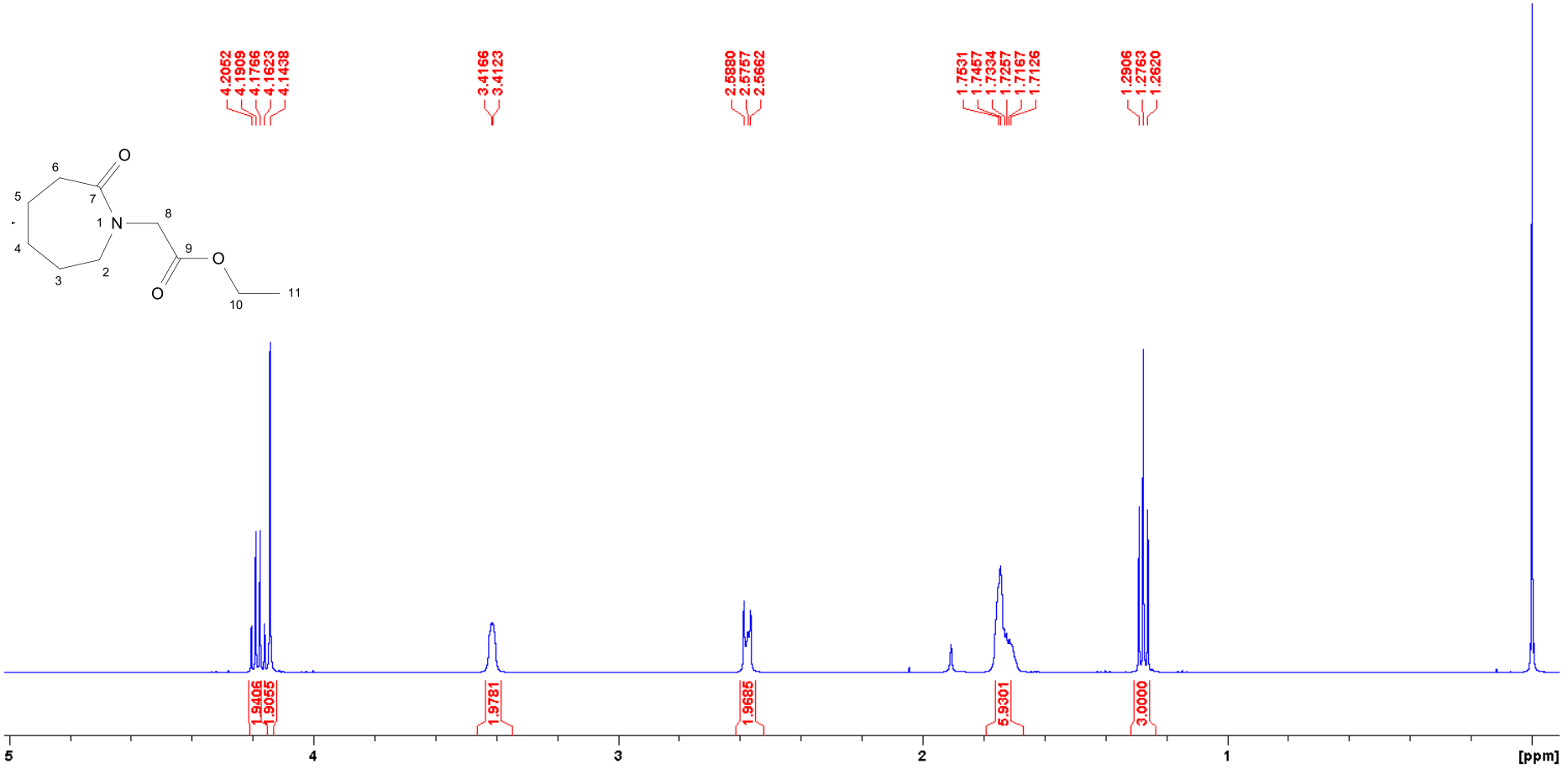
4.2052
4.1909
4.1766
4.1623
4.1438
3.4166
3.4123
2.5880
2.5757
2.5662
1.7531
1.7457
1.7334
1.7257
1.7167
1.7126
1.2906
1.2763
1.2620
1.9406
1.9055
1.9781
1.9685
5.9301
3.0000
5
4
3
2
1
[ppm]

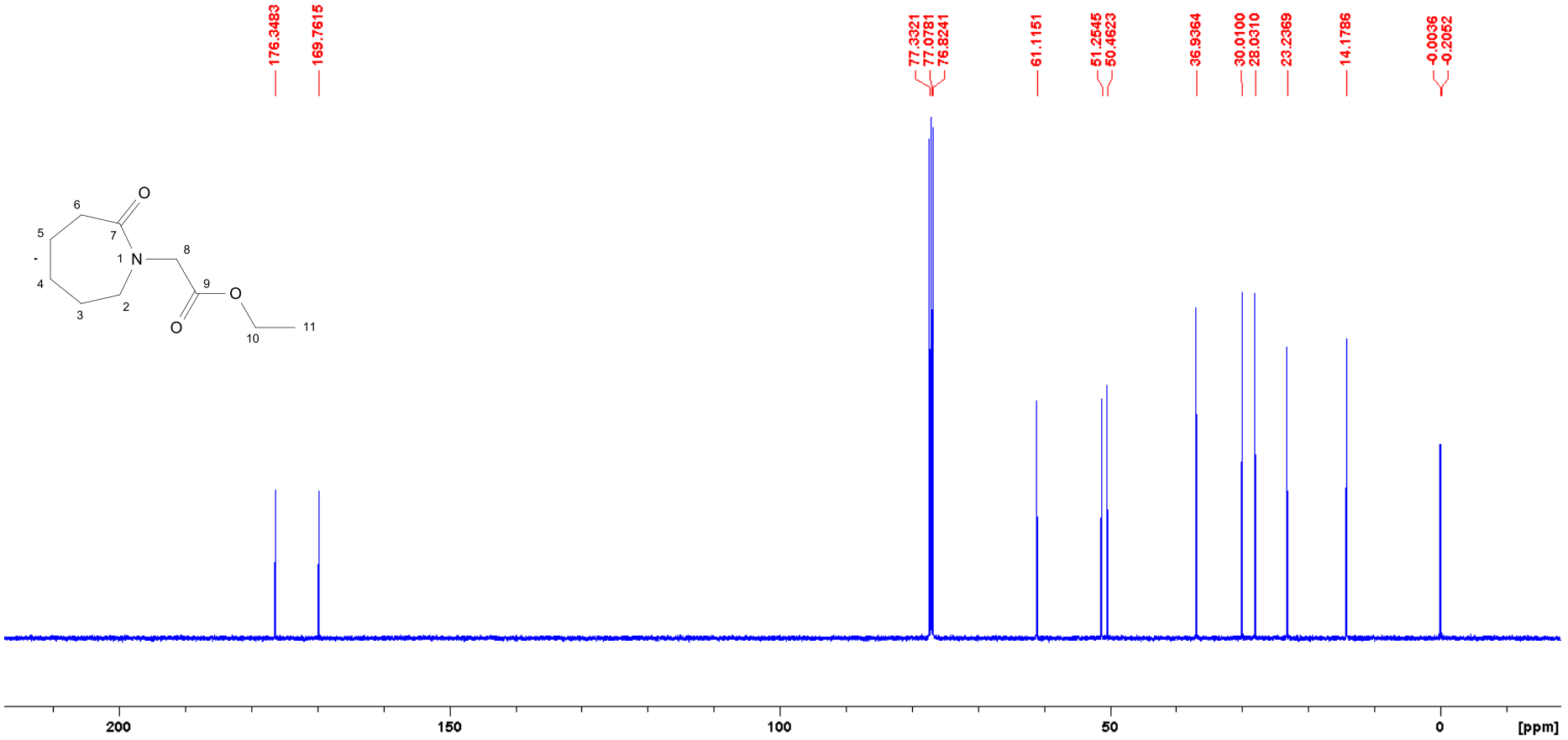
176.3483
169.7615
77.3321
77.0781
76.8241
61.1151
51.2545
50.4623
36.9364
30.0100
28.0310
23.2369
14.1786
-0.0036
-0.2052
O
6
5
7
1
N
8
4
9
O
2
3
O
10
11
200
150
100
50
0
[ppm]

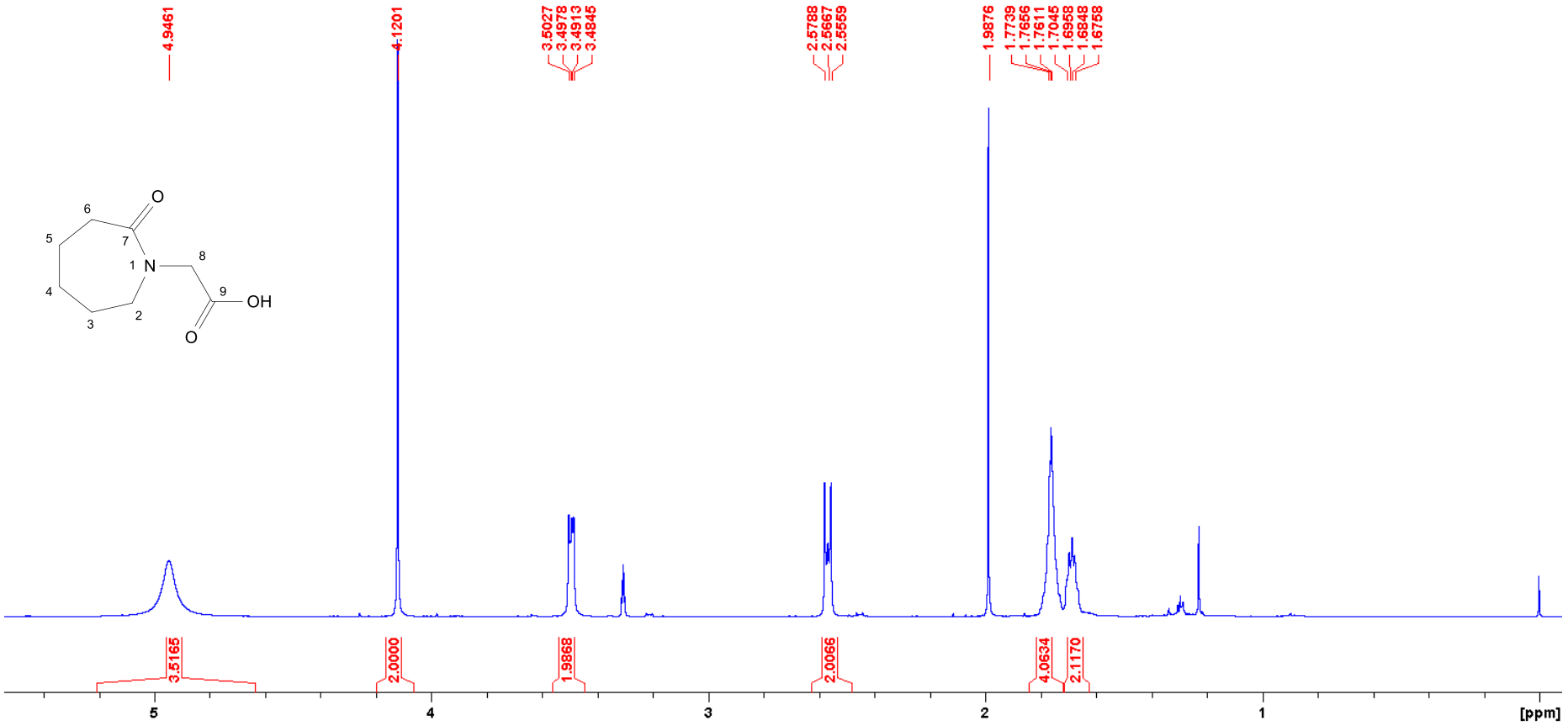
4.9461
4.1201
3.5027
3.4978
3.4913
3.4845
2.5788
2.5667
2.5559
1.9876
1.7739
1.7656
1.7611
1.7045
1.6958
1.6848
1.6758
O
6
5
7
1
N
8
4
9
OH
3
2
O
3.5165
2.0000
1.9868
2.0066
4.0634
2.1170
5
4
3
2
1
[ppm]